hexagon:2610.00678v4

Geometric Computation: Twin Helices and the Algebra of Flow

Benjamin Kaminsky*

November 20, 2026

Abstract

This work constructs a manifold consisting of twin helices to investigate the existence of computational geometric bordisms, as part of the broader program of the Cobordism Hypothesis. We use these structures to define a class of deterministic computational substrates, termed *Geometrically Computable Manifolds*, and study their geometric, algebraic, and computational properties. We show that, in a discrete regime, these manifolds encode arbitrary cyclic groups and support universal computation. This leads to a hypothesis describing the structural trade-offs in physical computation across distinct computational phases. We then analyze a regime in which abelian gauge computation is modeled with ordinary differential equations, linking the construction to continuous geometric dynamics. This signals a new research direction in physical mathematics at the intersection of geometry, gauge theory, and computability theory, termed *Geometric Computability Theory*, in which computation is treated as a property of geometric compositions. This perspective opens avenues for future investigation, motivating the development of a constructive computational gauge theory with applications to Yang–Mills theory. As of this writing, no complete unified compositional semantics yet exists for the full range of these manifolds; future work will develop such a formalism.

Keywords: geometric computation, higher gauge theory, prequantum geometry, Yang-Mills theory, cobordism hypothesis, helices, topological quantum field theory.

*benkaminskymath@gmail.com

Contents

Introduction **3**

1 Twin Helical Manifolds **4**
1.1 Volumetric Helices . . . 4
1.2 Chirality and Alignment . . . 5
1.3 Twin Helical Manifolds . . . 7

2 Geometrically Computable Manifolds **14**
2.1 GCMs and Geobits . . . 14
2.2 The Logic of Geometry . . . 17
2.3 The EVT Hypothesis and the Structure of Physical Computation . . . 23

3 Abelian Gauge Dynamics and Phase Geometry **32**
3.1 A New Kind of Computation . . . 33
3.2 Abelian Lattice Gauge Dynamics in the Quasi–Fluidic Mode . . . 36
3.3 Application of Lie Groupoids in Geometric Computation . . . 41
3.4 Connections and Phase Ledgers on a Trivial Helical Bundle . . . 46
3.5 Lancret's Ghost? . . . 48

4 Non-Abelian Geometric Computation **50**
4.1 Gauge Transport and Computational Memory . . . 51
4.2 The Algebra of Flow . . . 59
4.3 From Helical Holonomy to Spin-Network Coordinates . . . 68
4.4 On the Expressive Power of Physical Computation . . . 71
4.5 Constructive Computational Gauge Theory . . . 76

5 Geometric Computational Field Theory **86**
5.1 Euclidean Gauge Computation and Emergent Spacetime . . . 86
5.2 Reconstruction of Internal Gauge Symmetry . . . 93
5.3 On the Classification of Geometric Computational Field Theories . . . 102
5.4 From Geometric Semantics to Quantum Field Theory . . . 110
5.5 Psi-Geometric . . . 121

A Appendix **126**
A.1 "Hidden" Variables? . . . 126
A.2 Invariant Content Across Gauge and Duality Frames . . . 134
A.3 Higher Dimensional Algebra and Geometric Computational Field Theory . . . 138
A.4 Topological Kleene Field Theories and Computational Geometric Bordisms . . . 141
A.5 Reversible Computing and Gauge Processes . . . 143
A.6 Parallel Composition and Geometric E_∞-Structure . . . 146
A.7 Comparison with Real and Quantum Computation . . . 148
A.8 Fourier Mode Calculations . . . 149
A.9 Disclaimers . . . 152

Introduction

"In the long run, we hope that some theory of language expressiveness develops into a formal theory of the programming language design space."

— Mattias Felleisen, *On the Expressive Power of Programming Languages* (1991)

"A twisted version of four-dimensional supersymmetric gauge theory is formulated..."

— Edward Witten, *Topological Quantum Field Theory* (1988)

The following work constructs a geometric model of computation.

The gap between computer science and physics has been a long-standing one. While various attempts to bridge this divide have been made, the two fields still tend to begin from rather different primitives. Familiar models of computation are typically formulated in terms of discrete states and transition rules, whereas fundamental physics makes essential use of continuous geometry, symmetry, fields, and transport. This raises a natural question: in what sense are physical processes themselves computational? Penrose and others have questioned whether every physically relevant phenomenon should admit an algorithmic description, while ordinary scientific practice routinely treats continuous systems through numerical and analytic approximation. But a physical substrate already possesses geometry, symmetry, admissible deformations, boundary data, and modes of composition. These structures constrain which states can exist, how information may be transported, and which transformations can be performed. We therefore ask whether computation can be defined directly through the geometry of a smooth substrate, with symbolic and field-theoretic descriptions appearing as different regimes of the same underlying construction.

Section 1 constructs a deterministic geometric substrate from manifolds built out of joined helices. This naturally leads to coherence conditions imposed by chirality, torsion, and gluing, and from these conditions emerges a class of symbolic flow manifolds. We then analyze their basic group-theoretic behavior and define admissible regularity constraints.

Section 2 introduces the main computational objects of the paper: the *Geometrically Computable Manifold* and its associated state object, the *geobit*. The goal is to reconcile semantic expressiveness in computation with the structural stability and reversibility of geometric processes. Instead of treating semantics syntactically, we recast it geometrically in terms of moduli spaces of helices and their categorical behavior under symbolic flow. This leads to a regime in which symbolic computation is expressed through geometry itself, and from this analysis, we arrive at the central result of the paper: a generalized hypothesis governing the structure of physical computational behavior.

Section 3 passes from the symbolic regime to continuous abelian computation. The quasi-fluidic model enlarges a discrete geometric state by compact phase variables and quantized winding data, producing a natural commutative transport layer. We study this regime using local lattice-gauge dynamics, stroboscopic readout, Lie groupoids, decorated path data, connections, curvature, and phase ledgers. The purpose is to show how a deterministic geometric computer can carry continuous information while retaining local composition and finite observable readouts. This section also develops the moduli-space viewpoint needed once the geometry itself becomes a variable of the computation.

Section 4 develops the non-abelian regime. Connections and curvature are promoted from auxiliary descriptions to computational data, while holonomy records history-dependent transport and persistent geometric memory. The resulting *Algebra of Flow* describes the passage from commuting phase transport to order-sensitive composition, including the spinorial lift of helical frame geometry and the generation of non-abelian $SU(2)$ holonomy through independent rotation controls. We relate finite systems of graph holonomies to the representation theory underlying spin-network coordinates, examine the corresponding growth of physical expressive power, and formulate a constructive computational

gauge theory in which boundary conditions, gluing, constraints, and controlled effects become part of the computational semantics.

Section 5 asks how this geometric-computational structure may be organized as a field theory. We introduce *Geometric Computational Field Theory* (GCFT) as a framework for computationally decorated bordisms, boundary states, gauge transport, and local-to-global composition. Beginning with Euclidean gauge histories and the proposed emergence of spacetime and gravitational excitations, we develop a conditional geometric reconstruction of the internal gauge symmetries $U(1)$, $SU(2)$, and $SU(3)$, together with their prospective matter and Higgs sectors. The classification problem is formulated as a program rather than a completed application of the Cobordism Hypothesis. We then distinguish this compositional framework from the additional requirements of quantum field theory, including dynamical weighting, gauge reduction, locality, positivity, unitarity, continuum limits, spectra, and anomaly cancellation. The section concludes with a tentative ψ-geometric interpretation of quantum theory and its outstanding reconstruction problems.

The overall progression of the paper is therefore from finite geometric state, to symbolic computation, to abelian phase transport, to non-abelian gauge computation, and finally to a candidate field-theoretic semantics. These regimes are not introduced as independent analogies. They are successive enlargements of the same basic question: what computational structures become available when the state and process space of a machine are generated by smooth geometry?

Our task here, by its nature, is a work of synthesis as much as rigor. If its scope sometimes appears unruly, or its exposition occasionally ventures beyond traditional boundaries, it is only because the questions at hand have historically resisted treatment by *standard means*. I have aimed for clarity without sacrificing depth. So, if at times arguments feel *unconventional*?

I hope that patient reading and engagement will reward the effort.

Ultimately, my intent is not to assert authority, but to invite the reader to explore together an unexpected landscape that may, in time, help reshape our understanding of computation itself.

1 Twin Helical Manifolds

1.1 Volumetric Helices

Fix $R, H, \lambda, L > 0$, an apex-center $p_* = (x_*, y_*, z_*) \in \mathbb{R}^3$, a phase $\varphi_0 \in \mathbb{R}$, and signs $\chi, \omega \in \{-1, +1\}$. Define the conical helical spine by

$$\gamma_{\chi,\omega}(t) = p_* + e^{-\lambda t} \begin{pmatrix} R\cos(\chi\omega t + \varphi_0) \\ R\sin(\chi\omega t + \varphi_0) \\ -\omega H \end{pmatrix}, \qquad 0 \le t \le L. \tag{1}$$

The parameter runs from base ($t = 0$) toward apex ($t = L$). The distance from the axis and the axial coordinate are

$$r(t) = Re^{-\lambda t}, \qquad z(t) = z_* - \omega H e^{-\lambda t},$$

so the spine lies on a right circular cone:

$$r(t) = \frac{R}{H}\,|z(t) - z_*|.$$

The limiting cone vertex p_* is approached only as $t \to \infty$; it is not included in a finite regular unit helix.

The curve is an orbit of the one-parameter similarity flow

$$S_s(p_* + v) = p_* + e^{-\lambda s} R_z(\chi\omega s)v, \qquad s \in \mathbb{R},$$

where R_z denotes rotation about the z-axis. The sign ω gives the direction of axial advance from base to apex, while χ denotes intrinsic handedness. For this family, $\operatorname{sgn}\tau = \chi$, where τ is signed Frenet torsion.

Definition 1.1 (Volumetric Conical Helix)**.** Let $(T(t), N(t), B(t))$ be the Frenet–Serret frame of the regular spine (1) [Bis75]. Choose a sufficiently small $b > 0$, and let $a : [0, L] \to (0, \infty)$ be a smooth, nonincreasing cross-sectional radius satisfying

$$a(t) = be^{-\lambda t} \quad (0 \le t \le L - \delta), \qquad a'(L) = 0,$$

for some arbitrarily short terminal collar $0 < \delta < L$. The *volumetric conical helix* is the image of

$$\Phi(t, s, \phi) = \gamma_{\chi,\omega}(t) + s\big(\cos\phi\, N(t) + \sin\phi\, B(t)\big),$$

with

$$0 \le t \le L, \qquad 0 \le s \le a(t), \qquad 0 \le \phi < 2\pi.$$

We require b to be small enough that this tubular parametrization is embedded. The cross-sectional disk at $t = 0$ is the *base*; the terminal end at $t = L$ is the *apex end*.

Away from the short terminal collar, the cross-sectional thickness scales with the same factor $e^{-\lambda t}$ as the spine. This is the thickened conical geometry represented schematically in Fig. 1. Flattening $a'(L)$ in the collar permits a smooth apical cap without altering the screw–dilation law of the centerline.

Definition 1.2 (Apical Cap)**.** Write $a_L = a(L)$ and $(T_L, N_L, B_L) = (T(L), N(L), B(L))$. The apical cap is the hemispherical surface

$$S_{\mathrm{cap}}(u, v) = \gamma_{\chi,\omega}(L) + a_L \sin u\, T_L + a_L \cos u\big(\cos v\, N_L + \sin v\, B_L\big),$$

for $0 \le u \le \pi/2$ and $0 \le v < 2\pi$.

Because $a'(L) = 0$, the cap and the tube have matching tangent planes along their common terminal circle. With the usual rounding of any remaining base-edge corner, the capped body is an embedded compact 3-manifold with boundary, diffeomorphic to D^3, provided the tube and cap are chosen without self-intersection. Its distinguished core arc and base disk retain the geometric information relevant to subsequent gluing.

Remark 1.1. Choose the thickness below a tubular-neighborhood bound for the compact regular spine [Gra04], and require the apical cap to remain disjoint from the rest of the body. For fixed $L < \infty$, sufficiently small b gives an embedded capped tube. The limiting cone vertex at $t = \infty$ lies outside the regular volumetric helix.

Lie-algebraic structure of the helical flow. The one-parameter screw–dilation flow S_s is generated by

$$X = -\lambda D + \chi\omega J_z \in \mathfrak{sim}(3),$$

where D generates uniform dilation about p_* and J_z generates rotation about the helical axis. Since $[D, J_z] = 0$, the generator lies in the abelian subalgebra $\mathrm{span}\{D, J_z\} \subset \mathfrak{sim}(3)$. This distinguishes the conical helix from a cylindrical helix, whose centerline is an orbit of a screw motion in $SE(3)$, generated by a combination of axial translation and rotation. Thus the conical construction naturally belongs to similarity geometry rather than purely Euclidean rigid-motion geometry.

1.2 Chirality and Alignment

Definition 1.3 (Chirality)**.** A subset $O \subset \mathbb{R}^n$ is said to have *chirality* if it is not properly congruent to its mirror image. Equivalently, O is chiral if for every reflection r across a plane in $\mathbb{R}^n$, there exists no proper isometry, i.e., orientation-preserving Euclidean motion (translations or rotations), g such that $g(O) = r(O)$. We say that helices may possess either left-handed or right-handed chirality. For the conical family (1), chirality is the sign $\chi = \operatorname{sgn}\tau$ of the signed Frenet torsion, with $\chi = -1$ left-handed and $\chi = +1$ right-handed. The axial orientation ω is independent of this label.[1]

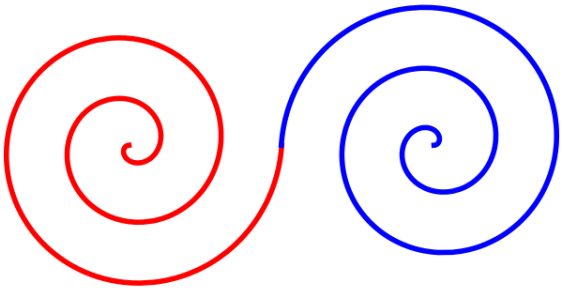
Lemma 1.1 (Matching-Phase Constraint for Offset Spirals)**.** *Let*

$$S_i(\theta) = C_i + a_i\theta \begin{pmatrix}\cos\theta\\ \sin\theta\end{pmatrix}, \qquad i = 1, 2,$$

be two Archimedean spirals in $\mathbb{R}^2$, with distinct centers $C_1 \neq C_2$ and equal pitch magnitude

$$|a_1| = |a_2| = a > 0.$$

[1] Here, *chirality* means literal geometric handedness of a helix: noncongruence with its mirror image under orientation-preserving Euclidean motions. It should not be confused with fermionic chirality in relativistic quantum field theory, which refers to left- and right-handed spinor representations or γ^5-eigenspaces.



The spirals intersect at a common nonzero phase θ if and only if

$$a_2 = -a_1$$

and

$$C_2 - C_1 = 2a_1\theta \begin{pmatrix} \cos\theta \\ \sin\theta \end{pmatrix}.$$

In particular, opposite chirality is necessary but not sufficient: the relative displacement of the centers must also satisfy the displayed matching condition.

Proof. Suppose first that the two spirals intersect at a common phase $\theta \neq 0$. Then

$$S_1(\theta) = S_2(\theta),$$

so

$$C_1 + a_1\theta \begin{pmatrix} \cos\theta \\ \sin\theta \end{pmatrix} = C_2 + a_2\theta \begin{pmatrix} \cos\theta \\ \sin\theta \end{pmatrix}.$$

Rearranging gives

$$C_2 - C_1 = (a_1 - a_2)\theta \begin{pmatrix} \cos\theta \\ \sin\theta \end{pmatrix}.$$

Since $C_1 \neq C_2$, the right-hand side is nonzero, and therefore $a_1 \neq a_2$. Because $|a_1| = |a_2|$, it follows that

$$a_2 = -a_1.$$

Substituting this relation yields

$$C_2 - C_1 = 2a_1\theta \begin{pmatrix} \cos\theta \\ \sin\theta \end{pmatrix}.$$

Conversely, suppose that $a_2 = -a_1$ and that, for some $\theta \neq 0$,

$$C_2 - C_1 = 2a_1\theta \begin{pmatrix} \cos\theta \\ \sin\theta \end{pmatrix}.$$

Then

$$C_1 + a_1\theta \begin{pmatrix} \cos\theta \\ \sin\theta \end{pmatrix} = C_2 - a_1\theta \begin{pmatrix} \cos\theta \\ \sin\theta \end{pmatrix},$$

and hence

$$S_1(\theta) = S_2(\theta).$$

Thus the two spirals intersect at the common phase θ. □

Remark 1.2. Matching phase does not by itself imply equality of the oriented tangent vectors. Define

$$e_r(\theta) = \begin{pmatrix} \cos\theta \\ \sin\theta \end{pmatrix}, \qquad e_\theta(\theta) = \begin{pmatrix} -\sin\theta \\ \cos\theta \end{pmatrix}.$$

Then

$$S_i'(\theta) = a_i\big(e_r(\theta) + \theta e_\theta(\theta)\big).$$

In the opposite-chirality case $a_2 = -a_1$, one obtains

$$S_2'(\theta) = -S_1'(\theta).$$

Thus the two branches determine the same unoriented tangent line but carry opposite parameter orientations. Reversing the parametrization of one branch aligns the first derivatives. Matching second-order data requires additional jet conditions or an interpolating splice and does not follow from phase matching alone.

Corollary 1.2 (Concentric Spiral Constraint)**.** *Let S_1 and S_2 be Archimedean spirals with the same center,*

$$C_1 = C_2,$$

and equal pitch magnitude. A noncentral matching-phase intersection at some $\theta \neq 0$ occurs if and only if

$$a_1 = a_2.$$

Consequently, two concentric spirals of equal pitch magnitude can meet at a common nonzero phase only when they have the same chirality; in that case, the two parametrized spirals coincide.

Proof. At a common phase θ, the intersection condition becomes

$$(a_1 - a_2)\theta \begin{pmatrix} \cos\theta \\ \sin\theta \end{pmatrix} = 0.$$

For $\theta \neq 0$, the vector

$$\begin{pmatrix} \cos\theta \\ \sin\theta \end{pmatrix}$$

is nonzero, so

$$a_1 = a_2.$$

Conversely, if $a_1 = a_2$ and $C_1 = C_2$, then

$$S_1(\theta) = S_2(\theta)$$

for every θ. □

Remark 1.3. The phase-matching condition therefore imposes a global placement constraint. For distinct centers, equal signed pitch is impossible, while opposite signed pitch permits an intersection only when the displacement $C_2 - C_1$ lies on the corresponding one-parameter matching locus. For concentric spirals, every noncentral matching-phase intersection forces equality of the signed pitches. These statements concern intersection and first-order alignment; the existence of a prescribed C^2 splice is a separate jet-matching problem.

1.3 Twin Helical Manifolds

We now form pairs of volumetric helices by gluing them along their base disks.

Definition 1.4 (Binary Orientation of a Helix)**.** Let H have spine (1), parameterized from base to apex by $t \in [0, L]$. Its axial orientation is

$$\omega(H) := \operatorname{sgn} \frac{dz}{dt} \in \{-1, +1\}.$$

In the conical family,

$$\frac{dz}{dt} = \omega\lambda H e^{-\lambda t},$$

so $\omega = +1$ means upward axial advance and $\omega = -1$ means downward axial advance. This is independent of the intrinsic chirality $\chi = \operatorname{sgn}\tau$. In particular, the azimuthal phase increases or decreases according to $\chi\omega$, so the base-to-apex parameter need not be an increasing angular coordinate. Later geometric regimes refine the same orientation channel by retaining additional phase information associated with rotation about the helical axis.

Definition 1.5 (Type 1 Twin Helix)**.** Fix $R, H, \lambda, L > 0$ and $\varphi_0 = 0$. Let

$$\gamma_A(t) = \begin{pmatrix} Re^{-\lambda t}\cos t \\ Re^{-\lambda t}\sin t \\ H(1-e^{-\lambda t}) \end{pmatrix}, \qquad 0 \le t \le L,$$

and let its reflection across the horizontal plane be

$$\gamma_B(t) = \begin{pmatrix} Re^{-\lambda t}\cos t \\ Re^{-\lambda t}\sin t \\ -H(1-e^{-\lambda t}) \end{pmatrix}.$$

Both spines start at the common base center $(R, 0, 0)$ and taper toward opposite axial directions. In the notation of (1), their labels are

$$(\chi_A, \omega_A) = (+1, +1), \qquad (\chi_B, \omega_B) = (-1, -1).$$

Thus the two unit helices have opposite intrinsic handedness and opposite axial orientation, as in Type 1 of Fig. 1. Their defining relation is the orientation-reversing reflection

$$\gamma_B = \Sigma_z \circ \gamma_A, \qquad \Sigma_z(x, y, z) = (x, y, -z),$$

with a smooth embedded volumetric representative obtained by gluing the abstract base disks and, where necessary, choosing a compatible local smoothing or bridge.

Forming the THM. Let H_A and H_B be volumetric helices, and let

$$B_A \subset \partial H_A, \qquad B_B \subset \partial H_B$$

be their distinguished base disks. Given a diffeomorphism

$$f : B_A \to B_B,$$

the *Twin Helical Manifold* associated to (H_A, H_B, f) is the quotient

$$H_{AB} = (H_A \sqcup H_B)/\sim, \qquad p \sim f(p) \quad (p \in B_A).$$

This quotient defines the abstract manifold obtained by gluing the two helices along their bases. In the present paper, we typically take f to be the identity in the natural cylindrical coordinates on the base disks. An embedded realization in $\mathbb{R}^3$ requires compatible boundary collars and clearance; for placements where this is feasible, we may interpolate between the two bases using a bridge.

Definition 1.6 (Embedded Bridge Realization)**.** Let P_A and P_B be the centers of the two base disks. Orient the joined spine by traversing helix A from apex to base, then the bridge from P_A to P_B, and then helix B from base to apex. Let $\mathbf{t}_A, \mathbf{t}_B$ be the unit tangents of the parent spines in their original base-to-apex parametrizations, and let $\mathbf{k}_A, \mathbf{k}_B$ be their curvature vectors (derivatives of the unit tangents with respect to arc length) at the bases. Fix a positive parameter speed ℓ and prescribe the compatible endpoint jets

$$\mathbf{m}_A = -\ell\,\mathbf{t}_A, \qquad \mathbf{m}_B = \ell\,\mathbf{t}_B, \qquad \mathbf{a}_A = \ell^2\mathbf{k}_A, \qquad \mathbf{a}_B = \ell^2\mathbf{k}_B.$$

Reversal of the first parent arc changes its tangent sign but not its curvature vector. The bridge spine is the quintic Hermite interpolant [dB78]

$$\begin{aligned}\Gamma_5(s) = {} & h_{00}(s)P_A + h_{01}(s)P_B + h_{10}(s)\mathbf{m}_A + h_{11}(s)\mathbf{m}_B \\ & + h_{20}(s)\mathbf{a}_A + h_{21}(s)\mathbf{a}_B, \qquad s \in [0, 1],\end{aligned}$$

with basis polynomials

$$\begin{aligned} h_{00}(s) &= 1 - 10s^3 + 15s^4 - 6s^5, & h_{01}(s) &= 10s^3 - 15s^4 + 6s^5, \\ h_{10}(s) &= s - 6s^3 + 8s^4 - 3s^5, & h_{11}(s) &= -4s^3 + 7s^4 - 3s^5, \\ h_{20}(s) &= \tfrac{1}{2}(s^2 - 3s^3 + 3s^4 - s^5), & h_{21}(s) &= \tfrac{1}{2}(s^3 - 2s^4 + s^5). \end{aligned}$$

The interpolant matches the positions, first derivatives, and second derivatives:

$$\Gamma_5(0) = P_A, \quad \Gamma_5(1) = P_B, \qquad \Gamma_5'(0) = \mathbf{m}_A, \quad \Gamma_5'(1) = \mathbf{m}_B,$$
$$\Gamma_5''(0) = \mathbf{a}_A, \quad \Gamma_5''(1) = \mathbf{a}_B.$$

These are the C^2 spine-matching conditions of theorem 1.4, with a common local parameter speed on the adjoining arcs.

For offset configurations, an interpolating bridge may develop a hairpin or meet one of the parent tubes. A clearance adjustment can be sought in the form

$$\widetilde{\Gamma}(s) = \Gamma_5(s) + \alpha s^3(1-s)^3\,\mathbf{n},$$

where $\mathbf{n}$ is a fixed transverse direction. Because the perturbation and its first two derivatives vanish at both endpoints, it preserves the prescribed 2-jets. Choose α, if possible, so that the bridge remains regular, embedded, and clear of the parent tubes.

Reparametrize a regular bridge by arc length σ, and use an orthonormal Bishop (rotation-minimizing) frame (T, E_1, E_2) along it, satisfying

$$\frac{dE_a}{d\sigma} = -\left\langle \frac{dT}{d\sigma}, E_a \right\rangle T, \qquad a = 1, 2.$$

Its tubular coordinates are

$$\Phi_{\mathrm{br}}(\sigma, r, \phi) = \widetilde{\Gamma}(\sigma) + r\big(\cos\phi\, E_1(\sigma) + \sin\phi\, E_2(\sigma)\big),$$

with r below a tubular-neighborhood bound. The Bishop frame remains defined at points of vanishing curvature. With compatible endpoint framings and sufficiently regular tubular collars, the construction gives a C^2 embedded local join whenever the bridge is regular and has sufficient clearance.

Remark 1.4. The spline bridge is *not* part of the abstract definition of a Twin Helical Manifold. It is one possible geometric realization when suitable clearance and endpoint matching can be achieved in $\mathbb{R}^3$. The gluing of the base disks determines the underlying manifold, while the particular bridge affects only the chosen embedded representative.

We call any such glued object a *Twin Helical Manifold* (THM), or more informally, a *Twin Helix*.

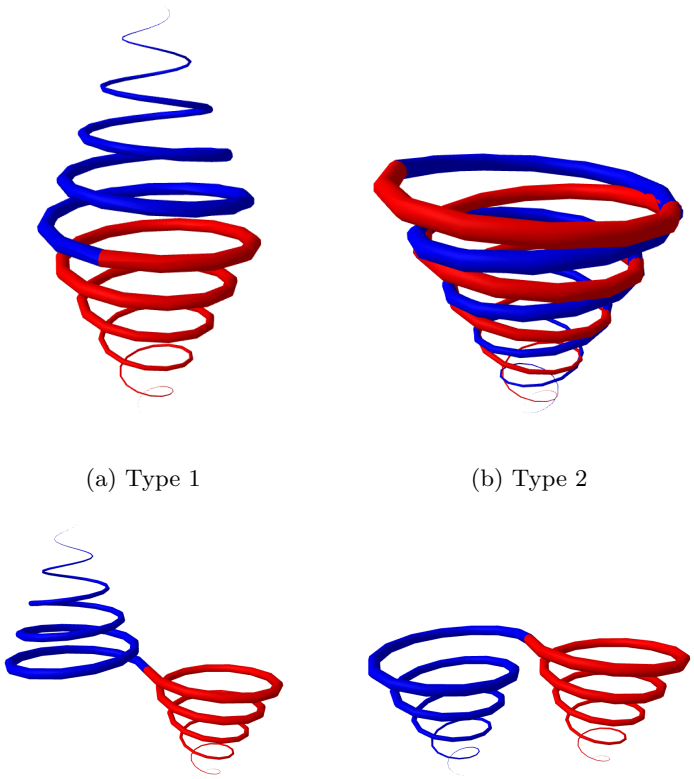
Definition 1.7 (Twin Helical Manifold and Unit Helices)**.** A THM consists of two embedded helical tubes $\Sigma_\pm \subset M$ whose distinguished base disks are identified along an interface $B \simeq D^2$, with boundary circle $\partial B \simeq S^1$. The orientations and boundary collars (modeled locally on $D^2 \times I$) are matched so that the glued object $\Sigma_+ \cup_B \Sigma_-$ is a smooth submanifold (no cone angle or cusp). A connection $A \in \Omega^1(M; \mathfrak{g})$ restricts smoothly across B; its curvature F is bounded (no measure concentration). The two helices composing a single THM are termed *unit helices*, denoted H_A and H_B.

By combining different chiralities and orientations, we define a geometric family of four canonical manifolds, denoted THM_4. This yields a total of 4 distinct invariant configuration states. However, our Type 2 twin helix has a small problem. A simple drawing shows that constructing a twin helix with the specified attributes becomes problematic in the previously defined $\mathbb{R}^3$ space. A closer investigation leads to the following conclusion.

Table 1: Essential type chart for twin helical manifolds

Type	**Chirality**	**Orientation**	**Axiality**	**Mnemonic**	**Map** $\Rightarrow H_B$
1	Opposite	Opposite	Coaxial	Helical Orb	Σ_z
2	Opposite	Same	Coaxial	Twisted Pair	Σ_y
3	Same	Opposite	Offset	Symmetrical Flow	$R_y(\pi), T$
4	Same	Same	Offset	Co-propagating Twins	$R_z(\pi), T$

Lemma 1.3 (Type-2 Intersection Lemma for the Canonical Coaxial Family)**.** *Let H_A and H_B be two coaxial helical centerlines parameterized by $t \in [0, 1]$, with the same radial function $r(t)$, the same*



(a) Type 1 (b) Type 2

(c) Type 3 (d) Type 4

Figure 1: The THM_4 geometric family.

axial function $z(t)$, the same number of turns N, and opposite chirality. Suppose that their angular coordinates differ only by a constant phase offset. If

$$N \geq \frac{1}{2},$$

then, for every constant phase offset, the two centerlines intersect at some $t \in [0, 1]$.

Proof. Write the angular phases with the common orientation ω as

$$\alpha_A(t) = 2\pi N \chi_A \omega t + \phi_A, \qquad \alpha_B(t) = 2\pi N \chi_B \omega t + \phi_B.$$

Here $\chi_B = -\chi_A$, and both curves have the same positive radial profile and axial coordinate. Relabeling if necessary, take $\chi_A = -1$ and $\chi_B = +1$. Then

$$\alpha_B(t) - \alpha_A(t) = 4\pi N \omega t + (\phi_B - \phi_A).$$

As t varies from 0 to 1, this continuous expression ranges over an interval of length $4\pi N$, regardless of the sign of ω. If $N \geq \frac{1}{2}$, the interval contains an integer multiple of 2π. At the corresponding parameter, the two angular coordinates agree modulo 2π; their radial and axial coordinates agree by hypothesis, so the centerlines intersect. □

Type-2 helices and separation in $\mathbb{R}^4$. The preceding lemma establishes an extrinsic obstruction for the canonical coaxial realization with matched radial and axial profiles: within this restricted family, a constant phase shift cannot separate the two centerlines in $\mathbb{R}^3$. This obstruction is specific to the three-dimensional realization rather than to the abstract pairing itself.

Passing to $\mathbb{R}^4$ supplies an additional normal direction in which the two branches may be separated while preserving the original helical geometry under projection to $\mathbb{R}^3$. For example, one may place the two centerlines at distinct constant values of the fourth coordinate; the same construction applies to

the corresponding volumetric tubes provided the separation exceeds their transverse thickness. Thus the fourth coordinate gives an explicit resolution of the intersection forced by the canonical Type-2 realization in $\mathbb{R}^3$.

From planar phase matching to spatial jet matching. Passing from planar spirals (1.1) to spatial helices introduces additional geometric data, but the order at which those data enter must be distinguished carefully. A direct C^1 splice is controlled by tangent matching, while a direct C^2 splice is controlled by the curvature vector. Torsion is a third-order invariant and becomes relevant only when one asks for C^3 compatibility. Consequently, chirality alone does not determine whether two helical arcs admit a C^2 splice: the answer depends on their complete endpoint 2-jets.

Proposition 1.4 (Jet Criterion for a Direct C^2 Splice)**.** *Let*

$$\gamma_1 : (-\varepsilon, 0] \longrightarrow \mathbb{R}^3, \qquad \gamma_2 : [0, \varepsilon) \longrightarrow \mathbb{R}^3$$

be regular C^2 curves, parameterized by arc length near 0. Assume that

$$\gamma_1(0) = \gamma_2(0) = P.$$

Define the piecewise curve

$$\gamma(t) = \begin{cases} \gamma_1(t), & t \le 0, \\ \gamma_2(t), & t \ge 0. \end{cases}$$

Then γ is C^2 at P if and only if

$$T_1(0) = T_2(0)$$

and

$$\kappa_1(0)N_1(0) = \kappa_2(0)N_2(0).$$

When both curvatures are nonzero, this is equivalent to

$$T_1(0) = T_2(0), \qquad \kappa_1(0) = \kappa_2(0), \qquad N_1(0) = N_2(0).$$

Proof. Continuity at the joining point is exactly the condition

$$\gamma_1(0) = \gamma_2(0).$$

Since the curves are parameterized by arc length near the join,

$$\gamma_i'(0) = T_i(0),$$

so the piecewise curve is C^1 precisely when

$$T_1(0) = T_2(0).$$

Likewise,

$$\gamma_i''(0) = \kappa_i(0)N_i(0),$$

and therefore the second derivatives agree precisely when

$$\kappa_1(0)N_1(0) = \kappa_2(0)N_2(0).$$

These are exactly the conditions for the piecewise curve to be C^2 at the joining point. □

Remark 1.5. Torsion is not part of the 2-jet of a regular space curve and therefore does not enter the criterion for a C^2 splice. For a unit-speed curve with nonzero curvature,

$$\gamma''' = -\kappa^2 T + \kappa' N + \kappa\tau B.$$

Thus a direct C^3 splice requires compatibility of the complete third-order Frenet data, including torsion.

Proposition 1.5 ($THM_4 \cong V_4$)**.** *The group of transformations generated by the Chirality Swap (X) and Orientation Swap (Y) operators, which acts on the set of four canonical THM types, is isomorphic to the Klein four-group, V_4.*

Proof. Let $H_{\text{types}} = \{\text{Type 1}, \text{Type 2}, \text{Type 3}, \text{Type 4}\}$, representing the four configurations of unit helices determined by combinations of chirality (Same vs Opposite) and orientation (Same vs Opposite).

Define the following transformations acting on H_{types}:

- Identity I: Trivial transformation. $I(T_i) = T_i$ for all $T_i \in H_{\text{types}}$.
- Chirality Swap X: Swap the chirality relationship (Same $\leftrightarrow$ Opposite), while preserving orientation.
- Orientation Swap Y: Swap the orientation relationship (Same $\leftrightarrow$ Opposite), while preserving chirality.
- Composite $Z = X \circ Y$: Acts by applying both swaps.

The action on the four manifold types proceeds as follows:

Type	(Chirality, Orientation)	X	Y
H_1	(O, O)	H_3	H_2
H_2	(O, S)	H_4	H_1
H_3	(S, O)	H_1	H_4
H_4	(S, S)	H_2	H_3

Composition rules:

$$\begin{aligned} Z = X \circ Y = Y \circ X \\ Z(H_1) = X(Y(H_1)) = X(H_2) = H_4 \\ Z(H_2) = X(Y(H_2)) = X(H_1) = H_3 \\ Z(H_3) = X(Y(H_3)) = X(H_4) = H_2 \\ Z(H_4) = X(Y(H_4)) = X(H_3) = H_1 \end{aligned}$$

All non-identity elements have order 2:

$$X^2 = I, \quad Y^2 = I, \quad Z^2 = (X \circ Y)^2 = X^2 \circ Y^2 = I$$

Pairwise compositions:

$$X \circ Y = Z, \quad Y \circ X = Z \quad \Rightarrow \quad X \circ Y = Y \circ X$$

$$X \circ Z = X \circ (X \circ Y) = (X \circ X) \circ Y = I \circ Y = Y$$

$$Y \circ Z = Y \circ (X \circ Y) = (Y \circ Y) \circ X = I \circ X = X$$

The set of transformations $G = \{I, X, Y, Z\}$ forms a group under composition. All elements have order 1 or 2, and the group is abelian. Thus, $G \cong V_4$. □

Table 2 displays the calculated finite-symmetry-group progressions computed with [GAP]. In addition, the generators of THM_{256} and lower orders are shown in table 3. These symmetries exhibit a progression toward non-abelian behavior as more generators and state permutations are introduced. We note that this group structure may not be unique to the present construction. Similar generator sets arise in various contexts of symmetry and braid groups. For our purposes here, we do not require all known symmetry groups, so the explicit relations and whole structure of THM_x are left open for further investigation as a pure mathematical exercise.

Table 2: Group progression of the THM_4

Group Structure	**Order**	**Defined by...**	**Type**
$V_4 \cong C_2 \times C_2$	4	Chirality and orientation combinations of the 4 canonical THM_4 types	abelian
$D_4 \cong (C_4) \rtimes C_2$	8	Chirality flips + swapping identity of the two helices	non-abelian
C_2^4	16	Independent flips of (c_A, c_B, d_A, d_B) for each unit helix	abelian
$C_2^4 \rtimes C_2$	32	Above + helix identity swapping symmetry	non-abelian
$(C_2^4 \rtimes C_2) \times C_4$	128	Adds 90° global rotation symmetry around z-axis	non-abelian
$(C_2^4 \rtimes C_2) \times C_{4h}$ $\cong (C_2^4 \rtimes C_2) \times (C_4 \times C_2)$	256	Full group including xy-plane reflection symmetry (σ_h)	non-abelian

Table 3: Generators of the THM_{256} symmetry group

Generator	**Action**
c_1	Flip chirality of Helix A
c_2	Flip chirality of Helix B
d_1	Flip orientation of Helix A (up/down)
d_2	Flip orientation of Helix B (up/down)
S	Swap identity of Helix A and Helix B
R_{90}	Global 90° rotation of the twin helix around the z-axis
σ_h	Reflect the entire twin helix across the xy-plane

Definition 1.8 (Regularity Principle for Geometric Computation)**.** A geometric computational state consists of an admissible manifold configuration together with a specified local evolution law (flow, pulse update, or hybrid dynamics). A necessary condition for well-posed computation is that the geometric data and the evolution law possess sufficient regularity to prevent singular breakdown and to make local updates unambiguous.

At minimum, the state manifold must admit the geometric structures used by the model (e.g., tangent directions, phase variables, curvature), and the associated vector field or update operator must be at least locally Lipschitz on the relevant state space. This ensures local existence and uniqueness of the induced ordinary differential evolution whenever the model is expressed in ODE form.

Definition 1.9 (Minimal Regularity by Computational Regime)**.** The required differentiability depends on which geometric invariants actively participate in the computation:

- **Abelian regimes** (symbolic and quasi-fluidic). It is generally sufficient that the geometric state be at least C^1 and that the local evolution law be locally Lipschitz (or C^1) in the active variables. This guarantees well-defined tangent/phase transport and deterministic local evolution. Higher regularity is often convenient but not essential.

- **Non-abelian regimes** (fully fluidic and gauge). When the computation depends explicitly on curvature, torsion, holonomy, or other higher-order geometric data, one typically requires at least C^2 regularity of the underlying geometric configuration, together with compatible regularity of the evolution law. In practice, C^k regularity for $k \geq 2$ (and often smoother) is preferable for stable geometric evolution.

Remark 1.6. Geometric computation must be regular enough for its update rules to be well-defined. In the symbolic and quasi-fluidic bands, this usually means controlling tangent and phase data; in the higher regimes, curvature and higher-order structure enter directly, forcing stronger regularity assumptions. Thus, singularities are not merely geometric defects: they mark a breakdown of the computational model itself.

2 Geometrically Computable Manifolds

We now begin the construction of a Turing Machine ("TM") from a lattice of THM. The feasibility of this approach rests on the fact that THM, unlike most manifolds, provides a rich but controlled symmetry space. It is precisely because most well-known shapes in this metric (e.g., circles, tori, spheres) possess too much symmetry—not too little—that they fail to offer the structural asymmetry needed for computational behavior. The THM construction breaks this impasse.

2.1 GCMs and Geobits

Definition 2.1 (Geometrically Computable Manifold)**.** A **GCM** on a space is:

$$\mathcal{G} \;=\; \big(\mathcal{M},\ \{R_i\}_{i\in I},\ \pi : E \to \mathcal{M},\ \mathcal{I},\ \mathsf{Ev}\big)$$

consisting of:

(a) **Smooth Manifold $\mathcal{M}$.** A smooth manifold (often a finite working region, possibly with boundary). A finite family of compact submanifolds $\{R_i\}_{i\in I}$ (cells) covers the working region and provides locality (finite overlap pattern).

(b) **State bundle $\pi : E \to \mathcal{M}$.** A smooth fiber bundle with finite-dimensional fibers. A *global state* is a section $\sigma \in \Gamma(E)$. Discrete/symbolic, toroidal/phase, and integer-valued components may all live in the fiber.

(c) **Interfaces $\mathcal{I}$.** For each nonempty overlap $R_i \cap R_j$, an interface map:

$$I_{ij} :\ \big(\sigma|_{R_i},\, \sigma|_{R_j},\, \text{local data}\big) \longmapsto \big(\sigma'|_{R_i},\, \sigma'|_{R_j}\big),$$

attached to a portion of $\partial R_i \cap \partial R_j$. Interfaces couple neighboring cells and enforce locality: updates at R_i depend only on σ over R_i and finitely many overlaps $R_i \cap R_j$.

(d) **Evolution Ev.** Either:

- discrete time: an update operator $U : \Gamma(E) \to \Gamma(E)$ that is local with respect to $\{R_i\}$, or
- continuous time: a flow of sections $(\sigma_t)_{t\in\mathbb{R}}$ solving $\dot\sigma_t = F(\sigma_t)$ for a smooth, fiber-wise vector field F over $\mathcal{M}$;

possibly accompanied by a base diffeomorphism $\Phi_t : \mathcal{M} \to \mathcal{M}$. In either case, evolution is nonsingular; it exists for all steps/times on admissible initial states and remains in a fixed finite-energy subset of E.

What a GCM is. A GCM is a manifold that can encode its computable properties. A single THM can qualify as a GCM. A lattice of THM is also a GCM—just with more computing capacity. We call $\mathcal{G}$ a GCM when its evolution is local, interface-driven, and closed under composition: finite products of such systems and gluing along matched interfaces yield new systems of the same kind.

Definition 2.2 (Geometric Bits — Symbolic and Enriched)**.** Fix an ambient manifold region $\mathcal{M} \subset \mathbb{R}^n$ and a twin helix template H (a pair of embedded tubular helices) together with a framing: a preferred axial direction $\hat z$ and a reference scale r_0. Let $\mathrm{Emb}^{\mathrm{fr}}(H, \mathcal{M})$ denote the set of framed embeddings $e : H \hookrightarrow \mathcal{M}$ modulo framed ambient isotopy that preserves the axial framing and the scale r_0 so that radius and orientation remain part of the state.
Let $H_{\mathrm{ext}} \le O(n)$ be a chosen ambient symmetry group (allowing reflections so that chirality changes are representable) and let H_{int} be a finite internal symmetry group acting on the labels of the twin (e.g. the swap of the two helices). Set $G := H_{\mathrm{ext}} \times H_{\mathrm{int}}$, acting on $\mathrm{Emb}^{\mathrm{fr}}(H, \mathcal{M})$ by pre/post–composition.

(a) **Symbolic geobit.** Define the symbolic geobit state set:

$$\mathbf{S}_{\mathrm{sym}} \;:=\; \Big\{\, [e;\chi,\omega] \;\Big|\; e \in \mathrm{Emb}^{\mathrm{fr}}(H,\mathcal{M}),\ \chi,\ \omega \Big\}\Big/ G,$$

where $[e;\chi,\omega]$ denotes a framed embedding decorated by chirality (χ) and axial orientation (ω) relative to $\hat z$, and the quotient is by the G–action, so states are defined up to global symmetry. A *symbolic geobit* is an element $s \in \mathbf{S}_{\mathrm{sym}}$. The finite subgroup generated by "flip chirality" C, "flip orientation" D, and (optionally) "swap" $S \in H_{\mathrm{int}}$ acts on $\mathbf{S}_{\mathrm{sym}}$; in the canonical twin helix unit this induces a $V_4 \cong \mathbb{Z}_2 \times \mathbb{Z}_2$ action on the labels (χ, ω).

(b) **Enriched (quasi–fluidic) geobit.** To allow compact phase and quantized charges, extend the label by a finite–type fiber:

$$P \;\cong\; (S^1)^m \times \mathbb{Z}^p \times F,$$

where the S^1–coordinates encode bounded phases (e.g. axial angle), the $\mathbb{Z}$–coordinates encode twist/winding/linking numbers, and F is a finite set of discrete tags (e.g. mode, parity). Set

$$\mathbf{S}_{\text{enr}} \;:=\; \Big\{\, [e;\chi,\omega,p] \;\Big|\; e \in \mathrm{Emb}^{\text{fr}}(H,\mathcal{M}),\ \chi,\ \omega,\ p \in P \Big\}\Big/G,$$

with G acting equivariantly on the S^1–factors (by rotation) and preserving the $\mathbb{Z}$–charges. An *enriched geobit* is an element of $\mathbf{S}_{\text{enr}}$. The G–action need not be transitive; its orbits in $\mathbf{S}_{\text{enr}}$ are the *geobit types*. The symbolic case is recovered by taking $m = p = 0$ and F trivial.

In both cases, the geobit is a G–set (not necessarily a group): the finite operations generated by C, D (and S when present) act on states, yielding the canonical V_4 action in the symbolic unit. The enrichment by P provides the quasi–fluidic degrees of freedom (compact phases and integer counters) used elsewhere in the text.

For the time being, we work only with S_{sym}. Now, let:

$$(H_1, H_2, H_3, H_4) \mapsto (00, 01, 10, 11)$$

where each H_n is a configuration from the THM_4 symmetry schema defined in table 1, preserving the order of the original type chart. We assign bit values based on symmetry: if the chirality and orientation of the unit helices are the same, assign bit value 1; if they differ, assign 0. This yields a total of 2 bits per THM_4 configuration.

Definition 2.3 (Readout Capacity of a Geobit)**.** Let X be the finite microscopic state space of a GCM cell, and let

$$\rho : X \longrightarrow B$$

be a chosen finite readout map. The observable state alphabet is

$$B_\rho := \mathrm{im}(\rho),$$

and the corresponding readout capacity is

$$\mathrm{Cap}_\rho(X) := \log_2 |B_\rho|.$$

Thus, geobit capacity is not an intrinsic function of the symmetry group alone; it is a property of the pair (X, ρ). If a group K acts on X by observational redundancies and ρ is K-invariant, then ρ factors through the orbit map

$$X \longrightarrow X/K.$$

When ρ distinguishes all K-orbits,

$$\mathrm{Cap}_\rho(X) = \log_2 |X/K|.$$

By contrast, a group whose elements implement admissible updates is not quotiented out merely because it acts on X.

Example 2.1 (Relational Readout of a Twin Helix). Let the microscopic symbolic state of a twin helix cell be

$$X = C_2^4, \qquad \alpha = (C_A, O_A, C_B, O_B),$$

where C_A, C_B encode the chiralities of the two unit helices and O_A, O_B encode their orientations. The microscopic state space has

$$|X| = 16, \qquad \log_2 |X| = 4.$$

The canonical THM_4 classification, however, records only the relative chirality and relative orientation of the two unit helices. Define

$$\rho_{\text{rel}} : C_2^4 \longrightarrow C_2^2$$

by

$$\rho_{\mathrm{rel}}(C_A, O_A, C_B, O_B) = (C_A \oplus C_B,\ O_A \oplus O_B).$$

Its image contains four relational states, corresponding to the four canonical twin helix types. Hence

$$\mathrm{Cap}_{\rho_{\mathrm{rel}}}(X) = \log_2 4 = 2$$

bits. The remaining two microscopic bits are not nonexistent; they are invisible to this relational readout. A finer observation map could retain them, while a coarser map could identify additional states.

The distinction between state symmetries and observational redundancies is essential. Let Γ denote a group of admissible transformations acting on X. Its elements may function as updates or gates, carrying one observable state into another. Such an action contributes to the transition structure of the geobit and should not ordinarily be divided out. A subgroup $K \leq \Gamma$ is quotiented only when its action represents a change of description that leaves every chosen observable unchanged:

$$\rho(k \cdot x) = \rho(x) \qquad \text{for all } k \in K,\ x \in X.$$

Accordingly, the relevant hierarchy is

$$\text{microscopic state space} \longrightarrow \text{redundancy quotient} \longrightarrow \text{chosen readout alphabet},$$

rather than a direct identification of capacity with group order. Commutativity does not by itself determine the number of distinguishable states. That number depends on the state space, the action, its stabilizers, and the chosen readout. The abelian/non-abelian distinction instead becomes important dynamically. In an abelian regime, successive updates commute and can often be represented by independent phase or parity channels. In a non-abelian regime, the order of updates may matter, producing path-dependent transport and holonomy memory. Non-abelian structure therefore changes the algebra of computation, not by generically reducing the cardinality of the state alphabet, but by enriching the structure of admissible transitions and readouts.

Remark 2.1. The embedding dimension for a THM symmetry group is the minimal integer n such that all distinct geometric configurations corresponding to the elements of the group can be realized as non-self-intersecting embedded submanifolds in Euclidean space. It is essential to note that global reflections or entire rotational symmetry groups do not contribute to the intrinsic geobit capacity in $\mathbb{R}^4$. These operations require action on the global geometry and do not alter the intrinsic state of the unit helices. Thus, group orders beyond 16 that arise from external symmetry do not increase state space in a symbolically computable sense. Table 4 compares geobits with their close cousin [NC10].

Table 4: Qubit vs. Geobit

Property	**Quantum qubit**	**Geometric geobit**
Pure state space	$\mathbb{C}P^1 \cong S^2$ (Bloch sphere)	Finite labels $\times$ continuous geometric parameters (e.g. chirality/orientation, phase)
Dynamics	Unitaries (e.g. $SU(2)$ rotations)	Geometric transformations (flips, rotations, deformations)
Measurement/Readout	Born rule (probabilistic)	Geometric probe/partition (deterministic given microstate)
Accessible classical info	≤ 1 bit per use	Depends on chosen encoding and symmetries
Elementary operations	Single-/two-qubit gates; entanglement via tensor product	Local geometric updates; composition by connecting/gluing components
Key feature	Coherence and entanglement central	Robustness tied to analog stability

Definition 2.4 (Geometric Kets)**.** We refer to an individual geobit ket array as "n-geobit," directly paralleling the usage of qubit arrays with ket-style notation. Following the same notation, we employ a modified bra-ket notation.

Let the microstate of a twin helix cell be

$$\alpha = (C_A, O_A, C_B, O_B) \in C_2^4.$$

Where C is chirality and O is orientation. We write the *state ket* $|\alpha\rangle := |C_A\, O_A\, C_B\, O_B\rangle$. Intrinsic flips act by the Klein-four group

$$V_4 = \{e,\ s_A,\ s_B,\ s_A s_B\},$$

where s_A flips O_A and s_B flips O_B, leaving the chirality coordinates unchanged. A 1-bit readout is any fixed function $r : C_2^4 \to C_2$ (e.g. parity $r = o_A \oplus o_B$ or equality $r = [o_A = o_B]$).

Example 2.2 (Update Step with V_4). Take parity readout $r = o_A \oplus o_B$ and the microstate

$$|\alpha\rangle = |1\,1\,0\,1\rangle.$$

Then $b = r(x) = 1 \oplus 1 = 0$. Suppose the next bit should be $b' = 1$. Apply any toggler in V_4, e.g. s_A:

$$s_A \cdot |\alpha\rangle \ = \ |1\,0\,0\,1\rangle, \qquad r(s_A \cdot \alpha) = 0 \oplus 1 = 1 = b'.$$

(If instead $b' = b$, use a parity-preserver e or $s_A s_B$.) Optionally, a coarse projection $\pi : C_2^4 \to C_2^2$ such as

$$\pi(C_A, O_A, C_B, O_B) = (C_A \oplus C_B,\ O_A \oplus O_B)$$

can be displayed as $|\pi(\alpha)\rangle$; for this relational projection both s_A and s_B descend to the same relative-orientation flip on C_2^2, although a general microscopic update need not descend through a chosen readout. The resulting projected ket is $|11\rangle$.

2.2 The Logic of Geometry

Definition 2.5 (GCM Lattice)**.** A *GCM Lattice* or *GL* is a finite or locally finite assembly of GCMs arranged over a graph. Formally, it is the data:

$$GL \ = \ \big(\, \mathcal{L},\ G = (I, E),\ \{\mathcal{G}_i\}_{i \in I},\ \{\iota_i\},\ \mathcal{I}^{\mathrm{lat}},\ \mathsf{Ev},\ \mu \,\big)$$

with:

(a) **Ambient region $\mathcal{L}$.** Smooth manifold (often a bounded working region) into which cells will be embedded.

(b) **Lattice graph $G = (I, E)$.** A finite or locally–finite graph (e.g. a box of $\mathbb{Z}^d$) with uniformly bounded degree; vertices index the cells, edges encode adjacency.

(c) **Cells $\{\mathcal{G}_i\}$.** For each $i \in I$, a GCM $\mathcal{G}_i = (\mathcal{L}_i, \{R_\alpha^i\}, \pi_i : E_i \to \mathcal{L}_i, \mathcal{I}_i, \mathsf{Ev}_i)$ as in definition 2.1.

(d) **Placements $\{\iota_i\}$.** Smooth embeddings $\iota_i : \mathcal{L}_i \hookrightarrow \mathcal{L}$ with pairwise disjoint interiors. The support of cell i is $\mathrm{supp}(i) := \iota_i(\mathcal{L}_i)$.

(e) **Lattice interfaces $\mathcal{I}^{\mathrm{lat}}$.** For each edge $(i, j) \in E$, a family of interface maps attached to portions of $\partial\mathrm{supp}(i) \cap \partial\mathrm{supp}(j)$,

$$I_{ij} : \ \big(\sigma|_{\mathrm{supp}(i)},\, \sigma|_{\mathrm{supp}(j)},\, \text{local flow data}\big) \ \longmapsto \ \big(\sigma'|_{\mathrm{supp}(i)},\, \sigma'|_{\mathrm{supp}(j)}\big),$$

which are local (depend only on a finite stencil around i, j) and equivariant with respect to the chosen cell symmetries.

(f) **Evolution Ev.** Either (a) a discrete, synchronous update $U : \Gamma(E) \to \Gamma(E)$ on the global state bundle $E := \bigsqcup_{i \in I} \iota_i E_i$, or (b) a continuous flow of sections $(\sigma_t)_{t \in \mathbb{R}}$ solving $\dot\sigma_t = F(\sigma_t)$ and compatible with all interfaces. Evolution is local and non-singular on admissible initial states.

(g) **Symbolic observation μ.** A readout map $\mu : \Gamma(E) \to \Sigma^N$ that, at each cell i, selects a coding $q_i : E_i \to \Sigma^{n_i}$ of its geobits; the total capacity is $N = \sum_{i \in I} n_i$.

We say that a GL is *computationally coherent* if the geometric evolution descends through the symbolic readout. In discrete time, this means that there exists a map

$$\Phi_s : \Sigma^N \longrightarrow \Sigma^N$$

such that

$$\mu \circ U = \Phi_s \circ \mu.$$

For continuous evolution, let

$$\varphi_t : \Gamma(E) \longrightarrow \Gamma(E)$$

denote the flow map generated by $\dot{\sigma} = F(\sigma)$. Computational coherence means that, for the admissible times under consideration, there exist maps

$$\Phi_t : \Sigma^N \longrightarrow \Sigma^N$$

such that

$$\mu \circ \varphi_t = \Phi_t \circ \mu.$$

Whenever the induced symbolic evolution is defined for all compatible times, these maps satisfy

$$\Phi_{t+s} = \Phi_t \circ \Phi_s.$$

Since Σ^N is discrete, no differentiable evolution of the symbolic readout is assumed. Threshold crossings may instead produce discrete events, and in applications one may restrict the factorization condition to designated pulse or sampling times.

Remark 2.2. A GCM does not presuppose the stored-program organization of a classical von Neumann machine. Its state, local update law, and admissible interfaces are encoded in the same geometric system; there is no primitive distinction between program memory and data memory, nor any required fetch–decode–execute cycle. The geometry *is* the computation. A single GCM may realize a finite-state process, while a GCM lattice supplies the spatial composition and unbounded family of local interactions required for cellular-automaton-type universality. Depending on the regime, the induced computation may be discrete, continuous, or hybrid, with symbolic behavior recovered through a specified readout.

Proposition 2.1. *A one-dimensional GL whose cells are THM_4 tiles with symbolic nearest–neighbor communication can simulate Rule 110.*

Proof. Each cell contains a twin helix with two binary orientation labels

$$(o_A, o_B) \in C_2 \times C_2,$$

and intrinsic orientation flips act by the Klein four-group

$$V_4 \;\cong\; C_2 \times C_2 \;=\; \{e,\, s_A,\, s_B,\, s_A s_B\},$$

where s_A flips o_A, s_B flips o_B, and $s_A s_B$ flips both.

Readout/encoding. Fix the bit readout as the parity (XOR)

$$r(o_A, o_B) \;:=\; o_A \oplus o_B \;\in\; \{0, 1\}.$$

Any fixed local encoding is acceptable; parity is chosen because s_A or s_B toggles r, while $s_A s_B$ preserves r.

Cellular update. Let $b_i^t := r(o_{A,i}^t, o_{B,i}^t)$ be the bit at site i and time t. Compute the Rule 110 local rule

$$b_i^{t+1} \;=\; \delta(b_{i-1}^t, b_i^t, b_{i+1}^t), \qquad \delta = 110 \to 1,\ 101 \to 1,\ 011 \to 1,\ 010 \to 1,\ 001 \to 1,\ \text{else } 0.$$

Now choose a group element $g_i^t \in V_4$ to enforce the new readout:

$$g_i^t \;=\; \begin{cases} e \text{ or } s_A s_B, & \text{if } b_i^{t+1} = b_i^t \quad \text{(preserve parity);} \\ s_A \text{ or } s_B, & \text{if } b_i^{t+1} \neq b_i^t \quad \text{(toggle parity).} \end{cases}$$

Table 5: Classical vs. Geometric Computation

Feature	**Classical Computation**	**Geometric Computation**
Basic substrate	Strings, tapes, registers, graphs of discrete symbols	Embedded geometric cells/manifolds arranged in a lattice or interface network
Primitive state	Symbol/bit / finite register value	Local geometric state (e.g. chirality, orientation/phase, and optional topological counters)
State space	Finite alphabet or discrete configuration space	Structured local fiber, typically discrete or hybrid: symbolic labels and, in richer regimes, continuous phase data and quantized invariants
Elementary operations	Rewrite rules, gate updates, transition functions	Admissible geometric transformations, local interface updates, and symmetry-respecting deformations
Dynamics	Discrete step semantics (FSM/TM/CA update)	Local evolution on geometric states: symbolic updates, driven pulses, or continuous flows with induced return maps
Composition	Product of machines, circuit wiring, cellular adjacency	Gluing/coupling of cells through interfaces, adjacency graphs, and local geometric compatibility conditions
Input	External symbol stream or initial tape/register contents	Boundary conditions, perturbations, forcing pulses, or initialized geometric configurations
Output	Tape contents, accepting state, register readout	Readout of geometric observables via a chosen projection/partition of the state space
Symmetry	Usually implicit or combinatorial	Explicit: finite groups in the symbolic regime, abelian phase symmetries and richer geometric symmetries beyond
Constraint structure	Logical consistency and finite update rules	Smoothness constraints, and admissibility of local geometric moves
Computational viewpoint	Computation is manipulation of discrete symbols	Computation is evolution of structured geometry, with symbolic data recovered as a readout of the substrate

Apply the intrinsic update

$$(o_{A,i}^{t+1}, o_{B,i}^{t+1}) \;=\; g_i^t \cdot (o_{A,i}^t, o_{B,i}^t).$$

This uses only nearest–neighbor bits to compute b_i^{t+1} and a local V_4 action to realize it; hence, the induced dynamics on the readout $\{b_i^t\}_{i\in\mathbb{Z}}$ is exactly Rule 110.

By Cook's theorem [Coo04], such a lattice simulates a cyclic tag system and therefore a Turing machine. Consequently, the GL with THM_4 cells and the above encoding is Turing complete. □

Orientation as a geometric alphabet. In a GCM, logic may be encoded geometrically rather than symbolically. The most basic mechanism is the orientation channel introduced in definition 1.4. In the symbolic regime, only its binary axial readout is retained. Once the rotational phase about the preferred axis is resolved, the same channel admits a continuous coordinate $\theta \in S^1$, from which finite n-ary readouts may be obtained. This enables a passage from binary logic to finite n–ary logic [Pos21, Zad65]. Fix a helical axis and let $\theta \in S^1 \cong \mathbb{R}/2\pi\mathbb{Z}$ denote the corresponding orientation

phase. For each integer $n \geq 2$, partition the circle into n equal sectors and define the discrete readout

$$b(\theta) \;:=\; \left\lfloor \frac{n\,\theta_{\mathrm{norm}}}{2\pi} \right\rfloor \in \{0, 1, \ldots, n-1\}, \qquad \theta_{\mathrm{norm}} \in [0, 2\pi).$$

This induces an n–valued logic on the orientation channel, which we call ω–*logic*. Equivalently, one may regard the underlying continuous phase as

$$s(\theta) \;:=\; \frac{\theta_{\mathrm{norm}}}{2\pi} \in [0, 1),$$

with the discrete alphabet obtained by thresholding s into n bins. In this way, binary, ternary, quaternary, and higher n–ary logics all arise from the same geometric mechanism: a cyclic phase together with a chosen readout.

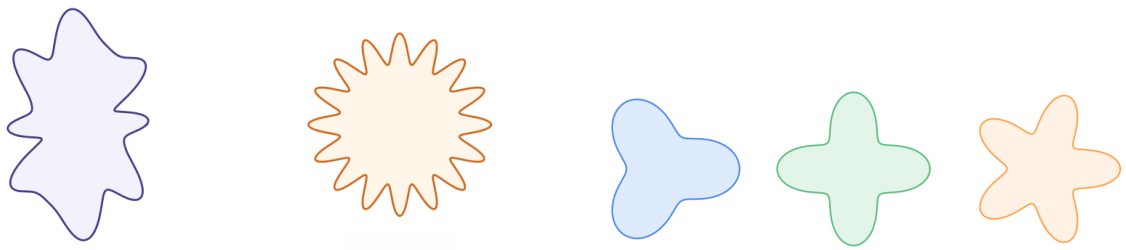
Definition 2.6 (ω–logic)**.** Let $n \geq 2$. The n–*ary orientation logic* of a unit helix is the map

$$\omega_n : S^1 \longrightarrow \{0, 1, \ldots, n-1\}, \qquad \omega_n(\theta) = \left\lfloor \frac{n\,\theta_{\mathrm{norm}}}{2\pi} \right\rfloor.$$

When $n = 2$, this recovers binary logic; when $n > 2$ it gives finite n–ary logic; and if one retains θ itself rather than thresholding, one obtains the continuous $U(1)$ phase corridor. Table 6 organizes a table of models.

Table 6: The chart of n–logics

Geometric Expressiveness	**Join Symmetry**	**Algebraic Closure Group**	**Result**
Extreme	—	$\mathrm{Diff}(M)$ (Maximal)	Computational gauge field
High	1-fold (360°)	C_1	Geometric chaotic analog flow
Medium	2-fold (180°)	C_2	Classical Boolean logic
Low	n-fold ($2\pi/n$), finite	C_n	Finite n–ary logic
Minimal	Full rotational symmetry	$U(1)$ (Lie)	Algebraic fuzzy analog flow



(a) Expressiveness in binary vs. hexadecimal

(b) n–logical gluing maps for 3-, 4-, and 5–ary logic

Figure 2: Cross-sectional shape families and the n–logic tradeoff.

A spectrum of physical logic. From the computational point of view, low-order cyclic logics such as C_2 or C_4 occupy a particularly stable region: they retain enough discrete algebraic structure to support verification and symbolic composition, while still allowing genuinely geometric realizations. At one extreme, the continuous $U(1)$ limit becomes an abelian phase medium; at the other, the loss of usable discrete closure drives the system toward geometric or chaotic analog behavior. In this sense, Boolean and low-order finite logic form a kind of *logical habitable zone* for physically stable symbolic computation.

Hence, even in an idealized, noiseless world, n-ary logical computers are "sandwiched" between two analog extremes. For n-ary logic, the cross-section of the THM can be any smooth closed manifold with at least n distinguished points on its boundary that realize the requisite "logical angularities." The primary family consists of sinusoidal perturbations ("clovers") that can be globally smooth and are easily visualized in polar coordinates—see fig. 2b. However, one can readily imagine richer forms that realize the required angular structure. Figure 2a illustrates such alternatives and compares expressiveness across different logical regimes.

A geometric tradeoff. The passage from C_2 to larger cyclic groups and finally to $U(1)$ exhibits a *systematic tradeoff*. Increasing rotational symmetry enlarges the continuity of the orientation channel, but at the same time restricts the available shape space and weakens finite algebraic closure. Conversely, low-order discrete symmetry yields fewer phase values but stronger symbolic verifiability. This motivates the following lemma.

Lemma 2.2 (Geometric Logic Conservation Lemma)**.** *Fix a THM G together with a chosen readout. Let $\mathcal{C}(G)$ denote the complexity of the induced algebra of local symbolic operations (for example, the size of the effective gate clone or finite symmetry algebra visible under the readout), and let $\mathcal{E}(G)$ denote the corresponding geometric expressiveness (for example, the number of orbit-distinguishable cross-sectional shapes or phase patterns available at fixed regularity). Then one expects a bounded tradeoff of the schematic form*

$$\mathcal{C}(G) + \mathcal{E}(G) \lesssim \Lambda(G),$$

where $\Lambda(G)$ depends on the ambient geometric constraints and symmetry class of the model.

Remark 2.3. The essential point is that the symmetry of the system's configuration space directly induces an invariant quantity in the system's dynamics. Every symmetry break in topology introduces a logical ambiguity, and vice versa. Although we are only in the initial regime of computation, we will eventually encounter higher-order regimes that devolve into pure fluidic computability, leaving discrete logic altogether and entering increasingly abstract and chaotic forms of analog computation.

Definition 2.7 (Geometric Expressiveness at Finite Cutoff)**.** Let $\mathcal{F}_K$ denote the space of real trigonometric polynomials of degree at most K,

$$r(\theta) = a_0 + \sum_{k=1}^{K} \big(a_k \cos(k\theta) + b_k \sin(k\theta)\big),$$

interpreted as smooth 2π–periodic radial functions. Let $\mathcal{F}_{n,K} \subseteq \mathcal{F}_K$ be the subspace of functions invariant under rotation by $2\pi/n$:

$$r(\theta + 2\pi/n) = r(\theta) \qquad \forall\, \theta.$$

The *relative geometric expressiveness* at symmetry level n and cutoff K is

$$E_K(n) \;:=\; \frac{\dim(\mathcal{F}_{n,K})}{\dim(\mathcal{F}_K)}.$$

Proposition 2.3 (Symmetry Collapses Cross-sectional Expressiveness)**.** *For a fixed cutoff K,*

$$\dim(\mathcal{F}_{n,K}) \;=\; 2\Big\lfloor \frac{K}{n} \Big\rfloor + 1, \qquad E_K(n) = \frac{2\lfloor K/n \rfloor + 1}{2K+1}.$$

In particular, for fixed K, $E_K(n)$ decreases monotonically with n, and

$$E_K(n) \to \frac{1}{2K+1} \qquad \text{as } n \to \infty.$$

At the level of smooth functions (without cutoff), full rotational symmetry forces the radial function to be constant; hence the cross-section is a circle.

Proof. If

$$r(\theta) = a_0 + \sum_{k=1}^{K} \big(a_k \cos(k\theta) + b_k \sin(k\theta)\big)$$

satisfies $r(\theta + 2\pi/n) = r(\theta)$ for all θ, then only those Fourier modes with frequency divisible by n may remain. Hence the allowed modes are $k = 0, n, 2n, \ldots, \lfloor K/n \rfloor n$, giving

$$\dim(\mathcal{F}_{n,K}) = 1 + 2\Big\lfloor \frac{K}{n} \Big\rfloor.$$

Since $\dim(\mathcal{F}_K) = 2K + 1$, the formula for $E_K(n)$ follows immediately. In the full smooth category, invariance under all rotations implies that only the constant Fourier mode survives, so the radial profile is constant, and the cross-section is a circle. □

Progression to algebraic analog flow. This is the essential phenomenon as the size of the rotational symmetry group grows. Even as the symmetry group becomes continuous, the system's logic remains identical to its geometry. This is the core idea behind geometric computation, and why such systems are not limited to discrete operations.

Definition 2.8 (χ–logic)**.** Let $\mathcal{C}$ be a class of framed geometric configurations equipped with a continuous *chiral observable*

$$\kappa : \mathcal{C} \longrightarrow \mathbb{R},$$

where κ may be realized, for example, by signed torsion, signed twist density, or another orientation-sensitive local invariant. The associated *chirality logic* is the map

$$\chi : \mathcal{C} \longrightarrow \{-1, 0, +1\}, \qquad \chi(x) := \operatorname{sgn}(\kappa(x)).$$

Thus:

- $\chi(x) = +1$ denotes a right-handed configuration,
- $\chi(x) = -1$ denotes a left-handed configuration,
- $\chi(x) = 0$ denotes the non-chiral or degenerate locus where the chiral invariant vanishes.

When the value 0 is admitted as a stable readable state, χ–logic is ternary. When the degenerate locus is excluded from the admissible state space, χ–logic reduces to a binary left/right channel.

The role of chirality. Unlike the orientation phase, chirality is not naturally a cyclic n–ary coordinate. Geometrically, a change of handedness requires the sign change of an orientation-sensitive invariant, such as signed torsion or local twist density. If

$$\kappa : \mathcal{C} \longrightarrow \mathbb{R}$$

denotes such an invariant on the configuration space $\mathcal{C}$, then

$$\chi(x) := \operatorname{sgn} \kappa(x) \in \{-1, 0, +1\}$$

defines a natural stratification

$$\mathcal{C} = \mathcal{C}_- \sqcup \mathcal{C}_0 \sqcup \mathcal{C}_+,$$

where $\mathcal{C}_\pm$ are the left- and right-handed sectors and $\mathcal{C}_0$ is the degenerate locus on which the chiral invariant vanishes. Any continuous interpolation between opposite handed sectors must intersect $\mathcal{C}_0$.

For the canonical twin helix register, only the nondegenerate sectors are taken as stable states,

$$\chi \in \{-1, +1\},$$

while $\chi = 0$ represents a transition or boundary stratum rather than an additional persistent symbol. Thus χ–logic should be understood primarily as a signed geometric grading, rather than as an n–ary phase alphabet analogous to ω–logic. Together with the binary orientation distinction, it supplies the two independent $\mathbb{Z}_2$ labels underlying the canonical THM_4 structure. At the same time, in continuous regimes it records whether admissible deformations and gluings preserve, reverse, or pass through a degeneration of handedness.

2.3 The EVT Hypothesis and the Structure of Physical Computation

We now formulate a proposed constraint on the design of physical computational systems. The central question is not merely which functions a machine can evaluate, but how the geometry of a physical substrate determines the states, transformations, histories, and readouts available to it.

In GCT, computation is treated as a process carried by a geometric substrate. Configurations serve as states, admissible deformations and transports serve as transformations, interfaces supply input and output conditions, and composition is realized through gluing. This places the present discussion within the broader process-theoretic correspondence among physics, topology, logic, and computation described by Baez and Stay [BS10].

Gauge structure enters at this level rather than being appended after the computational model has already been specified. A connection determines parallel transport along paths, and its curvature controls the infinitesimal generation of holonomy [AS53, SW13]. Accordingly, groups such as

$$C_n, \qquad U(1), \qquad SU(2), \qquad SU(3)$$

are not treated here as unexplained labels placed upon an otherwise independent substrate. They describe increasingly rich closure and transport structures generated by the admissible geometry.

Strictly speaking, a gauge group is not by itself the complete physical state space. The realized states also depend on the representation, bundle, boundary conditions, admissible controls, and quotient by gauge. It is the richness of this complete process structure, rather than the name or dimension of a group alone, that determines the expressive power of the physical computer.

Definition 2.9 (Physical Computational Substrate)**.** A *physical computational substrate* is a system

$$\mathfrak{S} = \big(X, \mathsf{P}, \mathsf{I}, \mathsf{R}\big),$$

where:

(a) X is a space of admissible physical configurations;

(b) P is a class of admissible transformations, trajectories, or boundary-to-boundary histories between configurations;

(c) I is a class of finite preparation, control, and boundary specifications;

(d) R is a family of observable readouts defined on the resulting configurations or histories.

The *reachable behavior* of $\mathfrak{S}$ consists of the states, histories, and observable input–output relations generated from admissible data in I by processes in P.

This definition is intentionally broad. In a finite symbolic machine, X may be a discrete state set and P a transition system. In an analog or gauge-theoretic machine, X may be a continuous configuration or moduli space, while P may contain flows, parallel transports, or field histories. The physical expressive power of the substrate depends on the total reachable behavior generated by these structures.

Expressive power. We adapt Felleisen's comparative distinction between eliminable and non-eliminable extensions [Fel91]. His framework was developed for programming languages, but the underlying idea applies more generally: an apparent increase in expressive power is genuine only when a uniform translation cannot remove it preserving the relevant semantics.

Definition 2.10 (Physical Expressive Power)**.** Let $\mathfrak{S}_0$ and $\mathfrak{S}_1$ be physical computational substrates with specified classes of admissible encodings and translations.

We say that

$$\mathfrak{S}_1 \succeq_{\mathrm{E}} \mathfrak{S}_0$$

if every reachable process and observable input–output relation of $\mathfrak{S}_0$ can be represented in $\mathfrak{S}_1$ by a uniform translation preserving the relevant interfaces, composition laws, and readouts.

The extension from $\mathfrak{S}_0$ to $\mathfrak{S}_1$ is *macro-expressive* when $\mathfrak{S}_1$ additionally realizes reachable transformations, histories, compositions, or observable distinctions that cannot be eliminated by any translation in the chosen class.

Physical expressive power is therefore relational. It is not identified with the cardinality of X, the dimension of a Lie group, the number of locally distinguishable symbols, or computational universality alone. These may contribute to expressive power, but only insofar as they enlarge the reachable process semantics.

An extension is merely *micro-expressive* when it enriches local notation, coordinates, primitive labels, or state encodings while remaining uniformly reducible to the original process structure. A larger local alphabet, for example, need not be macro-expressive if its states and transitions admit a uniform semantics-preserving encoding in the original substrate.

By contrast, new continuous degrees of freedom, new composition orders, new path-dependent transports, new boundary couplings, or new topological sectors may be macro-expressive when they create global behaviors that cannot be represented within the previous regime without loss of structure.

We denote the resulting comparative position of a substrate by its *expressiveness profile*

$$\mathcal{E}(\mathfrak{S}).$$

No universal scalar measure of expressive power is assumed. Numerical coordinates may be introduced only after fixing a particular comparison class and family of admissible translations.

Global algorithmic verifiability. Expressiveness should be distinguished from both observability and local rule checking. A symbolic state may be directly readable, and every individual update may be mechanically checked against a finite transition table, while nontrivial properties of the completed computation remain undecidable.

Thus

$$\text{local state legibility} \not\Longrightarrow \text{global algorithmic verifiability}.$$

The EVT Hypothesis concerns the second notion.

Definition 2.11 (Global Algorithmic Verifiability)**.** Let $\mathfrak{S}$ be a physical computational substrate, and let $\mathcal{Q}$ be a specified family of nontrivial properties of its reachable states, histories, outputs, or invariants.

A property

$$Q \in \mathcal{Q}$$

is *globally algorithmically verifiable* on a behavior class $\mathcal{B}$ if there exists a uniform terminating procedure which, from finite descriptions of

(a) the substrate and its relevant structural parameters;

(b) the preparation, boundary, and control data;

(c) the property Q;

correctly certifies whether Q holds for every admissible process in $\mathcal{B}$, without merely executing the complete physical process and reading its final result.

The *verifiability profile* of $\mathfrak{S}$ relative to $\mathcal{Q}$ and $\mathcal{B}$ is

$$\mathcal{V}_{\mathcal{Q},\mathcal{B}}(\mathfrak{S}) = \{Q \in \mathcal{Q} \mid Q \text{ is globally algorithmically verifiable on } \mathcal{B}\}.$$

The definition is property-relative. A system may admit complete certificates for conserved charges, topological sectors, or bounded reachability questions while admitting no uniform procedure for more general long-range behavior.

The qualifier *global* indicates that the property may depend on the completed history or on relations among widely separated parts of the computation. The qualifier *algorithmic* requires one uniform finite procedure rather than a different proof devised for each case. The qualifier *verifiable* refers here to pre-execution certification from the finite specification of the machine and its admissible data.

Post-execution inspection is a different notion. A machine may produce a result that is easy to read or check after the computation has finished even when that result could not have been certified in advance. Likewise, the local legality of every transition does not imply the global decidability of the resulting behavior.

Structural restrictions can enlarge the verifiability profile. Examples include finite closure, complete invariants, conserved quantities, integrability, totality, bounded recursion, type discipline, topological protection, restricted holonomy, and resource-sensitive control. Such structures compress classes of global histories into finite certificates.

Tractability. Verifiability asks whether a uniform certificate exists. Tractability asks what resources are required to construct, execute, control, simulate, or verify the corresponding process.

Definition 2.12 (Tractability)**.** Let $\mathfrak{S}$ be a physical computational substrate equipped with a resource model $\mathfrak{R}$.

The *tractability profile*

$$\mathcal{T}_{\mathfrak{R}}(\mathfrak{S})$$

records those admissible constructions, computations, predictions, and verification problems that can be carried out within the bounds designated as feasible by $\mathfrak{R}$.

Depending on the substrate, the resource model may include time, memory, energy, control precision, sample complexity, error tolerance, and preparation complexity. Polynomial time and space provide one important specialization in digital computation, but physical tractability is not exhausted by standard asymptotic complexity. A formally short analog computation may require exponentially increasing precision; an algebraically simple control may require physically inaccessible energy or stability; a verifiable process may require an impractically large certificate.

Human comprehensibility is also treated as an additional cognitive tractability criterion, particularly in programming-language design and formal verification. It should not, however, be identified with algorithmic complexity. A process may be efficiently executable but difficult to represent, explain, or audit, and the converse may also occur.

We consequently treat

$$\mathcal{E}(\mathfrak{S}), \qquad \mathcal{V}(\mathfrak{S}), \qquad \mathcal{T}(\mathfrak{S})$$

as comparative profiles rather than universal scalar quantities. Within a fixed family of substrates, questions, and resource models, these profiles may be normalized or represented by monotones. The EVT Hypothesis concerns the structural relation among them.

With these notions fixed, we can now state the hypothesis.

Conjecture 2.4 (**Expressiveness/Verifiability/Tractability ("EVT") Hypothesis**)**.** *The conjecture formally comprises two parts:*

(A) ***Loss of Global Verifiability in Macro-expressive Systems.*** *As the expressive power of a system of physical computation increases, the range of its globally algorithmically verifiable behaviors generally decreases unless additional structural restrictions are imposed.*

(B) ***Expressiveness/Verifiability/Tractability Trilemma.*** *Within such a system, every deterministic computational model is fundamentally constrained by a three-way tradeoff among* expressiveness *(geometric or semantic generality),* verifiability *(algebraic checkability or formal runtime assurance), and* tractability *(algorithmic or computational efficiency). These attributes shall satisfy the following trilemma:*

No system can simultaneously maximize all three properties. For any given model, at most two of the three can be optimized beyond a critical threshold, while the third must necessarily be sacrificed.

This is the central motivating hypothesis of this work. We take the phenomenon isolated in theorem 2.2 and generalize it from our geometric setting to physical deterministic computation more broadly.

The first half of the EVT Hypothesis should be read as a selection principle on physical substrate classes. It asks which structural features allow locally verifiable behavior to compose into globally verifiable behavior, and which features obstruct that passage. Later, in definition 4.5, we establish an obstruction to transport-compatible abelianization. Here we use the term in the comparative sense suggested by Felleisen [Fel91]: a substrate is macro-expressive when it supports genuinely new global processes or modes of composition that cannot be eliminated by a uniform semantics-preserving translation.

This distinction is useful because the present framework is not restricted to digital syntax, natural-number encodings, or Turing-style machines. Beginning directly with recursion-theoretic machinery already assumes a symbolic regime rich enough to support self-interpretation. The prior physical question is how a discrete, continuous, or hybrid substrate acquires new global computational behavior in the first place.

Microstates and macrostates describe the configurations of a system. A microstate is a particular geometric, algebraic, or dynamical configuration, whereas a macrostate is an equivalence class of such configurations under the relevant symmetry or observational relation. Micro-expression and macro-expression instead describe the processes available to the system. Micro-expression enlarges the local alphabet, state labels, or primitive rules without changing the global process semantics. Macro-expression introduces new ways of composing, transporting, or reading information that cannot be reduced to the previous regime. In brief,

$$\text{microstates/macrostates} \quad \text{describe what exists,}$$

whereas

$$\text{micro-/macro-expression} \quad \text{describe what can be done.}$$

The EVT therefore concerns not the mere proliferation of states, but the enlargement of the reachable process structure. A continuous state space may remain compositionally tame, while a substrate with a small local alphabet may acquire substantial global power through memory, feedback, path dependence, or unrestricted composition. In GCT, a principal witness of this transition is the passage from commuting transport to non-abelian, order-sensitive transport. Local operations can no longer always be certified independently and then assembled: the resulting observable may depend on the path, order, and history of the completed composition.

To state the thesis informally:

> *As a physical computational substrate acquires new global compositional structure—including non-abelian transport, path-dependent joins, or context-sensitive readouts—local verification no longer automatically extends to global verification. Recovering global guarantees then requires additional algebraic, geometric, topological, type-theoretic, or resource-sensitive constraints.*

Expressive enlargement as growth of the behavior space. A useful comparison comes from programming-language design. Languages such as Lisp, C++, and Haskell occupy very different regions of the design space: Lisp exposes unusually flexible metaprogramming and self-modification mechanisms; C++ combines a large collection of partially constrained paradigms and abstractions; Haskell places much of its expressive power behind a stronger static type and effect discipline. These examples should not be read as a strict linear ranking of language power. Rather, they illustrate that adding or restricting forms of composition changes the set of behaviors that a programmer can directly construct and the kinds of guarantees that can be obtained about those behaviors. Expressiveness and verifiability therefore depend not merely on how many local states a language possesses, but on the structure of the process space generated from them.

The same distinction appears physically in the sequence of computational regimes developed in GCT. A finite closure group C_n supports a discrete family of transformations; passage to $U(1)$ introduces a continuous phase and continuous transport; passage to $SU(2)$ introduces non-commuting, order-sensitive composition; and the larger non-abelian structure associated with $SU(3)$ further enlarges the family of coupled transports and globally distinguishable histories. The detailed geometric construction of this hierarchy is given later in section 5.2. What matters here is the common principle: each transition enlarges the *reachable behavior space* of the substrate by introducing qualitatively new modes of composition.

Such enlargements increase the burden carried by any system of global certificates, but they do not by themselves imply indeterminacy or undecidability. A highly expressive language may remain well controlled because its admissible programs are disciplined by a type system, effects, totality, or other invariants; likewise, a non-abelian physical system may possess integrable, protected, or otherwise verifiable sectors. The EVT concerns what happens when successive gains in expressive structure outpace the restrictions and invariants that make the resulting behavior globally certifiable. In this sense, increasing expressiveness through several structural jumps is a necessary enabling condition for the richest forms of indeterminate behavior, but it is not sufficient by itself.

Example 2.3 (Expressive Enlargement in Languages). The definitions above are intended to compare *reachable behavior spaces*, rather than merely the cardinality of local state sets. A familiar illustration comes from programming-language design.

Consider, for example, languages such as Lisp, C++, and Haskell. They should not be placed in a strict total ordering of expressive power: all support extremely rich computation, and the answer depends on the translations, effects, and properties being compared. Nevertheless, they expose different portions of their process spaces directly. Lisp makes code–data interchange, macros, and metalinguistic extension unusually accessible; C++ exposes mutable state, aliasing, templates, multiple abstraction mechanisms, and low-level control; Haskell supports higher-order and highly abstract computation while imposing a stronger type and effect discipline on many classes of programs.

Relative to a chosen comparison class, these design choices alter all three EVT profiles. Features such as reflection, unrestricted mutation, or runtime code generation may enlarge

$$\mathcal{E}(\mathfrak{S})$$

by making additional transformations directly constructible, while a type system, ownership discipline, total fragment, or restricted effect system may enlarge

$$\mathcal{V}_{\mathcal{Q},\mathcal{B}}(\mathfrak{S})$$

for a selected family of properties by excluding behaviors that would otherwise have to be analyzed dynamically. Either choice may improve or worsen

$$\mathcal{T}_{\mathfrak{R}}(\mathfrak{S})$$

depending on the relevant compilation, execution, verification, and human-control costs. The point is not that one of these languages is "more powerful" in every sense, but that changing the admissible process structure redistributes expressive freedom and available guarantees.

For a fixed property family $\mathcal{Q}$, a certificate system that separates all relevant behaviors in one regime need not remain complete after an expressive extension:

$$\mathfrak{S}_1 \succeq_{\mathrm{E}} \mathfrak{S}_0 \qquad \text{does not imply} \qquad \mathcal{V}_{\mathcal{Q},\mathcal{B}}(\mathfrak{S}_1) \supseteq \mathcal{V}_{\mathcal{Q},\mathcal{B}}(\mathfrak{S}_0).$$

Additional expressive power may preserve the old guarantees, weaken them, or require new structural machinery to recover them.

Why alphabet size is not the issue. Recall the spectrum of n-logics generated from join symmetry in table 6. The number of locally distinguishable symbols does not by itself determine the expressive power or verifiability of a computational substrate. A finite alphabet may make local states easy to observe and individual transitions easy to check, while the long-range behavior generated from those transitions remains globally difficult or undecidable. Thus,

$$\text{local symbolic legibility} \implies \text{global algorithmic verifiability}.$$

The relevant distinction is between a finite local alphabet and a finite global process space. A closed finite-state system may admit exhaustive analysis because its complete transition graph is finite. By contrast, a lattice, tape, or network built from the same finite alphabet may support unbounded memory, feedback, and composition. Once such a substrate becomes capable of universal symbolic computation, Rice-style barriers apply to its nontrivial extensional properties regardless of whether its local alphabet is binary, ternary, or n-ary [Ric53]. The obstruction is therefore not the number of local symbols, but the macro-expressive process structure generated from them.

Increasing the alphabet size is ordinarily only a micro-expressive change when the additional symbols and transitions admit a uniform semantics-preserving encoding in the original substrate. Greater verifiability is obtained not merely by adding local states, but by restricting the admissible global behavior: bounding memory or recursion, stratifying effects, imposing linear or affine use disciplines, preserving complete invariants, or requiring totality and strong normalization. Systems based on the Calculus of Constructions [CH88], for example, recover strong semantic guarantees by constraining term formation and recursion rather than by modifying the underlying alphabet.

The symbolic case therefore illustrates the general EVT distinction. Local states and update rules may remain completely transparent even as the reachable process space becomes too expressive for uniform global certification. Alphabet arity affects how information is represented; the decisive question is what histories and compositions the substrate can generate.

Symbolic universality as a limiting case. Self-reference and halting-type undecidability are not the general mechanism we observe in microscopic physical computation. They are the characteristic form taken by the loss of global verification once a substrate supports universal symbolic computation.

In classical recursion theory, evaluator-like mechanisms, self-application, and diagonalization provide the relevant obstructions. Kleene's Recursion Theorem and the *s-m-n* theorem make the structure of effective self-reference explicit [Kle52], while Turing's halting argument supplies the canonical undecidable decision problem.

The EVT addresses a prior and more general structural question: whether locally available certificates continue to determine global behavior as the reachable process structure of a substrate is enlarged. In GCT, the certification burden may increase through path-dependent transport, order-sensitive composition, nontrivial moduli, or global readouts even before a literal self-interpreter has been identified. These structures motivate the EVT, but they are not by themselves claimed to establish a Rice- or halting-type undecidability theorem.

The hypotheses of the symbolic results should therefore be kept explicit. Rice's theorem concerns nontrivial extensional properties of partial computable functions [Ric53]; Kleene-style fixed-point results require an effective programming structure rich enough to support the relevant translations and self-application. When universality, partiality, or unrestricted composition is withdrawn through totality, strong normalization, staging, bounded recursion, or stratification, substantial classes of semantic questions may again become decidable. This is not an exception to the EVT, but an instance of its central qualification: global verifiability is recovered by restricting the admissible process structure.

Why gauge theory appears. Gauge theory enters GCT because the state of a distributed geometric substrate need not admit a single preferred global description. Local states are represented relative to local frames or trivializations, and descriptions on overlapping regions must be related by transition functions. A connection specifies how such local data are compared along paths, curvature measures the obstruction to path-independent comparison, and holonomy records the resulting global transport.

This structure is already present in abelian gauge theory. Non-abelianity introduces an additional expressive jump: transports need no longer commute, and the result of a process may depend on the order and path by which it was assembled. The gauge-theoretic hierarchy therefore distinguishes two effects: local description and transport from order-sensitive global composition. The first motivates gauge structure itself; the second substantially enlarges the reachable process semantics.

This distinction is important for verifiability. In finite or abelian regimes, broad classes of histories may often be summarized by finite transition tables, additive phases, winding numbers, or other compact invariants. In a non-abelian regime, the observer may instead need to retain ordered holonomies, relations among several paths, and information about the completed history. Gauge-invariant readouts then preserve only selected features of this richer framed transport data. The difficulty is not merely that the state space is larger, but that a small collection of local or invariant certificates need no longer separate all globally distinct processes.

A bridge from physical expressiveness to operational indeterminacy. The EVT Hypothesis does not identify non-abelianity with randomness, nor does it presently derive quantum measurement probabilities. It supplies a more limited bridge. As the reachable process structure of a deterministic substrate becomes more expressive, outcome-relevant distinctions may cease to be represented in the finite preparation, control, and readout data available to an external observer.

Schematically, let

$$q : \Lambda \longrightarrow \Omega$$

send a complete physical configuration to its accessible operational description, and let

$$B : \Lambda \longrightarrow \mathcal{B}$$

assign the resulting classical output. The output is predictable from the operational description when there exists a map

$$\overline{B} : \Omega \longrightarrow \mathcal{B}$$

such that

$$B = \overline{B} \circ q.$$

When no such factorization exists, the complete substrate may still evolve deterministically, but the accessible description does not determine the individual output. Distinct complete histories can appear identical to the observer while producing different readouts.

The proposed connection to quantum indeterminacy lies at this level. Gauge-generated physical expressiveness can produce global, history-dependent distinctions that are not retained by a finite, context-dependent classical interface. A bare observer, supplied only with external preparation data and a restricted family of invariant readouts, may therefore be unable to pre-certify the output without reconstructing substantially more of the internal geometric process.

Later we will outline how we precisely perform such reconstruction (5.4). The claim is not that this reconstruction has already yielded a complete theory of quantum probabilities. It is that quantum-like operational indeterminacy becomes intelligible even within a deterministic ontology once the expressive power of the underlying process exceeds the separating power of the observer's accessible description.

The first half of the EVT should therefore be read as a constraint on how observer-side guarantees scale with physical expressive power. Increasing the range of admissible compositions does not automatically increase the range of globally certifiable behaviors. Verifiability can be recovered only by adding sufficient structure: complete invariants, restricted holonomy, integrability, topological protection, bounded controls, type discipline, or a more detailed reconstruction of the substrate itself.

The second half of the EVT Hypothesis sheds light on the odd "dual nature" observed in functional programming languages. On the one hand, languages with strong static typing offer stronger compile-time reasoning principles (e.g. type safety and, in suitable fragments, parametricity), at the cost of meta-linguistic restrictions during construction (Haskell). On the other hand, dynamically typed languages maximize meta-linguistic expressiveness at construction time (macros, reflection), while giving up static guarantees at runtime and shifting assurance to testing and contracts (Scheme).

Bridging attempts proceed along multiple axes: *gradual typing* [ST06] (Typed Racket) inserts types with higher-order contracts at typed/untyped boundaries, and *staging* [TS97] (MetaOCaml) separates compile-time code generation from runtime execution. From the proof-theoretic direction (Coquand), total dependent type theories recover strong guarantees by forbidding general recursion. From the pragmatic language research side, (Felleisen) shows how large untyped codebases can be migrated toward sound types via occurrence typing and higher-order contracts—at the cost of explicit blame and potential runtime overhead—an archetypal EVT tradeoff between meta-linguistic freedom and verifiability [THF06]. Here, the goal is not to re-formalize the trilemma, but to show how the second half of the EVT manifests concretely in real language design. When expressive features are pushed far enough, the same structural tension repeatedly reappears in practice through a small number of recognizable engineering symptoms:

The limits of expressive semantics. These bridges are inherently delicate. When many powerful features coexist, three recurring pressure points tend to appear:

(a) **Static complexity.** Extremely rich type features (GADTs, type families, dependent types) that can render inference undecidable, forcing annotations; combining dependency with effects or staging threatens phase separation unless carefully constrained.

(b) **Compile-time liveness.** Macros or multi-stage generation can diverge at compile time; expressive compile-time evaluators reintroduce fixed-point phenomena.

(c) **Runtime boundaries.** Gradual typing preserves type safety via contracts, but introduces blame and potentially unbounded overhead; interoperation across typed/untyped modules trades static guarantees for dynamic checks.

These are not accidents of particular implementations; they are manifestations of the EVT Trilemma: increased *macro-expressiveness* (reflection, self-interpretation, unconstrained composition) strains *global verifiability*, unless restrictions restore structure. Hence, an explicitly stated *upper bound in the space of physical computational behaviors* explains these difficulties.

The Von Neumann curtain. The reason this hypothesis has long gone unformulated is that its essential tradeoff has long been hidden in plain sight—embedded in the very architecture of classical computation we all use in our day-to-day lives! The Von Neumann model deliberately collapses program and data into a common memory space: the same substrate can store instructions, manipulate data, generate new code, and in sufficiently unrestricted settings modify its own future behavior. This gives general-purpose computers their *extraordinary* expressive flexibility via an endless array of syntax-based programming languages.

The price is that local transparency does not scale automatically to global guarantees. Individual instructions may be simple and directly inspectable, while the behavior of the complete machine becomes increasingly difficult to certify once mutable state, indirect control flow, reflection, concurrency, and unbounded composition are allowed. Global reasoning therefore survives only by reintroducing structure: types, protected memory, module boundaries, ownership rules, restricted effects, contracts, or other disciplines that constrain how the machine may use its expressive freedom.

At the opposite extreme, a substrate whose admissible states, operations, and transitions are fixed by a sufficiently rigid algebra may become much easier to predict and verify, precisely because many possible behaviors have been ruled out in advance. What is gained in global checkability is purchased by narrowing the reachable behavior space. The "Von Neumann curtain" is therefore the fact that we have spent most of the history of computation looking at this tradeoff from inside one exceptionally expressive architecture, where its costs are so familiar that they appear to be properties of computation itself rather than consequences of a particular way of organizing a physical computer.

The Turing tarpit. The tradeoff does not assert a single conservation equality. As we will see, there exist regimes in both classical (language-based) and physical (geometric) computation with both low expressiveness *and* low verifiability—the infamous "Turing tarpit". A space where everything is theoretically possible but practically inexpressible. The second half of the EVT is best read as a *no-free-lunch inequality* with phases: beyond a threshold of expressiveness and verifiability, tractability for humans and machines becomes increasingly difficult. Before this extreme limit is reached, there lie transitional corridors in which small feature additions *can* cause qualitative shifts in what can be expressed, verified, and/or computed.

Because these tradeoffs depend on ambient structure, the EVT treats *local* symmetries of a model or architecture rather than postulating a single global invariant across all substrates. In a Von Neumann setting, some of the most important local regularities are *cognitive* and *conventional*: programming idioms, abstractions, and composition patterns induce de facto invariants that temporarily "abelianize" parts of the system, while reflective or unrestricted features reintroduce non-commuting structure. **Pushing too far past the barriers above yields systems that remain formally expressive and verifiable in principle but become progressively less usable in human social, cognitive, and physical engineering practice.**[2]

Removing barriers to viewing computation. Regarding tractability, the present paper intentionally abstracts away many ordinary engineering bottlenecks. In an idealized geometric regime, one may treat the substrate as reconfigurable enough that the sharp distinction between hardware and program becomes less natural than it is in fixed Von Neumann architectures. This does *not* remove physical resource limits; rather, it allows the expressiveness/verifiability relation to be studied more directly, without immediately collapsing into familiar questions about instruction sets, compilers, and implementation overhead. For this reason, although the full trilemma must be stated as such, we do not pursue tractability in equal depth here. In the present paper, it functions chiefly as a reminder that human-built machines impose additional constraints beyond those intrinsic to the underlying geometric substrate.

So in our GCM-based setting, the expressiveness/verifiability relationship can be studied more transparently because there is *no fixed separation between logic and memory* of the usual Von Neumann sort. A GL is an idealized *non*-Von Neumann substrate defined directly in geometric and algebraic terms. By fusing logic and language into a single analog-geometric object, one can *see* how the operational semantics deforms the computational substrate, and model how the algebraic closure group constrains the geometry with every increasing bit!

The mathematicians' bargain. This tension between expressive freedom and structural discipline is not unique to programming languages; it is a recurring theme whenever algebraic power begins to dominate geometric intuition. As Baez [Bae22] writes in *Getting to the Bottom of Noether's Theorem:*

[2]The full account of how the EVT Trilemma manifests in macroscopic programming practice is given in [Kam26]. This outlines connections to resource theory and can be read as a companion piece.

> "Atiyah [Ati02] warned us of the dangers of algebra: *" ...algebra is to the geometer what you might call the Faustian offer. As you know, Faust in Goethe's story was offered whatever he wanted (in his case the love of a beautiful woman), by the devil, in return for selling his soul. Algebra is the offer made by the devil to the mathematician. The devil says: I will give you this powerful machine, it will answer any question you like. All you need to do is give me your soul: give up geometry and you will have this marvellous machine.*"

Baez notes that "While this is sometimes true, algebra is more than a computational tool: it lets us *express* concepts in a very clear and distilled way." We agree that the finest mathematics arises when algebra and geometry are brought into balance. But our contention here is that computation is one of the settings in which this balance becomes unusually unforgiving. Within an ordinary formal background such as ZFC, geometry and algebra can coexist without tension; but once a geometric system is required to *compute*, the act of doing so (in our case—the "gluing" 2.2) *enforces constraints* on *how* the flow can be structured. The bargain, in this case, is not rhetorical but structural, and the devil shall not be cheated.

But why physics? It is reasonable to ask why a hypothesis about computation belongs in a mathematical-physics paper.

First, differential geometry, topology, and gauge theory provide native languages for flow, locality, transport, gluing, invariants, defects, and boundary composition. These structures are not metaphors imposed on computation after the fact; they are mechanisms by which a physical substrate stores and transforms information.

Second, physical computers are constrained by more than syntactic decidability. Finite precision, noise, energy, time, stability, measurement back-action, causal structure, and control limitations determine which formal processes can actually be realized and read. A physical selection principle should therefore be stated at a level that applies to discrete, analog, geometric, and hybrid substrates.

Third, the physical setting prevents an easy conflation of unverifiability with symbolic diagonalization. A deterministic analog or field-theoretic process may fail to admit global pre-certification because of chaotic sensitivity, contextual readout, non-commuting transport, topological obstruction, or unresolved boundary data, even when it contains no literal self-interpreter.

This does not diminish the interest of the EVT Hypothesis for computer science or the philosophy of natural laws. Versions of the underlying tension have appeared in many domains, though rarely isolated as a single, explicit selection principle. A few recurring patterns (illustrative, not exhaustive) are:

- **Logic and programming.** As previously stated, total and strongly normalizing calculi increase verifiability by withdrawing general recursion; reflective and metaprogramming systems increase expressive freedom while transferring assurance to later phases.
- **Numerical analysis and PDEs.** Stability conditions such as CFL-type bounds restrict discretizations to preserve controlled evolution, while structure-preserving integrators restrict admissible updates to retain symplectic, conservative, or geometric information [CFL28].
- **Dynamical systems.** Integrable and symmetry-protected regimes may admit exact invariants and reduced descriptions, while generic perturbations can destroy those certificates without introducing any symbolic self-reference.
- **Many-body and field theory.** Uniform decision problems concerning infinite families of Hamiltonians can become undecidable; the spectral-gap result of Cubitt, Pérez-García, and Wolf supplies a particularly sharp example [CPGW15].
- **Quantum information.** Coherent transformations preserve a rich phase and correlation structure, while the accessible classical interface returns only a context-dependent finite outcome. The distribution may remain predictable even when the individual output does not descend from the operational state.

These examples do not establish one theorem with identical hypotheses. They motivate the search for a common physical design constraint: systems gain expressive power by enlarging their admissible process structure, while globally certifying and feasibly controlling that structure requires additional restrictions.

However, the most pressing applications of a *computational* selection principle are presently in *quantum gravity* and *lattice gauge theory*, where one must extract dynamics from large, ongoing physical computations (experiments or simulations) under resource and precision constraints. The EVT Hypothesis is intended to bound *how* such processes can behave and what can be recovered from them, independently of any particular quantization scheme.

In this manner, it is proposed as a *selection principle* for the behavior and modeling of computational processes: physical computation—discrete or analog—is not substrate-independent magic; it is a *gauge-constrained flow* carried by a geometric substrate, with invariant quantities and resource monotones that cannot be simultaneously optimized without limit. From this viewpoint, the structures that make computation possible (*how* we compute) are as consequential as the extensional outcomes (*what* we compute). Any physical theory of computation should, at a minimum, respect this geometric constraint.

3 Abelian Gauge Dynamics and Phase Geometry

Recent work on the computational richness of fluid dynamics provides a useful jumping-off point. Tao's universality program for the incompressible Euler equations shows that apparently compact local differential laws may support a remarkably large class of embedded dynamical behavior [Tao18]. Cardona et al. sharpened this connection by constructing a Turing-complete stationary Euler flow on a Riemannian S^3 [CMPSP21]. These results make an important distinction visible: the formal simplicity of a differential equation does not imply simplicity of its global solution space, nor does the existence of a solution theory by itself specify which features of those solutions should be regarded as computational states, transitions, or outputs.

The present section develops the first continuous regime of GCT with this distinction in mind. We introduce the *quasi-fluidic band*, in which a discrete geometric state is enlarged by compact abelian phase variables and quantized winding data. The resulting substrate is continuous, but its computational semantics remains organized by local interfaces, admissible transport, invariant structure, and specified readouts. In the simplest realization, the active continuous degree of freedom is a $U(1)$-valued phase, so that transport remains abelian and may be summarized by phase differences, winding ledgers, and curvature fluxes.

The role of differential equations in this regime is therefore important but deliberately separated from the definition of computation. A differential law specifies which histories of the substrate are dynamically admissible. The GCM structure specifies which features of those histories carry information, which local histories may be composed, which quantities survive deformation, and which observables constitute a readout. Schematically,

$$\text{differential law} \longrightarrow \text{admissible histories} \longrightarrow \text{compositional geometric structure} \longrightarrow \text{readout}.$$

The computation is identified with the latter structural organization of admissible histories, rather than with the task of reproducing the entire solution field.

This separation will become increasingly important later. In the abelian regime, the relevant structural data can often be compressed into phases and integer ledgers. In the non-abelian regime of section 4, the same principle is promoted to ordered transport, curvature, and holonomy. In section 5, histories themselves become inputs to a bordism- and field-theoretic semantics.

As a motivating example, consider the classic experiment in which a hose filled with running water is placed across a vibrating speaker. The resulting jet forms a visible oscillating pattern: the driving frequency controls coil tightness, amplitude controls the spiral radius, and phase controls the initial offset. This is an instructive caricature of the quasi-fluidic regime: periodic forcing induces an effective $U(1)$-phase along a geometric substrate, and the observable shape provides a coarse readout of that phase. In the language adopted later (3.1), the phase offset belongs to the T-layer (S^1 data), while winding/twist counts correspond to quantized Z-invariants; discrete readouts arise from coarse partitions of these quantities. Helical and twisted structures appear here not as an aesthetic choice, but as energetically natural carriers of phase and twist under periodic driving. A visual demonstration by [bru13] makes this phenomenon concrete.[3]

Computational geometric bordisms. The vibrating-hose experiment may be viewed as an analog of a *computational geometric bordism*: a smooth evolution mediating between boundary conditions

[3]Regarding an unconventional reference; the point is purely pedagogical: it is a compact way to visualize phase, winding, and coarse readout in a physical system.

(fixed endpoints, imposed phase/frequency, initial and final configurations). Here, the bordism is "internal" to the geometry of the evolving flow, and the computable content is not the PDE solution itself but the stable, gauge-invariant features one can read from it—see section A.4 for cobordism formalisms.

Proposition 3.1. *A GCM has information-bearing degrees of freedom, but the* effective *information content is relative to a chosen readout (coarse-graining). In particular, geometric computation is deterministic at the microstate level, while information is defined relative to an encoding.*

Unlike in classical computation—where the bit is treated as an absolute, context-free primitive—in geometric computation, the notion of a "geobit" is always specified with respect to a readout map (or partition) on the underlying state space. Concretely, one fixes an observable or coarse-graining

$$\rho : \Sigma \longrightarrow B,$$

where Σ is the (possibly structured) microstate space of the GCM and B is a finite label set used for symbolic computation. Once ρ is fixed, information becomes an objective property of the pair (Σ, ρ): the dynamics may be fully deterministic on Σ, yet the induced evolution on B depends on which features are chosen as readable and which are treated as hidden or irrelevant.

This is directly analogous to physics, where measurements and reference choices enter through specified observables rather than through subjectivity. The boundary between symbolic and quasi-fluidic computation is therefore not a matter of taste. Still, of modeling choice: symbolic regimes arise when the operative degrees of freedom are purely discrete (a finite B with static invariants), while the quasi-fluidic regime appears when one enlarges the local fiber to include compact abelian phases and quantized topological counters (the $B/T/Z$ structure of definition 3.1). Geometric deformation then permits interpolation between discrete and continuous logic *without* introducing probabilistic amplitudes.

The quasi-fluidic regime should therefore not be understood as an attempt to remove differential dynamics from continuous computation. Rather, it separates the dynamics of the carrier from the semantics of the computation carried by it. Earlier symbolic constructions used externally prescribed pulses and local update schedules acting on finite geometric labels. The quasi-fluidic mode promotes part of this control structure into the geometry itself: compact phases evolve continuously, integer quantities record isolated winding events, and finite readouts extract stable information from the resulting histories. Differential equations may govern these histories, but the computational content is specified by the invariant structures and interface relations selected from them.

3.1 A New Kind of Computation

The distinction between a differential law and the computational semantics carried by its solutions can be stated geometrically. Let

$$\pi : E \longrightarrow \Sigma$$

be a smooth field bundle. A regular finite-order differential equation may be represented by a differential relation

$$\mathcal{E} \hookrightarrow J^k E$$

inside the k-jet bundle of E. A section

$$\phi : \Sigma \longrightarrow E$$

is a solution when its jet prolongation satisfies

$$j^k \phi(\Sigma) \subseteq \mathcal{E}.$$

Higher prolongations

$$\mathcal{E}^{(r)} \subseteq J^{k+r} E$$

encode the differential consequences of the original equation. Formal integrability asks, roughly, whether this tower of prolongations closes compatibly rather than producing new hidden differential constraints at successive orders; standard criteria for nonlinear systems were developed by [Gol67].

This geometric viewpoint already moves substantially beyond identifying a PDE with a coordinate formula. More recently, Khavkine and Schreiber have reconstructed the formal theory of differential equations inside synthetic differential geometry, where the jet construction acquires a comonadic

formulation and formally integrable PDEs may be treated intrinsically in a setting that also accommodates higher and stacky geometry [KS17]. Their construction is motivated in part by the eventual treatment of locally variational field theories, including higher gauge fields. The lesson relevant here is not that PDEs disappear, but that differential equations themselves may be treated as geometric objects rather than as privileged coordinate syntax.

GCT makes a further, orthogonal separation. The differential relation $\mathcal{E}$ specifies the dynamically admissible histories, but it does not by itself specify their computational interpretation. For boundary data B_0, B_1, write schematically

$$\mathrm{Sol}_{\mathrm{adm}}\big(\mathcal{E}; B_0, B_1\big)$$

for the space of admissible solution histories connecting them. A GCM then equips such histories with additional structure: distinguished interfaces, allowed local transformations, equivalence relations, protected quantities, and readouts. A computational observable is a map of the form

$$R : \mathrm{Sol}_{\mathrm{adm}}\big(\mathcal{E}; B_0, B_1\big) \longrightarrow \mathcal{O},$$

where $\mathcal{O}$ may be finite, phase-valued, integer-valued, or in later regimes, a gauge-invariant moduli or holonomy space.

Thus, two dynamically distinct solutions need not represent distinct computations:

$$\phi_1 \sim_R \phi_2 \qquad \Longleftrightarrow \qquad R(\phi_1) = R(\phi_2).$$

Conversely, a computationally meaningful distinction need not be a pointwise property of the field. It may be carried by a winding number, a boundary transition, a defect event, an accumulated phase, or a global transport invariant. In this sense, the relevant computational object is not the full solution space alone, but its organization by admissible composition and observable quotient:

$$\mathrm{Sol}_{\mathrm{adm}}(\mathcal{E}) \longrightarrow \mathrm{Sol}_{\mathrm{adm}}(\mathcal{E})/\!\sim_R \longrightarrow \mathcal{O}.$$

We refer to this separation as *computation by structure*. The differential law answers

Which histories are dynamically permitted?

while the GCM semantics answers

Which permitted histories compose as computations, and what information do they carry?

Neither question replaces the other.

This distinction is particularly important for continuous media. The results of Tao and of Cardona et al. show that Euler dynamics may support extremely rich embedded computation. Such results demonstrate that a compact differential law can generate a solution space with nontrivial computational content. They do not, however, imply that every variable of the fluid is itself a computational register, or that computation is best identified with reconstructing the complete Euler solution. A computational interpretation still requires a choice of stable states, admissible controls, interfaces, and readouts.

The paradox of analog logic flow. Historically, analog and fluidic devices exploited continuous physics to implement nontrivial transformations. Their central difficulty is not simply that a governing equation may possess singular solutions. Continuous computation also raises questions of well-posedness, stability, conditioning, sensitivity to initial data, and the robustness of the chosen readout. A physical trajectory may remain perfectly well defined while becoming computationally ambiguous because nearby states cease to be distinguishable under the intended encoding.

If

$$\rho : \Sigma_{\mathrm{state}} \longrightarrow B$$

is a finite readout, then the relevant stability question is not only whether nearby trajectories remain nearby in the full state space, but whether perturbations preserve their observable class. A small geometric displacement may cross a readout boundary and induce a large change in the symbolic output. Analog fragility is therefore often a failure of the map from continuous dynamics to stable computational semantics rather than a literal failure of the underlying physics.

GCT responds by building the computational layer from invariant and compositional structure. A GCM update is a local admissible transformation at an interface, driven by specified boundary perturbations, pulses, or couplings. The ambient evolution may be described by ODEs or PDEs, but the computational semantics is carried by what may change, what must remain invariant, how local histories may be composed, and which quantities are retained by the readout. This is the sense in which the theory shifts emphasis from *solving the whole equation* to *controlling the structure of its admissible histories*.

The analytic obligations nevertheless remain. A proposed realization must still possess whatever existence, uniqueness, regularity, stability, continuation, and boundary-compatibility properties are required for its update laws to be well defined. Recasting computation geometrically does not remove these problems; it prevents them from being conflated with the separate question of what the resulting dynamics computes.

This structural viewpoint is also compatible with a broader movement in applied mathematics toward local interaction laws and networked descriptions of complex systems. Goriely and collaborators, for example, have modeled biological propagation through coupled local interaction mechanisms rather than treating the global phenomenon as a single undifferentiated state variable [TCK+20]. The relevance to GCT is methodological: complicated global behavior can be organized by local coupling structure even when continuous differential dynamics remain present underneath. The purpose is not to oppose PDE modeling, but to expose the compositional structure that a global equation alone does not identify.

Boundaries in Quasi-Fluidic GCMs. The passage from local differential dynamics to compositional computation requires boundary structure. A local differential law does not determine how independently specified regions may be assembled: one must also specify which boundary data are admissible, which traces of the fields are retained at an interface, and when two local histories are compatible under gluing.

Let M_1 and M_2 be neighboring regions meeting along an interface Y. For a differential relation $\mathcal{E}$, denote by

$$\mathcal{B}_{\mathcal{E}}(Y)$$

the relevant space of admissible boundary data on Y. Depending on the equation and variational problem, these data may consist of field values, normal derivatives, finite jets, connection data, conserved fluxes, or some constrained subset thereof. Two local histories

$$\phi_1 \in \mathrm{Sol}_{\mathrm{adm}}(\mathcal{E}; M_1), \qquad \phi_2 \in \mathrm{Sol}_{\mathrm{adm}}(\mathcal{E}; M_2)$$

may be glued only when their induced boundary data agree under the chosen interface identification.

Schematically, compatible histories therefore form a fiber product

$$\mathrm{Sol}_{\mathrm{adm}}(\mathcal{E}; M_1) \times_{\mathcal{B}_{\mathcal{E}}(Y)} \mathrm{Sol}_{\mathrm{adm}}(\mathcal{E}; M_2).$$

When the relevant analytic gluing problem is well-posed, such compatible data determine a history on

$$M_1 \cup_Y M_2.$$

This is the differential-geometric counterpart of the GCM interface law: composition is permitted only when the structures exposed at the common boundary are compatible.

In finite-order problems, these compatibility conditions may be expressed through traces of finite jets. This parallels the jet-matching conditions already encountered in section 1 for smooth helical splices, but now the jets belong to fields or state sections rather than only to embedded centerlines. Formal prolongation provides the natural language for checking whether such local differential constraints remain compatible at higher order.

The quasi-fluidic regime isolates a particularly controlled instance of this general picture. The boundary data retained by a cell consist of a finite symbolic sector, compact abelian phase variables, and quantized topological counters. Local evolution remains deterministic and nonsingular, while interfaces couple these data through equivariant maps. We now make this phase boundary precise.

Definition 3.1 (Quasi–Fluidic Computation and Regime Phases)**.** Given a GCM, we say it operates in the *quasi–fluidic regime* if each region R_i carries a finite–dimensional state fiber:

$$\mathcal{X}_i \;\cong\; B_i \times T_i \times Z_i,$$

as in definition 2.1 with the following structure:

(QF1) **Discrete core (symbolic).** B_i is finite, typically $B_i \cong (C_2)^{k_i}$; in the twin helix unit one has $k_i = 4$ for chirality/orientation bits.

(QF2) **Phase layer.** T_i is a continuous but compact abelian Lie group (a torus), $T_i \cong (S^1)^{m_i} \simeq U(1)^{m_i}$, encoding axial phase(s), orientation angles, or other bounded "analog" degrees of freedom.

(QF3) **Quantized invariants.** Z_i is a finitely generated abelian group (e.g. $\mathbb{Z}^{p_i}$), recording twist/winding/linking numbers or other topological charges.

(QF4) **Abelian symmetry and equivariance.** The local symmetry acting on Σ_i is

$$K_i \;\cong\; (C_2)^{k_i} \times (S^1)^{m_i},$$

and every interface map $I_{ij} \in \mathcal{I}$ and the induced flow on Σ_i are K–equivariant, that is, they depend on phase differences and commute with flips/rotations.

(QF5) **Flow coupling.** The ambient flow $\{\mathsf{Ev}_t\}$ transports the T–coordinates continuously (phase evolution) and can modify Z only by isolated, energy–threshold events (phase slips) prescribed by the interface rules; B updates by the same local rules. No non-abelian monodromy is present.

(QF6) **Non–singularity and bounded energy.** Trajectories have no finite–time blow-ups; curvature/torsion remain bounded; state updates at interfaces are well defined for all t.

A system is symbolic when $m_i = 0$ and Z_i is static; it is purely fluidic when B_i is trivial and non-abelian holonomy appears. The quasi–fluidic band sits between these: it combines a finite discrete core with $U(1)$–type phases and integer topological counters, all governed by abelian symmetry.

The $B/T/Z$ decomposition should therefore be read not merely as a taxonomy of state variables, but as a choice of boundary data adapted to composition. The B-sector records finite locally readable labels, the T-sector records compact phase data that may be transported continuously across interfaces, and the Z-sector records discrete invariants that remain constant on smooth strata and change only at prescribed threshold events. The purpose of this decomposition is to retain enough information for neighboring histories to be glued without requiring the complete microscopic solution on either side of the interface.

Composition of GCMs. In the symbolic regime, interfaces exchange finite readouts and induce local discrete updates. In the quasi-fluidic regime, the same compositional principle persists, but the interface data are enlarged to include compact phases and quantized invariants. Composition is therefore controlled by compatibility of the relevant $B/T/Z$ boundary data rather than by a purely discrete transition table. Reconfiguration corresponds to changing the admissible interface maps, coupling parameters, or boundary conditions, while preserving the local gluing rules of the GCM.

3.2 Abelian Lattice Gauge Dynamics in the Quasi–Fluidic Mode

In the QF band, the appropriate "computational" physics we should work with is not a discrete logic model as in the symbolic band but an *abelian lattice gauge dynamics*: compact phases transported and coupled locally, with evolution governed by a bounded local energy and (optionally) a driven-damped relaxation law. This section is *interpretive*; it provides a stable dynamical model for analyzing QF behavior, without elevating differential equations to the definition of geometric computability.

Lattice variables (QF state). Let $\Gamma = (V, E)$ be the interaction graph of a GL (cells/modules are vertices, interfaces are edges). For each cell $i \in V$, we take an internal phase (orientation layer)

$$\theta_i \in U(1) \cong \mathbb{R}/2\pi\mathbb{Z},$$

and for each interface $(i, j) \in E$ we take a *link phase* (a discrete connection 1–form)

$$A_{ij} \in \mathbb{R}/2\pi\mathbb{Z}, \qquad A_{ji} = -A_{ij},$$

equivalently $U_{ij} := \exp(iA_{ij}) \in U(1)$. (If one wishes to remain in the finite cyclic subband, replace $U(1)$ by C_N and interpret all equations below as a continuous approximation to a stroboscopically driven C_N update.)

Gauge redundancy. A $U(1)$ gauge transformation is a choice of angles $\alpha_i \in \mathbb{R}/2\pi\mathbb{Z}$ at each cell,

$$\theta_i \mapsto \theta_i + \alpha_i, \qquad A_{ij} \mapsto A_{ij} + \alpha_i - \alpha_j,$$

under which the *gauge–invariant phase difference*

$$\Delta_{ij} \;:=\; \theta_i - \theta_j - A_{ij} \pmod{2\pi}$$

is unchanged. In this sense, "independence of local modules" is a choice of gauge/frame, while couplings are encoded invariantly by Δ_{ij}.

Local energy (interface functional). A minimal gauge–invariant energy on Γ is

$$\mathcal{E}(\theta, A) \;=\; \sum_{(i,j)\in E} J_{ij}\,\big(1 - \cos(\Delta_{ij})\big) \;+\; \sum_{p\in \mathsf{P}} \kappa_p\,\big(1 - \cos((dA)_p)\big), \tag{2}$$

where $J_{ij} \geq 0$ are interface couplings and P is a chosen set of plaquettes (2–cells) with discrete curvature

$$(dA)_p \;:=\; \sum_{(i,j)\in \partial p} s_{p,ij}\, A_{ij} \pmod{2\pi}, \qquad s_{p,ij} \in \{\pm 1\}$$

the oriented sum around ∂p. The first term penalizes a mismatch between neighboring phases modulo the link variable; the second penalizes nonzero curvature ("flux") [Kog79].

Gradient–flow dynamics. A simple well-behaved evolution law is driven by gradient flow on the compact state space:

$$\dot\theta_i \;=\; -\gamma_\theta\,\frac{\partial \mathcal{E}}{\partial \theta_i} \;+\; \eta_i(t), \qquad \dot A_{ij} \;=\; -\gamma_A\,\frac{\partial \mathcal{E}}{\partial A_{ij}} \;+\; \eta_{ij}(t), \tag{3}$$

with mobilities $\gamma_\theta, \gamma_A > 0$ and external drives $\eta_i(t), \eta_{ij}(t)$ (global pulses, boundary forcing, or localized injections). Concretely, the Euler–Lagrange components are

$$\frac{\partial \mathcal{E}}{\partial \theta_i} = \sum_{j\sim i} J_{ij}\,\sin(\Delta_{ij}), \tag{4}$$

$$\frac{\partial \mathcal{E}}{\partial A_{ij}} = -J_{ij}\,\sin(\Delta_{ij}) \;+\; \sum_{p\ni(i,j)} \kappa_p\, s_{p,ij}\,\sin((dA)_p), \tag{5}$$

so (3) relaxes toward gauge–invariant consistency ($\Delta_{ij} \to 0$) and low curvature ($(dA)_p \to 0$) unless forced otherwise. Because the variables are compact and $\mathcal{E}$ is bounded below, this regime is dynamically stable and aligns with the QF "no blow-ups " philosophy.

Remark 3.1 (Scope and Interpretation). Equations (2)–(3) are not proposed as fundamental laws of GCT; they are a *normal form* for the abelian corridor: local couplings, compact phases, gauge redundancy, and dissipative relaxation. In particular, continuous flows of this type do *not* implement jump–style updates by themselves; any discrete "computational" layer is induced later by readout/partitioning (return maps).

Auxiliary geometric ODE variables. To retain an explicit connection to helix geometry, one may attach slowly varying, bounded geometric parameters to each cell,

$$r_i(t) \in \mathbb{R}_{>0} \qquad \text{(effective radius/scale)}, \tag{6}$$

$$\tau_i(t) \in \mathbb{R} \qquad \text{(effective twist rate)}, \tag{7}$$

$$\mathcal{L}_i(t) \in \mathbb{R}_{>0} \qquad \text{(effective length)} \tag{8}$$

and couple them to *local energy density* and/or *local phase current*. A simple choice is:

$$\dot r_i = -\lambda_r\,(r_i - r_0) \;+\; \alpha_r \sum_{j\sim i} \big(1 - \cos(\Delta_{ij})\big), \tag{9}$$

$$\dot\tau_i = -\lambda_\tau\,(\tau_i - \tau_0) \;+\; \alpha_\tau \sum_{j\sim i} \sin(\Delta_{ij}), \tag{10}$$

$$\dot{\mathcal{L}}_i = -\lambda_L\,(\mathcal{L}_i - \mathcal{L}_0) \;+\; \alpha_L\, r_i\,|\tau_i|, \tag{11}$$

with $\lambda_\bullet > 0$ ensuring relaxation to baseline values $(r_0, \tau_0, \mathcal{L}_0)$ and $\alpha_\bullet$ setting coupling strength. These equations encode the informal idea that mismatch/coupling stress can thicken the effective geometry (9), phase transport can bias twist (10), and geometry co-scales (11). One may also let the mobilities in (3) depend on τ_i (twist as a local "clock" factor), e.g. $\gamma_\theta = \gamma_\theta(\tau_i)$, without changing the gauge structure.

Synchronization limit: Kuramoto reduction. A useful special case of the QF phase dynamics is obtained by restricting to nearest-neighbor coupling on the $U(1)$ phase layer and passing to a co-rotating frame. In that case, the local phase evolution reduces to a Kuramoto-type system [ABV+05, Kur84]

$$\frac{d\theta_i}{dt} = \Omega_i + K \sum_{j \sim i} \sin(\theta_j - \theta_i),$$

where $\theta_i \in S^1$ is the phase of cell i, Ω_i is its intrinsic frequency, and K is the coupling strength.

This should be understood as a *synchronization limit* of the abelian gauge dynamics, not as the full semantics of quasi–fluidic computation. Physically, it describes the tendency of neighboring helices to phase-lock under local coupling; computationally, it captures the emergence of a shared clock or coherent phase carrier across a region of the lattice. In particular, when the $U(1)$ corridor is used only as a transport layer, Kuramoto synchronization provides a natural mechanism by which continuous phase variables may stabilize before a stroboscopic readout is applied.

Equivalently, if the local energy is taken to be of XY type,

$$E(\theta) = \sum_{(i,j) \in E(\Lambda)} \kappa_{ij} \big(1 - \cos(\theta_i - \theta_j)\big),$$

then the dissipative phase flow

$$\dot{\theta}_i = -\frac{\partial E}{\partial \theta_i}$$

recovers the Kuramoto form above up to the choice of sign convention and the addition of the drift terms Ω_i. Thus, the Kuramoto system is a familiar, physically interpretable subcase of the general QF lattice dynamics.

Example 3.1 (Plaquette Phase Slip and Integer Counter Update). Let p be an oriented plaquette in the lattice, and let

$$\Delta_e = \theta_{s(e)} - \theta_{t(e)} - A_e \qquad (\mathrm{mod}\ 2\pi)$$

denote the gauge–invariant phase difference on each oriented boundary link $e \in \partial p$. Along a continuous trajectory, choose continuous real lifts $\widetilde{\Delta}_e(t) \in \mathbb{R}$ and define the lifted circulation

$$\widetilde{\Gamma}_p(t) := \sum_{e \in \partial p} s_{p,e}\, \widetilde{\Delta}_e(t), \qquad s_{p,e} \in \{\pm 1\}.$$

Because each Δ_e is gauge invariant, so is $\widetilde{\Gamma}_p$ once its initial lift has been fixed.

At every time, decompose the lifted circulation uniquely as

$$\widetilde{\Gamma}_p(t) = \Gamma_p(t) + 2\pi z_p(t),$$

where

$$\Gamma_p(t) \in (-\pi, \pi], \qquad z_p(t) \in \mathbb{Z}.$$

The variable Γ_p is the principal compact $U(1)$ flux observed on the plaquette, while z_p records the number of complete 2π windings that have passed through the chosen branch.

As long as $\widetilde{\Gamma}_p(t)$ remains within a single branch interval, z_p is constant and the evolution lies entirely in the smooth phase layer. Suppose, however, that an applied drive causes $\widetilde{\Gamma}_p$ to cross a branch boundary at a time t_*. Then the principal phase wraps by 2π, while the integer counter changes by one:

$$z_p(t_*^+) - z_p(t_*^-) = \begin{cases} +1, & \dot{\widetilde{\Gamma}}_p(t_*) > 0, \\ -1, & \dot{\widetilde{\Gamma}}_p(t_*) < 0. \end{cases}$$

The compact quantity

$$\exp\big(i\widetilde{\Gamma}_p(t)\big) = \exp\big(i\Gamma_p(t)\big)$$

remains continuous throughout the event; the discrete change occurs in the lifted winding ledger z_p. This is a *phase slip*.

In the phase–only reduction $A_e = 0$, the same construction measures the winding of neighboring cell phases around the plaquette. In a continuum physical realization, the event corresponds to the passage or nucleation of a vortex through the plaquette; the phase-only description may then fail briefly at the defect core while the surrounding $U(1)$ phase remains well-defined. Thus, the Z–coordinate is not introduced independently of the continuous dynamics: it records isolated threshold events generated by the evolution of the T– layer.

Remark 3.2 (Smooth Core and Thresholded Boundary Events). The strict smooth QF core is obtained by restricting to trajectories for which every z_p remains fixed. Allowing the isolated events of example 3.1 enlarges this core by adjoining transitions between integer-labeled strata. Such phase slips do not by themselves introduce non-abelian holonomy: the structure group remains $U(1)$, but the evolution is no longer confined to a single smooth lift of the compact phase space. This thresholded extension supplies the natural bridge from abelian phase transport to vortex and defect dynamics.

Recovery of discrete readouts. The QF dynamics above are continuous (compact phases with local energy and gradient flow). As such, they do *not* natively implement jump–style updates. The bridge back to classical symbolic computation is therefore *stroboscopic*: we sample the system once per pulse and apply a *discretized readout* (a quantizer) to obtain an induced update on a finite alphabet. In this sense, discrete computation in the QF band is a *return–map phenomenon*, not an ODE phenomenon.

Definition 3.2 (Pulse Times and Stroboscopic Map)**.** Fix a pulse period $\Delta t > 0$ and define $t_n := n\Delta t$. Let $P : \mathcal{L}_{\mathrm{QF}} \to \mathcal{L}_{\mathrm{QF}}$ denote the time–Δt map on the global QF state space $\mathcal{L}_{\mathrm{QF}}$ induced by one pulse:

$$P \;:=\; \mathsf{Ev}_{\Delta t}.$$

We write $x^n \in \mathcal{L}_{\mathrm{QF}}$ for the post–pulse state at time t_n, so $x^{n+1} = P(x^n)$.

Because the abelian corridor carries gauge redundancy, any robust readout should be phrased in terms of *gauge–invariant local observables*. In the lattice–gauge normal form, the basic invariants are:

$$\Delta_{ij} = \theta_i - \theta_j - A_{ij} \pmod{2\pi} \qquad \text{and} \qquad (dA)_p = \sum_{(i,j)\in\partial p} s_{p,ij} A_{ij} \pmod{2\pi}.$$

We therefore define a cellwise observable $y_i = y_i(x)$ as a finite list of such invariants in a bounded neighborhood (e.g. the Δ_{ij} on links incident to i, and optionally nearby plaquette fluxes $(dA)_p$).

Definition 3.3 (Discretized Readout/Quantizer)**.** Fix a finite alphabet B and a (piecewise constant) quantizer

$$Q : \; \mathcal{Y} \longrightarrow B,$$

where $\mathcal{Y}$ is the range of local invariants y_i. The induced discrete configuration for a state $x \in \mathcal{L}_{\mathrm{QF}}$ is

$$b = \mathrm{Read}(x) \in B^V, \qquad b_i := Q\big(y_i(x)\big).$$

For example, one may partition S^1 into arcs and threshold a chosen invariant angle, or partition the flux $(dA)_p$ into bins. The specific partition is a modeling choice.

Definition 3.4 (Local QF Return Maps and Induced Symbolic Dynamics)**.** Let

$$P : \mathcal{L}_{\mathrm{QF}} \longrightarrow \mathcal{L}_{\mathrm{QF}}$$

be the time-Δt stroboscopic map introduced above. Finite-range coupling of the infinitesimal evolution law does not, by itself, imply that the exact finite-time map P has strictly finite propagation.

We therefore say that a pulse is *finite-propagating* if, for every cell i, there exists a finite neighborhood $N(i)$ such that the post-pulse state at i depends only on the pre-pulse states in $N(i)$:

$$x_i^{n+1} = U_i\big(\{x_j^n\}_{j\in N(i)}\big), \qquad x_i^n \in X,$$

where X is the local compact state space. If the lattice and update law are translation invariant, one may take $U_i = U$. Under this additional finite-propagation hypothesis, the stroboscopic dynamics is a continuous-alphabet cellular automaton.

Let the discretized readout be a surjection

$$\mathrm{Read} : \mathcal{L}_{\mathrm{QF}} \longrightarrow B^V.$$

An autonomous symbolic return map $F_B : B^V \to B^V$ exists precisely when the stroboscopic evolution preserves the readout fibers:

$$\mathrm{Read}(x) = \mathrm{Read}(y) \quad \Longrightarrow \quad \mathrm{Read}(Px) = \mathrm{Read}(Py).$$

When this holds, the induced map is uniquely determined by

$$F_B \circ \mathrm{Read} = \mathrm{Read} \circ P, \qquad F_B = \mathrm{Read} \circ P \circ \mathrm{Lift},$$

where $\mathrm{Lift} : B^V \to \mathcal{L}_{\mathrm{QF}}$ is any section of the readout; the expression is independent of the section. If V and B are finite and P is bijective (as for a complete smooth ODE flow at finite time), exact global descent forces F_B to be bijective as well.

For an effectively irreversible sampled update, instead choose a proper *forward-admissible readout domain*

$$\mathcal{L}_{\mathrm{adm}} = \bigsqcup_{b \in B^V} U_b \subsetneq \mathcal{L}_{\mathrm{QF}},$$

where the nonempty readable regions U_b have disjoint guard-banded interiors and satisfy $\mathrm{Read}|_{U_b} = b$. Require, at sampling times,

$$P(U_b) \subseteq U_{F_B(b)} \qquad (b \in B^V),$$

with the images separated from the destination threshold boundaries by a prescribed positive margin. Thus $P(\mathcal{L}_{\mathrm{adm}}) \subseteq \mathcal{L}_{\mathrm{adm}}$, but equality and surjectivity of the restricted map are not required. The continuous trajectory between samples may pass through the excluded threshold collars. This permits a non-injective finite symbolic update despite invertibility of the ambient flow, provided an appropriate trapping-domain construction exists.

Remark 3.3 (What is "Computed"?). In the QF corridor, the continuous dynamics are the physical substrate, and symbolic computation appears only after stroboscopic sampling and a specified discretized readout. The infinitesimal dynamics may be local even when the exact finite-time flow is not strictly finite-propagating. A genuine cellular-automaton description therefore requires either an explicitly local pulse scheme or the finite-propagation hypothesis of definition 3.4. For finite B^V, exact global descent of a bijective time map yields only reversible symbolic updates. Non-injective sampled updates instead use forward-admissible, guard-banded readout regions as in definition 3.4; the gradient-flow model in (3) motivates possible trapping regions but does not itself establish a particular logic gate.

The $U(1)$ Corridor and an E/V Paradox. Within the quasi-fluidic band, the ω-logic layer may be represented either by a finite cyclic alphabet C_N or by a continuous phase $U(1)$. The continuous S^1 limit is compact and abelian, yet it exposes a distinctive backfire within the expressiveness–verifiability tradeoff:

- **Low geometric expressiveness.** Pure $U(1)$ phase composition is commutative. As a result, sequencing power collapses: one cannot exploit non-commuting compositions to build richer path-dependent behavior, and the phase layer alone tends to support only limited families of smooth, energetically bounded dynamics. In this corridor, most "computational complexity" must therefore be carried either by the discrete core B (via readout and interface thresholds) or by leaving the abelian setting (e.g. via threshold events/topological defects or non-abelian holonomy).
- **Low algebraic verifiability.** Any *finite* readout must discretize phase (explicitly or implicitly) by thresholds. In the $U(1)$ corridor, near-resonant phase evolution makes this discretization brittle: small phase perturbations can move trajectories across readout boundaries, producing significant changes in the inferred discrete state. Moreover, phase-locking reduces redundancy (many degrees of freedom share a common "clock"), weakening independent cross-checks.[4]

[4] In essence, pure $U(1)$-logic has *too many* microstates, and this points toward a concrete mathematical reason why large-scale analog computers were mostly abandoned by the late 1950s.

Transition, not destination. For these reasons, the $U(1)$ phase limit is best regarded as a *critical corridor*: visually orderly and analytically tractable, yet brittle under discretized readout and shallow in purely geometric expressiveness unless supplemented by discrete structure. It serves as a staging layer for robust computation on B and as a boundary marker before the onset of genuinely non-abelian (fluidic/gauge) behavior.

3.3 Application of Lie Groupoids in Geometric Computation

In gauge theory, geometric data are assigned to fibers over a base manifold, and a connection determines how these data are transported and compared along paths. Such comparisons have specified source and target points, with composition defined only when endpoints agree. For a principal G-bundle $P \to M$, this structure is naturally organized by the gauge groupoid

$$\mathcal{G}(P) = (P \times P)/G \rightrightarrows M,$$

whose arrows represent equivariant identifications between fibers, while a connection supplies parallel transport and its associated holonomy. Lie groupoids provide the corresponding smooth framework, originating in the differential-geometric work of Ehresmann [Ehr59] and developed further by Pradines [Pra66]; see also [Mac05].

Informally, a Lie groupoid consists of smooth manifolds of objects and morphisms, with smooth structural maps (source, target, identity, inversion, and composition), where the source and target maps are submersions. Unlike a single global symmetry group, a Lie groupoid allows the available transformations to depend on their source and target, and morphisms compose only when their endpoints match. This makes Lie groupoids a natural framework for the reversible transport and local symmetry of GCMs. The additional admissibility conditions governing computational updates and boundary interfaces are specified by the chosen geometric and compositional structures.

We begin with a general decorated formalism, and then specialize it to the quasi-fluidic abelian regime.

Definition 3.5 (S–decorated Groupoid)**.** Let $(S, *)$ be a monoid with unit e, and let $\mathbf{B}S$ denote the one-object category whose endomorphism monoid is S. An *S–decorated groupoid* is a pair $(\mathcal{G}, d)$ consisting of a small groupoid $\mathcal{G}$ together with a functor

$$d : \mathcal{G} \longrightarrow \mathbf{B}S.$$

Equivalently, each morphism $f \in \mathrm{Mor}(\mathcal{G})$ is assigned a label $d(f) \in S$ such that

$$d(g \circ f) = d(g) * d(f), \qquad d(\mathrm{id}_x) = e$$

for all composable f, g and all objects x. Since functors preserve isomorphisms, every decoration of an arrow lies in the unit group $S^\times \subseteq S$.

Definition 3.6 (Morphisms of S–decorated Groupoids)**.** A morphism

$$(\mathcal{G}, d) \longrightarrow (\mathcal{H}, \delta)$$

of S–decorated groupoids is a functor $F : \mathcal{G} \to \mathcal{H}$ such that

$$\delta \circ F = d.$$

This defines the category $\mathrm{DecGrpd}_S$ of S–decorated groupoids.

Remark 3.4. The use of the term "decorated" follows modern geometric and categorical usage [Pen87, Fon15]. The point is to enrich a base compositional structure with auxiliary data while preserving functorial composition. In the present context, the decorations record geometric or computational quantities associated with paths, interfaces, or local transformations.

General decorated path data. Let M be a smooth manifold (or a stratified manifold when needed), and let $\mathcal{S}$ denote a specified collection of geometric or computational structures on M—for example, twist counts, phase accumulation, chirality labels, or local field values. The classical fundamental groupoid remembers only path homotopy classes. In geometric computation, however, one often needs a refinement that also records such auxiliary data.

Definition 3.7 (Decorated Fundamental Groupoid)**.** Let M be a smooth manifold and let S be a monoid. An *S–decorated fundamental groupoid* of M is an S–decorated groupoid

$$(\Pi_1^*(M), d)$$

whose underlying groupoid $\Pi_1^*(M)$ is chosen from a path groupoid naturally associated to M (for example, the ordinary fundamental groupoid, or the thin fundamental groupoid when differential invariants are to be preserved), and whose decoration functor

$$d : \Pi_1^*(M) \to \mathbf{B}S$$

records the specified geometric data along paths. Composition is induced by path concatenation together with the monoid law in S.

Remark 3.5. When the decoration depends only on ordinary homotopy classes, one may work with the usual fundamental groupoid $\Pi_1(M)$. When the decoration depends on differential data such as connection holonomy or thin geometric transport, one should instead use the thin fundamental groupoid $\Pi_1^{\mathrm{thin}}(M)$, since such invariants are constant under thin homotopy but need not factor through ordinary homotopy classes.

A geometric model for the twin helix. For geometric computation, a finite twin helix module is best modeled as a regular neighborhood of an embedded arc. Topologically, this gives

$$THM \;\cong\; D^2 \times I \;\cong\; B^3.$$

Thus, the underlying space is contractible: its ordinary homotopy type is trivial, and the undecorated fundamental groupoid carries no nontrivial loop information.

It means that the computationally relevant structure of a twin helix module is not encoded by the bare topology of the carrier space, but by the additional geometric data placed on it: phase fields, twist laws, chirality assignments, framings, and interface rules. In the symbolic and general decorated setting, one may attach labels such as chirality or twist to paths in this contractible space. In the quasi-fluidic abelian reduction developed later in this chapter, chirality is no longer treated as an actively updated path label, but instead as a choice of orientation convention for link variables.

Example 3.2 (Decorated Loops in a Finite Module). Let

$$THM \;\cong\; D^2_{(r,\varphi)} \times I_z,$$

and choose a smooth phase 1-form on the cross-sectional angular direction,

$$A \;=\; \Omega(r, \varphi, z)\, d\varphi.$$

For fixed (r, z), let $\gamma_{r,z}$ denote the loop obtained by traversing once around the circle of radius r in the cross-section $D^2 \times \{z\}$. As a loop in the contractible manifold THM, $\gamma_{r,z}$ is null-homotopic in the ordinary sense. Nevertheless, it may carry nontrivial geometric data.

For example, taking

$$S = U(1) \times C_2,$$

one may define a decoration on an appropriate refined path groupoid (for example, the thin fundamental groupoid) by

$$d([\gamma_{r,z}]) \;:=\; \left(\exp\Big(i \int_{\gamma_{r,z}} A\Big),\; \chi(\gamma_{r,z}) \right),$$

where the first component records the accumulated phase and the second records a chirality label determined by the chosen geometric structure [Bar91]. The resulting decorated class

$$([\gamma_{r,z}],\, d([\gamma_{r,z}]))$$

is computationally nontrivial even though the underlying ordinary homotopy class of $\gamma_{r,z}$ is trivial.

Thus, in a finite twin helix module, the computational content lives in the decoration rather than in the bare fundamental groupoid.

Remark 3.6. This is precisely why the general decorated picture and the later quasi-fluidic abelian reduction must be kept distinct. In the symbolic/general setting, chirality may legitimately appear as part of the decoration target S, and one works with a refined path groupoid because ordinary homotopy forgets too much. In the specialized $U(1)$ phase regime, by contrast, chirality is frozen into an orientation convention, and the active structure reduces to abelian phase transport.

Why Lie groupoids appear in the QF regime. The preceding decorated picture is intentionally broad. In the quasi-fluidic regime, however, the relevant structure simplifies dramatically. The active degree of freedom is no longer a freely manipulated chirality/twist label, but an abelian phase field. The correct object is therefore not a general decorated path groupoid, but a Lie groupoid encoding *gauge redundancy* of local $U(1)$ phase assignments on a lattice.

To provide a rigorous setting for this maximal abelian regime, we explicitly construct the corresponding Lie groupoid.

Definition 3.8 (S–decorated Lie Groupoid)**.** If $\mathcal{G} \rightrightarrows M$ is a Lie groupoid and S is a Lie group, an *S–decorated Lie groupoid* is a smooth functor

$$d : \mathcal{G} \to \mathbf{B}S,$$

where $\mathbf{B}S$ is the one–object Lie groupoid with endomorphism group S.

Definition 3.9 (Underlying Lattice/Graph Datum)**.** Fix a finite connected graph

$$\Gamma = (V, E),$$

for example, a finite patch of a GL, where V is the set of sites and E the set of undirected adjacency links. Choose an orientation on each undirected edge, written as a subset

$$E^+ \subseteq \vec{E},$$

so that every edge $\{i, j\} \in E$ appears exactly once as either $e : i \to j$ or $\bar{e} : j \to i$ in E^+. Write $s(e), t(e) \in V$ for the source and target of an oriented edge e.

Definition 3.10 (Core Configuration Space in the QF Regime)**.** The quasi-fluidic core state of the lattice is a *link phase assignment*

$$M_{\mathrm{QF}} \;:=\; U(1)^{E^+} \;\cong\; (S^1)^{|E^+|}.$$

An element $U \in M_{\mathrm{QF}}$ is a family $U = (U_e)_{e \in E^+}$ with $U_e \in U(1)$. The value on the oppositely oriented edge is determined by inversion:

$$U_{\bar{e}} \;:=\; U_e^{-1}.$$

Remark 3.7 (Chirality as Orientation Convention). In this quasi-fluidic interpretation, chirality is *not* a separate state coordinate. Instead, the handedness of the underlying helix selects (or suggests) a preferred orientation for reading the link phase; reversing that convention replaces U_e with U_e^{-1}. Thus, the earlier symbolic chirality label is absorbed into the orientation convention on each link and disappears from gauge-invariant observables.

Definition 3.11 (Gauge Group and Action on Link Phases)**.** Let the site gauge group be

$$G_{\mathrm{QF}} \;:=\; U(1)^V.$$

For $g = (g_i)_{i \in V} \in G_{\mathrm{QF}}$ and $U = (U_e)_{e \in E^+} \in M_{\mathrm{QF}}$, define the action

$$g \cdot U \in M_{\mathrm{QF}}$$

by the standard link transformation law

$$(g \cdot U)_e \;:=\; g_{s(e)}\, U_e\, g_{t(e)}^{-1}, \qquad e \in E^+.$$

Definition 3.12 (QF Core Lie Groupoid: the Gauge Action Groupoid)**.** The quasi-fluidic core Lie groupoid is the action groupoid

$$\mathcal{G}_{\mathrm{QF}} \;:=\; G_{\mathrm{QF}} \ltimes M_{\mathrm{QF}} \rightrightarrows M_{\mathrm{QF}}.$$

An arrow is a pair (g, U) with $g \in G_{\mathrm{QF}}$ and $U \in M_{\mathrm{QF}}$. The source and target maps are

$$s(g, U) = U, \qquad t(g, U) = g \cdot U,$$

and composition is

$$(h,\, g \cdot U) \circ (g, U) = (hg,\, U), \qquad h, g \in G_{\mathrm{QF}}.$$

For finite Γ, this is a finite-dimensional Lie groupoid.

Remark 3.8 (Gauge Invariants Live on the Quotient Stack). The physically meaningful quantities in the quasi-fluidic abelian regime are gauge–invariant functions on M_{QF} (equivalently, functions on the quotient stack

$$[M_{\mathrm{QF}}/G_{\mathrm{QF}}]).$$

The groupoid $\mathcal{G}_{\mathrm{QF}}$ records *gauge redundancy*, that is, equivalences of description rather than physical time evolution. Dynamics—for example, the gradient flow of a local gauge-invariant energy built from plaquette terms—is additional structure: a G_{QF}–equivariant flow on M_{QF} that descends to the quotient. We treat this dynamical layer separately from the gauge groupoid itself; see also [CFP18] as a reference.

The viewpoint adopted here is therefore two-tiered. At the general level, decorated groupoids package the local geometric and combinatorial data relevant to symbolic or hybrid computation. At the quasi-fluidic abelian level, this broad picture reduces to a concrete lattice $U(1)$ gauge groupoid whose arrows encode only local phase-frame redundancy. This distinction is intentional: transcendental or geometric data may decorate computation in general, whereas the $U(1)$ corridor isolates the simplest smooth abelian core on which the later return-map and phase-ledger constructions are built.

A warning on the Homotopy Hypothesis. It would be amiss not to mention the Grothendieck Homotopy Hypothesis [Gro21], but equally important not to overstate what follows from it. The classical principle concerns the equivalence between homotopy types and suitable ∞-groupoidal models of those homotopy types. It does *not* imply that arbitrary differential, geometric, dynamical, or computational decorations are themselves determined by the underlying homotopy type.

This distinction is essential in GCT. A connection, framing, phase field, chirality assignment, holonomy, interface law, or local computational constraint may distinguish two geometric systems whose underlying spaces have the same ordinary homotopy type. When such data factor through homotopy, the usual homotopy-theoretic classification is sufficient. When they do not, the correct object is not a new "homotopy type" in the classical sense, but a homotopy type equipped with *additional structure*—for example a thin, Lie, decorated, or higher groupoid, a bundle with connection, or an appropriate higher-geometric stack. Accordingly, decorated groupoids in this paper should not be read as a replacement for regular homotopy types.

Definition 3.13 (Homotopy Computation)**.** Fix a GCM lattice in the quasi-fluidic regime with configuration space M_{QF}, pulse map

$$P : M_{\mathrm{QF}} \to M_{\mathrm{QF}},$$

and readout

$$\mathrm{Read} : M_{\mathrm{QF}} \to B^V.$$

A *homotopy computation* is a finite or continuous state evolution

$$\gamma : [0,1] \longrightarrow M_{\mathrm{QF}}$$

such that γ is generated by admissible local dynamics of the model (for example, gradient flow segments, pulse updates, or their hybrid composition), together with its induced readout trajectory

$$\mathrm{Read} \circ \gamma : [0,1] \to B^V.$$

Two homotopy computations $\gamma_0, \gamma_1 : [0,1] \to M_{\mathrm{QF}}$ with the same endpoints are said to be *computationally equivalent* if there exists a homotopy

$$H : [0,1] \times [0,1] \longrightarrow M_{\mathrm{QF}}$$

such that:

(a) for each fixed $u \in [0,1]$, the path $t \mapsto H(t,u)$ is again an admissible computation,

(b) $H(t,0) = \gamma_0(t)$ and $H(t,1) = \gamma_1(t)$,

(c) the relevant observable data are preserved along the deformation (for example, the same decorated invariants, or the same induced symbolic readout up to the chosen notion of equivalence).

Interpretation. This definition is intentionally regime-dependent. In the symbolic regime, a homotopy computation reduces to a path through a finite transition graph. In the quasi-fluidic regime, it is a path in the continuous phase configuration space M_{QF}, typically observed only through the stroboscopic return map and the readout Read. Thus, the same underlying idea—computation as an admissible path modulo invariant-preserving deformation—specializes to both discrete and continuous settings.

Remark 3.9. The point of the terminology is not that every computation is literally a topological homotopy, but that admissible evolutions in configuration space form path-like objects whose equivalence is controlled by the invariants one chooses to preserve. In the abelian quasi-fluidic corridor, these are typically gauge-invariant phase observables and their induced symbolic readouts.

Lie algebroid chart and Atiyah's linearization of flow. Readers from differential geometry may reasonably ask why we do not take Lie algebras and Lie brackets as the primary algebraic language throughout. The short answer is that our computational semantics is organized by *global, composable transport data* (paths, holonomy, winding/phase, and gluing across interfaces), and these are most naturally encoded at the groupoid level rather than by infinitesimal generators. Nothing here rejects the Lie-algebraic viewpoint; rather, it appears as a *linearization chart*. Given a Lie groupoid $\mathcal{G} \rightrightarrows M$, its infinitesimal object is the Lie algebroid

$$A(\mathcal{G}) \;:=\; \ker(ds)\big|_M \;\longrightarrow\; M, \qquad \rho := dt\big|_{A(\mathcal{G})} : A(\mathcal{G}) \to TM,$$

whose bracket on sections encodes first-order commutator information of local bisections. This is the many-object analogue of "Lie algebra = infinitesimal Lie group" [Wei96]. Thus, whenever one restricts to a sufficiently smooth regime where a genuine local symmetry pseudogroup governs evolution, one can pass from the groupoid semantics to an algebroid bracket calculus.

Atiyah's gauge-theoretic instance. In particular, for a principal G–bundle $P \to M$, the gauge groupoid $(P \times P)/G \rightrightarrows M$ has associated Lie algebroid

$$A \;\cong\; TP/G \;\to\; M,$$

fitting into the short exact "Atiyah sequence"

$$0 \;\to\; \mathrm{ad}(P) \;\to\; TP/G \;\to\; TM \;\to\; 0,$$

introduced by Atiyah in his study of connections. This is precisely the setting in which the Lie bracket formalism is maximally effective: it governs infinitesimal deformations of connections and local curvature evolution [Ati57].

Why we do not build the theory around brackets. The point of the "Algebra of Flow" emphasized here (4.2, 5.1) is that many of the invariants relevant to computation are inherently global and persist under operations for which infinitesimal linearization is either insufficient or not stable. Accordingly, we treat Lie algebroids (and brackets) as a *derived* local chart available in the upcoming fluidic/gauge regimes, while keeping the groupoid/decorated-path level as the primitive semantic layer. Unlike Lie algebras, Lie algebroids need not integrate to global Lie groupoids without additional conditions; integrability is controlled by explicit obstructions [CF03]. This reinforces the methodological choice: our semantics is formulated on the global/compositional side, with infinitesimal calculus used when (and only when) the regime admits it.

Boundary of the groupoid formalism: CJS and Floer flow categories. The decorated Lie groupoids introduced above encode reversible transport, gauge equivalence, and path-dependent geometric data. Their arrows are invertible, as required for a groupoid, and the passage to the thin fundamental groupoid permits connection-dependent quantities such as holonomy to be retained even when ordinary homotopy is trivial. This should be distinguished from the categorical structure appearing in Morse–Floer theory. There the relevant arrows are not equivalences but directed trajectories between critical configurations. If x and y are critical points of a Floer functional, the corresponding morphism object is a compactified moduli space $\overline{\mathcal{M}}(x, y)$ of flow trajectories, whose boundary strata are assembled from broken trajectories,

$$\partial\overline{\mathcal{M}}(x, z) \supseteq \bigcup_y \overline{\mathcal{M}}(x, y) \times \overline{\mathcal{M}}(y, z).$$

Such data are naturally organized by a *flow category*, rather than by a groupoid.

The ordinary Floer chain complex retains only a severe algebraic compression of the trajectory geometry: in particular, zero-dimensional moduli spaces supply the coefficients of the Floer differential. Cohen, Jones, and Segal proposed that, when the compactified trajectory spaces admit sufficiently coherent stable framings, the entire flow category may instead determine a stable homotopy type whose ordinary homology recovers Floer homology [CJS95, Coh19]. This should be regarded as a *homotopy refinement problem*, rather than as a universally missing object (in particular, see section A.3). Stable homotopy refinements have been constructed in important settings, notably Seiberg–Witten Floer theory [Man03], and recent work of Abouzaid and Blumberg gives a stable ∞-categorical formulation in which flow categories and flow bimodules produce Floer homotopy types, including an implementation for Hamiltonian Floer theory [AB24].

For the present construction, the dividing line is therefore explicit. The decorated Lie groupoid records *transport through a geometric configuration*; it does not by itself encode the full moduli spaces of dynamically admissible histories between critical configurations. A Floer-type refinement of geometric computation would require an additional directed layer in which admissible histories form compactified moduli spaces, broken histories supply their boundary strata, and suitable orientation, framing, or bordism data survive gluing. Only at that stage would a comparison with the Cohen–Jones–Segal construction, or with a corresponding Floer homotopy type, become mathematically substantive.

3.4 Connections and Phase Ledgers on a Trivial Helical Bundle

The finite twin–helix module used in the basic construction is locally modeled by a regular neighborhood of an embedded arc, and is therefore topologically

$$D^2 \times I \;\cong\; B^3.$$

Thus, as a D^2–bundle over the interval I, the local helical model is topologically trivial. In particular, there is no intrinsic bundle monodromy in the D^2 fibers. This does *not* mean that the geometry is computationally trivial. Rather, it means that the bundle class itself does not carry the information relevant to computation, but that additional geometric structure is placed on this trivial scaffold: chosen phase fields, connections, deformations, and local interface rules.

This is the correct abelian analogue of the Aharonov–Bohm (AB) viewpoint [AB59]. In the AB effect, the underlying space may be locally simple while the physically meaningful information is carried by phase accumulation of a $U(1)$ connection around loops. The same lesson applies here: even on a topologically trivial helical module, one may impose a phase field on the transverse circular directions in each cross-section, and the resulting loop integral defines a nontrivial $U(1)$ response. Thus, the relevant invariant in the present setting is not topological twisting of the bundle, but phase accumulation determined by the chosen geometric control data.

We therefore use the above product structure to isolate the abelian structure that will persist in later sections: an S^1–valued phase accumulated around transverse circles in a fixed cross-section. In modern language, this is most naturally described by a $U(1)$ connection on a trivial circle bundle over such loops (equivalently, a Hermitian line bundle with unitary connection). However, in the present discussion only the elementary notions of phase, curvature, and holonomy are required. As an organizational comparison, the product structure also means that local differential data may be written globally in coordinates; in this limited sense, one avoids the extra cocycle bookkeeping that would arise on a genuinely nontrivial fibration.

Fix a longitudinal parameter value $z_0 \in I$, and work in the transverse disk

$$D^2 \times \{z_0\}.$$

For each radius r for which the circle

$$\gamma_r(\theta) \;:=\; (r, \theta, z_0), \qquad \theta \in [0, 2\pi],$$

lies in the interior of the disk, let

$$A \;:=\; \Omega(r,\theta)\, d\theta$$

be a $U(1)$ connection one–form on that transverse slice. Define the associated phase ledger by

$$U(r) \;:=\; \exp\Big(i \int_{\gamma_r} A\Big) \;=\; \exp\Big(i \int_0^{2\pi} \Omega(r,\theta)\, d\theta\Big) \;\in\; U(1).$$

Proposition 3.2 (Radial Shear Identity)**.** *Let*

$$A := \Omega(r,\theta)\,d\theta \qquad \text{and} \qquad F := dA = \partial_r \Omega(r,\theta)\,dr \wedge d\theta$$

on a fixed transverse slice $D^2 \times \{z_0\}$. For $r_1 < r_2$, let γ_{r_1} and γ_{r_2} denote the circles of radii r_1 and r_2, and let

$$\mathcal{A}_{r_1,r_2} := [r_1, r_2] \times S^1$$

denote the annulus between them. Then

$$U(r_2)\,U(r_1)^{-1} \;=\; \exp\Big(i \int_{\mathcal{A}_{r_1,r_2}} F\Big).$$

Equivalently, the relative phase between the two radii is determined by the curvature flux through the annulus. In particular, if $\partial_r \Omega \equiv 0$ (no radial shear), then $F = 0$ on the annulus and $U(r)$ is independent of r.

Proof. By definition,

$$U(r_k) = \exp\Big(i \int_{\gamma_{r_k}} A\Big), \qquad k = 1, 2.$$

Hence

$$U(r_2)\,U(r_1)^{-1} = \exp\Big(i \int_{\gamma_{r_2}} A - i \int_{\gamma_{r_1}} A\Big) = \exp\Big(i \int_{\partial \mathcal{A}_{r_1,r_2}} A\Big).$$

Applying Stokes' theorem on the annulus gives

$$\int_{\partial \mathcal{A}_{r_1,r_2}} A = \int_{\mathcal{A}_{r_1,r_2}} dA = \int_{\mathcal{A}_{r_1,r_2}} F,$$

which proves the identity. If $\partial_r \Omega \equiv 0$, then $F = 0$ and therefore the phase ledger $U(r)$ is constant in r. □

Example 3.3 (Gluing and Composition of Relative Phase Ledgers). Let

$$A_1 = [r_0, r_1] \times S^1, \qquad A_2 = [r_1, r_2] \times S^1,$$

be two annular regions equipped with $U(1)$ connection one-forms

$$A^{(1)} = \Omega_1(r,\theta)\,d\theta, \qquad A^{(2)} = \Omega_2(r,\theta)\,d\theta,$$

defined in compatible boundary trivializations. Suppose the outer boundary of A_1 is identified with the inner boundary of A_2, and that the connection data agree smoothly along the common circle. Then the glued annulus

$$A_{\mathrm{gl}} = A_1 \cup_{\{r_1\} \times S^1} A_2$$

inherits a $U(1)$ connection A_{gl}.

For $k = 0, 1, 2$, let

$$\gamma_{r_k}(\theta) = (r_k, \theta), \qquad U_k := \exp\left(i \int_{\gamma_{r_k}} A_{\mathrm{gl}}\right).$$

The relative phase ledgers across the two component annuli are

$$L_1 := U_1 U_0^{-1}, \qquad L_2 := U_2 U_1^{-1}.$$

The relative ledger across the glued annulus is

$$L_{\mathrm{gl}} := U_2 U_0^{-1}.$$

These satisfy

$$L_{\mathrm{gl}} = L_2 L_1,$$

since

$$U_2 U_0^{-1} = \left(U_2 U_1^{-1}\right)\left(U_1 U_0^{-1}\right).$$

Let

$$F^{(1)} = dA^{(1)}, \qquad F^{(2)} = dA^{(2)}, \qquad F_{\mathrm{gl}} = dA_{\mathrm{gl}}.$$

By Stokes' theorem,

$$L_1 = \exp\left(i \int_{A_1} F^{(1)}\right), \qquad L_2 = \exp\left(i \int_{A_2} F^{(2)}\right),$$

and therefore

$$L_{\mathrm{gl}} = \exp\left(i \int_{A_{\mathrm{gl}}} F_{\mathrm{gl}}\right) = \exp\left(i \int_{A_1} F^{(1)}\right) \exp\left(i \int_{A_2} F^{(2)}\right).$$

Equivalently,

$$\int_{A_{\mathrm{gl}}} F_{\mathrm{gl}} = \int_{A_1} F^{(1)} + \int_{A_2} F^{(2)}.$$

Thus, in the abelian $U(1)$ corridor, curvature contributions add under radial gluing, while the corresponding relative phase changes multiply. Absolute loop holonomies multiply only under concatenation of the underlying paths, not merely from gluing the regions that contain them.

3.5 Lancret's Ghost?

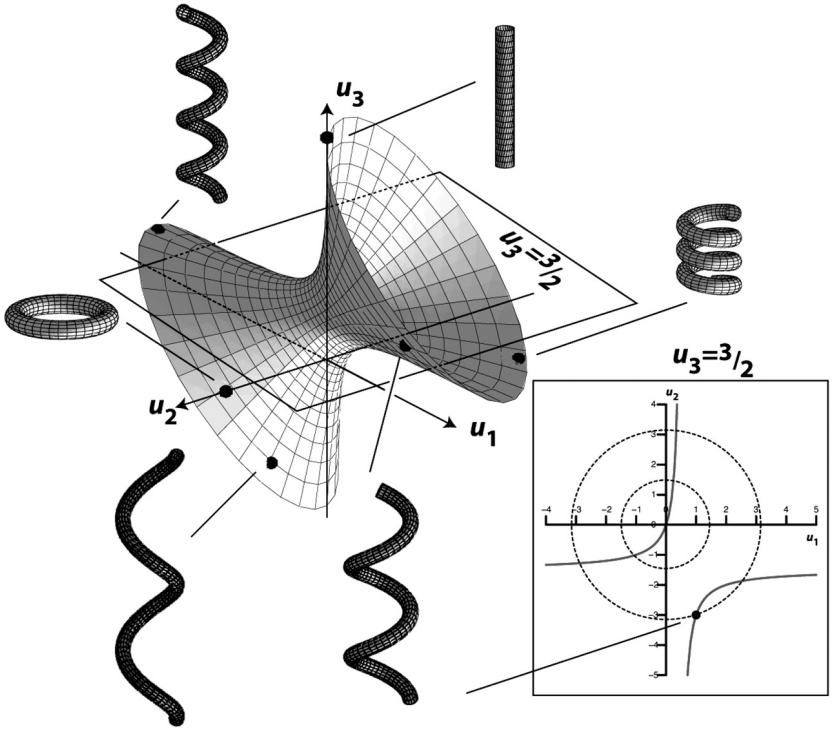


Figure 3: Homology, Helicity, and Hyperbolicity: a geometric "Rosetta Stone." *(Image Courtesy of Alain Goriely,"Helices" 2006)*

Helices are mathematical objects rich in dynamical variables—as explored in this section—whose properties interact synergistically but without the constraints of maximal symmetry. This flexibility has arguably obscured their structural significance. A helix is not merely a curve in space, but a framed, oriented 1–manifold carrying both axial and cyclic data. As earlier sections suggest, maximal symmetry tends to suppress geometric expressiveness, whereas physically useful computation requires enough asymmetry to support nontrivial state encoding and controlled transitions. Helices can dance with ones and zeros, but a sphere will never lie.

The helix presents a unique challenge in mathematical physics: despite its ubiquity in nature—from DNA to protein folding, to solitons—it resists easy classification. The standard helix relies on *transcendental* functions (e.g., $\gamma(t) = (a\cos t, a\sin t, bt)$) and as a result, it falls outside the traditional scope of algebraic geometry, which deals natively with polynomial varieties. In this sense, the helix

constitutes something of a disciplinary orphan: too smooth for pure combinatorics, too transcendental for algebraic geometry, and too continuous for discrete computation. Yet, for a theory of physical computation—especially one grounded in constructible geometric objects—this specific structure must take center stage.

Emergence of helices in nature. Helices occur constantly in physics, chemistry, and biology precisely because they integrate two forms of structure at once: cyclic phase and longitudinal transport. This tension may even be computationally significant. Recent work on the internal representations of large language models [KT25] suggests that gradient-based optimization can give rise to helical or helix-like internal organization for arithmetic tasks. Though such findings do not admit a universal interpretation, they at least reinforce the plausibility that helices are not merely common physical shapes, but natural carriers of computation whenever cyclic and linear degrees of freedom must be coordinated.

And while helices offer remarkable efficiency for encoding computational structure, it is essential to note that not all helices in nature are used for computation, nor do they dominate large-scale architectures. Helical forms excel at packing information, facilitating transmission, and exploiting symmetry at small scales (e.g., DNA and chiral molecules). However, at larger scales, nature often favors other symmetries—branching, fractal, planar, or modular structures—driven by stability, energetic, and functional constraints. Thus, the computational potential of helices arises not from their ubiquity but from their unique ability to localize and propagate information under appropriate conditions.

The helical moduli problem. Lancret's theorem (1802) already hints that "being helical" is not a local accident: a space curve $\gamma \subset \mathbb{R}^3$ is a general helix iff the Frenet invariants satisfy $\tau/\kappa \equiv C$. Equivalently, helices are integral curves of a geometric constraint in the 3-jet bundle of immersed curves [Bar97, Sau89]. In our setting, however, the computational objects are *thickened* and *decorated*: a helical *spine* carries a framed tubular neighborhood (cross-section data), marked boundary ports for gluing, and (in higher regimes) connection/holonomy data. The natural "moduli space" is therefore not a single finite-dimensional manifold, but a quotient of an infinite-dimensional configuration space by reparametrization and symmetry. Once one allows variation in framing, cross-section, pitch, chirality, and coupling data, the resulting parameter spaces become extremely large.

Definition 3.14 (Helical Moduli Stack, Working Model)**.** Fix a smooth compact *template* helical body H (e.g. a capped tube with marked base disk and chosen framing class) and a regularity class C^k (or Sobolev H^s) appropriate to the regime. Let $\mathrm{Emb}^k_{\mathrm{fr}}(H, \mathbb{R}^m)$ be the space of framed C^k-embeddings, and let $\mathrm{Diff}^k_{\mathrm{fr}}(H)$ act by reparametrization (preserving the marked boundary structure), together with the ambient Euclidean group $E(m)$ acting by rigid motion. We define the moduli *stack*

$$\mathfrak{M}^k_H \;:=\; \Big[\mathrm{Emb}^k_{\mathrm{fr}}(H, \mathbb{R}^m) \big/ \big(E(m) \times \mathrm{Diff}^k_{\mathrm{fr}}(H)\big)\Big],$$

and its coarse moduli space M^k_H as the corresponding orbit space when it is well-behaved. Allowing variable cross-sections amounts to fibering this construction over a shape space of embedded disks (or contours), which increases the functional degrees of freedom.

This formulation is concrete enough to state what must be constructed: local models (Banach/Fréchet charts depending on k or s), a stratification by singular phenomena (self-contact, self-intersection, knotting/linking type, degeneration to the torus-like and straight-rod limits), and gluing maps induced by the marked boundary ports. In particular, the difficulty is not naming the quotient; it is extracting computable invariants from it in a way that is stable under deformation and compatible with composition [EM70].

Once one treats computation or physics as *local-to-global* with observables defined locally on helical pieces and composed by gluing, one is forced toward an integration/pushforward formalism on a stratified quotient object. In other words, the analogue of a path integral or partition function in geometric computation is a functorial assignment built from (a) passage to moduli (quotienting by symmetry), and (b) a gluing law that behaves like a Fubini theorem for composition. Developing such an "integration on moduli of helical histories" is exactly the point at which one should expect derived/stacky and constructible techniques to enter, much as they do in Kontsevich-style theories of integration over highly singular, infinite-dimensional parameter spaces [Met03].

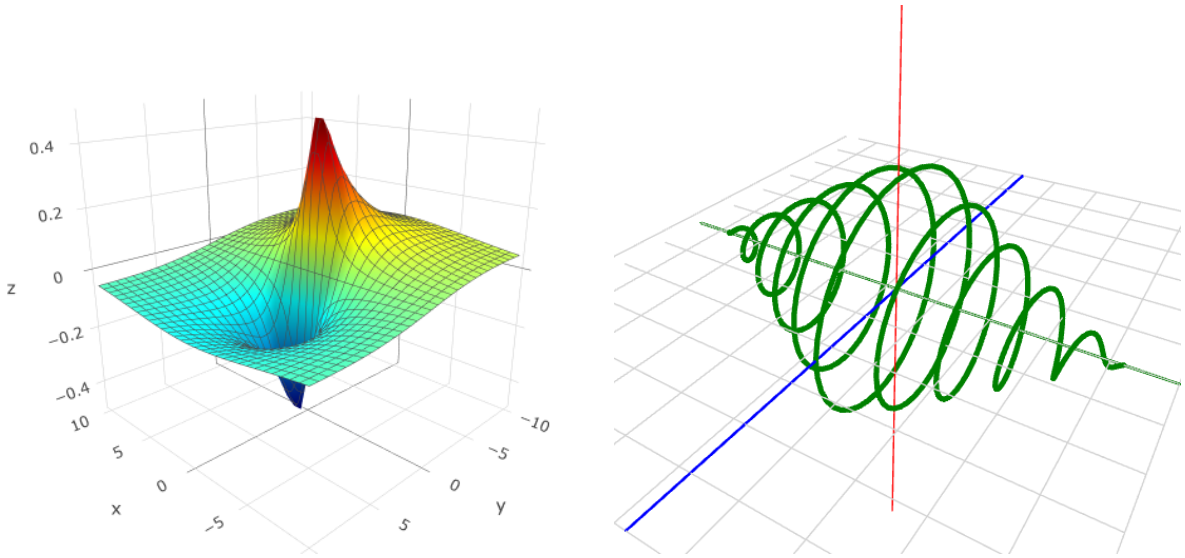
Overlooked but important reading on helicity. For a continuum–mechanics foundation on why helices are generic energy minimizers (and how curvature/torsion couple), see Goriely [Gor17]; for a crisp, canonical derivation of when minimizers are helical with pitch/radius set by constraints, see Chouaieb et al. [CGM06]. Developable–ribbon energetics and torsion–curvature locking—which motivate "channel" formation in cross–sections—are captured by Starostin van der Heijden [SvdH07]. On the geometric side that is often missed, Adachi [Ada09] provides a leading example of how (helical) Killing fields and foliations structure flows, aligning with our base–join transport picture. Ferrández Izquierdo's recent monograph [FI25] will also provide a focused, modern treatment of helical geometries to unify these threads for newcomers.

For all we know? Perhaps the key to modern quantum theory lurks quietly in the diagrams of a century-old German treatise [Lor02] on transcendental curves—waiting for someone to notice that helices and hyperboloids speak a universal geometric tongue.

4 Non-Abelian Geometric Computation

The abelian regime presents a remarkably economical picture of physical computation. A continuous geometric system may accumulate phase, retain winding information, and distinguish different paths while preserving a commutative algebra of transport. Yet this economy has a limit. Consider the familiar example of rotations in three-dimensional space: rotating an object about one axis and then another generally produces a different result from performing the same rotations in reverse. The individual transformations have not changed; what matters is their order of composition. In mathematical physics, Yang–Mills theory and non-abelian geometric phases provide a far-reaching generalization of this phenomenon. Internal transport is no longer adequately summarized by a single accumulated scalar phase, and the history of composition becomes part of the relevant geometric information.

For a theory of computation built from geometry, this raises a more fundamental problem than the introduction of additional continuous variables. If two individually admissible operations cannot be freely interchanged, then knowing the invariant content of each operation separately need not determine the invariant content of their composite. Local descriptions may remain perfectly well defined while their global assembly retains information that no independent collection of scalar phase ledgers captures. The challenge is therefore to formulate computation in a setting where ordered histories, geometric constraints, and invariant readouts coexist without sacrificing compositional consistency.



(a) BPST instanton: a finite-action, localized topological solution to the Yang–Mills equations, exhibiting geometric twist and winding [BPST75].

(b) Complex quantum wave: a superposition of oscillations, illustrating the intertwined, helical modes of computation.

Figure 4: Familiar examples of geometric configurations corresponding to Type 3 and Type 1 THM.

4.1 Gauge Transport and Computational Memory

The quasi–fluidic regime of the preceding section is governed primarily by abelian phase transport and finite local readouts. We now pass to the *fully fluidic* regime, in which the state of a geometric computer must be transported through a nontrivial bundle of local configurations. The appropriate language is therefore that of connections, curvature, holonomy, and their associated invariant data.

Gauge-geometric state space. Let

$$\pi : P \longrightarrow B$$

be a principal G-bundle over a computably presented base B, where B represents the working region of the geometric substrate. Let F be a finite-dimensional G-space describing the internal geometric variables carried by a twin helix cell, and let

$$E := P \times_G \mathsf{F} \longrightarrow B$$

be the associated state bundle.

A principal connection on P determines parallel transport between fibers. In a local trivialization $s : U \to P$, it is represented by a gauge potential

$$A = s^*\omega \in \Omega^1(U; \mathfrak{g}),$$

with curvature

$$F_A = dA + A \wedge A \in \Omega^2(U; \mathfrak{g}).$$

Globally, F_A is the corresponding adjoint-bundle-valued curvature two-form.

The connection specifies how local states may be transported; its curvature measures the infinitesimal obstruction to path-independent transport. A flat connection $F_A = 0$ may still possess nontrivial global holonomy when B is not simply connected, while a connection with $F_A \neq 0$ can exhibit local path dependence even when its structure group is abelian. Curvature therefore records local geometric memory, whereas holonomy records the accumulated transport around finite paths and cycles.

Within GCT, a *join* in this regime is no longer merely a symbolic identification of interfaces. It carries a transport map induced by the connection. Sequential composition of joins is therefore represented by composition of parallel transports.

Parallel transport and the interface groupoid. Let

$$\Pi_1^{\mathrm{thin}}(B)$$

denote the thin fundamental groupoid of B. Its objects are points of B, and its morphisms are paths modulo thin homotopy. A connection A defines a parallel-transport functor

$$\mathsf{PT}_A : \Pi_1^{\mathrm{thin}}(B) \longrightarrow \mathrm{Iso}(E),$$

where $\mathrm{Iso}(E)$ is the groupoid whose objects are fibers E_x and whose arrows are the transport isomorphisms between them.

We restrict this construction to the paths and boundary data admitted by the geometric computer.

Definition 4.1 (Interface Transport Groupoid)**.** The *interface transport groupoid*

$$\mathcal{J}_A$$

is the subgroupoid generated by parallel transports along admissible interface paths. Its objects are the boundary-state fibers associated with admissible interfaces, and a morphism

$$J : X \longrightarrow Y$$

is an admissible reversible transport from the state fiber X to the state fiber Y.

Composition in $\mathcal{J}_A$ is serial execution of transport, and path reversal determines inverse morphisms. Noninvertible operations such as coarse-graining, measurement, dissipation, or irreversible effects belong to the broader GCT process semantics and are not assumed to lie in $\mathcal{J}_A$.

For a path

$$\gamma : x \longrightarrow y,$$

we write

$$U_\gamma := \mathsf{PT}_A([\gamma])$$

for its parallel transport. After choosing local frames, this is represented by the familiar path-ordered exponential

$$U_\gamma = \mathcal{P} \exp\left(\int_\gamma A \right).$$

For a based loop $\gamma : x \to x$, the transport lies in the isotropy group

$$\mathrm{Aut}_{\mathcal{J}_A}(X_x),$$

and, in a chosen gauge, is represented by an element of G.

Definition 4.2 (Effective Holonomy Group)**.** For $x \in B$, the *effective holonomy group* of the connection at x is

$$\mathrm{Hol}_x(A) := \{ U_\gamma \mid \gamma : x \to x \},$$

with the appropriate closure when required. It is the subgroup of the structure group actually generated by closed admissible transports based at x.

The distinction between the nominal structure group G and the realized group $\mathrm{Hol}_x(A)$ is essential. A nonabelian structure group does not imply that a particular connection realizes noncommuting transport: the connection may reduce to an abelian subgroup. The computationally relevant question is therefore whether the *effective holonomy* is nonabelian.

Path dependence and relative holonomy. Two admissible transports can follow different geometric routes while having the same initial and terminal interfaces. Such parallel arrows cannot themselves be multiplied as though they were elements of a single group. Their difference is instead measured by closing them into a loop.

Definition 4.3 (Relative Join Holonomy)**.** Let

$$P, Q \in \mathrm{Hom}_{\mathcal{J}_A}(X, Y)$$

be two admissible transports having the same source and target. Their *relative join holonomy*, based at X, is

$$\Delta_X(P, Q) := Q^{-1} \circ P \in \mathrm{Aut}_{\mathcal{J}_A}(X).$$

Equivalently, one may base the comparison at Y:

$$\Delta_Y(P, Q) := P \circ Q^{-1} \in \mathrm{Aut}_{\mathcal{J}_A}(Y).$$

The two representatives are related by conjugation,

$$\Delta_Y(P, Q) = P \circ \Delta_X(P, Q) \circ P^{-1}.$$

Hence their conjugacy classes carry the same invariant information.

Thus

$$\Delta_X(P, Q) = \mathrm{id}_X$$

if and only if the two transports agree. Nontrivial relative holonomy records path dependence. It may occur already for an abelian connection with nonzero curvature.

This observation separates two notions that will play different roles below:

$$\boxed{\text{path dependence} \neq \text{noncommutativity.}}$$

Curvature can make transport path-dependent without making transport order-sensitive.

The join commutator. Order sensitivity is detected only after the relevant transports have been made into based cycles.

Definition 4.4 (Join Commutator)**.** Let

$$X \in \mathrm{Ob}(\mathcal{J}_A), \qquad J_1, J_2 \in \mathrm{Aut}_{\mathcal{J}_A}(X).$$

The *join commutator* of J_1 and J_2 is

$$[J_1, J_2]_X := J_1 \circ J_2 \circ J_1^{-1} \circ J_2^{-1} \in \mathrm{Aut}_{\mathcal{J}_A}(X).$$

The joins commute precisely when

$$[J_1, J_2]_X = \mathrm{id}_X,$$

or equivalently

$$J_1 \circ J_2 = J_2 \circ J_1.$$

We call the transport at X *order-sensitive* if there exist based join cycles J_1, J_2 such that

$$[J_1, J_2]_X \neq \mathrm{id}_X.$$

This construction is covariant under change of base object.

Proposition 4.1 (Covariance of the Join Commutator)**.** *Let*

$$K : X \longrightarrow Y$$

be an isomorphism in $\mathcal{J}_A$, and define

$$J_i^K := K \circ J_i \circ K^{-1} \in \mathrm{Aut}_{\mathcal{J}_A}(Y).$$

Then

$$[J_1^K, J_2^K]_Y = K \circ [J_1, J_2]_X \circ K^{-1}.$$

Consequently, the condition

$$[J_1, J_2]_X = \mathrm{id}_X$$

is independent of the chosen representative, and the conjugacy class

$$\big[[J_1, J_2]_X\big]$$

is invariant under transport of the base object.

Proof. Associativity and cancellation give

$$\begin{aligned}
[J_1^K, J_2^K]_Y &= (KJ_1K^{-1})(KJ_2K^{-1})(KJ_1^{-1}K^{-1})(KJ_2^{-1}K^{-1}) \\
&= K(J_1J_2J_1^{-1}J_2^{-1})K^{-1} \\
&= K[J_1, J_2]_X K^{-1}.
\end{aligned}$$

□

After choosing a local frame, based cycles are represented by ordinary holonomies $U_{\gamma_i} \in G$, and the categorical commutator becomes

$$[U_{\gamma_1}, U_{\gamma_2}] = U_{\gamma_1} U_{\gamma_2} U_{\gamma_1}^{-1} U_{\gamma_2}^{-1}.$$

A gauge transformation conjugates this element. Thus the statement that the commutator is trivial is gauge invariant, as are class functions of the commutator.

Remark 4.1 (Path Dependence versus Order Sensitivity). The two constructions measure genuinely different phenomena.

For two routes

$$P, Q : X \longrightarrow Y,$$

the condition

$$\Delta_X(P, Q) \neq \mathrm{id}_X$$

records path dependence. This can occur in a $U(1)$ theory.

By contrast,

$$[J_1, J_2]_X \neq \mathrm{id}_X$$

records the order dependence of two-based transport cycles. This requires a nonabelian effective holonomy group.

Accordingly, abelian curvature may already store geometric context, while a nontrivial join commutator supplies the additional resource of order-sensitive transport.

Curvature and the generation of holonomy. The relationship between curvature and holonomy is not merely heuristic. Infinitesimally, the curvature determines the leading failure of parallel transport around sufficiently small loops to close trivially. Globally, the Ambrose–Singer theorem identifies the Lie algebra of the holonomy group with the algebra generated by curvature transported back to a common base point [AS53].

Schematically,

$$\mathfrak{hol}_x(A) = \mathrm{span}\left\{ \mathrm{Ad}_{U_\eta^{-1}} F_y(u, v) \;\middle|\; \eta : x \to y,\ u, v \in T_y B \right\},$$

with the usual interpretation in the principal bundle.

Thus curvature provides the infinitesimal generators from which the effective holonomy algebra is assembled. In particular,

$$\mathrm{Hol}_x(A) \text{ abelian} \quad \Longrightarrow \quad [J_1, J_2]_X = \mathrm{id}_X$$

for every pair of based join cycles, whereas the existence of

$$[J_1, J_2]_X \neq \mathrm{id}_X$$

directly witnesses a nonabelian realized holonomy sector.

Notice that neither nonzero curvature nor nontrivial topology alone forces this conclusion. A $U(1)$ connection may have nonzero curvature and nontrivial global holonomy while all transports still commute. Handles, defects, and curvature enlarge the possible memory channels; noncommutativity appears only when the effective transport group itself is nonabelian.

Holonomy as computational memory. For a closed admissible path γ, the *holonomy*

$$U_\gamma = \mathcal{P} \exp\left(\oint_\gamma A \right)$$

stores the cumulative result of transport around the cycle. Under a change of gauge at the base point,

$$U_\gamma \longmapsto g(x) U_\gamma g(x)^{-1},$$

so the matrix representative is not itself an invariant. Its conjugacy class and class functions are.

In a representation

$$\rho : G \longrightarrow GL(V),$$

the Wilson-loop observable

$$W_\rho(\gamma) := \mathrm{tr}\big(\rho(U_\gamma)\big)$$

is the standard example [Wil74]. In GCT, this supplies a natural gauge-invariant readout of a closed execution cycle.

The computational interpretation is therefore:

(a) **Registers as cycles.** Distinguished loops or interface cycles carry holonomy data $\{[U_{\gamma_k}]\}$.

(b) **Updates as transport.** Control fields, deformations, and gluings modify the connection or the admissible path system and therefore modify the associated transports.

(c) **Relative memory as path comparison.** Distinct routes between the same interfaces are compared by $\Delta_X(P, Q)$.

(d) **Order-sensitive memory as commutator.** Noncommuting closed transports are detected by $[J_1, J_2]_X$.

(e) **Observable output.** Gauge-invariant readouts are extracted from conjugacy classes, characters, Wilson-loop traces, characteristic classes, spectral indices, or other invariant functions of the transport data.

The essential progression is therefore

$$\text{connection} \longrightarrow \text{parallel transport} \longrightarrow \text{relative holonomy} \longrightarrow \text{join commutator}.$$

The first two stages already occur in abelian phase geometry. The final stage detects the genuinely nonabelian resource: the output of a composite transport may depend on the order in which admissible cycles are executed.

From Berry phase to Wilczek–Zee transport. The preceding construction has a standard realization in adiabatic geometry. Suppose the relevant internal states form a Hermitian vector bundle

$$E \longrightarrow B.$$

For an isolated nondegenerate state, the adiabatic eigenspace is a line bundle, and its Berry connection has effective structure group $U(1)$ [Ber84]. Its holonomies are phases and therefore commute.

If instead an m-dimensional eigenspace remains degenerate over a region of parameter space, the adiabatic connection takes values in $\mathfrak{u}(m)$, producing Wilczek–Zee transport [WZ84]. Such a connection *may* have nonabelian holonomy. For $m = 2$,

$$U(2) \cong \frac{SU(2) \times U(1)}{\mathbb{Z}_2},$$

so after separating the central phase, the traceless part supplies an $SU(2)$-type transport sector.

Neither rank $m \geq 2$ nor degeneracy alone guarantees noncommuting holonomies: the realized connection may still reduce to an abelian subgroup. Symmetries, couplings, boundary conditions, and controlled deformations of the twin helix substrate determine whether the effective holonomy is genuinely nonabelian. In particular, anisotropy may either split an existing degeneracy or participate, together with couplings and constraints, in selecting a protected multidimensional subspace. The operational criterion remains

$$[J_1, J_2]_X \neq \mathrm{id}_X.$$

Chern–Weil readouts. Holonomy records transport around particular cycles. Chern–Weil theory supplies a complementary mechanism for compressing curvature into stable global invariants [BT82].

Let

$$p : \mathfrak{g}^{\otimes k} \longrightarrow \mathbb{R}$$

be an Ad-invariant polynomial. Then

$$p(F_A, \ldots, F_A)$$

is a closed $2k$-form, and its de Rham cohomology class is independent of the chosen connection. Familiar examples include representatives of Chern and Pontryagin classes. In particular, expressions of the form

$$\mathrm{tr}(F_A \wedge F_A)$$

encode four-dimensional characteristic data.

From the computational viewpoint, this provides a canonical instance of *curvature-as-readout*:

$$\text{local curvature data} \longrightarrow \text{closed characteristic form} \longrightarrow \text{deformation-stable global class}.$$

The characteristic class does not retain the full connection or all of its holonomy data; it is instead a controlled compression into a stable global sector label.

Chern–Simons forms provide the corresponding transgression data. In a local presentation,

$$d\,\mathrm{CS}_{2k-1}(A) = p(F_A, \ldots, F_A),$$

so a Chern–Simons quantity may be regarded as a boundary or history-dependent ledger whose change records the characteristic density swept out by a higher-dimensional interpolation. This relationship will reappear below when histories are treated as bordisms.

Topological memory channels. A twin helix configuration may also carry order-parameter fields independent of the connection itself. For example, an internal orthonormal frame can determine a unit vector field

$$n : B_0 \longrightarrow S^2$$

on an appropriate region $B_0 \subseteq B$. Depending on the relevant order-parameter space and spatial dimension, familiar topological sectors include

$$\pi_1(S^1) \cong \mathbb{Z}, \qquad \pi_2(S^2) \cong \mathbb{Z}, \qquad \pi_3(S^2) \cong \mathbb{Z}.$$

These correspond respectively to vortex or phase winding, skyrmion-type degree, and Hopf-type linking of preimages.

These homotopy classes should not themselves be identified with nonabelian gauge transport. A skyrmion or Hopf sector is a statement about the topology of an order-parameter map, whereas nonabelianity is a statement about composition in the effective holonomy group. When the texture is coupled to the gauge connection, however, the two structures may interact: a topological sector can constrain admissible connections, defects, boundary conditions, and hence the possible holonomy readouts.

GCT therefore distinguishes at least three sources of persistent memory:

$$\begin{aligned} \text{curvature} &: \text{local obstruction to path independence,} \\ \text{holonomy} &: \text{finite cyclic transport memory,} \\ \text{topological class} &: \text{deformation-stable sector memory.} \end{aligned}$$

None of these should be collapsed into the others.

Expressive consequence. The passage from $U(1)$ phase transport to nonabelian holonomy enlarges the available process algebra by introducing order-sensitive composition. Relative holonomy already distinguishes paths; a nontrivial join commutator additionally distinguishes the order of closed operations.

This supplies a natural candidate witness for the increase in expressiveness discussed in theorem 2.2, as one now jumps across within table 6 from a fuzzy ordered algebraic flow on one end to a chaotic form of geometric analog flow on the other. The claim must nevertheless be interpreted in the relational sense of the EVT framework: noncommuting transport does not prove that an arbitrary classical universal machine cannot simulate the corresponding matrix calculations. Rather, it demonstrates that a translation which is required to preserve the native geometric interfaces, transport composition, and gauge-invariant readouts cannot simply collapse the nonabelian regime back to the abelian phase semantics without discarding structure.

Example 4.1 (Spectral Flow as a Computable Readout). Let B be a compact odd-dimensional manifold, let

$$E \longrightarrow B$$

be a Hermitian vector bundle, and let

$$\{A_t\}_{t \in S^1}$$

be a smooth periodic family of unitary connections. Associated to this family, choose a smooth periodic family of self-adjoint Dirac-type operators

$$D_{A_t} : \Gamma(E) \longrightarrow \Gamma(E).$$

Assume that the operators are Fredholm with discrete spectrum and that zero is crossed only at isolated parameters.

The spectral flow

$$\mathrm{sf}\{D_{A_t}\}_{t \in S^1} \in \mathbb{Z}$$

is the signed number of eigenvalues crossing zero during one control cycle.

The periodic family, or a family periodic up to a specified gauge identification, determines the corresponding bundle

$$\widetilde{E} \longrightarrow B \times S^1$$

and the operator

$$\mathcal{D} = \frac{\partial}{\partial t} + D_{A_t}.$$

The spectral-flow index theorem gives

$$\mathrm{sf}\{D_{A_t}\}_{t\in S^1} = \mathrm{ind}(\mathcal{D}).$$

The Atiyah–Singer theorem [AS63] then expresses this integer topologically:

$$\mathrm{ind}(\mathcal{D}) = \int_{B\times S^1} \Big[\widehat{A}\big(T(B\times S^1)\big)\,\mathrm{ch}(\widetilde{E})\Big]_{\dim B+1}.$$

In the simplest abelian case, take

$$B = S^1, \qquad B\times S^1 = T^2,$$

and let

$$L \longrightarrow T^2$$

be a complex line bundle with curvature F. For the corresponding family of one-dimensional Dirac-type operators,

$$\mathrm{sf}\{D_{A_t}\} = \big\langle c_1(L), [T^2]\big\rangle = \frac{1}{2\pi}\int_{T^2} F \in \mathbb{Z},$$

with the conventional normalization of the connection understood. Thus a periodic control cycle produces an integer readout determined by the first Chern class.

For a nonabelian example, let

$$\dim B = 3$$

and let

$$\widetilde{E} \longrightarrow B\times S^1$$

carry an $SU(r)$-connection. The degree-four gauge contribution is governed, up to the chosen trace and sign convention, by the instanton number

$$k = \frac{1}{8\pi^2}\int_{B\times S^1} \mathrm{tr}(F\wedge F) \in \mathbb{Z}.$$

When the remaining tangent-bundle contribution is fixed or trivial in the regime under consideration, this characteristic number determines the corresponding gauge contribution to the index and hence to the spectral-flow readout.

Spectral flow therefore provides an explicit example of analytic compression where an integer index classifies a continuous family of operators. The integer may be obtained either from signed eigenvalue crossings or from the appropriate characteristic class on the mapping torus. It is the spectrum of the family $\{D_{A_t}\}$, rather than the spectrum of a single holonomy matrix, that undergoes spectral flow.

Remark 4.2 (Holonomy and Spectral Flow). Holonomy and spectral flow are distinct but complementary readouts. Holonomy assigns a transport automorphism, or invariantly its conjugacy class, to a closed path. Spectral flow assigns an integer to a closed family of self-adjoint operators. Curvature enters the former through parallel transport and the latter through the characteristic forms appearing in the index density.

Hamiltonian and contact presentations. The gauge description above does not require the fully fluidic state space to be symplectic. In regimes that additionally admit a Hamiltonian formulation, however, the same process semantics *can* be expressed in standard symplectic and contact language.

Let

$$(X,\omega)$$

be a symplectic phase space with Hamiltonian H, and let

$$\Sigma = H^{-1}(c)$$

Computational notion	Gauge-geometric realization
Local state description	Choice of local section, frame, or gauge representative
Admissible interface update	Parallel transport along an interface path
Sequential execution	Composition of transport morphisms
Alternative execution paths	Parallel arrows compared by relative holonomy
Closed execution cycle	Based loop and its holonomy
Order-sensitive execution	Nontrivial join commutator
Local geometric memory	Curvature and its gauge-covariant transport data
Persistent cyclic memory	Holonomy conjugacy class
Gauge-invariant scalar readout	Class function such as a Wilson-loop trace
Global sector readout	Characteristic class, index, or related topological invariant
Equivalent local descriptions	Gauge-related representatives preserving invariant observables

Table 7: Computational semantics of gauge transport. The correspondence is operational: local representatives may depend on a chosen frame, whereas observable output is extracted from gauge-invariant functions or equivalence classes of the resulting transport.

be a regular energy hypersurface of contact type. Thus, in a neighborhood of Σ, suppose

$$\omega = d\lambda$$

and

$$\alpha := \lambda|_{\Sigma}$$

is a contact form; equivalently, the associated Liouville vector field is transverse to Σ. The Reeb vector field R_α is defined by

$$\alpha(R_\alpha) = 1, \qquad d\alpha(R_\alpha, \cdot) = 0$$

[MS17, Gei08].

Since the restriction of X_H to a regular energy hypersurface lies in its characteristic line field, one has, for an appropriate choice of orientation,

$$X_H|_{\Sigma} = fR_\alpha$$

for a nonvanishing function f, positive after compatible orientation conventions. Closed Hamiltonian characteristics are therefore reparametrized periodic Reeb trajectories.

In such a presentation, robust periodic execution cycles in GCT may be studied using the action, index, and orbit invariants familiar from contact and Floer geometry. Symplectic field theory provides a much richer algebraic structure built from such Reeb data [EGH00]. We do not assume that machinery here. The point is instead that whenever a fully fluidic GCM admits a Hamiltonian/contact realization, its periodic computational cycles have a standard geometric interpretation for those readers familiar with Hofer-style dynamics. The contact/Reeb description is best viewed as a *change of mathematical presentation under additional hypotheses*, not an extra ontological postulate of GCT.

The Wu–Yang dictionary and its computational extension. The gauge-geometric ingredients used above are standard. In the Wu–Yang picture [WY75], the gauge potential is a local representative of a connection, the field strength is its curvature, gauge transformations relate local representatives, and nonintegrable phase factors are parallel transports or holonomies. The same language underlies the modern treatment of monopoles, instantons, calorons, and other nonperturbative gauge configurations.

Within GCT, these standard gauge-theoretic constructions acquire operational roles when the geo-

metric substrate is treated as a computational process:

$$\begin{aligned}
\text{connection} &\longleftrightarrow \text{transport/update law},\\
\text{curvature} &\longleftrightarrow \text{local path-dependent context},\\
\text{parallel transport} &\longleftrightarrow \text{admissible interface update},\\
\text{relative holonomy} &\longleftrightarrow \text{comparison of execution paths},\\
\text{join commutator} &\longleftrightarrow \text{order-sensitive composition},\\
\text{holonomy class} &\longleftrightarrow \text{persistent cyclic memory},\\
\text{transition function} &\longleftrightarrow \text{interface gluing rule},\\
\text{characteristic class} &\longleftrightarrow \text{global sector invariant}.
\end{aligned}$$

The resulting hierarchy clarifies what is meant here by *curvature as computation*. Curvature is not itself an instruction set, and a nonabelian gauge group is not automatically a computer. Rather, the connection specifies admissible transport, curvature controls its infinitesimal path dependence, topology supplies additional global sectors, and holonomy records the accumulated result of closed transport. When the effective holonomy becomes nonabelian, the join commutator adds an intrinsically order-sensitive layer of composition.

The fully fluidic regime therefore differs from the quasi–fluidic $U(1)$ corridor not merely by possessing more continuous degrees of freedom, but by admitting a richer compositional geometry:

$$\boxed{\text{phase} \longrightarrow \text{transport} \longrightarrow \text{curvature} \longrightarrow \text{holonomy} \longrightarrow \text{noncommuting composition}.}$$

This ordered transport structure is the starting point for the nonabelian Algebra of Flow developed in the following subsection.

4.2 The Algebra of Flow

The preceding section established that geometric computation may be organized by transport, curvature, and holonomy, with the join commutator distinguishing genuinely order-sensitive composition. We now return to the geometry of the twin helix itself. The question is no longer merely how nonabelian transport is represented, but how the geometric degrees of freedom of a helical substrate can supply the transformations from which such transport is constructed.

There are two related mechanisms. First, relaxing rotational symmetry enlarges the available cross-sectional geometry, admitting anisotropies, distinct angular channels, and additional couplings. Second, the moving orthonormal frame of a helix naturally takes values in $SO(3)$, whose spinorial double cover is $SU(2)$. When the corresponding rotation directions become independently controllable, they provide the algebraic ingredients for noncommuting transport.

These mechanisms should be distinguished. Breaking the rotational symmetry of a cross-section does not itself produce a non-abelian connection, and the existence of an $SU(2)$ spinorial lift does not itself establish nontrivial Yang–Mills curvature. Nevertheless, together they identify a natural geometric route from helical form to a non-abelian algebra of admissible operations.

Cross-sectional symmetry and geometric freedom. Recall the cross-sectional shape families introduced in section 2.2. A circular cross-section is invariant under every rotation about its central axis. A general smooth cross-section need not possess this symmetry.

To quantify the distinction, consider the space of smooth, strictly positive radial profiles

$$\mathcal{S} := \left\{ r \in C^\infty(S^1, \mathbb{R}) \;\middle|\; r(\theta) > 0 \right\}.$$

Each profile determines a star-shaped embedded contour

$$\Gamma_r(\theta) = r(\theta) \begin{pmatrix} \cos\theta \\ \sin\theta \end{pmatrix}.$$

The positivity condition ensures that this parametrization defines a regular simple closed curve. The space $\mathcal{S}$ is an infinite-dimensional smooth configuration space, modeled on the Fréchet space $C^\infty(S^1, \mathbb{R})$.

A radial profile admits a Fourier expansion

$$r(\theta) = a_0 + \sum_{k=1}^{\infty} \left(a_k \cos(k\theta) + b_k \sin(k\theta) \right),$$

where the coefficients decay sufficiently rapidly to represent a smooth function.

Full rotational invariance requires

$$r(\theta + \varphi) = r(\theta) \qquad \text{for every } \varphi \in S^1,$$

and therefore forces

$$r(\theta) = a_0.$$

Thus, within this family, continuous rotational symmetry reduces the cross-sectional shape space to a one-dimensional family of circles.

By contrast, imposing only finite rotational symmetry of order n requires

$$r\left(\theta + \frac{2\pi}{n}\right) = r(\theta),$$

which permits every Fourier harmonic whose index is divisible by n. Even this restricted space remains infinite-dimensional in the unrestricted smooth category.

Proposition 4.2 (Rotational Symmetry and Angular Mode Capacity)**.** *Let*

$$\mathcal{F}_K = \left\{ a_0 + \sum_{k=1}^{K} \left(a_k \cos(k\theta) + b_k \sin(k\theta) \right) \right\}$$

be the real vector space of trigonometric polynomials of degree at most K. Let

$$\mathcal{F}_{n,K} = \left\{ r \in \mathcal{F}_K \;\middle|\; r\left(\theta + \frac{2\pi}{n}\right) = r(\theta) \right\}$$

be its C_n-invariant subspace.

Then

$$\dim \mathcal{F}_K = 2K + 1,$$

and

$$\dim \mathcal{F}_{n,K} = 2 \left\lfloor \frac{K}{n} \right\rfloor + 1.$$

Consequently, the fraction of permitted angular modes is

$$E_K(n) = \frac{2\lfloor K/n \rfloor + 1}{2K + 1}.$$

For fixed K, this quantity is nonincreasing with n. When $n > K$, only the angular zero mode remains.

Proof. Under rotation by $2\pi/n$, the complex Fourier basis transforms according to

$$e^{ik\theta} \longmapsto e^{2\pi ik/n} e^{ik\theta}.$$

Invariance requires

$$e^{2\pi ik/n} = 1,$$

which holds precisely when

$$k \in n\mathbb{Z}.$$

Within the cutoff $|k| \le K$, the permitted frequencies are therefore

$$k = 0,\ \pm n,\ \pm 2n, \ldots, \pm \left\lfloor \frac{K}{n} \right\rfloor n.$$

Counting these frequencies gives

$$\dim \mathcal{F}_{n,K} = 2 \left\lfloor \frac{K}{n} \right\rfloor + 1.$$

Division by $\dim \mathcal{F}_K = 2K + 1$ proves the result. □

The proposition gives a finite-cutoff measure of a more general phenomenon. In the unrestricted smooth category, removing continuous rotational symmetry releases an infinite family of angular shape parameters. The finite-dimensional approximation records how many of these parameters survive a prescribed residual symmetry.

This is a statement about *geometric configuration freedom*, not yet about computational macro-expressiveness. In particular, the dimension of a shape space does not by itself determine the range of admissible computations.

Fourier selection rules and transport channels. The Fourier calculation has a second interpretation. Suppose a linearized transport or coupling operator

$$L : \mathcal{H} \longrightarrow \mathcal{H}$$

acts on an angular function space $\mathcal{H}$ and commutes with a C_n rotation operator T_n:

$$LT_n = T_n L.$$

Then L preserves the isotypic decomposition of $\mathcal{H}$ under the C_n action.

In the Fourier basis, this means that matrix elements between angular modes vanish unless

$$m \equiv m' \pmod{n}.$$

Equivalently, the operator decomposes into blocks indexed by angular momentum modulo n.

This is the familiar origin of symmetry selection rules. A residual rotational symmetry restricts which angular channels can couple, while symmetry breaking permits additional off-diagonal couplings. The corresponding calculation for cross-sectional flow fields is recorded in section A.8.

Importantly, block diagonalization does not imply that all operators acting within a block commute. A multidimensional isotypic component may support noncommuting internal transformations. The selection rule determines which channels may interact; the algebra of the permitted interaction operators determines whether their compositions commute.

Thus the passage

$$SO(2) \longrightarrow C_n \longrightarrow \{e\}$$

describes a progressive relaxation of spatial rotational constraints. It should not be confused with a change from an internal $U(1)$ gauge group to $SU(2)$. The two structures are mathematically related through the available geometric controls, but they are distinct group actions.

The moving-frame origin of $SU(2)$. The second mechanism is intrinsic to the helical spine. A regular space curve with nonvanishing curvature carries a Frenet–Serret frame

$$R(s) = \begin{pmatrix} T(s) & N(s) & B(s) \end{pmatrix} \in SO(3),$$

where s is arc length and the frame is positively oriented.

The Frenet–Serret equations are

$$\begin{aligned} T' &= \kappa N, \\ N' &= -\kappa T + \tau B, \\ B' &= -\tau N, \end{aligned}$$

with curvature $\kappa(s)$ and torsion $\tau(s)$.

In matrix form,

$$R^{-1}\frac{dR}{ds} = \Omega(s) = \begin{pmatrix} 0 & -\kappa & 0 \\ \kappa & 0 & -\tau \\ 0 & \tau & 0 \end{pmatrix}.$$

Writing J_a for the standard generators of $\mathfrak{so}(3)$, we obtain

$$\Omega(s) = \tau(s)J_1 + \kappa(s)J_3.$$

Thus the differential geometry of a helix directly supplies two rotational directions, associated with torsion and curvature. They belong to the Lie algebra

$$\mathfrak{so}(3),$$

whose simply connected covering group is

$$\mathrm{Spin}(3) \cong SU(2).$$

The standard double covering

$$p : SU(2) \longrightarrow SO(3)$$

has kernel

$$\ker p = \{\pm I\},$$

and consequently

$$SO(3) \cong SU(2)/\{\pm I\}.$$

In the fundamental representation, the covering map is characterized by

$$U(\mathbf{v} \cdot \boldsymbol{\sigma})U^\dagger = \big(p(U)\mathbf{v}\big) \cdot \boldsymbol{\sigma},$$

where

$$\boldsymbol{\sigma} = (\sigma_1, \sigma_2, \sigma_3)$$

denotes the triple of Pauli matrices.

Proposition 4.3 (Spinorial Lift of Helical Frame Transport)**.** *Let*

$$\gamma : I \longrightarrow \mathbb{R}^3$$

be a unit-speed C^3 curve with nonvanishing curvature, and let

$$R : I \longrightarrow SO(3)$$

be its Frenet–Serret frame.

After choosing a lift of the initial frame, there exists a unique lifted path

$$\widetilde{R} : I \longrightarrow SU(2)$$

such that

$$p \circ \widetilde{R} = R.$$

With the standard Pauli-matrix convention,

$$\widetilde{R}^{-1}\frac{d\widetilde{R}}{ds} = -\frac{i}{2}\left(\tau(s)\sigma_1 + \kappa(s)\sigma_3\right).$$

If the frame traces a closed loop in $SO(3)$, the endpoint of its lifted path differs from the initial lift by an element of $\{\pm I\}$. The sign detects the corresponding class in

$$\pi_1(SO(3)) \cong \mathbb{Z}_2.$$

Proof. The map

$$SU(2) \longrightarrow SO(3)$$

is a covering map, so the path-lifting property gives a unique lift once its initial value is specified.

Under the standard Lie-algebra identification, an infinitesimal spatial rotation with angular velocity

$$\boldsymbol{\omega} = (\omega_1, \omega_2, \omega_3)$$

is represented in $\mathfrak{su}(2)$ by

$$-\frac{i}{2}\boldsymbol{\omega} \cdot \boldsymbol{\sigma}.$$

The Frenet–Serret matrix Ω corresponds to the angular-velocity vector

$$\boldsymbol{\omega} = (\tau, 0, \kappa).$$

Substitution gives the asserted lifted generator.

For a closed frame loop, the two endpoints of the lift project to the same element of $SO(3)$, and therefore differ by an element of the covering kernel $\{\pm I\}$. This distinction agrees with the two homotopy classes of loops in $SO(3)$. □

The proposition identifies a natural spinorial representation of helical frame transport. A full 2π spatial rotation returns an ordinary frame to its original orientation, while its lifted action on the fundamental spin representation is

$$\widetilde{R}(2\pi) = -I.$$

The lift returns to $+I$ after a 4π rotation.

This double-cover structure is not imposed as an independent symmetry of the twin helix. It arises from the ordinary rotational geometry of its moving frame.

There is, however, an essential limitation. The differential form

$$R^{-1}dR$$

is a pure-gauge frame connection wherever the frame is globally defined. Its spinorial lift

$$\widetilde{R}^{-1}d\widetilde{R}$$

satisfies the Maurer–Cartan equation and has vanishing curvature. The existence of the spin lift therefore does not by itself generate a nonflat $SU(2)$ gauge field.

Moreover, the moving frame of the single conical helix defined in (1) has variable curvature and torsion, but their ratio satisfies Lancret's condition $\tau(s)/\kappa(s) = q$ for a constant q. Its lifted Frenet–Serret generator consequently takes the form

$$-\frac{i}{2}\kappa(s)(q\sigma_1 + \sigma_3).$$

Generators at different points of the spine are thus proportional to the same element of $\mathfrak{su}(2)$ and commute. The spinorial evolution remains in a single one-parameter subgroup: screw–dilation changes the magnitude of the generator, not its Lie-algebra direction.

The additional ingredient required for non-abelian computation is independent control over distinct rotation directions, together with a connection for which their associated transports do not reduce to a single commuting subgroup.

Independent geometric controls and non-abelian curvature. The twin helix construction provides several candidate mechanisms for such control: variations in curvature and torsion, cross-sectional anisotropy, coupling between the two helical strands, and boundary conditions which select distinct internal transport channels.

To exhibit the algebraic mechanism explicitly, consider a two-dimensional control region

$$D \subset \mathbb{R}^2$$

with coordinates (u, v), equipped with a rank-two Hermitian state bundle. The two control directions are taken to act through independent spinorial rotation generators.

Choose an $\mathfrak{su}(2)$-valued connection

$$\mathcal{A} = -\frac{i}{2}\left(a\sigma_1\, du + b\sigma_3\, dv\right), \qquad a, b \in \mathbb{R} \setminus \{0\}.$$

We use the convention

$$\nabla = d + \mathcal{A}, \qquad \mathcal{F} = d\mathcal{A} + \mathcal{A} \wedge \mathcal{A}.$$

The two generators are motivated by the torsion and curvature directions appearing in the lifted Frenet–Serret equations. The connection is an explicit controlled model; its realization by a particular twin helix interaction law remains a separate dynamical requirement.

Proposition 4.4 (Non-Abelian Holonomy from Independent Helical Rotation Channels)**.** *Let $D \subset \mathbb{R}^2$ be a connected, simply connected open control region, and let*

$$\mathcal{A} = -\frac{i}{2}\left(a\sigma_1\, du + b\sigma_3\, dv\right)$$

be the connection defined above, with $a, b \neq 0$.

Then

$$\mathcal{F} = \frac{iab}{2}\sigma_2\, du \wedge dv \neq 0,$$

and the holonomy Lie algebra is

$$\mathfrak{hol}(\mathcal{A}) = \mathfrak{su}(2).$$

Consequently, the holonomy group is $SU(2)$.

Proof. The connection coefficients are constant, so

$$d\mathcal{A} = 0.$$

The curvature is therefore determined by the commutator of the two connection components:

$$\mathcal{F}_{uv} = [\mathcal{A}_u, \mathcal{A}_v].$$

Using

$$[\sigma_1, \sigma_3] = -2i\sigma_2,$$

we obtain

$$\begin{aligned}\mathcal{F}_{uv} &= \left[-\frac{ia}{2}\sigma_1, -\frac{ib}{2}\sigma_3\right] \\ &= \frac{iab}{2}\sigma_2.\end{aligned}$$

The curvature initially supplies the σ_2 direction. Parallel transport of curvature along the two control directions supplies the remaining generators.

Indeed, the gauge-covariant derivatives satisfy

$$D_u\mathcal{F}_{uv} = [\mathcal{A}_u, \mathcal{F}_{uv}] = \frac{ia^2b}{2}\sigma_3,$$

and

$$D_v\mathcal{F}_{uv} = [\mathcal{A}_v, \mathcal{F}_{uv}] = -\frac{iab^2}{2}\sigma_1.$$

Since $a, b \neq 0$, these three directions span

$$\operatorname{span}_{\mathbb{R}}\{i\sigma_1, i\sigma_2, i\sigma_3\} = \mathfrak{su}(2).$$

By the Ambrose–Singer description of the holonomy algebra, curvature values transported to a common base point generate the holonomy Lie algebra. The displayed covariant derivatives arise as infinitesimal variations of those transported curvature values, and therefore belong to that algebra.

It follows that

$$\mathfrak{hol}(\mathcal{A}) = \mathfrak{su}(2).$$

Since the control region is simply connected, the holonomy group is connected. Its Lie algebra is the full $\mathfrak{su}(2)$, so the holonomy group is $SU(2)$. □

This proposition supplies an explicit non-abelian transport model using the same two rotation directions that arise naturally in the helical moving-frame description.

It should not be interpreted as asserting that every twin helix generates this connection. Rather, it establishes that independently controlled spinorial frame directions admit a nonflat connection whose holonomy is genuinely non-abelian.

The geometric realization problem is now precise: determine which admissible deformations, couplings, and boundary controls of the twin helix induce connections of this type, and which restrictions on those controls preserve or reduce the resulting holonomy group.

The algebra of noncommuting execution. The distinction from the abelian regime can be seen directly in the fundamental representation.

Consider two $SU(2)$ transformations

$$U_1 = \exp(i\alpha\sigma_1), \qquad U_3 = \exp(i\beta\sigma_3).$$

Using the Pauli-matrix relations, one obtains

$$U_1U_3 - U_3U_1 = 2i\sin\alpha\sin\beta\,\sigma_2.$$

For generic values of α, β, the two execution orders therefore differ.

When these transformations are realized as based holonomies, their group commutator

$$[U_1, U_3] = U_1 U_3 U_1^{-1} U_3^{-1}$$

is a nontrivial instance of the join commutator introduced in definition 4.4.

By contrast, for scalar phase transports

$$u_1 = e^{i\alpha}, \qquad u_2 = e^{i\beta},$$

one always has

$$u_1 u_2 = u_2 u_1.$$

An abelian connection may distinguish different paths through curvature or global monodromy, but it cannot distinguish the order of two based transports through their group commutator.

The passage to non-abelian holonomy therefore changes the algebra of admissible composition. It introduces ordered operations whose collective behavior is not determined merely by multiplying independent scalar phases.

Joint holonomy as computational information. A further distinction concerns the information retained by gauge-invariant readouts.

For an individual closed transport cycle, the conjugacy class

$$[U_\gamma]$$

or a character such as

$$\mathrm{tr}(U_\gamma)$$

provides a gauge-invariant observable.

For several cycles based at the same interface, however, the individual conjugacy classes need not determine the gauge-invariant relations among their transports. Under a simultaneous gauge transformation,

$$(U_1, \ldots, U_m) \longmapsto (gU_1 g^{-1}, \ldots, gU_m g^{-1}).$$

The relevant invariant object is therefore the simultaneous-conjugation class

$$[(U_1, \ldots, U_m)] \in G^m/G.$$

In particular, two holonomies may possess identical individual trace data while their ordered products are distinguishable.

For example, let

$$U = \exp(i\alpha\sigma_1),$$

and compare

$$V_\parallel = \exp(i\beta\sigma_1), \qquad V_\perp = \exp(i\beta\sigma_3).$$

Then

$$\mathrm{tr}(V_\parallel) = \mathrm{tr}(V_\perp) = 2\cos\beta,$$

but

$$\mathrm{tr}(UV_\parallel) = 2\cos(\alpha + \beta),$$

whereas

$$\mathrm{tr}(UV_\perp) = 2\cos\alpha\cos\beta.$$

Thus the individual cycle readouts agree, while the composite readouts generally differ. The relative orientation of the internal transport channels carries additional gauge-invariant information.

This provides a useful computational distinction. A collection of loop registers cannot always be treated as independent scalar memories. Their mutual transport relations may themselves form part of the readable state.

A precise obstruction to abelianization. The preceding phenomenon has a direct connection to the notion of physical macro-expressiveness introduced in definition 4.5. However, the nonexistence of a semantics-preserving translation must be established relative to a specified class of translations. Noncommuting matrix operations are not, by themselves, beyond ordinary classical simulation. We therefore isolate the particular obstruction relevant to transport-preserving comparisons.

Definition 4.5 (Transport-Compatible Abelianization)**.** Let H be a realized based holonomy group with a specified family of gauge-invariant readouts

$$\mathcal{R} = \{r_\lambda : H \to \mathcal{O}_\lambda\}.$$

A *transport-compatible abelianization* consists of an abelian group A, a group homomorphism

$$\phi : H \longrightarrow A,$$

and functions

$$\overline{r}_\lambda : A \longrightarrow \mathcal{O}_\lambda$$

such that

$$r_\lambda = \overline{r}_\lambda \circ \phi$$

for every $r_\lambda \in \mathcal{R}$.

Thus the translation preserves composition and every designated readout. This is a restricted class of the semantics-preserving translations considered in the general definition of physical expressive power.

Proposition 4.5 (Obstruction to Abelianizing Holonomy Readouts)**.** *Let*

$$H \subseteq SU(2)$$

be a realized holonomy group containing elements U, V with

$$[U, V] \neq I.$$

Suppose the designated readouts include the fundamental character

$$\chi(W) = \mathrm{tr}(W), \qquad W \in H.$$

Then no transport-compatible abelianization of H exists that preserves this character on every element of H.

Proof. Suppose such an abelianization exists, with

$$\phi : H \longrightarrow A,$$

where A is abelian.

Because ϕ preserves multiplication,

$$\phi([U, V]) = [\phi(U), \phi(V)] = e_A.$$

But

$$\phi(I) = e_A$$

as well.

If the fundamental character factors through ϕ, then

$$\chi([U, V]) = \chi(I).$$

In the fundamental representation of $SU(2)$, every element has eigenvalues $e^{i\theta}$ and $e^{-i\theta}$. Consequently,

$$\mathrm{tr}(W) = 2 \quad \Longleftrightarrow \quad W = I.$$

Since

$$[U, V] \neq I,$$

we obtain

$$\mathrm{tr}([U, V]) \neq 2 = \mathrm{tr}(I),$$

contradicting the assumed factorization. Therefore no such abelianization exists. □

This result identifies a genuine compositional distinction between the two regimes. An abelian transport model cannot simultaneously preserve the multiplication law and all character readouts of a nonabelian $SU(2)$ holonomy system.

It does not follow that an ordinary Turing machine, matrix computer, or suitably enriched abelian system cannot simulate the corresponding behavior by a different encoding. Rather, the proposition identifies the obstruction encountered when the admissible translation must preserve the native transport algebra and its readouts.

Geometric freedom and physical expressiveness. We can now distinguish three levels of the construction.

- **Kinematic freedom.** Relaxing rotational symmetry enlarges the space of cross-sectional shapes and admits additional angular modes, anisotropies, and coupling patterns. The Fourier calculation quantifies this freedom at finite cutoff.
- **Representation structure.** The orthonormal moving frame of a helix takes values in $SO(3)$, and its spinorial lift takes values in $SU(2)$. This supplies a mathematically natural two-dimensional complex representation of helical rotations.
- **Dynamical transport.** When independent admissible controls generate a connection whose effective holonomy is nonabelian, the resulting operations acquire order-sensitive composition. At this level, relative holonomies, join commutators, and jointly gauge-invariant readouts become computationally significant.

These levels may be summarized as

$$\begin{gathered}\text{cross-sectional symmetry breaking}\\ \Downarrow\\ \text{additional geometric control channels}\\ \text{helical moving frame} \longrightarrow SO(3) \longleftarrow SU(2)\\ \Downarrow\\ \text{spinorial transport representation}\\ \Downarrow\\ \text{independently controlled connection}\\ \Downarrow\\ \text{nonabelian holonomy and ordered composition.}\end{gathered}$$

The arrows involving the moving frame and spin double cover are established geometric constructions. The passage from available geometric controls to a particular nonflat connection is a dynamical realization problem. The explicit connection of theorem 4.4 demonstrates the mathematical possibility of this passage, without asserting that every THM realizes it.

To clarify the role of degenerate internal state spaces we note that an isolated rank-one adiabatic band carries abelian Berry transport, whereas a degenerate rank-m subbundle permits a $U(m)$-valued Wilczek–Zee connection [Ber84, WZ84]. For $m = 2$, the traceless transport sector is naturally $\mathfrak{su}(2)$-valued. Degeneracy permits such transport, but does not force its effective holonomy to be nonabelian. Likewise, cross-sectional anisotropy can supply mixing terms, but may also split degeneracies unless additional symmetries or constraints protect the relevant subspace. Physical consequences of this moduli are explained in section A.1.

Computational consequences. The principal distinction between the abelian and nonabelian regimes is therefore not a universal ranking of predictability, complexity, or computational speed.

Abelian continuous systems can possess complicated and even chaotic dynamics. Conversely, nonabelian systems may be integrable or admit strong invariant constraints. Neither geometric complexity nor noncommutativity alone implies algorithmic undecidability.

What changes is the native compositional structure. In a commuting phase sector, the order of based holonomy operations is immaterial. In a nonabelian sector, a computation may depend on the ordered history of its transport operations, even when each individual operation has a simple local description.

From the standpoint of verification, this makes the choice of observable data especially important. Separate local readouts may fail to distinguish globally different compositions, while suitable joint holonomy invariants can retain the relevant differences.

The EVT Hypothesis consequently applies here not as a theorem that nonabelian computation is necessarily less verifiable, but as a question about the adequacy of local certificates under richer forms of composition. The admissible translation class, the protected invariants, and the chosen readout must all be specified before a claim of macro-expressive increase can be established.

From transport algebra to graph coordinates. The resulting algebra does not require the complete smooth connection to be retained as a computational register. For a chosen finite family of admissible paths, one may record their transport matrices, impose gauge equivalence at shared endpoints, and study invariant functions of the resulting graph-level data.

This provides the natural bridge from the moving-frame description of helices to graph holonomies and their representation-theoretic decomposition. The next subsection develops precisely this finite reduction, relating the transport structure to the standard mathematics of spin-network coordinates.

4.3 From Helical Holonomy to Spin-Network Coordinates

Although our program does not aim to adjudicate debates over quantum gravity, aspects of the geometric computation model do resonate with the combinatorial, categorical, and background-independent *perspectives* emphasized in Loop Quantum Gravity [SMO04].

The relationship is most naturally expressed through their shared use of holonomy, representation theory, and combinatorial descriptions of geometric states. Although the two frameworks differ in their foundational assumptions, the passage from continuous geometric transport to graph-based observables provides a useful mathematical point of contact.

In GCT, the underlying twin-helical geometry remains smooth, with information carried by admissible flows, connections, and their associated holonomies. By selecting a finite graph of interfaces and transport paths, one can retain a discrete combinatorial description of this continuous structure. Assigning holonomies to edges and imposing gauge compatibility at vertices leads naturally to the representation-theoretic data familiar from spin networks, including edge labels and intertwiners [Pen71, RS95]. Spin-foam constructions provide a related language for histories interpolating between such boundary data.

The distinction is one of interpretation. We do not assume that the graph constitutes the fundamental geometry, nor that its representation labels already define a quantum theory. Rather, spin-network coordinates arise as a finite, gauge-invariant presentation of selected geometric transport data. This leaves open the possibility that discrete quantum-geometric observables emerge as stable effective structures of an underlying continuous substrate, rather than being imposed at the microscopic level.[5]

Helix-adapted graph reduction. Let

$$\pi : P \longrightarrow B$$

be a principal G-bundle over a working region B, where G is a compact Lie group, and let

$$A \in \Omega^1(P; \mathfrak{g})$$

be a connection. Choose a finite oriented graph

$$\Gamma = (V, E)$$

embedded in B, with edges following admissible transport channels of the GCM lattice and vertices located at interfaces or junctions. Unlike the minimal loops used for Wilson-loop readouts, the edges of Γ are generally open paths. Closed transport cycles are obtained by composing these edges.

After choosing a frame in the fiber over each vertex, parallel transport along an oriented edge e defines an element

$$h_e(A) := \mathrm{Hol}_e(A) = \mathcal{P} \exp\left(\int_e A\right) \in G.$$

The connection therefore determines a finite graph configuration

$$\mathrm{Hol}_\Gamma(A) = \big(h_e(A)\big)_{e \in E} \in G^E.$$

[5] Also: "Spacetime is doomed." — NAH [AHT14]

Proposition 4.6 (Graph-Holonomy Reduction)**.** *Let $P \to B$, A, and $\Gamma = (V, E)$ be as above. There is a graph-holonomy map*

$$\mathrm{Hol}_\Gamma : \mathcal{A}(P) \longrightarrow G^E, \qquad A \longmapsto \big(h_e(A)\big)_{e\in E},$$

where $\mathcal{A}(P)$ denotes the space of connections on P.

With the convention that a vertex gauge transformation

$$g = (g_v)_{v\in V} \in G^V$$

acts on an edge holonomy by

$$h_e \longmapsto g_{s(e)} h_e g_{t(e)}^{-1},$$

the graph-holonomy map is equivariant with respect to the restriction of the continuum gauge action to the vertices. It therefore induces a map of quotient groupoids

$$[\mathcal{A}(P)/\mathcal{G}(P)] \longrightarrow [G^E/G^V].$$

Proof. Parallel transport along an edge produces a G-equivariant map between the fibers over its source and target. Choosing frames at those fibers identifies this transport with an element $h_e(A) \in G$. Changing the frames by $g_{s(e)}$ and $g_{t(e)}$ changes the group element according to

$$h_e(A) \longmapsto g_{s(e)} h_e(A) g_{t(e)}^{-1}.$$

This is precisely the vertex gauge action on G^E, establishing equivariance. □

Remark 4.3. The map depends on the chosen graph and on the chosen vertex frames. It is a finite graph-level reduction of the connection data, not a claim that finitely many holonomies determine a continuum connection. The frame dependence is removed by passing to the quotient groupoid $[G^E/G^V]$.

The reduction is compatible with refinement. If an edge is decomposed as a concatenation

$$e = e_2 \circ e_1,$$

then parallel transport satisfies

$$h_e(A) = h_{e_2}(A) h_{e_1}(A).$$

Thus a refinement of the helix-adapted graph replaces a coarse holonomy by an ordered product of finer holonomies. This is the precise sense in which geometric composition descends to graph transport.

Spin-network coordinates. The classical graph configuration space is G^E, equipped with the vertex gauge action of G^V. Its standard kinematical quantization is the Hilbert space

$$\mathcal{H}_\Gamma := L^2\left(G^E, d\mu_{\mathrm{Haar}}^{\otimes E}\right),$$

with the gauge-invariant subspace

$$\mathcal{H}_\Gamma^{\mathrm{inv}} := L^2\left(G^E, d\mu_{\mathrm{Haar}}^{\otimes E}\right)^{G^V}.$$

A Wilson loop is a special gauge-invariant function obtained by taking a class function of the holonomy around a closed cycle. Spin-network functions provide a basis for the full gauge-invariant graph space, including configurations with many edges and junctions.

Proposition 4.7 (Spin-Network Expansion)**.** *Let G be a compact Lie group and let $\Gamma = (V, E)$ be a finite oriented graph. The Peter–Weyl theorem gives an orthonormal basis of $\mathcal{H}_\Gamma^{\mathrm{inv}}$ indexed by:*

(a) *an irreducible unitary representation*

$$\rho_e : G \longrightarrow U(V_{\rho_e})$$

assigned to each edge $e \in E$;

(b) *an invariant tensor*

$$\iota_v \in \mathrm{Inv}\left(\bigotimes_{e:t(e)=v} V_{\rho_e} \otimes \bigotimes_{e:s(e)=v} V_{\rho_e}^*\right)$$

assigned to each vertex $v \in V$.

The corresponding spin-network function is obtained by taking the matrix coefficients

$$\rho_e(h_e)$$

on each edge and contracting their indices at every vertex using the intertwiners ι_v.

For $G = SU(2)$*, the irreducible representations are indexed by*

$$j_e \in \frac{1}{2}\mathbb{N},$$

so a basis element is conventionally denoted

$$\big(\Gamma, \{j_e\}, \{\iota_v\}\big).$$

Proof. By the Peter–Weyl theorem,

$$L^2(G) \cong \widehat{\bigoplus}_{\rho\in\widehat{G}} V_\rho \otimes V_\rho^*.$$

Taking one copy for each edge gives a decomposition of $L^2(G^E)$ into tensor products of representation spaces and their duals. The action of G^V acts independently on the indices incident at each vertex. Passing to the invariant subspace therefore selects precisely the invariant tensors, or intertwiners, at the vertices. □

The representation label j_e should not be confused with the spectrum of a particular holonomy h_e. A holonomy is a group element, whereas j_e labels an irreducible Fourier mode in the Peter–Weyl decomposition of functions on the group. The spin-network description is therefore a representation-theoretic expansion of the graph-holonomy state space, not a direct assignment of one spin to each holonomy eigenphase.

Four-valent vertices and quantum tetrahedra. Suppose the helix-adapted graph contains a four-valent vertex v. For $G = SU(2)$, the gauge-invariant vertex data lie in the intertwiner space

$$\mathcal{I}_v = \mathrm{Inv}\left(V_{j_1} \otimes V_{j_2} \otimes V_{j_3} \otimes V_{j_4}\right),$$

where orientations have been suppressed using the self-duality of finite-dimensional $SU(2)$ representations. This is the standard intertwiner space associated with a quantum tetrahedron.

The chosen interface graph supplies the four-valence. The representation labels and intertwiner arise from the $SU(2)$ quantization of its holonomy variables. This construction is distinct from the finite

$$V_4 \cong C_2 \times C_2$$

symmetry of the symbolic twin helix register. The two structures may coexist in a coarse cell, but V_4 does not by itself generate the $SU(2)$ intertwiner or determine the spin labels.

In this sense, the quantum tetrahedron enters GCT conditionally: once a four-valent transport graph and an $SU(2)$ gauge sector are present, the standard graph quantization assigns an intertwiner space of tetrahedral type. The helix geometry supplies a possible microscopic origin for the transport graph, but the quantum-geometric interpretation belongs to the subsequent representation-theoretic quantization.

Computational bordisms and spin-foam carriers. A history of graph configurations may be represented by a two-dimensional cell complex

$$\mathcal{F},$$

whose faces trace the evolution of graph edges, whose edges trace the evolution of graph vertices, and whose vertices record elementary changes of the interface structure. Gluing successive histories corresponds to composition of the resulting two-complexes.

This gives a natural interface with spin-foam constructions [Bae98]. After quantization, one may label the faces of $\mathcal{F}$ by irreducible representations and its edges by intertwiners. However, a genuine spin-foam model requires more than the underlying two-complex and its labels: one must additionally specify face, edge, and vertex amplitudes, together with a measure or refinement prescription. These weights are not determined merely by the existence of the helix geometry or by products of Wilson-loop class functions.

Accordingly, a computational bordism supplies a candidate geometric carrier for a spin foam, but the passage

$$\text{GCM history} \longrightarrow \text{spin-foam amplitude}$$

requires an additional quantization and weighting rule. Establishing such a rule is a problem for the future development of Geometric Computational Field Theory.

Remark 4.4 (Status of the Correspondence). The mathematically established correspondence in this section is conditional but precise:

$$\begin{gathered}\text{a GCM connection and a chosen helix-adapted graph} \\ \Longrightarrow \text{graph holonomies in } G^E, \\ \text{compact-group quantization and gauge reduction} \\ \Longrightarrow \text{a spin-network basis.}\end{gathered}$$

This does not yet prove that spin networks are uniquely determined coarse invariants of all helix configurations, nor that the quantum kinematics of LQG emerge without an additional quantization step. It does show that once the continuous geometric dynamics are reduced to a finite system of gauge transports, spin-network coordinates arise by a standard and non-arbitrary mathematical procedure.

Gauge invariance should likewise be distinguished from background independence. Passing from G^E to its G^V-invariant sector removes dependence on local gauge frames. Full background independence would additionally require control of graph embeddings, graph refinement, and diffeomorphism equivalence.

Summary. The role of spin networks in GCT is not to replace the underlying manifold by fundamental discrete atoms. Rather, they provide representation-theoretic coordinates for the gauge-invariant holonomy data extracted from a chosen network of geometric transport channels. The helix lattice supplies the continuous geometry and interface structure; graph reduction supplies finite holonomies; and compact-group quantization supplies the discrete spin labels and intertwiners. Spin foams may then describe quantized histories of these graph data, provided an additional amplitude prescription is supplied.

These examples are not members of one uniform solution class. What they share is a local-to-global mechanism: ordinary gauge potentials are defined chartwise, while the computationally relevant information is carried by their compatibility, transport, curvature, and placement inside a global configuration space.

4.4 On the Expressive Power of Physical Computation

Before stating our final claim, we collect several gauge-theoretic solutions exhibiting recurring mechanisms of phase and matrix holonomy: periodicity, compactification twists, unstable saddles, and chiral transport.

- **Calorons.** Periodic instantons on $\mathbb{R}^3 \times S^1$, whose Euclidean time compactification enforces a helical/phase structure along the circle [Kv98].
- **Twisted solutions.** Gauge fields on compactified or cylindrical backgrounds with nontrivial boundary conditions; the twist enforces a globally enforced phase (or matrix) winding [tH79].

- **Sphalerons.** Unstable saddle points in electroweak theory; they sit atop energy barriers and encode large, topological reconfigurations (holonomy changes) along interpolation paths [KM84].
- **Witten's twisted constructions.** Lower–dimensional/topologically twisted reductions where the effective degrees of freedom are organized by holonomy classes and cohomological data [Wit88].
- **Non-abelian plane waves.** Chiral, order-sensitive transport in non-abelian gauge theory; parallel transport along wavefronts produces noncommuting holonomies [Col77].

Taken together, these exemplars highlight three recurring themes: (a) *periodic/compactified directions* that act as helical axes (calorons, twisted sectors), (b) *unstable saddles* that mediate large holonomy moves (sphalerons), and (c) *intrinsically chiral, non-abelian transport* (plane waves). In what follows, we leverage exactly these mechanisms—now encoded by holonomy class functions on chosen loops—to motivate the usage of geometric computation.

While this discussion does not claim to exhaust the intricate connections between geometric computation and modern field theory, it is instructive (cf. fig. 4a) that gluing two helical manifolds along a common boundary produces patching data directly related to the clutching that underlies BPST instantons. We now enter the final of the four computational regimes, *emergent gauge*.

Local connection data and descent. Let

$$\pi : P \longrightarrow M$$

be a principal G-bundle over a smooth manifold M, where G is a compact Lie group. Choose an open cover

$$M = \bigcup_{i \in I} U_i$$

and local sections of P over the U_i. On an overlap $U_i \cap U_j$, the two local trivializations are related by a transition function

$$g_{ij} : U_i \cap U_j \longrightarrow G.$$

On triple overlaps, the transition functions satisfy the cocycle condition

$$g_{ij} g_{jk} = g_{ik}.$$

A connection is represented locally by one-forms

$$A_i \in \Omega^1(U_i; \mathfrak{g})$$

satisfying

$$A_j = g_{ij}^{-1} A_i g_{ij} + g_{ij}^{-1} dg_{ij}$$

on $U_i \cap U_j$. Their curvatures

$$F_i = dA_i + A_i \wedge A_i$$

obey

$$F_j = g_{ij}^{-1} F_i g_{ij}.$$

Thus the local potentials are not independent fields. They are representatives of a single global connection reconstructed by descent. The transition functions encode changes of local frame, while gauge-invariant information must descend through these changes of description. In the language of GCT, the individual chart representatives are local computational states, the transition functions are interface data, and the global connection is the coherent state obtained after the interface constraints have been satisfied.

A pair of joined unit helices may provide a concrete geometric cover by chart domains U_A and U_B, but the gluing of their underlying base regions does not by itself produce a nontrivial gauge bundle. Nontrivial bundle topology resides in the homotopy class of the transition data. For example, the standard clutching description of an $SU(2)$ bundle over S^4 uses a transition function on the equatorial S^3,

$$g : S^3 \longrightarrow SU(2),$$

whose degree lies in

$$\pi_3(SU(2)) \cong \mathbb{Z}.$$

The integer degree determines the second Chern class and hence the instanton sector [BPST75, ADHM78]. The helix-interface analogy is therefore an analogy at the level of chartwise gluing and transport: to obtain an instanton sector, one must additionally specify topologically nontrivial gauge descent data.

Ambient gauge group and effective holonomy. A connection A determines parallel transport along admissible paths and hence a holonomy functor

$$\mathrm{Hol}_A : \Pi_1^{\mathrm{thin}}(M) \longrightarrow G\text{-}\mathbf{Tor}.$$

After choosing a frame over a base point $x \in M$, closed paths based at x generate the holonomy group

$$\mathrm{Hol}_x(A) \subseteq G.$$

The ambient structure group does not by itself determine the computational regime. Even when G is non-abelian, the effective holonomy may lie in a common abelian subgroup

$$\mathrm{Hol}_x(A) \subseteq H \subseteq G, \qquad [H, H] = \{e\}.$$

In that case, the transport visible to the chosen family of paths remains effectively abelian. Conversely, genuinely order-sensitive transport requires both

$$\mathrm{Hol}_x(A) \text{ non-abelian}$$

and a readout capable of distinguishing the relevant ordered compositions. Non-abelianity is therefore a structural possibility, not by itself a complete computational semantics.

This distinction is especially important after gauge reduction. Open parallel transports retain endpoint-frame data and transform covariantly. Closed-loop holonomies transform by conjugation, so gauge-invariant readouts are class functions such as Wilson-loop traces. Passing from framed transport to class functions may identify processes that were distinct before quotienting. The observable computation is therefore determined not only by the connection, but by the pair

$$\big(\text{admissible transport}, \text{chosen invariant readout}\big).$$

Finite-action histories with boundary. Let X be a compact oriented Riemannian 4-manifold whose boundary is decomposed as

$$\partial X = \overline{Y}_0 \sqcup Y_1,$$

where Y_0 is the incoming boundary and Y_1 is the outgoing boundary. Let

$$P \longrightarrow X$$

be a principal G-bundle, and fix boundary connections

$$A_0 \in \mathcal{A}(P|_{Y_0}), \qquad A_1 \in \mathcal{A}(P|_{Y_1}).$$

Write

$$\mathcal{G}_0(P) = \{u \in \mathcal{G}(P) \mid u|_{\partial X} = \mathrm{id}\}$$

for the group of gauge transformations fixed at the boundary.

The anti-self-dual boundary-value moduli space is

$$\mathcal{M}_{\mathrm{ASD}}(X; A_0, A_1) := \frac{\left\{\mathbb{A} \in \mathcal{A}(P) \;\middle|\; F_{\mathbb{A}}^+ = 0,\ \mathbb{A}|_{Y_0} = A_0,\ \mathbb{A}|_{Y_1} = A_1\right\}}{\mathcal{G}_0(P)}.$$

When nonempty, this space records gauge-equivalence classes of finite-action histories connecting the prescribed boundary data. A single instanton number does not specify such a history completely: different points or components of the moduli space may carry the same topological charge.

For the product cylinder

$$X = Y \times [0,1],$$

choose temporal gauge and write the four-dimensional connection as a path $A(t)$ of connections on Y. Then

$$F_{\mathbb{A}} = F_{A(t)} + dt \wedge \dot{A}(t).$$

With the product metric and a fixed orientation convention, the anti-self-duality equation

$$F_{\mathbb{A}}^{+} = 0$$

becomes

$$\dot{A}(t) = - *_Y F_{A(t)}.$$

This is the negative L^2-gradient-flow equation for the Chern–Simons functional. Thus a four-dimensional instanton history may be viewed as a trajectory in the reduced configuration space of three-dimensional connections.

The relevant computational object is therefore not merely a field configuration at one instant, but a boundary-to-boundary process

$$[A_0] \longrightarrow [A_1]$$

represented by a class in an appropriate moduli space. Boundary readouts determine which such histories are operationally distinguishable.

Chern–Simons transgression as a boundary ledger. Fix an invariant pairing on $\mathfrak{g}$ normalized so that the corresponding characteristic number is integral on closed four-manifolds. For a connection A on a closed oriented three-manifold Y, define

$$\mathrm{CS}(A) = \frac{1}{8\pi^2} \int_Y \mathrm{tr}\left(A \wedge dA + \frac{2}{3} A \wedge A \wedge A \right).$$

Under a large gauge transformation, $\mathrm{CS}(A)$ changes by an integer. Hence it is naturally an $\mathbb{R}/\mathbb{Z}$-valued functional unless a boundary framing or lift has been fixed.

For a connection $\mathbb{A}$ on X, define its relative four-dimensional charge by

$$Q(\mathbb{A}) = \frac{1}{8\pi^2} \int_X \mathrm{tr}\left(F_{\mathbb{A}} \wedge F_{\mathbb{A}} \right).$$

When the boundary trivializations are fixed, the transgression identity gives

$$Q(\mathbb{A}) = \mathrm{CS}(A_1) - \mathrm{CS}(A_0),$$

up to the sign determined by the orientation and trace conventions. Without fixed lifts, the equality is understood modulo $\mathbb{Z}$. On a closed four-manifold, the same integral gives the corresponding characteristic number

$$Q(\mathbb{A}) \in \mathbb{Z}.$$

This is the precise sense in which Chern–Simons data form a boundary ledger: a four-dimensional curvature history produces a three-dimensional record of the net sector change. The charge $Q(\mathbb{A})$ grades the process, but it is not a complete description of the process. In computational language, it is a stable global output associated with a history rather than a gate table that uniquely determines the intermediate evolution.

If two compatible histories

$$\mathbb{A}_{01} \quad \text{on} \quad X_{01} : Y_0 \longrightarrow Y_1$$

and

$$\mathbb{A}_{12} \quad \text{on} \quad X_{12} : Y_1 \longrightarrow Y_2$$

are glued along their common boundary data; then their characteristic charges add:

$$Q(\mathbb{A}_{02}) = Q(\mathbb{A}_{01}) + Q(\mathbb{A}_{12}).$$

Equivalently, the Chern–Simons contributions telescope:

$$\mathrm{CS}(A_2) - \mathrm{CS}(A_0) = \big(\mathrm{CS}(A_2) - \mathrm{CS}(A_1)\big) + \big(\mathrm{CS}(A_1) - \mathrm{CS}(A_0)\big).$$

This additivity supplies a genuine compositional law for sector-changing histories.

The core mechanism of regimes. At the level of *computational role*, effectively abelian regimes correspond to the stable carriage of information: state is propagated in a periodic, order-insensitive, and comparatively reversible manner, so that the dominant behavior is storage, transmission, or recurrence rather than structural transformation. By contrast, non-abelian regimes are characterized by order-sensitive evolution, where the flow itself performs the computation: composition is no longer reducible to simple commutative propagation, and state is actively reshaped through mixing, routing, and nontrivial transition. In the highest regime—*emergent gauge*—computation becomes genuinely history-dependent and topological. There, the relevant logical content is carried not only by the states themselves but by the global manner in which one state is connected to another, so that transition processes—for example, sphaleron-type [Man19] barrier crossings—become part of the computation itself. The working hypothesis of GCT is not that every Yang–Mills [YM54] solution is literally a twin helix but that helical geometry supplies a constructive family of carriers for the same basic mechanisms that recur throughout gauge theory: cyclic transport, path ordering, curvature-supported memory, descent, and topologically graded interpolation.[6]

Table 8: Computational regimes in GCT and the geometric structures that realize them.

Regime	**Computational signature**	**Primary state carrier**	**Topological role**	**Representative physical exemplars**
Symbolic	Discrete, stable, addressable states; local read/write behavior; robust storage.	Local occupation values, boundary conditions, or effectively commuting observables.	Topology is present but inactive; it serves as a fixed background structure rather than as the active computational variable.	Classical bits, digital memory, effectively abelian electromagnetic storage modes.
Quasi-fluidic	Cyclic or clocked evolution; recirculating transport; finite memory carried through repeated traversal of a loop.	Holonomy, phase accumulation, or other history-bearing data associated with motion around a compact direction.	Topological content is accumulated and reassembled over a cycle rather than expressed as a single isolated transition.	Calorons, periodic instantons, finite-temperature Yang–Mills configurations with nontrivial holonomy.
Fluidic	Distributed continuous transformation; order-sensitive mixing; non-commutative transport across an extended medium.	Flow profile, relative ordering of non-commuting updates, chiral or braided propagation patterns.	Topology is secondary to transport dynamics; the main effect is transformation by extended flow rather than sector change.	Non-abelian plane waves, helical or twisted Yang–Mills solutions, propagating chiral field configurations.
Gauge	Global, history-dependent update between sectors; computation by topological event rather than by local rewriting.	Bundle class, winding data, Chern-type invariants, or other global sector labels.	Topology is primary and active: the computation is identified with tunneling, obstruction crossing, or sector change.	Instantons, sphalerons, vacuum tunneling configurations, topological transition events.

Interpretation of the regime labels. The classifications in table 8 are *computational* rather than group-theoretic. They do not assert that all examples in a given column are abelian or non-abelian as gauge fields. Instead, they classify the *role* played by the configuration in the computational picture.

In particular, calorons are genuinely non-abelian Yang–Mills configurations, but they are placed in the quasi-fluidic regime because their operative structure is cyclic and holonomy-driven: state is transported around a compact S^1 direction, and memory is encoded by recurrence and phase accumulation. By contrast, instantons appear in the gauge regime when the emphasis is on isolated topological sector change.

Example 4.2 (The Computational Consequences of Non-Abelian Plane Waves). As a motivating ex-

[6] As to why the Universe chooses to *express itself* this way? The author kindly asks that such questions be directed *elsewhere* (cf. [Pen89]).

ample of one solution cited above, consider the appearance of non-abelian plane waves:

$$L = -\frac{1}{4}\mathrm{tr}(F_{\mu\nu}F^{\mu\nu}) = \frac{1}{2}\sum_{a=1}^{n}\left[(E^a)^2 - (B^a)^2\right] =: \frac{1}{2}(E^2 - B^2).$$

This is discussed by [Kas83], where he notes (with some exasperation) that plane–wave solutions with equal electric and magnetic energy densities satisfy $E^2 = B^2$ and hence $L = 0$. In the non-abelian case, such waves carry internal structure: along the propagation direction, the gauge potential undergoes nontrivial parallel transport, yielding non-vanishing holonomy in the gauge group. Equivalently, the field configuration traces a nontrivial path in the group manifold even though the local scalar invariant $E^2 - B^2$ vanishes.

Within a geometric–computational viewpoint, this slice $L = 0$ may be regarded as a *switching hypersurface* in configuration space: crossing it changes the group–theoretic state realized by the parallel transport while preserving the light-like character of the wave. The family of such plane waves thus furnishes a controlled alphabet of *signal trajectories*: each solution implements a definite group action (holonomy) along its world-volume, so compositions of waves correspond to compositions of group elements, with path ordering in the non-abelian case. In this sense, classical Yang–Mills solutions encode a concrete logic of state transitions, with the group providing the algebra and the spacetime evolution providing the flow.

4.5 Constructive Computational Gauge Theory

We feel that it is a useful exercise to frame gauge theory (and, by extension, quantum gravity) as a problem of *expressiveness* versus *verifiability*. If we allow "all histories" (arbitrary geometries, gauge redundancy, unbounded recursion in the construction of spacetimes), amplitudes can become ill-defined and intractable. If we clamp down too hard, we lose physically relevant states and dynamics.

Our proposal for a constructive computational gauge theory therefore occupies a middle ground. The aim is not to quantize every admissible geometry at the outset, nor to reduce the theory to a purely topological field theory. Instead, we seek a typed, resource-sensitive, total-core, effect-controlled calculus of geometric histories in which admissibility, composition, constraint propagation, and observable readout are made explicit.

At its most basic level, boundary/interface data play the role of types; computational geometric bordisms play the role of terms; and gluing is composition. In a four-dimensional realization, the boundary objects will often be three-dimensional. Still, the construction itself is not tied to a preferred spacetime dimension or to an already-emergent Lorentzian metric. The relevant boundary data may include bundle and connection data, framing, discrete topological labels, allowed mode or defect sectors, constraint data, and a chosen family of readouts. This gives a compositional semantics familiar from TQFTs but designed to scale beyond purely verifiable/topological settings (e.g., Chern-Simons [CS74]). Readers are asked to consider the correspondences in table 9.

Types. The proposed helical primitives (1.7) provide one concrete family of generators of histories: smooth geometric carriers equipped with orientation, chirality, framing, phase, and, in higher regimes, connection and holonomy data. This marries the "continuous versus discrete" tension: spectra and curvature are continuous objects; quantum numbers arise as stable, counted winding data.

A type is therefore best understood as a *geometric interface specification*. Schematically, one may write

$$\Sigma = (Y, \sigma),$$

where Y is the underlying boundary/interface manifold and σ denotes the additional structure required by the computational regime under consideration. This structure may include a principal bundle or associated state bundle, restricted connection data, framing, winding or charge labels, admissible mode sectors, defect data, regularity conditions, and a specified family of observable readouts.

Thus a type is more than a boundary condition in the ordinary functional-analytic sense. It declares what geometric structures may consistently enter or leave a region and what information about them is retained by the computational semantics.

Where a boundary supports a finite or controlled internal mode space $\mathcal{V}_\Sigma$, that mode space should be regarded as part of the type data. This becomes important in the non-abelian regime, because gluing may then induce an interaction map of the schematic form

$$\Gamma_f : \mathcal{V}_{\Sigma_1} \otimes \mathcal{V}_{\Sigma_2} \longrightarrow \mathcal{V}_{\Sigma_3},$$

Table 9: Constructive semantic structures and their geometric role

Semantic Structure	**Geometric/Gauge-Theoretic Role**
Types	Boundary/interface data: geometry, bundle data, constraints, mode or defect sectors, and declared readouts
Terms	Computational geometric bordisms carrying admissible geometric and gauge data
Composition	Gluing of compatible histories along matched boundary/interface data
Linear/resource discipline	No implicit duplication or erasure of declared boundary resources; explicit accounting of charge, flux, and other conserved data
Total core	Termination and well-defined evaluation of the restricted semantic core; not quantum-amplitude normalization
Dependent constraints	Gauge, diffeomorphism, regularity, charge-sector, and interface-compatibility conditions carried as part of admissibility
Descent/coherence	Compatibility of local geometric data on overlaps, including higher gluing conditions and obstruction data
Effects and handlers	Controlled coarse-graining, renormalization, noise, approximation, and change of scale or presentation
Readout	Gauge-invariant or otherwise quotient-stable observables extracted from a completed history
Type extensions	Enlargement of the admissible theory by new matter, defect, topology-changing, or nonperturbative sectors

so that the geometry of the interface constrains which combinations of modes are actually composable.

Terms. A *term* is a computational geometric bordism in the sense of definition A.3, equipped with a declared typing judgment. Thus,

$$W : \Sigma_{\text{in}} \longrightarrow \Sigma_{\text{out}}$$

denotes a compact geometric history whose boundary restrictions recover the declared input and output types and whose interior carries the required computational structure.

Terms are therefore not symbolic expressions standing in for geometry. They are geometric histories viewed operationally as processes between typed interfaces. In the symbolic or quasi-fluidic regimes such a history may be a controlled phase-carrying cylinder, junction, or lattice region. In the fluidic and gauge regimes it may carry nontrivial curvature, ordered holonomy, defect data, or changing moduli.

Crucially, a well-typed term need not yet be a dynamically realized history. We distinguish:

$$W : \Sigma_{\text{in}} \to \Sigma_{\text{out}} \qquad \text{(kinematic / well-formed history)},$$

$$W \models \mathcal{E} \qquad \text{(history satisfying the chosen dynamical equations)},$$

and

$$\text{Read}(W) \in \mathcal{O} \qquad \text{(observable or computational readout)}.$$

The differential or variational law determines which well-formed histories are dynamically admissible; the computational semantics determines how such histories compose and what information they carry.

Composition. *Composition* is gluing. Given

$$W_1 : \Sigma_0 \longrightarrow \Sigma_1, \qquad W_2 : \Sigma_1 \longrightarrow \Sigma_2,$$

with compatible boundary data, their sequential composition is obtained by identifying the common interface:

$$W_2 \circ_{\Sigma_1} W_1 : \Sigma_0 \longrightarrow \Sigma_2.$$

Parallel composition is given by disjoint union.

The gluing condition is stronger than agreement of the underlying topological boundaries. The geometric, gauge, mode, defect, and constraint data exposed on the common interface must also be

compatible. Composition therefore expresses the physical statement that the outgoing admissible structure of one region becomes the incoming admissible structure of the next.

At the level of observables, composition must preserve the declared equivalence relation on boundary data. In an abelian regime this may amount to preserving total phase, flux, or winding. In a non-abelian regime the relevant readouts may instead be conjugacy classes of holonomy or class functions such as Wilson-loop traces.

Moduli semantics. Gauge theories should not generally be modeled by spaces of representatives alone. Gauge transformations and other automorphisms are part of the semantic structure. Accordingly, for a boundary type Σ we write schematically

$$\mathfrak{M}(\Sigma)$$

for the corresponding moduli groupoid or stack of admissible boundary data modulo the appropriate redundancies.

Likewise, a term W determines a moduli object $\mathfrak{M}(W)$ together with restriction maps

$$\mathfrak{M}(\Sigma_{\mathrm{in}}) \xleftarrow{s} \mathfrak{M}(W) \xrightarrow{t} \mathfrak{M}(\Sigma_{\mathrm{out}}).$$

Thus a geometric process is represented semantically not merely by a function between state spaces, but by a correspondence between boundary moduli.

Composition of histories is then reflected schematically by a fiber product over the shared boundary data,

$$\mathfrak{M}(W_2 \circ W_1) \simeq \mathfrak{M}(W_1) \times_{\mathfrak{M}(\Sigma_1)} \mathfrak{M}(W_2),$$

with the ordinary fiber product replaced by an appropriate homotopy or derived fiber product when gauge automorphisms or higher coherence data make this necessary. The point is not to place the full syntax inside homotopy type theory, but to allow the denotational semantics to retain the groupoid or stack structure actually required by gauge redundancy. This separation between geometric/prequantum data and subsequent quantization is consonant with the higher-geometric approach of [Sch14].

Descent and coherence. Local compatibility must extend beyond pairwise gluing. Let

$$W = \bigcup_i U_i$$

be a cover by computational regions. Local geometric data on U_i must agree on overlaps $U_i \cap U_j$, and the corresponding transition data must satisfy the required coherence conditions on triple and higher overlaps. For an ordinary principal bundle, for example, transition functions satisfy

$$g_{ij} g_{jk} g_{ki} = e$$

on triple intersections. In higher gauge settings, analogous compatibility may itself hold only up to specified higher morphisms.

We therefore treat descent as a genuine semantic obligation. A collection of locally well-typed computations does not automatically define a global computation; the local data must descend to a coherent global object. Presheaf and sheaf language provide the ordinary version of this requirement, while moduli stacks and higher groupoids retain the automorphism and coherence data lost by a coarse quotient.

A restricted dynamical gluing criterion. The preceding descent statement concerns geometric and gauge data. For a history to be a solution of a differential equation, one must additionally match the analytic data on its interface. The following elementary criterion specifies one regime in which the distinction can be made exact.

Proposition 4.8 (Finite-Order Gluing of Classical Solution Histories)**.** *Let $W = W_1 \cup_Y W_2$ be a smooth manifold obtained by identifying collared boundaries along a common smooth hypersurface Y. Fix a smooth field bundle $E \to W$ and a local differential relation $\mathcal{E} \subseteq J^k E$ of finite order $k \geq 1$. Suppose ϕ_i are C^k sections on the closed pieces W_i, solve $j^k \phi_i \in \mathcal{E}$ on their interiors, and have matching k-jets along Y under the specified collar and bundle identifications. Then the piecewise section $\phi = \phi_1 \cup_Y \phi_2$ is C^k on W and satisfies $j^k \phi \in \mathcal{E}$ everywhere, provided $\mathcal{E}$ is closed in the relevant jet topology. Conversely, every global C^k solution restricts to such compatible local solutions.*

Proof. Matching the normal and tangential derivatives through order k in the common collar charts is precisely the C^k pasting criterion. Consequently ϕ is a well-defined C^k section with $j^k\phi|_{W_i} = j^k\phi_i$. The differential relation holds away from Y by hypothesis and extends to Y by continuity of the k-jet and closedness of $\mathcal{E}$. Restriction of a global solution gives the converse. □

For gauge fields, the statement is applied after specifying compatible bundle identifications and connection data on the collars; gauge equivalences must be retained in the corresponding moduli groupoid. This result does not assert that arbitrary independently prescribed boundary conditions admit solutions, that the resulting gauge boundary-value problem is well-posed, or that weak solutions or bubbling limits obey the same pasting criterion. Those stronger analytic statements remain separate obligations of the dynamical GCFT sector.

Several distinct guardrails govern the constructive core. They should not be confused with physical consequences that must be derived only at later stages.

Linearity and resource discipline. *Linearity* is used here in the resource-sensitive sense: declared boundary data cannot be copied or discarded implicitly [Gir87, Wad90]. A composition must account explicitly for where charge, flux, mode content, or other tracked resources enter and leave.

This discipline is useful for enforcing conservation bookkeeping at interfaces, but it does not by itself derive a physical conservation law, quantum no-cloning, or unitarity. Those require additional physical structure. A conservation law must be included as a constraint or invariant of the model; linearity ensures that the corresponding resource cannot silently disappear from the formal composition.

Totality. By *totality* we mean that the restricted *core evaluator* terminates and returns a well-defined semantic value on every well-formed core term. Schematically,

$$\mathrm{Eval}_{\mathrm{core}}(W)$$

must terminate and return the declared boundary object, invariant, or computable readout.

This is a property of the formal calculus, not a claim that nature is finite and not a statement that a quantum amplitude is normalized. The total fragment is the portion of the semantics for which one intends to prove compositionality, constraint preservation, and effective evaluation without importing the entire analytic burden of continuum QFT. Processes whose evaluation requires uncontrolled limits, divergent expansions, or non-total search lie outside this core until they are supplied with additional certified structure.

Effective evaluation of controlled holonomy. A continuous state space does not by itself prevent effective readout. The relevant question is whether a specified connection and path admit algorithms with certified approximation errors. The following result isolates a non-abelian fragment of the constructive core without assuming that an arbitrary Yang–Mills solution is computable.

Proposition 4.9 (Effective Wilson-Holonomy Readout)**.** *Let G be a compact matrix Lie group with a specified finite-dimensional unitary representation $\rho : G \to U(d)$. Let $\gamma : [0,1] \to M$ be a based piecewise-C^1 loop, and let A be a connection whose pullback along γ, expressed in a computably presented trivialization along the loop with identified endpoint frames, gives*

$$K(t) = \rho_*\big(A_{\gamma(t)}(\dot\gamma(t))\big) \in \mathfrak{u}(d).$$

Assume that K is uniformly computable on each smooth segment, with an effective modulus of continuity and a computable uniform bound $\|K(t)\| \le M_0$. Then, for every positive rational ε, a terminating algorithm produces a complex rational approximation w_ε such that

$$|w_\varepsilon - \operatorname{tr}\rho(\mathrm{Hol}_A(\gamma))| < \varepsilon.$$

The target trace is invariant under gauge transformations acting at the base point by conjugation. If a real-valued function of this trace is computable and its value is supplied with a certified positive margin from a finite readout threshold, the corresponding threshold decision is also computable.

Proof. In the chosen trivialization, parallel transport solves the matrix equation $U'(t) = -K(t)U(t)$, $U(0) = I$. The ordered integral (Dyson) expansion is

$$U(1) = I + \sum_{j=1}^{\infty}(-1)^j \int_{0\le t_j\le\cdots\le t_1\le 1} K(t_1)\cdots K(t_j)\,dt_j\cdots dt_1.$$

The operator norm of the tail beyond order N is bounded by

$$\sum_{j=N+1}^{\infty} \frac{M_0^j}{j!},$$

which can be made effectively smaller than any prescribed rational tolerance. Each retained iterated integral is computable to arbitrary precision by effective uniform continuity on the finitely many smooth segments. Since $|\operatorname{tr} T| \le d\|T\|$, the resulting approximation to $\operatorname{tr} U(1)$ has a certified error bound. A gauge transformation changes a based-loop holonomy by conjugation, leaving its trace unchanged. Finally, if the selected real readout is at distance at least $\delta > 0$ from every decision threshold, an approximation with error below $\delta/2$ determines its readout class. □

The result is deliberately restricted: the required effective descriptions and bounds are part of the input, not consequences of bare smoothness, compactness, or gauge invariance. It proves computability of specified finite-dimensional holonomy readouts, not computability of general moduli, continuum limits, gauge-fixing operations, or nonperturbative Yang–Mills solutions. Nor does it guarantee finite-time threshold decisions when the observable may lie exactly on a readout boundary.

Effects and handlers. Processes that change the scale or presentation of a geometric computation are treated as explicit *effects* rather than silently incorporated into the core semantics. Examples include coarse-graining, renormalization, stochastic or noisy coupling, controlled approximation, and changes of resolution [Mog91, PP09].

A handler acts on a well-typed geometric history and produces another well-typed history together with a declaration of what observable information has been preserved, modified, or discarded. Thus a handler is not merely a rewrite of geometry; it is a certified transformation between semantic descriptions.

Example 4.3 (Coarse-Graining as a Handled Effect.). Let

$$W : \Sigma_{\text{in}} \to \Sigma_{\text{out}}$$

contain microscopic helical loops

$$\gamma_1, \dots, \gamma_k$$

in some interior region. A coarse-graining handler replaces this subterm by an effective history W_{eff} together with a certificate relating the chosen boundary readouts.

In an abelian regime this may require preservation of total phase, winding, or flux. In a non-abelian regime it may require preservation of specified class functions of holonomy, for example Wilson-loop traces. More generally, one may permit a controlled error bound

$$d_{\mathcal{O}}\left(\operatorname{Read}(W), \operatorname{Read}(W_{\text{eff}})\right) \le \varepsilon.$$

The coarse-graining is therefore a semantics-controlled transformation rather than an arbitrary geometric simplification.

Soundness obligations for handlers. To prevent the effect layer from collapsing into informal manipulation, any declared handler—RG flow, coarse-graining, noise model, or controlled approximation—must satisfy an explicit contract:

(a) **Functoriality.** Handling must commute with sequential composition up to the declared equivalence.

(b) **Monoidality.** Handling must respect parallel composition so that independently prepared subsystems are not coupled implicitly.

(c) **Gauge and descent compatibility.** The transformation must respect the relevant gauge/diffeomorphism equivalences and map coherent local data to coherent effective data.

(d) **Observable control.** The handler must state which readouts are preserved exactly, which are preserved only up to equivalence, and which acquire controlled error.

(e) **Resource and defect accounting.** Any creation, removal, or transfer of tracked degrees of freedom must be explicit; lost energy, charge, flux, or topological content must appear as declared residual or defect data rather than disappearing silently.

(f) **Dynamical compatibility.** If the handler is claimed to send physical histories to effective physical histories, the relation between the microscopic equation $\mathcal{E}$ and the effective equation $\mathcal{E}_{\text{eff}}$ must itself be specified.

Dependent types. Gauge, diffeomorphism, regularity, charge-sector, and interface conditions may be carried as dependent typing data [ML84]. A boundary object is then admissible only together with the data or certificate required to satisfy its declared constraint structure.

The intended benefit is mechanical propagation of constraints through composition. But well-typedness is not proof that the physical theory is gauge complete or anomaly-free. The formal task is instead to prove a subject-reduction-style statement: if the input histories satisfy the declared constraints and the gluing rule is admissible, then the composite continues to satisfy them.

Coherence and obstruction data. Global consistency conditions should be represented separately from ordinary resource typing. A computation may be locally admissible yet fail globally because transition data do not descend, because a characteristic or obstruction class is nontrivial, or because a proposed quantum measure cannot be made gauge invariant.

The constructive core may therefore track explicit obstruction data and, where available, a chosen trivialization of those obstructions. What it may certify is that the *declared* coherence conditions of the geometric model are satisfied.

This should not be identified with quantum anomaly cancellation. In a genuine quantum field theory, anomalies are obstructions to the consistent quantization or functorial composition of the quantum theory, and additional data may be required to cancel or absorb them [Sch14]. The relationship between geometric coherence obstructions and physical quantum anomalies is therefore a theorem to be earned, not a consequence of typing alone.

Prequantum semantics and the quantization boundary. The construction above is intentionally prequantum. It specifies geometric histories, their moduli, their composition, and their invariant readouts. It does not yet assign quantum amplitudes to histories.

A later quantization step, if one exists for a chosen sector, should be treated as an additional functorial construction. Schematically, the correspondence

$$\mathfrak{M}(\Sigma_{\text{in}}) \xleftarrow{s} \mathfrak{M}(W) \xrightarrow{t} \mathfrak{M}(\Sigma_{\text{out}})$$

might be sent to a linear operation of the form

$$\mathcal{Q}(W) : \mathcal{H}_{\Sigma_{\text{in}}} \longrightarrow \mathcal{H}_{\Sigma_{\text{out}}},$$

or, in a pull–push presentation,

$$\mathcal{Q}(W) \sim t_!(K_W \otimes s^*(-)),$$

where K_W contains whatever dynamical weight, action, measure, or generalized cohomological data the chosen quantization requires. This schematic form marks the additional weighting data required to pass from geometric process semantics to a quantum realization.

The separation is important. Sheafification or descent may construct globally compatible histories from local data, and evaluation may extract gauge-invariant readouts from those histories. Still, neither operation by itself supplies a quantum measure, interference law, positivity structure, or unitary evolution. These remain part of the later reconstruction problem developed in section 5.4.

Type extensions and topology change. Not every enlargement of the theory should be represented as an ordinary effect. Some extensions change the class of admissible objects or morphisms themselves. New matter sectors, new classes of stable defects, different boundary categories, and genuine topology-changing processes may therefore require *type extensions* rather than handlers acting inside a fixed calculus.

This distinction is particularly important for topology change [AGM93, AGM94]. A coarse-graining handler may rewrite one representative of a fixed semantic process, but a topology-changing history can enlarge the bordism class through which composition is defined. Such an extension must therefore specify new admissible types and morphisms together with the new gluing, coherence, and obstruction conditions they satisfy.

The same principle applies to nonperturbative sectors: they should be added only when the extended theory supplies an explicit semantic role and compatible composition law, rather than being inserted as unconstrained new histories.

Stated goals. Practically, the workflow is therefore: specify typed boundary data; construct a computational geometric bordism; verify the kinematic and constraint judgments; impose the chosen dynamical law where appropriate; compose compatible regions by gluing; evaluate the total core semantics and declared readouts; and only then apply controlled handlers or type extensions when the physical problem demands them.

Our aim is a language *expressive* enough to describe nontrivial gauge transport, curvature, defects, changing moduli, and eventually field-theoretic dynamics, yet *restricted* enough that well-formedness, core termination, composition, descent, constraint preservation, and observational equivalence can be proved rather than assumed.

Extensions—including matter content, nonperturbative sectors, and topology change—are then added modularly as controlled effects or type extensions, together with new proof obligations as the expressive power of the theory is widened. In this sense, constructive computational gauge theory is intended to provide a semantics in which geometric processes may be calculated, composed, and certified without pretending that the full analytic and quantum theory has already been constructed.

Constructive and compositional precedents. Several established frameworks provide complementary precedents for the present programme. Constructive quantum field theory develops rigorous analytic methods for constructing field-theoretic models and recovering quantum structures from Euclidean data [OS73, GJ87]. Algebraic quantum field theory instead emphasizes local observable algebras and their compatibility across spacetime regions [HK64, BSZ92], while factorization algebras develop a complementary local-to-global organization of classical and quantum observables [CG17].

Our proposal differs from these approaches in taking admissible geometric processes, typed boundaries, transport, and composition as the initial semantic data. The objective is not to replace the analytic constructions of quantum field theory with formal syntax, but to establish a computational-geometric calculus in which well-formedness, gluing, and invariant preservation can be verified prior to any subsequent quantum reconstruction.

On QFT and foundational description. We do not dispute the empirical success of quantum field theory, nor its central role as a unifying mathematical framework in modern physics. For present purposes, however, we treat QFT not as a primitive ontology, but as a highly developed local-to-global description of continuous physical processes. Its essential structures—local fields and observables, symmetry, gauge transport, composition across regions, and controlled change of description across scales—provide a canonical template for smooth non-commutative analog computation. At the same time, in strongly coupled and nonperturbative regimes, these structures are not generally captured by a single globally transparent continuum construction; perturbation theory, regularization, renormalization, effective field theory, and lattice methods instead provide complementary presentations of the same underlying physical content.

Our proposal therefore begins one layer earlier. Rather than taking quantum fields, functional measures, or probabilistic amplitudes as primitive, we begin from a constructive geometric substrate in which local admissible operations, transport, and gluing are specified directly. Gauge-theoretic and probabilistic descriptions are then expected to arise as stable coarse-grained readouts of this underlying process. QFT is thus retained as an indispensable effective language and structural guide; the claim is only that the computational-geometric architecture it captures may admit a more primitive realization than the continuum quantum formalism itself. If successful, such a formulation could also have a practical methodological benefit in the EVT (2.4) sense: by encoding admissibility, composition, and invariant preservation directly into the substrate, it may shift part of the burden from brute-force calculation and after-the-fact consistency checks toward verification by construction, making difficult nonperturbative and multiscale problems more *tractable* for both human and machine-assisted analysis.

Compactness modulo gauge. A fundamental analytic precedent for controlling geometric degeneration is Uhlenbeck compactness. For connections over a compact n-dimensional manifold, suitable uniform L^p bounds on curvature, with $p > n/2$, yield weak subsequential compactness modulo gauge [Uhl82]. The critical four-dimensional case is more delicate. Under the appropriate Yang–Mills or anti-self-duality hypotheses, sequences with bounded L^2 curvature energy may develop concentration at finitely many points. After suitable gauge transformations, convergence can be recovered away from these points, while the lost curvature energy and topological information must be accounted for by bubbling or ideal-connection data [Sed82].

This distinction is essential for constructive computational gauge theory. Gauge fixing does not

eliminate every form of geometric degeneration, and a limiting connection alone need not retain the complete invariant content of the original sequence. In our proposed semantics, such limits motivate a handled effect that records both the surviving geometric data and any additional defect information. Preservation of specified boundary observables must then be established as a separate compatibility condition.

Compactness, however, must not be confused with computability. These theorems provide subsequential limits under analytic hypotheses; they do not generally supply algorithms for finding those limits or effective convergence rates. Constructive evaluation additionally requires computable representations, effective estimates, and certified control of the selected observables. We therefore require two distinct forms of discipline: analytic compactness to control geometric degeneration, and effectivity to make the resulting semantics computational rather than merely existential.

From external lattices to an intrinsic, lattice gauge calculus. Lattice gauge theory [Oec05] discretizes a continuum on an external grid: links carry group elements, plaquettes carry curvature, and one hopes to recover physics in a subtle continuum limit. But computability is not baked in; it is delegated to numerics.

By contrast, GCM lattices are of a different kind. The "lattice" is the 1–skeleton generated by minimal holonomy loops of the helix geometry itself; nodes are join interfaces (Gauss constraints), edges are Wilson–loop registers, faces carry curvature flux. No continuum limit is imposed from outside: the cell structure is induced by the manifold's own group–theoretic and topological constraints. Spectral gaps and forbidden transitions then arise from intrinsic geometry rather than from a choice of mesh.[7]

- **State space.** A presheaf or stack of local moduli [MLM92] over a helix-adapted cover; descent or sheafification enforces compatibility and produces globally admissible states.
- **Evaluation.** The typed core evaluates declared gauge-invariant observables or computational readouts on globally compatible states. This evaluation is required to be total on the core fragment, but it is not identified with quantum-amplitude normalization.
- **Scale change.** Refinement and coarse-graining are explicitly handled transformations of the cover and moduli data, accompanied by certificates specifying the readouts or effective structures they preserve.

Example 4.4 (Sheafification/Evaluation on an Intrinsic Helical Chain). Let $X = U_1 \cup U_2 \cup U_3$ be a helical working region whose open sets are centered on three consecutive intrinsic holonomy loops $\gamma_1, \gamma_2, \gamma_3$, with overlaps $U_{12} = U_1 \cap U_2$ and $U_{23} = U_2 \cap U_3$, and no triple overlap. Assume these opens as coming from the geometry of the GCM itself, rather than from an externally imposed cubic grid.

Let $\mathcal{M}(U)$ be the presheaf assigning to each open set $U \subseteq X$ the groupoid of $U(1)$-connections on the trivial line bundle over U, modulo gauge, together with the induced Wilson-loop values on the intrinsic loops contained in U. A local section over U_i is represented by a connection A_i and its holonomy

$$u_i := \mathrm{Hol}_{\gamma_i}(A_i) \in U(1).$$

The local data glue precisely when the restrictions align to gauge overlaps:

$$A_2|_{U_{12}} = A_1|_{U_{12}} + g_{12}^{-1} dg_{12}, \qquad A_3|_{U_{23}} = A_2|_{U_{23}} + g_{23}^{-1} dg_{23}.$$

After sheafification, the admissible global states are therefore not arbitrary triples (u_1, u_2, u_3), but compatible glued sections

$$A \in \Gamma(X, \mathcal{M}^{\#}).$$

Now choose the outgoing loop γ_{out} obtained by concatenating the three intrinsic channels. In the abelian corridor, the functoriality of holonomy gives

$$\mathrm{Hol}_{\gamma_{\mathrm{out}}}(A) = u_3 u_2 u_1.$$

Thus, the intrinsic lattice calculus does not "sum over histories" on an external mesh; it first constructs the global section by gluing local moduli, and only then evaluates the observable.

[7] "It's nice to have a framework where you can only have one Lagrangian, but it would be even nicer to have some reason that this particular algebra would inevitably appear as an answer to some question." —E. Witten [Int14]

The constructive evaluator is the gauge-invariant map

$$\mathrm{ev}_X : \Gamma(X, \mathcal{M}^{\#}) \longrightarrow U(1), \qquad \mathrm{ev}_X(A) := \chi(\mathrm{Hol}_{\gamma_{\mathrm{out}}}(A)),$$

where in the simplest abelian case one may take $\chi(z) = z$, or more generally a thresholded readout to a finite alphabet.

This also exhibits the effect-handler viewpoint. A coarse-graining handler may replace the pair (U_1, U_2) by a single effective region U_{12} with effective holonomy

$$u_{12} := u_2 u_1.$$

The rewritten term has local data (u_{12}, u_3), but the boundary observable is unchanged:

$$\chi(u_3 u_{12}) = \chi(u_3 u_2 u_1).$$

Hence, coarse-graining is not an informal simplification; it is a semantics-preserving rewrite certified by preservation of the boundary class function.

In the non-abelian lift, the same example survives with ordered transport:

$$U_{\mathrm{out}} = U_3 U_2 U_1, \qquad \mathrm{ev}_X(A) = \mathrm{tr}_\rho(U_3 U_2 U_1),$$

so the only change is that composition becomes path-ordered, and the evaluator passes from a scalar phase to a class function on holonomy.

Remark 4.5 (Why Not Classical $\mathbb{R}$?). In the fluidic/gauge band, one is tempted to model directly over the classical continuum. However, unrestricted real computation (cf. A.7) admits hyper–Turing power and brittle pathologies (exact tests, branch–on–sign over nonrobust inputs, oracle–like primitives). This undermines the two pillars we require: *executability* (every step is effectful but total) and *verifiability* (small perturbations do not change the decision class). Our constructive stance preserves smooth geometry while preventing hidden oracles.

Geometric reals? We separate *semantics* (smooth reasoning) from *execution* (effective approximation):

(a) **Computable reals** $\mathbb{R}_{\mathrm{comp}}$. Externally, numerical data (couplings, boundary values, readouts) live as computable reals given by fast Cauchy names (or, when possible, algebraic numbers with exact arithmetic). Equality is replaced by interval refinement; separation proofs guard branching. This is the target of all executable algorithms [Wei00].

(b) **Synthetic/smooth reals.** $\mathbb{R}_{\mathrm{syn}}$ internally, differential reasoning uses the smooth reals of a well–adapted SDG model (Kock–Lawvere axiom [Koc06], nilpotent $d\varepsilon = 0$), so vector calculus and curvature remain first–class without appeal to pointwise limits.[8]

(c) **A bridge.** A semantic–to–execution functor sends internal smooth expressions (curvatures, class functions on holonomy) to external names in $\mathbb{R}_{\mathrm{comp}}$, with *proof obligations* discharged by our effect handlers (for limits/coarse–graining).

The two-level scalar semantics retains smooth continuum reasoning alongside effective computation. Parameters are measured to finite precision, and algorithms require effective representations. Thus we use rationals/algebraics/$\mathbb{R}_{\mathrm{comp}}$ for execution, while $\mathbb{R}_{\mathrm{syn}}$ supplies calculus internally. This pragmatic split aligns with the observation (cf. [Szu12]) that physical models do not require arbitrary reals to be *expressed* or *simulated*, even if smooth structure is invaluable for *reasoning*.

Design axioms: equality, limits, and effects. We enforce three constraints in the core calculus:

- **No exact branching on undecidable predicates.** Tests are certified by separation bounds (or deferred as obligations).
- **Limits are effects.** Completion, closure, and renormalization are algebraic effects with handlers that carry witnesses of convergence/stability.

[8] Any well–adapted model suffices; no commitment to a specific topos is needed, but an implementation is provided in section 5.3 for convenience.

- **Gauge invariants only.** Readouts are class functions of holonomy (e.g. traces), ensuring stability under small perturbations and gauge changes.

Remark 4.6 (Effective Computability of Continuum Quantities). Our setting concerns analog geometrodynamics on a noncompact configuration space. Gaps (i.e., mixing rates, spectral edges of transfer generators) are typically defined by nested sup / inf over unbounded domains. In general, these constants need not be uniformly computable from the defining data. We therefore (a) state results in terms of *semi–decidable* or *effectively approximable* quantities, or (b) confine genuinely noncomputable constants to effectful interfaces outside the core (they cannot influence totality/normalization proofs). The present model cannot resolve the Clay Yang–Mills existence and mass-gap problem [JW06], which requires a rigorous construction of four-dimensional *quantum* Yang–Mills theory and proof of a positive mass gap.

Analytic obligations and intended advantage. A viable constructive realization must still establish the relevant Yang–Mills PDE results—including existence and regularity of admissible solutions, gauge fixing, a priori energy and curvature estimates, boundary compatibility, compactness modulo gauge, and control of bubbling or defect formation—together with stability and convergence under refinement. The proposed advantage is instead organizational. Rather than attacking the continuum theory as a single global configuration-space problem, GCFT decomposes it into typed local histories with explicit boundary data, gauge equivalences, and gluing laws, so that one may seek estimates and compactness statements that are stable under composition and propagate from local regions to larger histories. In this sense, the analytic task substantially differs from the standard Yang–Mills mass-gap problem: the Clay problem asks directly for the construction of a nontrivial four-dimensional quantum Yang–Mills theory with a positive mass gap, whereas the computational program inserts an intermediate regulated and compositional layer and asks whether the required continuum and spectral estimates can be assembled from uniformly controlled local data. If this decomposition fails to simplify or localize the necessary estimates, then the constructive apparatus supplies only a reorganization of the problem rather than a shortcut to its solution.

On finite information and intuitionist physics. We concur with the operational point that experimental data carry finite information, and that uncountable precision should not be a primitive of algorithms, as brought up by [Gis19]. Where we differ is methodological: we retain a smooth internal semantics ($\mathbb{R}_{\text{syn}}$) to keep geometry local and functorial, while ensuring that *every* externally visible quantity is realized in $\mathbb{R}_{\text{comp}}$ with certified error control. Thus, the continuum remains a modeling tool; computation proceeds on effectively presentable numbers.

Choosing a constructive base allows us to retain the familiar analytic language where needed while ensuring that each step of the formalism remains executable. The framework developed here treats physical dynamics as smooth, often chiral/transcendental flow, while treating topology and quantization as mechanisms of coarse-graining that project this flow onto the discrete structures accessible to observation. In this sense, the continuum substrate and the discrete emergent layer are not competitors but complementary levels of description. What we call "physical computation" is the geometric process that occurs at their interface, with its behavior constrained by the EVT Trilemma. Nothing in the present approach depends on sub-Planckian assumptions, nor do we take uncountable structure as primitive in the dynamics. We hope that the fully constructive classification outlined in (5.3) provides a more precise setting in which longstanding questions, including those surrounding Yang–Mills, can be reformulated and studied. A high-level road map toward the Yang–Mills mass gap in computational gauge theory is outlined below:

(a) **Define computational semantics for gauge theory.** Define a typed, resource-sensitive, total-core, effect-controlled calculus whose types encode boundary/interface data (3-geometries with gauge labels) and whose terms encode computational geometric bordisms (4-dimensional histories composed by gluing).

(b) **Build computable geometric bundles.** Give the calculus a denotational semantics in terms of computably presented bundles, connections, parallel transport, and their gauge moduli, formulated in a constructive/synthetic differential setting where appropriate. This preserves the differential structure while requiring effective evaluation on the designated constructive core.

(c) **Assess the scaling limit to continuum Yang–Mills.** Prove that families of regulated computational models approximate continuum Yang–Mills in a controlled scaling limit. Concretely,

a "differential computational jet calculus" would provide local error bounds under refinement, while the corresponding gauge-invariant observables—including Wilson loops and, after the appropriate quantum reconstruction, correlation functions—must converge to those of continuum Yang–Mills (see section A.3).

(d) **Prove the gap and its stability.** Establish a spectral gap (a uniform lower bound on excitation energies) for the constructive model using the required energy estimates, compactness modulo gauge, and spectral analysis; then show that this lower bound survives the scaling limit, yielding a continuum mass gap. Here, the constructive setting aims to organize the global problem through local-to-global invariants, admissible gluing, and certified control of the regulated models, without replacing the analytic compactness and continuum estimates required by Yang–Mills theory.

Geometric interpretation of the Yang–Mills mass gap. The Yang–Mills mass-gap problem poses a particularly sharp test. For a four-dimensional quantum Yang–Mills theory with compact simple gauge group, the question is whether the physical Hamiltonian possesses a strictly positive spectral gap above its vacuum:

$$\Delta_{\mathrm{YM}} := \inf\big(\mathrm{spec}(H_{\mathrm{phys}}) \setminus \{E_0\}\big) - E_0 > 0.$$

The gap concerns the energy spectrum of gauge-invariant physical excitations, not a discrete separation between geometric configurations, topological sectors, or computational readout values. Classical connections may vary continuously without implying the existence of arbitrarily low-energy physical particles.

From the perspective of GCFT, the problem is therefore to explain how continuous, non-Abelian geometric dynamics can produce a positive minimum excitation energy after the relevant gauge constraints and physical reconstruction have been imposed. The underlying connection admits continuously varying curvature and holonomy, but the spectrum of admissible physical excitations need not inherit this continuity down to zero energy. Under appropriate spectral assumptions, a positive gap is reflected in exponential decay of connected Euclidean correlation functions of suitable gauge-invariant observables, with a finite correlation length set by the lightest physical excitation.

Such behavior cannot be inferred from noncommuting holonomy or geometric closure alone. A genuine derivation must recover the relevant nonperturbative dynamics, the generation of a physical mass scale, and a positive-energy spectrum in the continuum and infinite-volume limits. This motivates a program in which the spectrum and correlations of physical excitations are reconstructed from admissible geometric histories, rather than postulated as primitive properties of an abstract field operator.

5 Geometric Computational Field Theory

The constructive calculus developed above is formulated at the level of typed geometric histories, gluing operations, and gauge-invariant readouts. To connect this formal architecture with familiar physical spacetime, however, one must explain how its Euclidean computational presentation relates to causal evolution, metric structure, and the effective Lorentzian theories used in physics. Our constructions are not introduced as an additional fundamental ontology, but as controlled presentations of the same underlying gauge computation to show how Lorentzian spacetime, gravitational response, and particle-like excitations may emerge as effective semantics of a deeper Euclidean geometric process.

5.1 Euclidean Gauge Computation and Emergent Spacetime

Euclideanization and clocking. The physical Yang–Mills mass gap concerns a relativistic quantum field theory on Minkowski spacetime $\mathbb{R}^{1,3}$, whereas our constructive model is formulated on a *Euclidean* 4-manifold. The problem of time in canonical quantum gravity is well known: the Hamiltonian constraint obstructs the identification of an external evolution parameter with physical time, leading in the Wheeler–DeWitt formalism to a seemingly "frozen" global state [Ish92]. We do not attempt to resolve this problem here. Rather, GCT distinguishes mathematical parameters used to organize admissible geometric histories from physical time defined relationally through internal clocking and observable correlations.

The fourth Euclidean coordinate supplies an additional geometric direction for resolving chirality obstructions (e.g., Type 2 *THM*) without identifying that direction with Lorentzian time or imposing

a preferred temporal foliation. Formally, Euclidean and Lorentzian field-theoretic descriptions are related by Wick rotation $t \mapsto -i\tau$, subject to the appropriate analytic and reconstruction conditions.

Operationally, pulses and flow propagation organize geometric evaluations, while stable recurrent subsystems may furnish internal clocks through their phases and correlated readouts. Lorentzian observables are recovered, where the necessary reconstruction conditions hold, from Euclidean correlation functions satisfying the Osterwalder–Schrader axioms, including reflection positivity [OS73]. In our calculus, "Wick rotation" is a controlled effect: Euclidean evaluation (for existence/compactness) and Lorentzian reconstruction (for causal dynamics and, with further assumptions, scattering) are separate, typed phases of the same program. This retains the computational advantages of a 4D Euclidean setting while providing a conditional route to physical predictions in $\mathbb{R}^{1,3}$, without presupposing a universal background clock.

The landscape of twistor theory. Twistor theory provides a complementary complex-analytic description of selected four-dimensional geometric and gauge-theoretic structures. Originating in the work of Penrose and collaborators [PM73], the Penrose transform relates appropriate sheaf cohomology classes on twistor space to solutions of linear massless field equations, while the Ward correspondence relates suitable holomorphic vector bundles to (anti-)self-dual Yang–Mills connections. These correspondences are especially useful because they reorganize differential equations and gauge constraints into holomorphic or cohomological problems. They do not, however, imply that general non-Abelian Yang–Mills dynamics become linear or algorithmically decidable.

Reader's compass. For our purposes, "twistor phase" means a regime where inherently noncommuting spacetime/gauge data admit a holomorphic reparametrization that turns analysis into cohomology. The symmetry group at play is the full conformal group $\mathrm{SU}(2,2) \cong \mathrm{Spin}(2,4)$; it is *not* an abelian corner. Thus, the twistor limit is best read as a complex-analytic chart in which selected self-dual or holomorphically constrained sectors admit more tractable descriptions through cohomology and integrability, even though the underlying gauge content may remain non-abelian. This can improve the calculation and certification of particular invariants without establishing global algorithmic verifiability. Nothing in this viewpoint licenses literal real-valued "infinite computation": finite-information bounds [Bou02] still apply. The twistor phase should be read as a *cohomological* linearization window, not as physical hypercomputation.

Finally, our framework is naturally compatible with holomorphic tools that also appear in parts of the Geometric Langlands (cf. [KW07]) and with twistor approaches to scattering amplitudes; see, e.g., the mathematical discussion noted in [Woi22]. These correspondences motivate the possibility that distinct holomorphic, gauge-theoretic, and categorical presentations may preserve a common structure of boundary observables and admissible compositions. We propose to interpret such dualities as changes of computational presentation wherever the appropriate equivalence can be established, rather than assuming that they are ordinary coordinate changes within a single fixed gauge theory. Our work does not require the full program, but it motivates the principle that physical/gauge computation should respect these categorical re-factorizations.

On Calabi–Yau manifolds and stable loci. The present viewpoint is not a String-theoretic construction. Still, it shares with string theory a geometry-first emphasis on extended objects, moduli, and the extraction of physical structure from constrained geometric deformation. On a compact Kähler manifold with $c_1 = 0$, Yau's theorem [Yau78] guarantees a unique Ricci-flat Kähler metric in each Kähler class. This furnishes a geometrically constrained background with powerful linear tools (Hodge theory, period maps, variation of Hodge structure) and controlled deformations.

Reader's compass. In our setting, Calabi–Yau (CY) [Pic19] structures are proposed as *stable bookkeeping loci*: constrained regions of geometric moduli in which selected curvature, flux, and deformation data admit controlled cohomological descriptions. This does not require the underlying gauge connection to become abelian; indeed, generic irreducible Calabi–Yau threefolds possess non-abelian $SU(3)$ Riemannian holonomy. Rather, the harmonic representatives of cohomology classes provide linear "ledgers" for suitable fluxes and charges, while Hodge decomposition and intersection pairings supply rigid accounting for the corresponding invariant data. For threefolds, the $(1,1)$ and $(2,1)$ sectors describe Kähler and complex-structure deformations, respectively. We propose that these sectors may furnish controlled models of computational capacities and admissible morphisms, with selected verification problems reducible to cohomological linear algebra.

Technically, three mechanisms are relevant to these proposed calibration loci:

(a) In abelian and maximally abelian quasi-fluidic regimes, suitable coefficient objects may carry an E_∞ structure, making parallel composition coherently commutative and compatible with the excisive constructions used below.[9]

(b) Twisted and equivariant K-theory can organize stable topological classes of charges and geometric channels, while period integrals and Picard–Fuchs equations describe variations of the relevant cohomological data.

(c) Transport around singular loci or boundary regions of Calabi–Yau moduli, including conifold and large-complex-structure limits, can produce monodromy and Picard–Lefschetz transformations. Such transformations may be noncommutative and complicate global accounting even when local cohomological descriptions remain available.[10]

Hence, CY manifolds are not a generic case; we propose them as *integrable gate points*—distinguished geometric settings in which selected invariant data admit cohomological or holomorphic descriptions and verification becomes more accessible. In GCT, they serve as candidate calibration loci for the lower abelian and quasi-fluidic regimes, and as possible transition charts toward richer gauge-theoretic presentations. Their significance is not that generic Calabi–Yau dynamics are linear or that their holonomy becomes abelian, but that constrained sectors can admit exceptionally effective mathematical descriptions. The identification of these loci with physical computational phase boundaries remains a dynamical question: motion through Calabi–Yau moduli does not, by itself, activate non-abelian gauge holonomy or require passage to a twistor regime.

Hyperkähler geometry and protected gauge moduli. A hyperkähler manifold $(\mathcal{M}, g, I, J, K)$ carries three covariantly constant complex structures satisfying the quaternionic relations

$$I^2 = J^2 = K^2 = IJK = -1,$$

with corresponding Kähler forms

$$\omega_I(\cdot,\cdot) = g(I\cdot,\cdot), \qquad \omega_J(\cdot,\cdot) = g(J\cdot,\cdot), \qquad \omega_K(\cdot,\cdot) = g(K\cdot,\cdot).$$

Equivalently, the same underlying real geometry admits a $\mathbb{CP}^1$-family of compatible complex structures whose holomorphic symplectic data are assembled by the associated twistor space. Hyperkähler geometry therefore occupies a special position between the Calabi–Yau and twistor presentations discussed above: it is Ricci-flat and cohomologically rigid enough to support controlled geometric accounting, while remaining naturally adapted to non-abelian gauge moduli and their holomorphic reconstruction. Indeed, moduli spaces of anti-self-dual instantons, monopoles, and solutions of Hitchin's equations frequently arise as hyperkähler quotients

$$\mathcal{M} = \boldsymbol{\mu}^{-1}(0)/\mathcal{G}, \qquad \boldsymbol{\mu} = (\mu_I, \mu_J, \mu_K),$$

where the moment-map equations impose the gauge-theoretic constraints and division by $\mathcal{G}$ removes frame-dependent descriptions [HKLR87, Hit87a]. For Hitchin systems, the resulting moduli space additionally admits an algebraically completely integrable fibration, allowing non-abelian gauge data to be reorganized through spectral curves and commuting Hamiltonians [Hit87b]. In GCFT, such a metric should not be regarded as a primitive structure on the computational substrate. Rather, it is a derived geometry on a constrained quotient of admissible configurations: the pre-metric theory specifies interfaces, joins, transport, curvature, and gauge equivalence, while the hyperkähler metric measures deformation, stability, and effective motion within the resulting moduli space. The $\mathbb{CP}^1$-family then supplies multiple holomorphic presentations of the same real process space, allowing nonlinear gauge data to be reorganized through spectral, symplectic, or twistor coordinates without changing the underlying computational semantics. In protected supersymmetric sectors, BPS and wall-crossing data may further determine corrections to a semiflat approximation and thereby reconstruct the twistor data of the hyperkähler metric [GMN10, GMN13]. Hyperkähler loci are thus best interpreted as protected non-abelian corridors—regions in which path ordering and holonomy remain active, but additional integrability makes the corresponding moduli sufficiently rigid for exact or asymptotic calculation. Selected reductions, such as ADHM-, Nahm-, or Hitchin-type sectors, may provide computable test cases for the future GCFT evaluator.

[9] E_∞ here denotes coherent homotopy-commutativity; see section A.6.

[10] This monodromy belongs to the variation of geometric data over moduli and should be distinguished from the holonomy of a physical Yang–Mills connection.

Table 10: Classification of computational regimes by data type and algebraic structure

Symmetry Regime	**Algebraic Structures**	**Data Types**
Discrete / symbolic (finite cyclic C_n)	Finite rings/Boolean algebras	Bits, n-its
Analog abelian ($U(1)$)	Real/complex fields, Lie algebra $\mathfrak{u}(1)$	Circle phases, amplitudes
Analog non-abelian (($SU(2)$, $SU(3)$); gauge group actions)	Principal bundles, moduli spaces, ∞-groupoids; (co)homology operations	Global classes (characteristic classes/Chern, Floer/Donaldson-type)

Interactions of regimes within emergent gauge behavior. The presentations of the discrete and abelian regimes in section 2 and 3 are intentionally given at the level of their *readouts*—coarse projections that isolate the symbolic (C_n) and commutative ($U(1)$) components of the substrate. In the full interaction picture, where non-abelian transport and defect/gluing data are active, the resulting dynamics are *not* adequately described by a standalone $C_n/U(1)$-valued cellular automaton. For expository purposes, we can collapse the final four-regime classification of section 5.3 into the three-band summary of table 10, and then indicate how the emergent gauge regime reorganizes the lower readouts.

Regimes as readouts of a single substrate. Table 10 should not be read as a list of unrelated theories, but as a hierarchy of *coarse-grained readouts* of one underlying flow. Concretely, let $\mathcal{S}$ denote the space of full substrate states (helical geometry, joins/defects, and transport data). The three rows of table 10 correspond to progressively richer "decoding maps"

$$\pi_{\mathrm{C_n}} : \mathcal{S} \to \mathcal{S}_{\mathrm{C_n}}, \qquad \pi_{U(1)} : \mathcal{S} \to \mathcal{S}_{U(1)}, \qquad \pi_{\mathrm{gauge}} : \mathcal{S} \to \mathcal{S}_{\mathrm{gauge}},$$

where $\pi_{\mathrm{C_n}}$ forgets geometric transport and retains only local symbolic degrees of freedom (a cellular automaton shadow), $\pi_{U(1)}$ retains a commutative phase/flux bookkeeping (an "abelianized" quasi-fluidic shadow), and π_{gauge} retains full non-abelian parallel transport and defect/gluing data (the fluidic/gauge regime). Thus, entering into π_{gauge} does not replace the lower regimes; it means we stop applying the early projections. The lower regimes remain present as *shadows* of the full dynamics, i.e. as the observables that survive after discarding non-commuting transport information.

Gauge back-reacts on lower readouts. Once non-abelian transport is active, the lower readouts inherit three systematic features:(a) *sectorization* by global topological labels (bundle/defect classes); (b) *twisting* of coefficients (fields become sections of associated bundles/local systems); (c) *center/trace observables* (the surviving abelian data is typically class-function data of holonomy). Concerning cohomology, near CY strata it may serve primarily as a linear *ledger* of invariant data within a selected sector, while more general gauge and twistor presentations may expose its additional roles in classifying sectors, obstructions, monodromy, and wall-crossing. These roles need not correspond to distinct physical phases; their relationship depends on the admissible dynamics and the chosen computational presentation.

Example 5.1 (A Three-band Toy Model on T^3: Abelian Ledger Twisted Gauge Readout). This example makes explicit how a non-abelian gauge regime induces (a) sector labels, (b) twisted coefficients, and (c) trace/center observables in the lower abelian/quasi-fluidic readouts.
Base. Let $X = T^3 = \mathbb{R}^3/\mathbb{Z}^3$ with coordinates $x_1, x_2, x_3 \in \mathbb{R}/\mathbb{Z}$. Then

$$H^1(T^3;\mathbb{Z}) \cong \mathbb{Z}^3, \qquad H^2(T^3;\mathbb{Z}) \cong \mathbb{Z}^3, \qquad H^2(T^3;\mathbb{Z}_2) \cong (\mathbb{Z}_2)^3.$$

Band A: $U(1)$ ledger (commutative transport). A $U(1)$-connection A on a line bundle $L \to T^3$ splits into topological flux and a flat holonomy part:

(a) *Flux ledger (H^2).* The Chern class $c_1(L) \in H^2(T^3;\mathbb{Z}) \cong \mathbb{Z}^3$ may be represented by an integral curvature form

$$\frac{F}{2\pi} = n_1\, dx_2 \wedge dx_3 \;+\; n_2\, dx_3 \wedge dx_1 \;+\; n_3\, dx_1 \wedge dx_2, \qquad n_i \in \mathbb{Z},$$

so (n_1, n_2, n_3) is a literal cohomological "ledger" of $U(1)$ fluxes.

(b) *Holonomy ledger (H^1).* A flat connection may be written

$$A_0 = 2\pi(\alpha_1\, dx_1 + \alpha_2\, dx_2 + \alpha_3\, dx_3), \qquad \alpha_i \in \mathbb{R}/\mathbb{Z},$$

with holonomies around the coordinate 1-cycles γ_i given by

$$\mathrm{Hol}_{A_0}(\gamma_i) = e^{2\pi i \alpha_i} \in U(1).$$

Thus, the abelian/quasi-fluidic readout is linear: integers in H^2 plus phases in $H^1(-;\mathbb{R}/\mathbb{Z})$.

Band B: Flat $SU(2)$ holonomy (non-abelian gauge readout). A flat $SU(2)$-connection on T^3 is equivalent to a representation

$$\rho : \pi_1(T^3) = \mathbb{Z}^3 \longrightarrow SU(2),$$

i.e. a commuting triple

$$(g_1, g_2, g_3) \in SU(2)^3$$

modulo simultaneous conjugation. Since commuting elements in $SU(2)$ lie in a common maximal torus $T \cong S^1$, any such triple may be simultaneously conjugated to

$$g_i = \begin{pmatrix} e^{i\theta_i} & 0 \\ 0 & e^{-i\theta_i} \end{pmatrix}, \qquad \theta_i \in \mathbb{R}/2\pi\mathbb{Z}.$$

The residual conjugation preserving the maximal torus is the Weyl group

$$W = N(T)/T \cong \mathbb{Z}_2,$$

which acts diagonally by simultaneous inversion,

$$(\theta_1, \theta_2, \theta_3) \longmapsto (-\theta_1, -\theta_2, -\theta_3).$$

Hence the coarse flat moduli space is

$$\mathcal{M}_{\mathrm{flat}}(T^3, SU(2)) \;\cong\; \mathrm{Hom}(\mathbb{Z}^3, SU(2))/SU(2) \;\cong\; T^3/W,$$

where W acts by simultaneous inversion. Equivalently,

$$\mathcal{M}_{\mathrm{flat}}(T^3, SU(2)) \;\cong\; (S^1)^3/\big((z_1, z_2, z_3) \sim (z_1^{-1}, z_2^{-1}, z_3^{-1})\big).$$

The important point is that the Weyl action is simultaneous: one does not independently identify each θ_i with $-\theta_i$, since gauge equivalence acts by a single simultaneous conjugation of the whole representation ρ.

This immediately exhibits two of the three claimed effects:

(c) Trace/character observables. Gauge-invariant observables factor through simultaneous conjugacy classes, and hence through class functions of the holonomies. For the coordinate generators one obtains

$$\mathrm{tr}(g_i) = e^{i\theta_i} + e^{-i\theta_i} = 2\cos(\theta_i).$$

More generally, traces of words in the commuting holonomies, such as

$$\mathrm{tr}(g_i g_j) = 2\cos(\theta_i + \theta_j),$$

define gauge-invariant class functions on the simultaneous conjugacy class. Thus the "abelian shadow" of non-abelian transport is not the raw holonomy matrix, but character/class-function data extracted from holonomy.

(b) Twisted coefficients. Fixing ρ, infinitesimal deformations of the flat connection are governed by cohomology with *twisted* coefficients. At a regular point of the flat moduli space, the reduced tangent directions are captured by

$$T_{[\rho]}\mathcal{M}_{\mathrm{flat}} \;\cong\; H^1\big(T^3; \mathrm{ad}_\rho\big),$$

where ad_ρ is the local system with fiber $\mathfrak{su}(2)$ and monodromy

$$\mathrm{Ad} \circ \rho : \pi_1(T^3) \longrightarrow \mathrm{Aut}(\mathfrak{su}(2)).$$

For a generic diagonal triple, the adjoint local system splits as

$$\mathrm{ad}_\rho \;\cong\; \underline{\mathbb{R}} \cdot \sigma_3 \;\oplus\; \mathcal{L}_{2\theta},$$

where $\underline{\mathbb{R}} \cdot \sigma_3$ is the trivial rank-1 Cartan subsystem and $\mathcal{L}_{2\theta}$ is the real rank-2 local system on which the coordinate loops act by rotation through angles $2\theta_i$. For generic holonomy, the rotating summand contributes no degree-1 cohomology, so one obtains

$$H^1(T^3; \mathrm{ad}_\rho) \;\cong\; H^1(T^3; \mathbb{R}) \;\cong\; \mathbb{R}^3.$$

Thus the surviving linear behavior is not ordinary untwisted cohomology from the outset; it is the Cartan component that remains after accounting for twisting by the background holonomy.

Band C: sector labels via $SO(3)$ and w_2. On T^3, every $SU(2)$-bundle is topologically trivial, so bundle-class sectorization is muted at the simply-connected level. Passing to the adjoint form $SO(3) \cong SU(2)/\{\pm I\}$ restores genuine topological sectors: principal $SO(3)$-bundles are classified by

$$w_2(P) \in H^2(T^3; \mathbb{Z}_2) \cong (\mathbb{Z}_2)^3.$$

Thus, the same H^2-type bookkeeping that served as an abelian "flux ledger" becomes, in the emergent gauge regime, a discrete *sector label* (a lifting obstruction for holonomy data), i.e., cohomology functions as governance rather than ledger [vB96].

Interpretation. This toy model exhibits the general mechanism used throughout the paper: the abelian/quasi-fluidic regimes record linear ledger data (classes/periods), while turning on non-abelian transport forces (a) decomposition into global sectors, (b) twisted coefficient systems for linearization, and (c) passage to trace/character class functions as the stable abelian shadows of gauge-invariant content.

Diffeomorphism invariance and the forced move to moduli invariants. In the highest (gauge) regime, the effective closure is not merely a compact structure group G acting on fibers, but the full redundancy of the geometric substrate: diffeomorphisms of the base (and their induced action on bundles and connections) as gestured towards in table 6. Concretely, the relevant symmetry is the gauge–diffeomorphism groupoid generated by $\mathrm{Diff}(M)$ together with bundle gauge transformations. Once computation must be invariant under this action, coordinate-level quantities cease to be meaningful: only invariants of the resulting quotient spaces (moduli of connections/flows up to gauge and diffeomorphism) remain as stable readouts. This is precisely the point at which Floer/Donaldson-type constructions become natural [Flo88, Don83], since they are designed to extract computable cohomological data from such moduli spaces.

Index theory and Seiberg–Witten benchmarks. Index theory provides a standard mechanism by which analytic field data acquire stable topological content. For a suitable elliptic Dirac-type operator D, the Atiyah–Singer theorem identifies its analytic index with a topological expression,

$$\mathrm{ind}(D) = \dim \ker D - \dim \mathrm{coker}\, D = \mathrm{ind}_{\mathrm{top}}(D)$$

[AS63]. Spectral flow of a family of self-adjoint Dirac-type operators is likewise related to an index on an associated higher-dimensional operator. In gauge theory, the same index-theoretic machinery enters the analysis of zero modes and perturbative anomaly data.

For GCFT, these results should be regarded as reconstruction benchmarks rather than consequences of the present type system. A constructive evaluator may record boundary conditions, admissible gluing, conserved charges, and obstruction classes, but agreement with continuum field theory requires that the resulting compositional semantics reproduce the relevant index data when a Dirac operator or corresponding elliptic complex is present. In particular, anomaly coefficients or zero-mode counts should not be regarded as guaranteed merely by typing; they constitute invariant data that a successful continuum reconstruction must preserve.

The Seiberg–Witten equations provide a complementary four-dimensional benchmark [SW94]. They couple a $U(1)$ connection on a determinant line bundle to a spinor and, after quotienting by gauge

and imposing the appropriate analytic hypotheses, give rise to moduli spaces from which smooth four-manifold invariants may be extracted. Their significance here is structural: a nonlinear gauge-theoretic PDE can admit a priori estimates, compactness properties, finite-dimensional moduli after elliptic reduction, and deformation-stable invariant output.

Seiberg–Witten theory thus supplies a benchmark for the analytic compression that a future GCFT reconstruction would need to reproduce:

$$\text{field equations} \longrightarrow \text{gauge quotient} \longrightarrow \text{controlled moduli space} \longrightarrow \text{invariant readout}.$$

A mature constructive gauge theory should therefore be judged in part by whether its geometric and compositional data can recover comparable index, compactness, and moduli-theoretic structures in regimes where the corresponding continuum theory is known.

Effective geometric layers. Geometric computation begins from a pre-metric configuration space, with propagation and readout structures supplying the first effective spacetime data. In particular, causal and optical behavior may be organized by an effective constitutive tensor χ; in near-equilibrium regimes, χ may become metric-induced, $\chi = \chi[g]$, thereby recovering Lorentzian geometry in the sense of pre-metric and constructive approaches to electromagnetism and gravity [Sch20]. Once this Lorentzian regime is available, quantum fields and observers should be interpreted with the usual curved-spacetime discipline: local observable algebras, admissible states, and horizon effects are part of the effective semantics rather than external additions [Wal95].

At still larger scales, gravitational dynamics are expected to appear as thermodynamic relations among the coarse-grained degrees of freedom of the substrate. This is consonant with Jacobson's derivation of the Einstein equation as an equation of state [Jac95], and with Padmanabhan's broader emergent-gravity program, in which the horizon or spacetime degrees of freedom satisfy thermodynamic/equipartition relations [PAD10]. Thus Schuller, Wald, Jacobson, and Padmanabhan occupy distinct effective layers: propagation selects causal structure, local quantum observables live on the recovered Lorentzian background, and coarse-grained horizon thermodynamics supply the macroscopic gravitational equation of state.

Effective field theory is therefore understood as an emergent description, valid only within an appropriate coarse-grained regime. We do not assume a priori that the effective dynamics are Markovian or that infrared and ultraviolet degrees of freedom admit a clean separation. The scale dependence of non-Abelian gauge interactions, exemplified by asymptotic freedom [GW73], underscores the importance of understanding the strongly coupled sector before attempting a complete reconstruction of macroscopic gravitational phenomena. Accordingly, we regard nonperturbative gauge dynamics as an intermediate problem in the emergence of spacetime thermodynamics and black-hole observables, whose detailed treatment is deferred to future work.[11]

Status of gravitons. Gravity is not quantized at the metric level in the present construction: we neither postulate a fundamental path integral over Lorentzian metrics nor take the metric itself to be a microscopic Yang–Mills-type field. Instead, a gravitational sector can arise only after coarse-graining produces an effective Lorentzian metric $g_{\mu\nu}$ together with a suitable long-wavelength action. If, in an appropriate regime, this effective action contains the Einstein–Hilbert term,

$$S_{\text{eff}}[g] = \frac{1}{16\pi G_{\text{eff}}} \int_M d^4x \, \sqrt{-g} \, \big(R - 2\Lambda_{\text{eff}}\big) + S_{\text{higher}}[g],$$

then small fluctuations about a background solution,

$$g_{\mu\nu} = \bar{g}_{\mu\nu} + h_{\mu\nu},$$

are governed at leading order by the quadratic part of S_{eff}. The perturbation $h_{\mu\nu}$ inherits the linearized diffeomorphism redundancy

$$h_{\mu\nu} \sim h_{\mu\nu} + \bar{\nabla}_\mu \xi_\nu + \bar{\nabla}_\nu \xi_\mu,$$

and, on a suitable vacuum background, the corresponding constraint equations remove the gauge and nondynamical components, leaving the two transverse-traceless propagating polarizations of a massless spin-2 field. Quantizing these effective normal modes yields helicity-± 2 excitations conventionally

[11] This caution is informed in part by [Bar25], which develops the role of non-Markovian, indivisible stochastic dynamics in a stochastic reconstruction of quantum phenomena.

called gravitons. Thus GCFT does *not* deny gravitons; it assigns them the status of quasiparticles of an emergent metric sector, analogous in logical status to phonons in an elastic medium, rather than fundamental constituents of the substrate.

A substantive reconstruction problem therefore lies one level below perturbative graviton physics. First, one must explain how its underlying computational dynamics, boundary constraints, and gluing laws generate a Lorentzian metric readout whose infrared effective action has the required diffeomorphism symmetry and spin-2 kinetic structure. Only after such a limit has been established is the usual graviton description [Hol06] warranted.

5.2 Reconstruction of Internal Gauge Symmetry

The preceding sections develop a sequence of increasingly rich transport structures: finite symbolic symmetry, compact abelian phase transport, and nonabelian frame holonomy. We now ask how far this hierarchy can be pushed toward the local gauge structure of the Standard Model. The aim of this subsection is not to derive the full Standard Model from first principles. In particular, we do not derive the observed hypercharge assignments, the chiral matter spectrum, generation multiplicity, Yukawa matrices, or anomaly cancellation. The narrower question is whether the internal gauge factors

$$SU(3)_c \times SU(2)_L \times U(1)_Y$$

can arise from geometric and representation-theoretic structures already present, or naturally generated, in the GCT hierarchy.

The primitive ω- and χ-channels should not be identified directly with electroweak and color gauge groups. They belong to the symbolic geometry of the twin helix substrate: ω supplies a cyclic phase channel, while χ supplies a signed geometric grading. The continuous gauge factors arise only after passing to internal transport spaces, their connections, and the holonomy groups generated by admissible controls.

The abelian phase factor. The $U(1)$ sector is the most direct. The abelian phase geometry developed in section 3.2 assigns to a one-dimensional complex transport channel a Hermitian line. Its norm-preserving automorphism group is

$$U(1) = \left\{ e^{i\theta} \;\middle|\; \theta \in \mathbb{R}/2\pi\mathbb{Z} \right\}.$$

Thus a compact phase ledger already carries the minimal continuous unitary gauge symmetry $U(1)$. In the Standard Model comparison below this supplies a candidate abelian factor; identifying its generator with physical hypercharge Y additionally requires the matter representation data introduced later.

Spinorial frame transport and the $SU(2)$ factor. The $SU(2)$ sector has a more explicitly geometric origin. A regular helical spine with nonvanishing curvature carries a Frenet–Serret frame

$$R(s) \in SO(3),$$

whose rotations admit the spinorial double cover

$$\mathrm{Spin}(3) \cong SU(2), \qquad SO(3) \cong SU(2)/\{\pm I\}.$$

As established in theorem 4.3, the lifted infinitesimal frame transport takes the form

$$\widetilde{R}^{-1}\frac{d\widetilde{R}}{ds} = -\frac{i}{2}\left(\tau(s)\sigma_1 + \kappa(s)\sigma_3\right),$$

where κ and τ are the curvature and torsion of the helical spine. The underlying geometry therefore supplies a natural two-dimensional complex spinorial representation of frame rotation.

A single rigid helix does not by itself generate nonabelian holonomy: its spinorial transport lies in a fixed one-parameter subgroup. The additional ingredient is independent control over distinct rotation directions. Since

$$[\sigma_1, \sigma_3] = -2i\sigma_2,$$

two independently controlled directions generate the full Lie algebra $\mathfrak{su}(2)$. The explicit connection constructed in theorem 4.4 realizes precisely this mechanism and has effective holonomy group $SU(2)$. Equivalently, on a protected rank-two Hermitian internal state bundle, the traceless unitary transport sector is naturally $\mathfrak{su}(2)$-valued. The identification of this generic geometric $SU(2)$ transport with the physical weak-isospin factor $SU(2)_L$ additionally requires the chiral matter representations discussed below.

The finite V_4 skeleton and the origin of a three-channel internal space. The color factor is less immediate. Unlike $SU(2)$, it is not obtained from a spin double cover of the ordinary moving frame. The starting point is instead the finite symmetry already established for the canonical twin helix register,

$$K \cong V_4 \cong C_2 \times C_2.$$

The important object here is not an identification of the three nonidentity elements of V_4 with red, green, and blue. Rather, we use the representation theory of the finite symmetry as a possible finite skeleton for a later internal transport space.

Let

$$\widehat{K} := \mathrm{Hom}(K, U(1))$$

be the complex character group. Since $K \cong V_4$, one has

$$\widehat{K} = \{1, \chi_1, \chi_2, \chi_3\},$$

with three nontrivial one-dimensional characters. Moreover,

$$\mathrm{Aut}(K) \cong GL(2, \mathbb{F}_2) \cong S_3,$$

and this automorphism group acts transitively on the three nontrivial characters.

Proposition 5.1 (Automorphism-symmetric Enrichment of the V_4 Skeleton)**.** *Let $K \cong V_4$. Suppose an internal complex enrichment of the symbolic K-sector contains at least one nontrivial character line and is required to remain closed under the full action of* $\mathrm{Aut}(K)$*. After removing the K-invariant singlet sector, the smallest such enrichment is*

$$V_c^{(0)} := \bigoplus_{\chi \in \widehat{K} \setminus \{1\}} \mathbb{C}_\chi,$$

and therefore

$$\dim_{\mathbb{C}} V_c^{(0)} = 3.$$

Equivalently, $V_c^{(0)}$ is the reduced complex regular representation of V_4.

Proof. Because K is finite abelian, every finite-dimensional complex representation decomposes into one-dimensional character spaces. The group

$$\mathrm{Aut}(K) \cong S_3$$

acts transitively on

$$\widehat{K} \setminus \{1\} = \{\chi_1, \chi_2, \chi_3\}.$$

Hence any $\mathrm{Aut}(K)$-stable representation containing one nontrivial character must contain all three. Removing the invariant trivial character leaves the direct sum of the three nontrivial character lines, which has complex dimension three. This is precisely the reduced regular representation. □

This proposition supplies a possible origin for a three-dimensional internal space without identifying chirality, orientation, or any individual twin helix type with a color label. The assumption is instead a symmetry-completeness condition: if the continuous enrichment does not privilege one of the three nontrivial V_4 character sectors, then the minimal nontrivial internal multiplet on which the full finite automorphism symmetry acts has three complex components.

Choose the character basis of $V_c^{(0)}$. The V_4 action may then be written as

$$\rho(K) = \{I, D_1, D_2, D_3\},$$

where

$$D_1 = \begin{pmatrix} 1 & 0 & 0 \\ 0 & -1 & 0 \\ 0 & 0 & -1 \end{pmatrix}, \qquad D_2 = \begin{pmatrix} -1 & 0 & 0 \\ 0 & 1 & 0 \\ 0 & 0 & -1 \end{pmatrix}, \qquad D_3 = \begin{pmatrix} -1 & 0 & 0 \\ 0 & -1 & 0 \\ 0 & 0 & 1 \end{pmatrix}.$$

Each nonidentity element reverses two character directions and preserves the third, so

$$\det D_i = 1.$$

Thus the finite V_4 skeleton already admits a canonical realization inside a determinant-one unitary three-channel space.

From the V_4 skeleton to a rank-two torus and the A_2 signature. The preceding finite representation has a useful continuous envelope. Consider the determinant-one diagonal torus

$$T := \{\mathrm{diag}(z_1, z_2, z_3) \mid z_i \in U(1),\ z_1 z_2 z_3 = 1\} \cong U(1)^2.$$

Its two-torsion subgroup is

$$T[2] := \{t \in T : t^2 = I\} = \rho(K) \cong V_4.$$

The appearance of rank two is therefore not obtained by promoting geometric chirality itself to a second $U(1)$ phase. Rather, the finite V_4 symmetry is recovered as the complete two-torsion skeleton of a rank-two determinant-one torus acting on the symmetry-complete three-channel enrichment.

The same construction carries the characteristic Weyl signature of type A_2. The automorphism group

$$\mathrm{Aut}(V_4) \cong S_3$$

permutes the three nontrivial two-torsion elements, while the Weyl group of $SU(3)$ is

$$W(A_2) \cong S_3.$$

Equivalently, the three weight directions are permuted while only two independent diagonal phases remain because

$$\theta_1 + \theta_2 + \theta_3 = 0 \pmod{2\pi}.$$

Among irreducible compact rank-two root systems, the possibilities

$$A_2, \qquad B_2 = C_2, \qquad G_2$$

have Weyl groups of orders 6, 8, and 12, respectively. Thus a rank-two semisimple continuous closure whose Weyl action is faithful on the V_4 two-torsion skeleton and exhausts its full S_3 automorphism symmetry has root system A_2 and Lie algebra

$$\mathfrak{su}(3).$$

This is a structural selection principle, not yet a dynamical derivation. The abstract automorphism group of V_4 exists whether or not the microscopic geometry physically realizes all of its elements. In particular, chirality swap and orientation swap have distinct geometric meanings in the symbolic regime. A genuine color reconstruction therefore requires a higher regime in which the relevant coarse-grained transport no longer privileges these microscopic distinctions and realizes the required symmetry on the enriched internal space.

Constructive $SU(3)$ closure from overlapping $SU(2)$ transport. A more direct realization uses the $SU(2)$ transport mechanism already available in the theory. Write

$$V_c^{(0)} = L_1 \oplus L_2 \oplus L_3$$

for the three character lines. Suppose admissible geometric controls realize determinant-one unitary mixing on two overlapping pairs,

$$L_1 \oplus L_2, \qquad L_2 \oplus L_3,$$

while fixing the complementary line. These define the standard embedded subgroups

$$SU(2)_{12}, \qquad SU(2)_{23} \subset SU(3).$$

These pairwise $SU(2)$ groups are subgroups of the candidate color transport sector; they should not be confused with the physical weak-isospin group $SU(2)_L$.

Proposition 5.2 (A_2 Closure from Overlapping Pairwise Mixers)**.** *Let*

$$H \subseteq SU(V_c^{(0)})$$

be a connected effective holonomy group. If its holonomy Lie algebra contains the two embedded subalgebras

$$\mathfrak{su}(2)_{12} \qquad \textit{and} \qquad \mathfrak{su}(2)_{23},$$

acting respectively on $L_1 \oplus L_2$ *and* $L_2 \oplus L_3$*, then*

$$\mathfrak{hol}(H) = \mathfrak{su}(3)$$

and consequently

$$H = SU(3).$$

Proof. Let E_{ij} denote the elementary matrix sending the jth basis vector to the ith. For $i < j$, define

$$X_{ij} := E_{ij} - E_{ji}, \qquad Y_{ij} := i(E_{ij} + E_{ji}), \qquad H_{ij} := i(E_{ii} - E_{jj}).$$

Then

$$\mathfrak{su}(2)_{12} = \mathrm{span}_{\mathbb{R}}\{X_{12}, Y_{12}, H_{12}\},$$

and

$$\mathfrak{su}(2)_{23} = \mathrm{span}_{\mathbb{R}}\{X_{23}, Y_{23}, H_{23}\}.$$

Their commutators generate the missing 1–3 mixing directions. For example,

$$[X_{12}, X_{23}] = X_{13},$$

while mixed commutators generate Y_{13}. The two diagonal elements H_{12} and H_{23} span a rank-two Cartan subalgebra. Hence the Lie algebra generated by the two overlapping $\mathfrak{su}(2)$ subalgebras contains

$$X_{12}, Y_{12}, \quad X_{23}, Y_{23}, \quad X_{13}, Y_{13}, \quad H_{12}, H_{23},$$

which are eight linearly independent generators spanning $\mathfrak{su}(3)$. Therefore

$$\mathfrak{hol}(H) = \mathfrak{su}(3).$$

Since H is connected and lies in $SU(3)$ with the same Lie algebra, it follows that

$$H = SU(3).$$

□

The proposition isolates the precise dynamical burden of the color reconstruction. The rank-three internal space is supplied by the automorphism-symmetric enrichment of the finite V_4 skeleton, while the continuous nonabelian closure requires two overlapping pairwise mixing channels. The $SU(2)$ mechanism established earlier supplies the appropriate local model for each pair; the genuinely new requirement is that the substrate realize those pairwise mixers coherently on the three-channel space. Once this occurs, the 1–3 channel is generated by Lie closure rather than inserted independently.

The proposed chain is therefore

$$\boxed{V_4 \longrightarrow V_c^{(0)} \cong \mathbb{C}^3 \longrightarrow T^2, \quad T[2] \cong V_4 \longrightarrow \{SU(2)_{12}, SU(2)_{23}\} \longrightarrow A_2 \longrightarrow SU(3)}.$$

The first arrow is representation-theoretic and conditional on the automorphism-symmetry requirement; the pairwise-mixing step is dynamical.

Dynamical selection of internal transport channels. The preceding constructions establish algebraic sufficiency conditions for non-Abelian holonomy, but leave open the physical origin of the required independent controls. The existence of suitable generators in an abstract representation is distinct from their physical accessibility as coupled geometric motions.

A complete dynamical account must identify an admissible evolution law, geometric action, or constraint system from which these control directions arise. In particular, it must determine which deformations, boundary conditions, or interactions activate the relevant transport channels; whether their combined evolution generates the required effective holonomy algebra; and whether the resulting structure persists under perturbation and coarse-graining. The distinction is one of dynamical selection rather than algebraic closure. Once the independent channels are physically realized, their non-Abelian compositions follow from the established Lie-algebraic constructions. What remains to be derived is why the geometric substrate realizes those channels, with the required couplings and stability properties, rather than a reduced commuting subgroup or some alternative transport structure.

Accordingly, the passage from V_4 through $SU(2)$ to the candidate $SU(3)$ color sector should be understood as a hierarchy of conditional geometric realizations. The present results constrain the algebra of admissible transport; a future dynamical theory must determine which of those algebraic possibilities are physically selected.

From $SU(2)$ Frame Transport to $SU(3)$ Color Webs. The passage from the $SU(2)$ to the $SU(3)$ regime should not be understood as a simple enlargement of the four twin helix types, nor as another instance of the transition from commuting to noncommuting transport described in section 4.2. The new ingredient is the organization of three internal transport channels into a common representation space, together with overlapping pairwise rotations whose Lie closure generates the A_2 root system. Whereas the $SU(2)$ construction arises directly from the spinorial lift of the helical moving frame, the proposed $SU(3)$ construction proceeds through the automorphism-symmetric enrichment of the finite V_4 skeleton and the subsequent closure of admissible nonabelian mixing operations.

Once this three-channel structure is realized, the familiar Hermitian-volume characterization of $SU(3)$ becomes a consequence and consistency check rather than an independent assumption about the rank of the color fiber. Let

$$(V_c, h_c), \qquad V_c \cong V_c^{(0)} \cong \mathbb{C}^3,$$

carry the Hermitian form induced from the reduced regular representation, and choose a nonzero complex volume form

$$\Omega_c \in \Lambda^3 V_c^*.$$

The unitary automorphism group of (V_c, h_c) is $U(3)$, while

$$U^*\Omega_c = (\det U)\Omega_c.$$

Consequently,

$$\mathrm{Aut}(V_c, h_c, \Omega_c) = \{U \in U(3) : \det U = 1\} \cong SU(3).$$

The volume form therefore records the determinant-one structure selected by the A_2 closure; it need not be postulated in order to manufacture the number of color directions.

The corresponding Lie algebra is

$$\mathfrak{su}(3) = \left\{ X \in \mathrm{End}(V_c) \;\middle|\; X^\dagger = -X,\ \mathrm{tr}\, X = 0 \right\},$$

with

$$\dim_{\mathbb{R}} \mathfrak{su}(3) = 3^2 - 1 = 8.$$

In the conventional physics normalization, these eight infinitesimal directions are represented by the Hermitian generators

$$T_a = \frac{\lambda_a}{2}, \qquad a = 1, \dots, 8,$$

where the λ_a are the Gell–Mann matrices. The gluon connection is therefore locally

$$A = -ig_s A_\mu^a T_a \, dx^\mu \in \Omega^1(M; \mathfrak{su}(3)), \qquad T_a = \frac{\lambda_a}{2}.$$

At the level of local Lie algebra and fundamental representation, this is the standard color connection. Its identification with physical $SU(3)_c$ additionally requires that the resulting matter sector realize the observed fundamental and conjugate color representations and the correct global gauge structure.

Color representations and gauge-field interactions. The conventional red, green, and blue labels are basis choices in V_c, not three independently observable geometric channels. A quark is represented by a spinorial matter mode valued in the fundamental representation,

$$q \in \mathbf{3} \simeq V_c,$$

while an antiquark transforms in the conjugate representation,

$$\bar{q} \in \overline{\mathbf{3}} \simeq V_c^*.$$

Anticolor is therefore not a second primitive alphabet. It is the conjugate representation of the same color transport space. The gluon field belongs to the adjoint connection sector. Representation-theoretically,

$$\mathbf{3} \otimes \overline{\mathbf{3}} \cong \mathbf{1} \oplus \mathbf{8},$$

so the adjoint octet is obtained by removing the trace singlet from the color–anticolor endomorphism space.

The preserved complex volume form supplies the familiar alternating invariant

$$\epsilon_{abc} : \mathbf{3} \otimes \mathbf{3} \otimes \mathbf{3} \longrightarrow \mathbf{1},$$

so a baryonic singlet may be written

$$\epsilon_{abc} q_1^a q_2^b q_3^c.$$

A mesonic singlet instead uses the binary evaluation pairing

$$\overline{\mathbf{3}} \otimes \mathbf{3} \longrightarrow \mathbf{1}, \qquad \bar{q}_a q^a.$$

Thus binary and trivalent invariant contractions coexist. In the baryonic color-flow sector, the alternating invariant may be represented geometrically by a trivalent Y-junction, but the junction is a representation-theoretic fusion vertex rather than an additional twin helix type.

The valence of perturbative gluon vertices belongs to yet another layer. Writing

$$F_{\mu\nu}^a = \partial_\mu A_\nu^a - \partial_\nu A_\mu^a + g_s f^{abc} A_\mu^b A_\nu^c,$$

the Yang–Mills term

$$-\frac{1}{4} F_{\mu\nu}^a F^{a\mu\nu}$$

contains schematically

$$(\partial A)^2 + g_s (\partial A) A^2 + g_s^2 A^4.$$

QCD therefore contains both three-gluon and four-gluon self-interactions. Their valence follows from the nonabelian curvature term

$$F = dA + A \wedge A$$

and should not be confused with the dimension of the fundamental color fiber or with the trivalent baryonic invariant. Fundamental color rank, invariant matter fusion, and perturbative gauge-field vertex valence are distinct pieces of structure.

Interaction vertices and geometric normal forms. Three distinct constructions must not be identified. First, the three- and four-gluon vertices arise from the cubic and quartic terms of the Yang–Mills action. They are perturbative interaction vertices of the adjoint connection, not literal spatial junctions of three or four helical carriers. Second, the baryonic Y-junction is governed by the invariant contraction

$$\epsilon_{ijk} : \mathbf{3}^{\otimes 3} \longrightarrow \mathbf{1},$$

acting on three fundamental color lines, whereas the three-gluon interaction is governed by the adjoint structure constants f^{abc}. These are different invariant tensors acting on different representations.

Third, the Type 2 and Type 4 normal forms considered in section A.1 concern proposed geometric representatives of composite or extended field configurations. Their two-strand geometry does not count constituent gluons, and their type numbers do not determine interaction- vertex valence. A confined flux network may contain branching junctions while individual segments admit local helical representatives, but no correspondence between vertex valence and twin helix type follows. In particular, the conditional reconstruction of $\mathfrak{su}(3)$ establishes neither confinement nor a specific composite-field geometry.

The strong-force extension is consequently better summarized as

$$\begin{aligned} THM &\longrightarrow \text{symmetry-complete internal enrichment} \\ &\longrightarrow \text{nonabelian holonomy} \\ &\longrightarrow \text{Wilson-line transport} \\ &\longrightarrow SU(3) \text{ representation webs and invariant fusion.} \end{aligned}$$

The center

$$Z(SU(3)) \cong \mathbb{Z}_3$$

supplies a still coarser representation-theoretic label, namely color triality. This $\mathbb{Z}_3$ should not be confused with the existence of three color basis states: the fundamental color space is the continuous vector space

$$V_c \cong \mathbb{C}^3,$$

whereas triality records the action of the center on a representation.[12]

[12] Echoing our previous disclaimer on chirality and spinors, the word *helicity* retains its standard meaning in QCD:

Gauge sector	Standard mode	GCFT interpretation
$U(1)$: abelian phase transport; scalar holonomy and phase ledger.	Hypercharge before electroweak symmetry breaking; the surviving electromagnetic direction after symmetry breaking is $U(1)_{\mathrm{em}}$.	Interpreted as an abelian connection channel carrying phase and holonomy data.
$SU(2)_L$: nonabelian internal frame transport.	Weak bosons W^1, W^2, W^3, which after mixing with hypercharge produce $W^{\pm}$, Z, and the photon.	Interpreted as internal spinorial/frame-rotation modes whose effective holonomy is generated by independently controlled noncommuting directions.
$SU(3)_c$: nonabelian color-frame transport.	Eight gluon fields G^a_μ, $a = 1, \ldots, 8$, valued in $\mathfrak{su}(3)$.	Interpreted as connection modes on the automorphism-symmetric three-channel internal space, with color-singlet readouts organized by invariant tensors, Wilson lines, flux tubes, and confinement-scale observables.

Table 11: Gauge sectors and their geometric-computational interpretation. The $U(1)$ factor is associated with abelian phase transport; the $SU(2)$ factor with spinorial frame transport and noncommuting rank-two holonomy; and the $SU(3)$ factor with the V_4-symmetric three-channel enrichment and its A_2 closure. Gauge bosons are connection modes of the framed substrate rather than additional helical bodies.

Fermionic matter and weak chirality. Fermionic matter enters the present field theory not as an additional family of helical bodies, but as spinorial modes supported by the framed gauge-computational substrate. Let M admit a spin structure with chiral spinor bundles

$$S = S_L \oplus S_R, \qquad P_{L,R} = \frac{1 \mp \gamma^5}{2},$$

and let $P \to M$ be a principal Standard Model gauge bundle. For a gauge representation

$$\rho : G_{\mathrm{SM}} \to GL(V_\rho),$$

the corresponding matter fields are sections of the associated spinor bundle

$$\psi \in \Gamma(S \otimes E_\rho), \qquad E_\rho = P \times_\rho V_\rho,$$

with gauge-covariant Dirac operator

$$\not{D}_{A,\rho} = \gamma^\mu \left(\nabla^{\mathrm{spin}}_\mu + \rho_*(A_\mu) \right).$$

The chiral character of the electroweak interaction is a representation-theoretic statement rather than a statement about visible geometric handedness. The left-handed quark and lepton sectors transform as weak doublets,

$$Q_L : (\mathbf{3}, \mathbf{2})_{1/6}, \qquad L_L : (\mathbf{1}, \mathbf{2})_{-1/2},$$

whereas the right-handed charged fermions transform as $SU(2)_L$ singlets,

$$u_R : (\mathbf{3}, \mathbf{1})_{2/3}, \qquad d_R : (\mathbf{3}, \mathbf{1})_{-1/3}, \qquad e_R : (\mathbf{1}, \mathbf{1})_{-1}.$$

Thus $SU(2)_L$ acts nontrivially on the left-Weyl bundles while the corresponding right-Weyl sectors are weak singlets. GCFT does not yet derive this chiral representation content from the microscopic

the spin projection of a massless gauge excitation along its momentum. It should not be identified with geometric handedness of the twin helix substrate or with the three-channel construction above. Any relation is indirect, through the geometry of spin and gauge transport.

helix geometry. A successful derivation would require the spin-lifted defect sector to produce the appropriate chiral zero-mode multiplicities and gauge representations. In Euclideanized backgrounds, this may be formulated through a chiral Dirac operator

$$D_A^+ : \Gamma(S_L \otimes E_\rho) \longrightarrow \Gamma(S_R \otimes E_\rho),$$

with index

$$\mathrm{ind}(D_A^+) = \dim\ker D_A^+ - \dim\ker D_A^-,$$

so that nontrivial topology or defect data can distinguish left- and right-chiral mode content.

At the level of the present geometric dictionary, propagating weak gauge bosons are therefore closest to Type 1-like connection waves (cf. A.1), but this is only a normal-form correspondence: the fields W_μ^a are $SU(2)_L$-valued nonabelian connection modes, and after electroweak symmetry breaking, the charged combinations $W^\pm$ and the neutral mixed mode Z become massive, while the orthogonal photon remains massless. Type 3 geometry may instead occur in nonperturbative electroweak sectors such as instanton histories and sphaleron-mediated transitions.

The existence of three fermion generations presents a further reconstruction problem. Within GCFT, a possible strategy is to interpret generations as distinct, stable zero-mode sectors of a common spinorial transport structure. In an appropriate defect or compactified background, the spectrum of a twisted chiral Dirac operator may admit multiple normalizable modes carrying identical Standard Model gauge representations. Their multiplicity could be constrained by topological indices, defect winding, and admissible gluing conditions, while their differing geometric profiles could produce non-identical Yukawa couplings through overlap with the Higgs sector. The index measures net chirality and does not, by itself, select exactly three families. Establishing the observed multiplicity, its stability across the fermion representations, and the resulting flavor hierarchies remains an open dynamical problem.

The Higgs sector and fermion mass generation. The Higgs field is represented by a section of the electroweak bundle associated to the representation

$$\Phi \in \Gamma(E_H), \qquad E_H = P_{\mathrm{EW}} \times_{\mathbf{2}_{1/2}} \mathbb{C}^2,$$

with the usual symmetry-breaking potential

$$V(\Phi) = -\mu^2 \Phi^\dagger \Phi + \lambda (\Phi^\dagger \Phi)^2.$$

For $\mu^2, \lambda > 0$, the vacuum selects a nonzero orbit

$$\langle \Phi \rangle = \frac{1}{\sqrt{2}} \begin{pmatrix} 0 \\ v \end{pmatrix},$$

thereby reducing

$$SU(2)_L \times U(1)_Y \longrightarrow U(1)_{\mathrm{em}}.$$

The broken gauge directions acquire masses

$$m_W = \frac{gv}{2}, \qquad m_Z = \frac{v}{2}\sqrt{g^2 + g'^2},$$

while the orthogonal electromagnetic combination remains massless.

Fermion masses arise through gauge-invariant Yukawa pairings,

$$\mathcal{L}_Y = -\bar{Q}_L Y_d \Phi\, d_R - \bar{Q}_L Y_u \widetilde{\Phi}\, u_R - \bar{L}_L Y_e \Phi\, e_R + \mathrm{h.c.}, \qquad \widetilde{\Phi} = i\sigma_2 \Phi^*.$$

After Φ acquires its vacuum expectation value, these terms become

$$M_d = \frac{v}{\sqrt{2}} Y_d, \qquad M_u = \frac{v}{\sqrt{2}} Y_u, \qquad M_e = \frac{v}{\sqrt{2}} Y_e.$$

Geometrically, the relevant structure is a gauge-equivariant trilinear pairing

$$E_L^* \otimes E_H \otimes E_R \longrightarrow \underline{\mathbb{C}},$$

whose evaluation on the Higgs vacuum couples otherwise distinct chiral spinorial sectors. In GCFT language, the Higgs may therefore be interpreted as an order-parameter sector that changes the admissible gluing of internal frame and spinorial data. This interpretation does not determine the Yukawa matrices, flavor hierarchy, CKM/PMNS mixing, or generation multiplicity. Likewise, the minimal Standard Model contains no right-handed neutrino field, so observed neutrino masses require additional structure beyond the minimal construction.

Why the electroweak and strong sectors separate. The low-energy factorization should not be identified directly with the primitive ω- and χ-logic channels. Those labels demonstrate that independent geometric data can coexist at the substrate level, but the gauge-theoretic split occurs later, through a decomposition of the effective internal transport algebra,

$$\mathfrak{g}_{\mathrm{int}} \simeq \mathfrak{su}(3)_c \oplus \mathfrak{su}(2)_L \oplus \mathfrak{u}(1)_Y .$$

The factors act on distinct components of the internal state space and therefore commute at the level of the direct-sum gauge algebra. The electroweak factors are distinguished dynamically from color because the Higgs order parameter transforms nontrivially under

$$SU(2)_L \times U(1)_Y$$

but is a singlet under $SU(3)_c$. Its vacuum therefore mixes and breaks only the electroweak transport sector,

$$SU(2)_L \times U(1)_Y \longrightarrow U(1)_{\mathrm{em}},$$

while leaving color transport intact. In GCFT terms, the observed electroweak/strong split is thus interpreted as a stable decomposition of the effective holonomy structure into commuting internal transport modules.

Global form and the $\mathbb{Z}_6$ quotient. The local Lie algebra does not by itself determine the global gauge group. For the Standard Model matter representations, the centers of the three local factors act with correlated phases. Writing

$$t \in \mathbb{Z}_3$$

for color triality,

$$s \in \mathbb{Z}_2$$

for weak-doublet parity, and

$$y = 6Y \in \mathbb{Z}$$

for integer-normalized hypercharge, the observed representations satisfy

$$2t + 3s + y \equiv 0 \pmod 6.$$

Consequently, a diagonal $\mathbb{Z}_6$ subgroup acts trivially on the Standard Model matter content, so the maximal faithful quotient is

$$G_{\mathrm{SM}} = \frac{SU(3)_c \times SU(2)_L \times U(1)_Y}{\mathbb{Z}_6}.$$

This quotient is not derived from the finite V_4 skeleton alone. It is a compatibility condition on the joint matter representations and therefore belongs to the global reconstruction problem rather than to the local Lie-algebra derivation.

Disclaimer regarding GUTs. The present theory does not exclude a GUT-like phase at higher energies. What it does *not* presently anticipate is that such unification *must* or *would* take the form of a single primitive Lie-group embedding. A more natural GCFT possibility is a symmetry-enhanced locus

$$\mathfrak{M}_{\mathrm{unif}}$$

in the moduli of geometric-computational states, equipped with a unified transport or coherence structure

$$\mathcal{G}_{\mathrm{unif}} \rightrightarrows \mathfrak{M}_{\mathrm{unif}}.$$

The familiar low-energy gauge sectors could then arise through distinct reductions, projections, or stabilized readouts,

$$\mathcal{G}_{\mathrm{unif}} \longrightarrow \mathcal{G}_3, \qquad \mathcal{G}_{\mathrm{unif}} \longrightarrow \mathcal{G}_2, \qquad \mathcal{G}_{\mathrm{unif}} \longrightarrow \mathcal{G}_1,$$

with effective local descriptions modeled by $SU(3)$, $SU(2)$, and $U(1)$, respectively. A conventional simple group such as $SU(5)$ might still appear at a particularly symmetric point or chart—for example, as an isotropy group

$$G_m = \mathrm{Aut}_{\mathcal{G}_{\mathrm{unif}}}(m), \qquad m \in \mathfrak{M}_{\mathrm{unif}},$$

but it would represent a local algebraic compression of the phase rather than necessarily its fundamental ontology.

An interpretational clue for this stance can be drawn from [WW20]. Using cobordism-theoretic anomaly classification and symmetric gapped-boundary arguments, Wang and Wen show that anomaly-free chiral gauge structures associated with familiar grand-unified groups admit nonperturbative local lattice realizations: in particular, the 15-Weyl-fermion $SU(5)$ theory can be realized by a $(3+1)$-dimensional local fermionic lattice model, while the 16-fermion Spin(10) theory admits an even stronger bosonic/qubit realization. This does not establish $SU(5)$ or Spin(10) as fundamental symmetries. Instead, it provides an instructive example in which GUT-like algebraic structure appears together with anomaly cancellation, locality, and nonperturbative consistency. From the present perspective, such results are compatible with viewing a GUT Lie group as the effective symmetry of a particularly coherent locus or phase rather than as the primitive symmetry of the underlying substrate.

Hence, the claim made here is deliberately limited but not merely classificatory. The $U(1)$ factor is tied to compact phase transport; the $SU(2)$ factor is tied to spinorial frame transport with independently controlled noncommuting directions; and a candidate $SU(3)$ color factor can be obtained by a two-stage construction in which the finite V_4 skeleton selects an automorphism-symmetric three-channel representation and overlapping pairwise $SU(2)$ mixers close to the A_2 algebra.

What would count as success or failure? The framework should be evaluated by the mathematical stability of its proposed invariants and by its agreement with established physical constraints. It gains support if its phase distinctions yield stable and nontrivial differences in observables, if its abelian and quasi-fluidic regimes recover familiar gauge-theoretic behavior in a more unified way, and if its computational predictions continue to align with known constraints on expressiveness, verifiability, and reversibility. It would be weakened, or potentially falsified, if the proposed geometric strata fail to produce mathematically meaningful invariants, if the claimed transitions between regimes do not correspond to genuine differences in computational behavior, or if the framework proves unable to recover the standard structures it is intended to subsume.

5.3 On the Classification of Geometric Computational Field Theories

We can now classify *geometric computational field theories* by specifying three layers of structure and composing the canonical maps between them:

$$\begin{array}{c} \text{decorated state/transition groupoid} \\ \downarrow{\scriptstyle \text{higher rep.}} \\ \text{fully dualisable object in a symmetric monoidal } (\infty,n)\text{-category} \\ \downarrow{\scriptstyle \text{Cobordism Hyp.}} \\ \text{fully extended } (\infty,n)\text{-TFT} \end{array}$$

Existence–uniqueness [BD95, Lur09] identifies the last arrow once a fully dualizable object is supplied; the first arrow is where GCFT lives, turning helix–decorated paths and bordisms into higher representations with explicit operational semantics.

Operational layer (constructive evaluator). As in section 4.5, the operational semantics is organized by typed boundary data and computational geometric bordisms between them, with composition given by gluing. Linearity supplies a resource-sensitive discipline on boundary data, while totality refers only to the termination and well-definedness of evaluation on the designated core fragment. Coarse-graining, renormalization, and related changes of scale or presentation enter as declared effects whose handlers must preserve the stated compositional and observational structure. Across the regimes below, the same general pattern persists: histories compose along compatible interfaces, while readout is taken through the appropriate invariant data—characters, holonomy classes, Wilson-type line or surface observables, or their higher analogues. The resulting topological theories should be understood as classification targets for the corresponding core structures; metric-dependent Yang–Mills dynamics enters separately through the evaluator.

Regime ladder.

(a) Symbolic. *Input.* Decorated fundamental groupoid with finite abelian labels V_4 and $(C_2)^3$. *Higher representation.* Finite-group 2-representations, with twist sectors as objects and path homotopies as 1-morphisms. *Dualisability.* A suitable finite semisimple target may supply duals; full

dualisability must still be checked in the chosen higher category. *Topological target.* Two-dimensional Dijkgraaf–Witten theory [DW90]. *Operations.* Commuting joins, with characters χ_g as readouts.

(b) Quasi-fluidic. *Input.* A finite higher-form truncation using $(C_2)^4$ with 1- and 2-form flux labels; this is a topological sector of, not a replacement for, the continuous quasi-fluidic $U(1)$ regime. *Higher representation.* 3-representations or crossed-module representations. *Dualisability.* Finite higher-group data are candidate inputs; duals and higher adjoints depend on the representation target and require verification. *Topological target.* Three-dimensional higher-form Dijkgraaf–Witten/Yetter quantum double [Yet92]. *Operations.* Loops and surfaces serve as registers; higher Wilson observables provide readouts; coarse-graining is organized through 2-sheafification.

(c) Fully fluidic. *Input.* The symmetry $D_4 \ltimes (C_2)^4$ of a THM cell acting on a decorated Π_1. *Higher representation.* 4-representations or, in the toy non-abelian sector, 2-connections on principal 2-bundles. *Dualisability.* Compactness alone supplies no full-dualisability theorem; one must choose a suitable finite or otherwise controlled target and construct the required higher adjoints. *Topological target.* Four-dimensional BF theory is a candidate topological core; the Yang–Mills term is introduced separately through the evaluator. *Operations.* Joins are noncommutative; class functions of holonomy supply readouts; renormalization is treated as a controlled handler.

(d) Emergent gauge. *Input.* A bundle of simple Lie data, for example $SU(2)$, over helix-adapted charts. *Higher representation.* Candidate algebraic or categorical objects associated with line bundle and boundary observables in Alg_∞, potentially including suitable E_2-algebras. *Dualisability.* Full dualisability requires the appropriate duals and iterated adjoints in a fixed symmetric monoidal target; compactness, rigidity, or factorization data alone do not establish it. *Topological target.* Candidate fully extended three-dimensional Chern–Simons and four-dimensional BF/CS-like topological sectors; Yang–Mills again enters through the metric-sensitive evaluator. *Operations.* The same boundary-compositional interface persists, while intertwiners in the corresponding representation category represent node constraints.

Scope of the dualisability entries. A finite group, a compact Lie group, a rigid monoidal category, or a topological BF action does not by itself provide a fully dualizable object in an unspecified (∞, n)-category. Full dualisability is a property of the chosen point datum *in its target*, including the requisite iterated adjoints. Accordingly, the assignments in the ladder and table below are candidates to be realized after fixing the target and proving these conditions; they are not four established fully extended TFT constructions. In particular, the finite higher-form row describes a controlled topological truncation of the quasi-fluidic regime, not its full continuous $U(1)$ dynamics.

Remark 5.1 (Conditional Cobordism-Hypothesis Classification). The preceding regime ladder should be read as a collection of candidate topological cores rather than as a completed classification theorem.

Suppose that, for a fixed computational regime, one has constructed:

(a) a fully extended structured bordism (∞, n)-category carrying the relevant geometric and computational decorations;

(b) a symmetric monoidal target (∞, n)-category $\mathcal{D}$;

(c) a symmetric monoidal functor
$$Z : \mathrm{Bord}_n^{\mathrm{comp}} \longrightarrow \mathcal{D};$$

(d) a fully dualizable object
$$X := Z(\mathrm{pt}) \in \mathcal{D},$$
together with the equivariance data required by the chosen tangential or geometric structure.

Under these hypotheses, the Cobordism Hypothesis identifies the fully extended topological theory Z, up to the appropriate notion of equivalence, with the theory classified by X. The present work does not construct all of this higher-categorical data. It identifies the decorated state, transition, bordism, gluing, and readout structures from which such a construction would have to proceed.

Table 12: Candidate regime data and topological classification targets (conditional on full dualisability).

Group Type	**Candidate point datum**	**Core (n)-TFT**	**Comments**	**Dualisability guardrails**
Abelian	Finite-group *2-representation* of the decorated groupoid (V_4)	2D Dijkgraaf-Witten	Factors through finite sets $\to$ Vect; commuting joins	Finite separable algebra or appropriate finite semisimple target
Maximally abelian	Discrete *3-representation* of $(C_2)^4$ with higher gauge 2-forms	3D DW / Yetter double	$\mathbb{Z}_2$ higher-form lattice models; surfaces as registers	Finite higher-group truncation and suitable higher linearization; verify higher adjoints
Non-abelian	Smooth *4-representation* of $D_4 \ltimes (C_2)^4$ inside decorated Π_1	4D BF; Yang-Mills via effect	Noncommuting holonomies; renorm as certified handler	Controlled finite or topological sector; specify a higher target admitting the required duality structure
Simple Lie	Bundle of dualisable objects in Alg_∞ (e.g. E_2 of $SU(2)$ lines)	Chern-Simons / (∞, n)-TFT; YM via effect	Conditional extension to a structured TFT	Quantized categorical or factorization algebras; establish full dualizability in the selected target

Guardrails in 4D: Topological Core vs. Metric Effects. In four dimensions, the Cobordism Hypothesis classifies *fully extended* topological field theories by *fully dualizable* objects in an appropriate symmetric monoidal (∞, n)-category. This classification is inherently *topological*: it is driven by local-to-global gluing, duals/evaluations, and functoriality under bordism composition, rather than by metric-dependent dynamics [Fre12].

Pure Yang–Mills is therefore not an acceptable *core* object for dualisability statements: the Yang–Mills action depends on a choice of metric through the Hodge operator $*$, and it carries propagating local degrees of freedom. To keep the 4D semantics fully compositional, we isolate a metric-free *BF topological core* [BT91] and treat the metric-sensitive Yang–Mills term as an *effect* handled by the constructive evaluator. Concretely, one may regard Yang–Mills in first-order form as a deformation of BF theory:

$$S_{\mathrm{BFYM}}(A, B) \;=\; \int_M \mathrm{tr}(B \wedge F_A) \;+\; \frac{g^2}{2} \int_M \mathrm{tr}(B \wedge *B),$$

where A is a connection with curvature F_A and B is an adjoint-valued 2-form. The BF term is topological (metric-free), while the second term is precisely where metric/scale enters via $*$. In the formal "topological limit" $g \to 0$, one recovers BF theory; integrating out B recovers the usual second-order Yang–Mills action.

This mirrors the Plebanski [Ple77] paradigm: four-dimensional gravity can be presented as *constrained BF theory*, [FS12] where a BF-type action is supplemented by *simplicity constraints* (or, equivalently, constraint potentials) to recover metric geometry and propagating modes. In our setting, the analogy is operational:

- **Core (candidate for dualisable semantics).** BF-type topological data may support a Cobordism-Hypothesis classification only after a fully extended construction and the necessary dualisability checks.

- **Effects (non-topological).** Metric-dependent dynamics (YM terms, constraint potentials, coarse-graining/RG) implemented as controlled effect-handlers in the evaluator.
- **Soundness criterion.** Effect-handlers must preserve symmetric monoidality (gluing/parallel composition) and must respect boundary gauge-invariant observables (e.g., class functions of holonomy such as Wilson loop traces).

On the BF/Yang–Mills presentation. Any proposed full-dualisability statement in this paper concerns a suitably constructed topological core, not continuum BF theory merely by virtue of being topological; the Yang–Mills sector enters only after the additional dynamical structure described above is supplied. This separation should not be read as a new field-theoretic formulation of Yang–Mills theory. First-order and BF-type presentations of Yang–Mills are well established: Yang–Mills may be formulated as a deformation of topological BF theory [MZ96, CCRF+98], and the broader class of actions consisting of a BF sector together with a B-dependent deformation has long been used in state-sum and spin-foam constructions [FK99]. The relation is nevertheless subtler than the formal slogan "BF plus a metric term": in four dimensions the topological limit carries an enlarged gauge symmetry, and equivalent semi-topological formulations may require auxiliary fields and an enlarged BRST complex [CCRF+98]. Modern BV–BFV treatments sharpen this point further by showing that the equivalence between first- and second-order Yang–Mills can be formulated compatibly with boundary data and cutting/gluing [CMR14, CSCS23].

Our use of this established decomposition is therefore semantic rather than field-theoretically novel. We assign the BF-type and Yang–Mills-type structures different roles inside the geometric-computational architecture, with the distinction organized by typed helical data, holonomy-sensitive readouts, and regime-dependent evaluation. The claim is not that BF theory is literally the microscopic theory from which Yang–Mills is obtained by a naive continuous limit, but that the known first-order decomposition provides a natural interface between the compositional structure of the geometric calculus and the additional data required for propagating gauge dynamics.

Geometric Computational Field Theory. GCFT organizes smooth geometric processes together with their computational structure through a compositional semantic architecture. In the language of section 4.5, boundary/interface specifications play the role of types, admissible geometric histories play the role of terms, and composition is realized by gluing. The corresponding field-theoretic structure is therefore organized by the sequence

$$\text{typed geometric bordisms} \longrightarrow \text{semantic evaluation} \longrightarrow \text{gauge-invariant observable extraction.}$$

We first specify the ambient smooth setting in which these objects and their moduli are interpreted.

Definition 5.1 (Differentially Cohesive Ambient Topos for GCMs)**.** Let

$$\mathcal{E}_{\mathrm{GCM}}$$

be a higher differentially cohesive topos, for example a suitable smooth ∞-topos of sheaves on Cartesian spaces, in which smooth spaces, bundles, connections, curvature, differential cocycles, moduli stacks, and holonomy may be represented internally. We assume the usual cohesive adjoint modalities

$$\Pi \dashv \flat \dashv \mathrm{id} \dashv \sharp$$

together with a de Rham shape modality

$$\mathrm{dR} : \mathcal{E}_{\mathrm{GCM}} \longrightarrow \mathcal{E}_{\mathrm{GCM}},$$

so that the geometric and differential-cohomological structures used throughout the construction admit an internal formulation [Sch13].

The role of $\mathcal{E}_{\mathrm{GCM}}$ is ambient rather than computational: it is the semantic universe in which the relevant smooth, gauge, higher-geometric, and moduli data live. The computational structure is carried by distinguished boundary objects, histories, their composition laws, and the observables retained under readout.

Definition 5.2 (GCM Boundary Type)**.** A *GCM boundary type* is a pair

$$\Sigma = (Y, \sigma),$$

where Y is a compact smooth $(n-1)$-manifold, possibly with the boundary or stratified structure required by the application, and σ denotes the additional data needed to specify an admissible computational interface.

Depending on the regime, σ may include bundle and connection data, framing, orientation or chirality sector data, phase or winding variables, conserved charges, allowed mode or defect sectors, regularity conditions, constraint data, obstruction or trivialization data, and a declared family of observable readouts.

The corresponding moduli object of admissible realizations of the boundary type is denoted

$$\mathcal{M}(\Sigma) \in \mathcal{E}_{\mathrm{GCM}}.$$

Gauge transformations, diffeomorphisms, and other automorphisms are retained in $\mathcal{M}(\Sigma)$ rather than removed by passage to a naive orbit space.

Definition 5.3 (GCM-structured Bordism)**.** Let

$$\Sigma_0 = (Y_0, \sigma_0), \qquad \Sigma_1 = (Y_1, \sigma_1)$$

be GCM boundary types. A *GCM-structured bordism*

$$W : \Sigma_0 \longrightarrow \Sigma_1$$

is a compact n-dimensional smooth bordism with collared boundary

$$\partial W \cong \overline{Y_0} \sqcup Y_1,$$

equipped with geometric, gauge, computational, constraint, and readout data whose restrictions recover σ_0 and σ_1 and which satisfy the declared kinematic admissibility and descent conditions of the theory.

The moduli object of admissible realizations of W is denoted

$$\mathcal{M}(W),$$

with restriction morphisms

$$\mathcal{M}(\Sigma_0) \xleftarrow{s} \mathcal{M}(W) \xrightarrow{t} \mathcal{M}(\Sigma_1).$$

A well-typed bordism need not, by definition, solve a chosen dynamical equation. As in section 4.5, we distinguish the kinematic judgment

$$W : \Sigma_0 \to \Sigma_1$$

from a dynamical admissibility condition

$$W \models \mathcal{E},$$

where $\mathcal{E}$ denotes the differential or variational law imposed in the physical sector under consideration.

Definition 5.4 (GCM Bordism Category)**.** Let

$$\mathsf{Bord}_n^{\mathrm{GCM}}$$

denote the symmetric monoidal higher category whose objects are admissible GCM boundary types and whose morphisms are GCM-structured bordisms, taken with the appropriate higher morphisms implementing gauge transformations, diffeomorphisms, homotopies, and coherence data.

Sequential composition is gluing along a matched typed interface:

$$W_1 : \Sigma_0 \to \Sigma_1, \qquad W_2 : \Sigma_1 \to \Sigma_2$$

compose to

$$W_2 \circ_{\Sigma_1} W_1 : \Sigma_0 \longrightarrow \Sigma_2.$$

Parallel composition is disjoint union,

$$\Sigma \otimes \Sigma' = \Sigma \sqcup \Sigma', \qquad W \otimes W' = W \sqcup W',$$

with the monoidal unit being the empty boundary.

At the level of moduli semantics, gluing is represented schematically by

$$\mathcal{M}(W_2 \circ_{\Sigma_1} W_1) \simeq \mathcal{M}(W_1) \times^h_{\mathcal{M}(\Sigma_1)} \mathcal{M}(W_2),$$

where the ordinary fiber product may be replaced by the appropriate homotopy or derived fiber product when gauge automorphisms or higher coherence data are present.

Remark 5.2 (Locality, Descent, and Path Data). The notation $\mathsf{Bord}_n^{\mathrm{GCM}}$ does not mean that a single decoration group encodes all additional structure. Different components of a boundary type obey different composition laws: connections restrict and glue by descent, charges may add, defect sectors may compose through specified interface laws, and constraint or obstruction data may require higher coherence conditions.

Likewise, transport data need not factor through the ordinary fundamental groupoid. A connection with nonzero curvature naturally defines transport on the thin path groupoid

$$\Pi_1^{\mathrm{thin}}(M),$$

while higher connections may require higher path-groupoid or differential-cohomological refinements; ordinary homotopy data are recovered only in flat or topological reductions.

Definition 5.5 (GCM Semantic Target)**.** Let

$$\mathcal{C}_{\mathrm{GCM}}$$

be a symmetric monoidal higher category of GCM-structured states and processes, internal to or presented in $\mathcal{E}_{\mathrm{GCM}}$. Its objects are the semantic values assigned to admissible boundary types, and its morphisms are the corresponding semantic processes assigned to admissible geometric histories. Its symmetric monoidal product represents parallel composition of independent systems.

The purpose of $\mathcal{C}_{\mathrm{GCM}}$ is denotational: it records the geometric-computational content of a process after gauge redundancy, moduli structure, descent, and the declared equivalence relations have been retained at the appropriate categorical level.

Definition 5.6 (Geometric Computational Field Theory)**.** An n-dimensional *Geometric Computational Field Theory* is a symmetric monoidal functor

$$Z : \mathsf{Bord}_n^{\mathrm{GCM}} \longrightarrow \mathcal{C}_{\mathrm{GCM}}.$$

Thus, to each admissible boundary type Σ, the theory assigns a semantic state object

$$Z(\Sigma) \in \mathcal{C}_{\mathrm{GCM}},$$

and to each computational geometric bordism

$$W : \Sigma_0 \to \Sigma_1,$$

it assigns a morphism

$$Z(W) : Z(\Sigma_0) \longrightarrow Z(\Sigma_1),$$

with

$$Z(W_2 \circ W_1) = Z(W_2) \circ Z(W_1)$$

up to the coherence data appropriate to the higher-categorical setting, and

$$Z(W \sqcup W') \simeq Z(W) \otimes Z(W').$$

The functor Z should not be identified with a quantum amplitude assignment. At the present stage it supplies compositional geometric semantics: it records how typed boundary data, moduli, transport, defects, constraints, and admissible histories compose. A subsequent quantization may act on suitable sectors of this semantic structure, but quantization is not built into the definition of GCFT.

Definition 5.7 (Execution Ambient and Observable Extraction)**.** Let

$$\mathcal{D}_{\mathrm{exec}}$$

be a symmetric monoidal category with finite limits whose objects and morphisms admit effective external representation, for example through finite symbolic data, rational or algebraic quantities, computable reals, or other effectively represented observable structures.

Let

$$\mathcal{C}_{\mathrm{GCM}}^{\mathrm{obs}} \subseteq \mathcal{C}_{\mathrm{GCM}}$$

denote the subcategory generated by admissible gauge-invariant observables and observable-preserving transformations. An *extraction functor* is a left-exact symmetric monoidal functor

$$\mathrm{Ex} : \mathcal{C}_{\mathrm{GCM}}^{\mathrm{obs}} \longrightarrow \mathcal{D}_{\mathrm{exec}},$$

which sends gauge-invariant semantic observables—for example, class functions of holonomy, differential-cohomological quantities, conserved or topological invariants, and stable boundary readouts—to effectively representable outputs.

The resulting semantic pipeline is therefore

$$\mathsf{Bord}_n^{\mathrm{GCM}} \xrightarrow{Z} \mathcal{C}_{\mathrm{GCM}} \supseteq \mathcal{C}_{\mathrm{GCM}}^{\mathrm{obs}} \xrightarrow{\mathrm{Ex}} \mathcal{D}_{\mathrm{exec}},$$

with all smooth, gauge, moduli, and higher-geometric data interpreted in the ambient universe

$$\mathcal{E}_{\mathrm{GCM}}.$$

Remark 5.3 (Modalities as Semantic Projections). The cohesive modalities organize several useful reductions of the ambient geometric semantics. Schematically,

- Π extracts homotopy-level or topological content;
- $\flat$ isolates flat or discrete structure, including sectors useful for symbolic verification;
- dR records de Rham and differential-cohomological information;
- $\sharp$ suppresses cohesive structure when codiscrete or externally controlled data are required.

These projections act on the ambient geometry and should not be identified with the executable extraction functor Ex. The former reorganize internal semantic structure; the latter selects effectively accessible observables for external readout.

Operationally, GCFT does not take a functional sum over arbitrary histories as primitive. Local geometric and gauge data are assembled by descent into globally admissible objects of $\mathcal{E}_{\mathrm{GCM}}$; the typing and constraint structure determines which bordisms belong to the computational process calculus; a chosen dynamical law further selects the physically realized histories; and Z assigns their compositional semantic values. Gauge-invariant observables may then be passed through Ex to produce executable readouts. Sheafification and descent are therefore components of the constructive semantic architecture, not substitutes for quantum weighting, interference, positivity, or a measure on histories.

Conjecture 5.3 (Computational Cobordism Hypothesis)**.** *In a fully extended version of the theory, such functors are expected to be controlled by appropriate dualizability data, namely by suitable fully dualizable objects in a symmetric monoidal higher-categorical completion of the GCM semantic target, equipped with the tangential, geometric, and computational structure required by the theory.*

We therefore conjecture that fully extended GCFTs admit a classification principle analogous to the Baez–Dolan Cobordism Hypothesis: up to the relevant notion of equivalence, a fully extended GCFT is determined by the fully dualizable datum assigned to a point together with its geometric and computational decoration data [BD95]. When the additional computational structure is trivial, or when the relevant connection and decoration data are flat and factor through ordinary homotopy information, the construction should reduce to the corresponding topological or functorial field-theoretic case.

Operational interpretation. The construction separates three semantic levels. At the local level, state and transport data are represented by the appropriate groupoid, Lie groupoid, moduli stack, or higher path object. At the process level, computational control flow is represented by typed GCM bordisms and their gluing. At the semantic level, the symmetric monoidal functor Z assigns compositional meanings to these bordisms, while Ex selects those invariant outputs that admit effective external readout.

Remark 5.4 (Reduction to Simpler Regimes). The general construction contains several familiar limits. If all additional structure is discrete and factors through ordinary homotopy data, the theory approaches the formal regime of finite-group or topological field theories. If the active transport data are continuous but abelian, such as a $U(1)$ connection or compact phase variable, the semantics remains order-independent at the level of the corresponding transport group. Non-abelian connection data instead introduce path ordering and history-sensitive holonomy, so that gauge-invariant class functions such as Wilson-loop traces become natural readouts. Higher differential or cohomological structure may be retained in $\mathcal{E}_{\mathrm{GCM}}$ without requiring it to be encoded by a single universal decoration group.

Example 5.2 (Helical Bordism Computation). Let $I = [0, L]$, and let $M \cong D^2 \times I$ be the tubular working region of a regular conical unit helix with core $\Gamma(s) = \gamma_{\chi,\omega}(s)$, cross-sectional radius $a(s)$, and fixed chirality $\chi \in C_2$, as in definition 1.1. Let $(N(s), B(s))$ be its smooth Frenet normal frame. The interval parameter s runs from the base toward the apex end, and $r \in [0, 1]$ denotes a normalized transverse radius; the physical transverse radius is $ra(s)$. The underlying space is a 3-ball, while the framing, scale profile, connection, and chirality are additional geometric data.

Fix $0 < r < 1$. The surface $W_r = S^1 \times I$ has the embedded representative

$$\Phi_r(\varphi, s) = \Gamma(s) + ra(s)\big(\cos\varphi\, N(s) + \sin\varphi\, B(s)\big),$$

with $\varphi \in \mathbb{R}/2\pi\mathbb{Z}$. Provided the thickness obeys the embedded-tube condition of Chapter 1, W_r is a smooth 2-dimensional bordism between the transverse circles S^1_0 and S^1_L. Its abstract topology is cylindrical, but its embedding inherits the conical scale profile.

Let A be a $U(1)$ connection on the trivial circle bundle over M, with curvature $F_A = dA$. Its parallel transport defines a functor on the thin path groupoid,

$$\mathrm{Hol}_A : \Pi_1^{\mathrm{thin}}(M) \longrightarrow BU(1).$$

The label χ is retained as fixed geometric sector data, not multiplied as though it were another path holonomy. For $i \in \{0, L\}$ the boundary type $\Sigma_i = (S^1_i, \sigma_i)$ includes the restricted connection, framing, chirality sector, and chosen phase readout. The decorated cylinder determines an admissible GCM-structured bordism

$$W_r : \Sigma_0 \longrightarrow \Sigma_L.$$

The gauge-invariant boundary holonomies are

$$u_i = \exp\left(i \oint_{S^1_i} A\right) \in U(1), \qquad i \in \{0, L\}.$$

With the boundary orientation $\partial W_r = \overline{S^1_0} \sqcup S^1_L$, Stokes' theorem gives the boundary compatibility law

$$u_L u_0^{-1} = \exp\left(i \int_{W_r} F_A\right).$$

Consequently, for fixed curvature flux and compatible boundary data, its abelian phase-transfer component is the map

$$\mathcal{T}_{W_r} : U(1) \longrightarrow U(1), \qquad \mathcal{T}_{W_r}(u) = \exp\left(i \int_{W_r} F_A\right) u.$$

Here $\mathcal{T}_{W_r}$ expresses the relation between boundary observables; for a fixed connection the input and output holonomies are constrained by that same connection, rather than being independent choices.

If two cylinders W_{01} and W_{12} have matching connection and boundary data at their common circle, curvature integrals add under gluing. Hence

$$\mathcal{T}_{W_{12} \circ W_{01}} = \mathcal{T}_{W_{12}} \circ \mathcal{T}_{W_{01}}.$$

This is the explicit compositional law in the abelian readout sector. In the general notation of GCFT, $Z(W_r)$ denotes the semantic morphism of a proposed full theory, whereas $\mathcal{T}_{W_r}$ is only its phase-transfer component. The extraction functor Ex retains the gauge-invariant boundary phases when these observables are given effectively representable data. This example does not require a complete construction of Z or a quantum amplitude assignment.

For a concrete smooth connection, use framed transverse polar coordinates (ρ, φ) and take

$$A = \frac{\beta}{2}\rho^2\, d\varphi, \qquad \beta \in \mathbb{R}.$$

The 1-form is smooth at the core because $\rho^2 d\varphi$ is smooth in Cartesian disk coordinates. On W_r we have $\rho = ra(s)$, so

$$u_s = \exp\bigl(i\pi\beta r^2 a(s)^2\bigr), \qquad \int_{W_r} F_A = \pi\beta r^2\bigl(a(L)^2 - a(0)^2\bigr).$$

The scale profile therefore changes the boundary phase even though all transverse loops are contractible in M. For a flat connection those loop holonomies are trivial, illustrating that the nontrivial phase readout comes from differential-geometric transport rather than ordinary homotopy alone.

Remark 5.5 (Scope of the Categorical Formulation). The preceding conjecture should be read as a proposed semantic envelope for GCFT is not a complete proof of a classification theorem. The role of the categorical language is to organize the data already present in geometric computation: boundary states, admissible histories, gluing, holonomy, and gauge-invariant readout. The fully extended classification problem requires additional higher-categorical infrastructure, including a precise choice of target $\mathcal{C}_{\mathrm{GCM}}$, a notion of decorated dualizability, and a treatment of higher morphisms between computational histories. These are left as part of the future formal development of the theory.

Relation to geometric field theory and structured bordism. The use of the phrase "geometric computational field theory" is meant to distinguish the present construction from existing frameworks for *geometric field theories*. In particular, Ludewig–Stoffel developed a general framework for geometric functorial field theories, in which bordisms are equipped with geometric structures and field theories are required to vary smoothly in families [LS21]. Their one-dimensional classification, where geometric field theories over a manifold are related to vector bundles with connection, is especially close in spirit to the transport-theoretic intuition used here. In the present work, however, the emphasis is not on classifying geometric field theories in general, but on isolating a particular computational enrichment of such structures.

Similarly, Grady–Pavlov's Geometric Cobordism Hypothesis provides a broad classification framework for fully extended field theories on bordisms carrying geometric structure, including metrics, connections, complex and symplectic structures, principal bundles with connection, and geometric string structures [GP21]. This work should be viewed as complementary to that program rather than as a replacement for it. The role of GCFT is to specify a particular kind of geometric structure whose data are computational: helical state, local update laws, admissible interface gluing, holonomy readouts, regularity constraints, and resource-sensitive observational equivalence.

5.4 From Geometric Semantics to Quantum Field Theory

The preceding sections have supplied a geometric and categorical semantics for computation: states are represented by structured boundary data, histories by admissible geometric processes, composition by gluing, and observable content by gauge-invariant readout. None of this, by itself, constitutes a quantum field theory. A GCFT may organize the geometry of fields and their compositional behavior while still lacking the additional analytic and probabilistic structures required of QFT: a suitable notion of quantization, a physical state space, locality and factorization, positivity, gauge reduction, continuum control, and a prescription for amplitudes or correlation functions. The purpose of this section is therefore to identify the precise point at which geometric semantics must be supplemented to recover conventional quantum field theory. We begin with geometric quantization and higher prequantum geometry, since these provide the most immediate mathematical comparison to the connection, curvature, holonomy, and moduli data already developed above.

Why geometric quantization is not taken as primitive. The use of the term *prequantum geometry* in the present work requires some clarification. There is an established mathematical meaning of

geometric prequantization and geometric quantization, originating in the Kostant–Souriau construction. Given a symplectic manifold

$$(X, \omega),$$

geometric prequantization asks for a Hermitian line bundle

$$L \longrightarrow X$$

equipped with a compatible unitary connection ∇ whose curvature reproduces the symplectic form, up to the conventional normalization,

$$F_\nabla = -\frac{i}{\hbar}\omega.$$

Such a prequantization exists only when the corresponding cohomology class satisfies the appropriate integrality condition. Geometric quantization then introduces further structure, most notably a polarization and, where appropriate, metaplectic or half-form corrections, to pass from the prequantum data to a quantum state space and an operator representation of a suitable class of classical observables [Kos70, Sou70].

We do not adopt this procedure as the foundational quantization mechanism of GCT. The reason is not an incompatibility with geometric quantization, but an ordering of structures. Ordinary geometric quantization begins with a classical phase space and its symplectic form already specified. In the present framework, however, the phase space itself is not regarded as primitive. The earlier sections instead begin with geometric computational substrates, local state bundles, admissible interfaces, transport laws, gauge identifications, and boundary readouts. Only after these structures have been assembled and reduced by the relevant equivalences may an effective symplectic or presymplectic state space emerge. To impose geometric quantization at the outset would therefore assume part of the structure that GCFT is intended to explain.

Schematically, the distinction is

$$\text{geometric quantization:} \qquad (X, \omega) \longrightarrow \text{prequantum bundle} \longrightarrow \text{polarized quantum state space},$$

whereas the present program proceeds through:

$$\begin{aligned} \text{helical types} &\longrightarrow \text{transport and gluing} \\ &\longrightarrow \text{gauge-reduced moduli/process geometry} \\ &\longrightarrow \text{effective phase-space data} \longrightarrow \text{possible quantization}. \end{aligned}$$

This distinction is already visible in the quasi-fluidic regime. There, a $U(1)$-connection on a helical module supplies a phase ledger through holonomy, and curvature measures the failure of phase transport to remain radially constant. These data resemble ordinary prequantum data, but the connection is introduced first as part of the computational transport structure, not as the prequantization of an independently specified symplectic manifold. A genuine identification with geometric prequantization requires an additional step: one must exhibit a closed integral 2-form ω on the relevant effective state or moduli space and identify the connection as a differential refinement satisfying

$$\mathrm{curv}(\nabla) = \omega$$

with the appropriate normalization. Accordingly, the existence of phase, connection, or holonomy data alone should not be called a completed geometric quantization.

Covariant phase space as a dynamical bridge. A natural intermediate construction is the covariant phase space of a chosen local field theory. Given a Lagrangian n-form L on a field bundle, its first variation has the local form

$$\delta L = \mathcal{E}(\phi) \cdot \delta\phi + d\theta(\phi; \delta\phi),$$

where $\mathcal{E}(\phi) = 0$ denotes the Euler–Lagrange equations and θ is the presymplectic potential current. Its antisymmetrized field-space variation determines the presymplectic current

$$\omega(\phi; \delta_1\phi, \delta_2\phi) = \delta_1\theta(\phi; \delta_2\phi) - \delta_2\theta(\phi; \delta_1\phi), \qquad \Omega_\Sigma = \int_\Sigma \omega,$$

for a hypersurface Σ and suitable tangent variations of solutions [LW90]. On shell, $d\omega = 0$ for linearized solutions; independence of Ω_Σ from the hypersurface requires the corresponding boundary symplectic flux to vanish or be accounted for. Gauge directions may lie in the presymplectic kernel, but transformations with nontrivial boundary charges need not do so.

This construction is pertinent to GCFT because a dynamically admissible bordism, together with an appropriate variational problem, can determine a relation between the presymplectic data on its incoming and outgoing boundaries. Under additional regularity, reduction, and flux hypotheses, such relations may be modeled by Lagrangian correspondences. The geometric-computational typing and gluing rules do not themselves supply L, θ, or Ω_Σ: these emerge only after a specified dynamical theory and its boundary conditions have been introduced. Covariant phase space therefore provides a possible bridge from computational histories to the effective phase-space structures required by geometric quantization, without conflating prequantization with quantum reconstruction.

Higher prequantum geometry. A substantially closer point of contact is provided by higher prequantum geometry. In the formulation developed by Fiorenza, Rogers, and Schreiber, ordinary prequantization is expressed in terms of the moduli object

$$\mathbf{B}U(1)_{\mathrm{conn}},$$

which classifies principal $U(1)$-bundles, equivalently Hermitian line bundles, equipped with a connection. A prequantization of (X, ω) may then be represented by a differential cocycle

$$\nabla : X \longrightarrow \mathbf{B}U(1)_{\mathrm{conn}}$$

whose curvature is ω. Higher prequantization replaces this by

$$\nabla : X \longrightarrow \mathbf{B}^n U(1)_{\mathrm{conn}},$$

where the target classifies higher $U(1)$-bundles, or gerbes and their higher analogues, with connection, and where the curvature is a closed $(n+1)$-form. In this way, symplectic prequantization becomes the lowest nontrivial member of a hierarchy of pre-n-plectic geometries [FRS16, Sch16].

This formulation is especially relevant to GCFT because it treats prequantum data globally and gauge-covariantly. In the cohesive formulation, differential cohomology simultaneously records the underlying topological class, its smooth refinement, connection data, and curvature. Higher Chern–Weil maps then relate moduli of gauge fields to higher differential cocycles and provide prequantum structures for Chern–Simons-type theories and their boundaries and defects [Sch13]. This is considerably closer to the language used here than a bare Hilbert-space quantization procedure: GCFT likewise organizes connections, curvature, holonomy, moduli, defects, and gluing before a Hilbert-space reconstruction has been chosen.

The appearance of $U(1)$ in higher prequantum geometry should not be confused with a restriction of the underlying physical gauge theory to an abelian gauge group. These are logically distinct structures. A non-abelian gauge field may have structure group

$$G = SU(2),\ SU(3), \ldots,$$

while a morphism encodes its prequantum data into a higher $U(1)$-connection object. In higher Chern–Weil theory one may, for example, have a differential characteristic morphism of the schematic form

$$\mathbf{B}G_{\mathrm{conn}} \longrightarrow \mathbf{B}^n U(1)_{\mathrm{conn}}.$$

Here G governs the non-abelian field and transport degrees of freedom, while the higher $U(1)$ object records the differential-cohomological phase or action data used in prequantization. Consequently, the transition in GCT from abelian $U(1)$ transport to $SU(2)$- or $SU(3)$-type holonomy does not imply that higher prequantum geometry has ceased to apply. The two uses of group structure occur at different levels.

A possible GCFT realization. This suggests a more precise interpretation of the phrase *prequantum geometry* in the present program. Let

$$\mathcal{M}_{\mathrm{GCM}}$$

denote an appropriate moduli object of geometric-computational configurations, including the active geometric structure, connection data, boundary conditions, defects, and gauge equivalences of the regime under consideration. If this moduli object carries a closed integral differential form

$$\Omega_{\mathrm{GCM}} \in \Omega^{n+1}_{\mathrm{cl}}(\mathcal{M}_{\mathrm{GCM}}),$$

then a technical higher prequantization would consist of a differential refinement

$$\nabla_{\mathrm{GCM}} : \mathcal{M}_{\mathrm{GCM}} \longrightarrow \mathbf{B}^n U(1)_{\mathrm{conn}}$$

such that

$$\mathrm{curv}(\nabla_{\mathrm{GCM}}) = \Omega_{\mathrm{GCM}}.$$

Nothing in the present paper proves that such a refinement exists for every GCM or every computational regime. Rather, this equation records the additional structure required for the broad prequantum language used here to coincide with higher prequantum geometry in its established technical sense.

The relation to the earlier holonomy construction is then transparent. In the ordinary $n = 1$ case, a connection classified by

$$\nabla_A : M \longrightarrow \mathbf{B}U(1)_{\mathrm{conn}}$$

induces parallel transport on the thin path groupoid and hence a holonomy functor

$$\mathrm{Hol}_A : \Pi_1^{\mathrm{thin}}(M) \longrightarrow BU(1).$$

The latter is therefore a transport-level shadow of the richer differential cocycle: the connection object determines thin transport, thin transport determines loop holonomy, and holonomy supplies the phase readout used by the computational semantics. In schematic form,

$$\mathbf{B}U(1)_{\mathrm{conn}} \longrightarrow \text{connection/transport} \longrightarrow \text{thin holonomy} \longrightarrow \text{gauge-invariant phase readout}.$$

This places the phase-ledger construction of section 3.4 naturally inside the ordinary differential-geometric boundary of higher prequantum geometry without identifying the two formalisms prematurely.

What GCFT adds. Higher prequantum geometry and GCFT therefore address different parts of the construction. Higher prequantum geometry supplies a natural language for the differential-cohomological refinement of field and phase data: connections, higher connections, curvature, characteristic cocycles, transgression, and their organization over moduli stacks. GCFT adds a computational interpretation to the source geometry. Its primitive data include admissible updates, interfaces, boundary types, gluing laws, computational histories, regime changes, and executable gauge-invariant readouts. The central claim of GCFT is not merely that such geometric data exist, but that their compositional structure may itself constitute computation.

Accordingly, the intended relation is not GCT versus higher prequantum geometry but rather a bridge from computationally structured geometry to higher prequantum refinement to quantization and QFT reconstruction. When an appropriate higher prequantum cocycle exists, it should be regarded as part of the semantic data of the corresponding GCFT sector. The subsequent passage to a quantum theory still requires the additional structures listed below: a measure or weighting, locality and factorization, positivity, gauge resolution, continuum control, and ultimately a physical Hilbert space or equivalent quantum representation. Higher prequantization is therefore not itself the completion of the quantum theory, just as the existence of a connection and holonomy is not.

For this reason, we also refrain from identifying the extraction map

$$\mathrm{Ex} : \mathcal{C}^{\mathrm{obs}}_{\mathrm{GCM}} \longrightarrow \mathcal{D}_{\mathrm{exec}}$$

with a polarization. A polarization in geometric quantization selects an admissible subspace of prequantum states from which the quantum state space is constructed. The extraction functor instead records which gauge-invariant geometric observables admit effective external readout. The two operations may eventually interact, but no equivalence between them is assumed here.

The conservative position of the present work is therefore as follows. Geometric quantization is not rejected; it is postponed until a GCFT sector has produced the phase-space structure on which geometric quantization acts. Higher prequantum geometry is closer to the present ontology and provides a natural candidate language for differential-cohomological refinement of GCFT moduli. GCT, however, addresses an earlier question: how the geometric, gauge, and compositional structures that are subsequently prequantized acquire physical and computational meaning in the first place.

Effects, semantic data, and QFT obligations. In the tradition of lattice gauge theory, we may interpret the constructive tooling as a regulator with admissibility built in. Rather than beginning with an unrestricted formal path integral over all field histories and imposing gauge, locality, or regularity conditions only afterward, we restrict the space of admissible histories at the level of geometric formation rules. Boundary data, gluing constraints, transport data, and regime-dependent readouts are not external decorations; they are part of the syntax of the theory. In this sense, GCFT aims to reduce the space of possible histories before analytic or quantum-field-theoretic reconstruction begins.

This should not be misunderstood as avoiding the ordinary obligations of quantum field theory. A constrained geometric semantics must still supply, or make possible the construction of:

(a) a local action or other weighting of admissible histories;

(b) a gauge-reduced measure or equivalent quantization prescription;

(c) a local and factorizing algebra of observables;

(d) positivity conditions sufficient for Hilbert-space reconstruction;

(e) unitary Lorentzian evolution or an equivalent unitary representation of the reconstructed physical symmetries;

(f) a nontrivial and controlled continuum limit;

(g) a spectrum of physical excitations;

(h) anomaly and global-symmetry data;

(i) well-defined boundary, defect, and bulk observables.

These are not effects in the programming-language sense, nor optional additions to an otherwise completed theory. They are the conditions by which a compositional geometric semantics becomes a physical quantum field theory rather than merely a kinematic or topological model.

In particular, the term *effect* is not meant as a catch-all for every analytic or quantum-field-theoretic obligation. Effects are controlled operations internal to the semantic framework: examples include Wick rotation, coarse-graining, measurement-induced boundary updates, quotient/readout projections, renormalization-like scale changes, and the introduction of metric-sensitive Yang–Mills dynamics over a more topological compositional core. These operations may transform the semantic data of the theory, but they do not by themselves replace that data.

Wick rotation. For example, Wick rotation may be regarded as an effect because it changes the presentation of a geometric-computational history from a Lorentzian dynamical regime to a Euclidean or moduli-sensitive regime in which instanton-like sectors, compactness phenomena, and tunneling configurations become more visible. But the legitimacy of this operation is not automatic. A Wick-rotated presentation must still satisfy the relevant reconstruction conditions, such as reflection positivity, if it is to define a physical Lorentzian quantum theory. Thus, Wick rotation may be an effect, while reflection positivity is a constraint on that effect.

Structure	Role in GCFT
Action/local weight	Assigns dynamical preference, phase, or statistical weight to admissible histories.
Measure	Defines semantic weighting or integration over the reduced space of histories.
Locality/factorization	Controls how observables assigned to local regions compose, descend, and reconstruct global observables.
Positivity	Supplies the positivity condition required for Hilbert-space reconstruction from Euclidean data.
Unitarity	Requires the reconstructed Lorentzian evolution and symmetry action to preserve the physical inner product.
Gauge resolution	Removes or resolves redundant field descriptions, for example through gauge fixing, BRST cohomology, or the BV formalism.
Continuum limit	Provides a scaling or refinement theorem relating the regulated geometric model to a continuum theory.
Spectrum	Records the physical excitations and reconstructed dynamical generators of the theory.
Anomalies	Encode obstructions, inflow data, and global consistency conditions.
Observables	Form the gauge-invariant readout algebra or semantic target of the theory.
Effects	Implement controlled changes of regime or presentation, such as Wick rotation, coarse-graining, or readout projection.

Locality and factorization. The gluing law of GCFT supplies only the geometric skeleton of locality. A physical field theory must additionally assign observables to regions in a way that is compatible with inclusion, separation, and local-to-global composition. Schematically, for pairwise disjoint regions

$$U_1, \dots, U_k \subset V,$$

one expects structure maps

$$\mathcal{O}(U_1) \otimes \cdots \otimes \mathcal{O}(U_k) \longrightarrow \mathcal{O}(V)$$

that are associative, symmetric up to the appropriate grading, and compatible with refinement of the chosen regions. A sufficiently strong descent or factorization condition then determines observables on a larger region from compatible local data [CG17].

In a Lorentzian reconstruction, locality also includes causal compatibility. For spacelike-separated regions U and V, the corresponding physical observables should commute, or graded-commute:

$$[\mathcal{O}(U), \mathcal{O}(V)]_{\pm} = 0.$$

This is the familiar local-algebraic condition of quantum field theory [HK64]. It is stronger than the claim that geometric histories can be glued. The present GCM interface structure provides a candidate local decomposition, but one must still prove that the resulting observable assignment satisfies the required factorization, descent, and causal-commutativity properties.

This distinction is especially important in the gauge regime. Gauge constraints may prevent the physical Hilbert space or observable algebra from factorizing naively across a spatial boundary. Boundary charges, edge modes, and Gauss-law constraints can couple the two sides even when their microscopic carriers are spatially separated. Accordingly, locality should be formulated at the level of the appropriate boundary and observable categories rather than assumed from a tensor-product decomposition of microscopic state spaces.

Unitarity and reconstruction. Reflection positivity is one route from a Euclidean presentation to a unitary Lorentzian theory, but positivity and unitarity should not be identified. Given Euclidean correlation functions satisfying the Osterwalder–Schrader conditions, one may reconstruct a Hilbert space, a vacuum, and Lorentzian fields with the corresponding unitary structure [OS73]. Reflection positivity is therefore a constraint on the Euclidean semantic data from which unitarity may be reconstructed.

Once a Lorentzian clock or time-translation structure has been identified, physical evolution should act by operators

$$U(t) : \mathcal{H}_{\mathrm{phys}} \longrightarrow \mathcal{H}_{\mathrm{phys}}$$

satisfying

$$U(t+s) = U(t)U(s), \qquad U(t)^\dagger U(t) = \mathrm{id},$$

together with the relevant continuity and spectral conditions. More generally, the reconstructed spacetime and internal symmetries should act unitarily on the physical Hilbert space.

Neither reversibility of the microscopic geometric dynamics nor linearity of the proposed type system proves this condition. Linearity expresses a resource and composition discipline; microscopic reversibility says that an update can be inverted. Unitarity is an additional analytic statement about the physical inner product, probabilities, and reconstructed symmetry representation. GCFT must therefore show how its deterministic geometric evolution gives rise to a positive physical state space and unitary observable dynamics rather than treating unitarity as a consequence of compositionality alone.

Cluster decomposition and infrared independence. A further requirement of physical reconstruction is cluster decomposition: the recovery of effective independence between widely separated local observables. Geometric compositionality and causal locality do not by themselves guarantee this property. For gauge-invariant local observables $A(x)$ and $B(y)$ in a suitable vacuum sector, one expects the connected correlation function

$$\langle A(x)B(y)\rangle_c = \langle A(x)B(y)\rangle - \langle A(x)\rangle\langle B(y)\rangle$$

to vanish as the spacelike separation between x and y becomes large. In a massive theory, appropriate spectral assumptions may yield exponential clustering, whereas massless excitations can produce algebraically decaying correlations. The precise statement depends on the vacuum, spectrum, and choice of local observable algebra.

This requirement is especially relevant to GCFT because spatially separated geometric excitations may retain common holonomy, boundary constraints, or topological data. Such global relationships do not necessarily represent persistent connected correlations between local observables. Conversely, the existence of a common gauge configuration does not establish cluster decomposition. A successful low-energy reconstruction must therefore distinguish nonlocal topological information and gauge constraints from ordinary connected correlations, and demonstrate that the latter exhibit the appropriate long-distance behavior within the physical sector under consideration. Cluster decomposition is thus an additional infrared consistency condition, not an automatic consequence of geometric gluing, gauge invariance, or compositional closure.

Gauge fixing, BRST, and BV resolution. The quotient by gauge transformations also requires more than an informal declaration that gauge-equivalent histories represent the same state. A naive integral over the space of connections

$$\mathcal{A}(P)$$

overcounts entire gauge orbits. One must either integrate directly over an appropriate quotient object

$$[\mathcal{A}(P)/\mathcal{G}(P)]$$

or choose a resolution that handles the redundancy while preserving the physical observables.

In conventional perturbative gauge theory, gauge fixing introduces auxiliary fields and ghost variables, while BRST symmetry packages the residual gauge invariance cohomologically. Physical observables are represented by BRST cohomology classes rather than arbitrary gauge-dependent functions of the fields [BRS76]. For reducible, open, or field-dependent gauge symmetries, the Batalin–Vilkovisky formalism enlarges the field space by ghosts and antifields and replaces the naive quotient by a derived resolution. At the classical level, the extended action S_{BV} satisfies the classical master equation

$$\big(S_{\mathrm{BV}}, S_{\mathrm{BV}}\big) = 0,$$

while quantization requires an appropriately regularized and renormalized solution of the quantum master equation [BV81].

In GCFT terms, gauge fixing is not a physical effect that changes the computational state. It is an auxiliary choice of presentation used to evaluate a quotient by redundancy. BRST or BV data belong to the quantization and consistency layer: they ensure that the measure, renormalization prescription, and observable algebra descend correctly to gauge-invariant information. Different gauge choices must therefore produce equivalent boundary readouts and correlation functions.

A complete gauge-computational field theory would ultimately require one of two constructions:

(a) a direct stacky or derived integration theory on the moduli of geometric-computational histories; or

(b) a BRST/BV-type resolution whose cohomology computes the same gauge-invariant observable content.

The present paper supplies the underlying groupoid, boundary, and holonomy data, but does not yet construct this full quantum gauge resolution.

Spin and statistics as a reconstruction constraint. Recovering spinorial degrees of freedom is not by itself sufficient to recover fermionic matter. Spin specifies how a field transforms under the relevant spacetime symmetry, while statistics specifies how multiparticle states behave under exchange. In relativistic quantum field theory these structures are tied together by the spin–statistics connection: under the standard assumptions of relativistic covariance, positive energy, and causal locality, half-integer-spin fields obey fermionic statistics while integer-spin fields obey bosonic statistics [Pau40].

This distinction matters for GCFT. A geometric construction may produce spinor bundles, chiral modes, or defect sectors transforming in spinorial representations without yet establishing the exchange law of the corresponding excitations. A successful reconstruction must also show that multiparticle composition carries the appropriate $\mathbb{Z}_2$-grading, so that spacelike-separated fields satisfy the corresponding graded locality condition

$$\mathcal{O}_1(x)\mathcal{O}_2(y) = (-1)^{|\mathcal{O}_1||\mathcal{O}_2|}\mathcal{O}_2(y)\mathcal{O}_1(x), \qquad (x-y)^2 < 0,$$

for homogeneous observables of definite parity.

From the present viewpoint, spin–statistics is therefore a local-to-global consistency requirement. Local geometric data determine the transformation type of an excitation, but the statistics of identical excitations is a rule governing their global composition and exchange. GCFT does not presently derive this rule from helical microgeometry. It requires that any Lorentzian reconstruction claiming to recover ordinary fermionic and bosonic sectors reproduce the standard spin–statistics relation.

CPT symmetry as a reconstruction constraint. The discrete geometric operations available in the helical substrate should not be identified directly with charge conjugation, parity, and time reversal in relativistic quantum field theory. In particular, spatial chirality reversal does not by itself implement conjugation of gauge representations, and reversal of a geometric history need not define a physical time-reversal symmetry. The present construction therefore neither assumes a primitive CPT symmetry nor predicts its violation. Rather, CPT invariance is required of any effective Lorentz-covariant, local quantum field theory reconstructed from the geometric-computational substrate under the standard hypotheses of the CPT theorem. Establishing those hypotheses, or equivalently constructing the corresponding effective CPT operation, remains an open obligation of the program.

Measurement, continuum limits, and anomalies. Measurement may alter boundary conditions, admissible continuations, or the readout data available to an observer, and in this limited sense it may be represented by an effect-like operation. The probabilities of its outcomes, however, require additional semantic data: a measure, state, or weighting on the relevant space of admissible configurations or histories. Likewise, the observable algebra is not itself an effect. It specifies which features of the underlying process survive as physical readouts, including holonomy traces, Wilson-loop-type observables, defect charges, boundary operators, spectral quantities, and moduli invariants. Thus one should distinguish the change of presentation or boundary data from weighting of histories and extraction of physical observables.

The continuum limit has a similarly distinct status. Coarse-graining and renormalization may be implemented as transformations between regulated descriptions, but the existence of a nontrivial continuum theory is not an operation that can be postulated. It is a limiting statement to be established. A finite or regulated helical system may possess gaps, stable sectors, conserved quantities, or finite-dimensional readouts; the physical question is whether an appropriate family of such structures persists under refinement. One must therefore identify a directed family of regulated theories, specify the observables being compared, and show that their correlation, spectral, or transport data approach a well-defined continuum limit. In a Yang–Mills realization, for example, any proposed mass gap must remain separated from zero uniformly in the continuum limit rather than being merely a feature of a finite regulator.

Anomalies play an even more structural role. Classically compatible local symmetry data need not admit a globally consistent quantum realization. An anomaly is precisely such an obstruction: the local gauge, symmetry, or gluing rules cannot be promoted to globally well-defined quantum data without additional structure [AW84, Fre14]. Accordingly, anomaly cancellation is not an optional consistency check performed after the theory has been constructed; it is a condition on whether the proposed local semantics can exist globally at all.

In geometric terms, the obstruction may appear through the failure of a partition function or state assignment to descend to an ordinary function on the quotient by gauge. Instead, it may transform as a section of a nontrivial line bundle, or more generally define higher cocycle data over the relevant moduli space. Local anomalies are detected infinitesimally, while global anomalies can remain even when the local anomaly polynomial vanishes. Anomaly inflow supplies a corresponding repair mechanism: an anomalous boundary theory may become consistent as the boundary of a higher-dimensional invertible theory whose variation cancels the boundary obstruction [Fre14].

This makes anomalies especially natural from the present viewpoint. GCFT is built around the passage

$$\text{local geometric data} \longrightarrow \text{compatible gluing} \longrightarrow \text{global process semantics}.$$

An anomaly records a failure of this passage after quantization. It is therefore closely related to failed descent, nontrivial cocycle data, boundary inflow, and obstructions to defining a globally consistent observable theory. Any proposed gauge-computational semantics must reproduce the anomaly structure of the effective field theory it claims to recover; otherwise the local geometric model and the quantum theory do not define the same global physics.

The intended architecture is therefore as follows:

(a) **Core geometry.** Helical local normal forms, admissible interfaces, transport, connections, curvature, and defects.

(b) **Compositional semantics.** Boundary objects, geometric histories, gluing, disjoint union, and observational equivalence.

(c) **Dynamical weighting.** Local actions, statistical weights, or phase assignments on admissible histories.

(d) **Gauge resolution.** Quotient-stack, gauge-fixing, BRST, or BV data sufficient to remove redundant descriptions without changing physical observables.

(e) **Observable locality.** A local net or factorization structure for bulk, boundary, and defect observables, together with the required descent and causal-commutativity conditions.

(f) **Effects.** Wick rotation, measurement-induced boundary updates, coarse-graining, renormalization, and quotient/readout projection.

(g) **Reconstruction and consistency.** Positivity, unitarity, gauge invariance, covariance, anomaly cancellation or inflow, and compatibility with gluing.

(h) **Scaling and outputs.** A nontrivial continuum limit, reconstructed Hilbert spaces, spectra, gaps, correlation functions, scattering data, and deformation-stable invariants.

This separation is essential. The effect structure organizes changes of presentation and regime, but it does not excuse the theory from reconstructing the physical content normally supplied by quantum field theory. Rather, the goal is to reorganize where these obligations enter. GCFT seeks to build admissibility into the geometric syntax of histories, then recover measures, observables, spectra, and continuum behavior from the resulting constrained semantic structure. If successful, the framework would not eliminate the analytic burdens of quantum field theory. Still, it would relocate them to a setting in which the allowed histories, boundary data, and gauge-compatible readouts are already geometrically disciplined.

On topological Lagrangians. A useful historical precedent for the present viewpoint is the Atiyah–Jeffrey [AJ90] reinterpretation of Donaldson–Witten theory through the Mathai–Quillen formalism. In that setting, the topological gauge action is not merely a dynamical functional placed into a formal path integral. Rather, it may be understood as the field-theoretic realization of an infinite-dimensional Mathai–Quillen representative of a Thom or Euler class. Schematically, the relevant section is given by the anti-self-dual curvature condition

$$s(A) = F_A^+,$$

so that the resulting cohomological theory localizes onto the zero locus

$$F_A^+ = 0$$

and hence onto the corresponding moduli space of gauge-equivalence classes of solutions. The action therefore packages geometric information about the solution space into a form suitable for invariant evaluation.

This provides a useful precedent for GCFT, but the analogy should be stated carefully. In the present field theory, compositional semantics, dynamical weighting, and observable extraction are distinct operations. The functor

$$Z : \mathsf{Bord}_n^{\mathrm{GCM}} \longrightarrow \mathcal{C}_{\mathrm{GCM}}$$

assigns semantic content to admissible geometric histories; a Lagrangian or analogous weighting selects or weights dynamically relevant histories; and the extraction functor

$$\mathrm{Ex} : \mathcal{C}_{\mathrm{GCM}}^{\mathrm{obs}} \longrightarrow \mathcal{D}_{\mathrm{exec}}$$

records which gauge-invariant observables admit effective external readout. Atiyah–Jeffrey supplies a precise example in which the dynamical/cohomological weighting itself has a geometric localization interpretation, rather than functioning as an opaque weighting of arbitrary configurations.

The comparison is consequently strongest in topological and cohomological sectors, where localization compresses an infinite-dimensional field space onto deformation-stable moduli data. It does not imply that generic metric-dependent gauge dynamics can be replaced by topological localization, nor does it supply the constructive, typed, or executable semantics sought here. In particular, it does not resolve the genuinely dynamical problems of four-dimensional Yang–Mills. Its relevance is instead structural: it demonstrates that a gauge-theoretic action can, in an appropriate sector, encode a geometric localization mechanism whose output is invariant information associated with a moduli problem.

Why Lagrangians appear: local scoring, gluing, and invariance. Given the above comparison, a recurring question from the physics side is why, then, our dynamics are presented (in the fluidic/gauge regimes) via an "action principle" in the first place. In the present framework, this is not an aesthetic choice but a structural one. Once one insists that (a) evolution is *local*, (b) composite processes are formed by *gluing*, and (c) the description is *coordinate/gauge invariant*, the natural notion of "cost" for a geometric process is provided by Lagrangian densities compatible with these requirements.

Local scoring and additivity under gluing. Let M be a spacetime region (or computational bordism) and let ϕ denote the relevant geometric field data (e.g. a connection, framing field, or helix-state field) subject to prescribed boundary conditions on ∂M. We seek a functional

$$S_M[\phi] \in \mathbb{R}$$

interpreted as the score/cost of realizing the process ϕ on M. The minimal structural requirements are:

(a) **Locality.** $S_M[\phi]$ depends on ϕ through its local jets (a finite number of derivatives), so that modifications supported in a small region only affect the score locally.

(b) **Gluing additivity.** If $M = M_1 \cup_\Sigma M_2$ is obtained by gluing along an interface Σ and ϕ restricts compatibly, then

$$S_M[\phi] \;=\; S_{M_1}[\phi|_{M_1}] \;+\; S_{M_2}[\phi|_{M_2}],$$

up to boundary/interface terms that depend only on the glued data on Σ [Ati88].

(c) **Invariant symmetry.** S is invariant under the relevant redundancy group: diffeomorphisms (when applicable) and gauge transformations for connection-valued data.

Under these hypotheses, the functional must be representable (up to boundary terms) as an integral of a *local density*,

$$S_M[\phi] \;=\; \int_M \mathcal{L}(\phi, \nabla\phi, \ldots)\,,$$

where $\mathcal{L}$ is built from coordinate- and gauge-invariant contractions of the available geometric tensors (metric, volume form, curvature, covariant derivatives, etc.). This is the precise sense in which a Lagrangian is the canonical "local score" compatible with gluing and invariance.

Stationarity, not optimization. The variational condition

$$\delta S_M[\phi] = 0$$

does not assert that Nature "minimizes" S in a global sense; rather, it singles out histories that are *stable under first-order perturbations* with fixed boundary data, yielding Euler–Lagrange equations [Arn89]. This stationarity principle is the natural compatibility condition between local scoring and compositional evolution, and it is the mechanism by which continuous field descriptions produce constraint equations and conservation laws via Noether-type arguments [Noe18].

Topological core versus evaluator. In the GCFT viewpoint, an action decomposes conceptually into a *compositional core* that depends only on topological/geometric structure needed for gluing and typing of interfaces, and an *evaluator term* that penalizes "difficulty" (curvature/strain/instability) and selects physically realizable histories. This mirrors our BF/Yang–Mills split. BF-type terms are first-order, local, and naturally compatible with gluing; they encode kinematic constraints (flatness, defect charges, coupling to sources). Yang–Mills-type terms introduce a metric-sensitive cost for curvature and thereby define an effective dynamics/regularization. Concretely, for a connection A with curvature F_A, one has the paradigmatic pair

$$S_{\mathrm{BF}}(A, B) = \int_M \mathrm{tr}(B \wedge F_A), \qquad S_{\mathrm{YM}}(A) = \int_M \|F_A\|^2 \,\mathrm{vol}_g,$$

where S_{BF} supports gluing-amenable constraint semantics and S_{YM} acts as an evaluator (a resource/energy functional) selecting stable configurations. In our setting, the "fully fluidic" regime corresponds to the existence of such a local invariant evaluator; lower regimes (quasi-fluidic, symbolic) arise when only coarser readouts of the geometry are verifiable or when dissipation/coarse-graining dominates.

Dissipation and arrows. Finally, many effective evolutions used in modeling (including ours in certain regimes) are not strictly Hamiltonian. This is compatible with the above: one may pass to Euclidean signature or introduce a dissipation functional so that evolution follows a gradient-like flow for the evaluator (a Lyapunov monotone). In that case, the Lagrangian/action continues to serve as the correct local score compatible with gluing. At the same time, the *effective* time evolution becomes a semigroup on the verifiable state space.

The role of the action. GCFT does not reject Lagrangian or action-based formulations. It rejects the stronger claim that an action functional, by itself, specifies the complete ontology and semantics of a physical theory.

Let

$$\mathrm{Hist}_{\mathrm{adm}}(Y_0, Y_1)$$

denote the space or groupoid of geometrically admissible histories between boundary data Y_0 and Y_1. The geometric formation rules determine which histories belong to this space. An action is then additional data

$$S : \mathrm{Hist}_{\mathrm{adm}}(Y_0, Y_1) \longrightarrow \mathbb{R}$$

in the Euclidean case, or a phase-valued functional in the Lorentzian case.

Classically, the stationary points of S select distinguished histories. In a quantum or statistical reconstruction, S contributes a weight such as

$$e^{-S_E} \qquad \text{or} \qquad e^{iS/\hbar}.$$

Thus the action weights or selects admissible geometry; it does not define admissibility, gauge equivalence, boundary composition, or the observable algebra by itself.

Compatibility with gluing requires locality of the action. For compatible histories $W_1 : Y_0 \to Y_1$ and $W_2 : Y_1 \to Y_2$, one expects

$$S(W_2 \circ W_1) = S(W_1) + S(W_2),$$

up to the boundary and corner terms required by the chosen variational problem. In this sense, Lagrangian data enter GCFT as a local weighting of the computational bordism semantics rather than as its primitive foundation.

Noether currents and Ward identities. The symmetry of the action must also survive in the observable dynamics. For an ordinary continuous global symmetry of a local action, Noether's theorem associates the invariance of the variational problem with a conserved current. Schematically,

$$\delta_\epsilon S = 0 \qquad \Longrightarrow \qquad \nabla_\mu J^\mu = 0$$

on solutions of the equations of motion.

Local gauge symmetry requires a slightly different interpretation. Because gauge transformations represent redundancies of description, their infinitesimal invariance gives Noether identities among the field equations rather than an independent physical conserved charge for each gauge parameter. The distinction is important in GCFT: a symmetry that acts physically on boundary or observable data must be distinguished from a gauge transformation that merely changes the representative of the same physical configuration.

After quantization, the corresponding symmetry constraints appear as relations among correlation functions and amplitudes. In the abelian case these take the form of Ward–Takahashi identities [War50]; in non-abelian Yang–Mills theory the corresponding relations are encoded by the Slavnov–Taylor identities [Tay71]. Their precise form depends on the fields, gauge-fixing prescription, and observable algebra, but their structural role is the same: the quantum theory must preserve the symmetry relations inherited from the classical local dynamics.

For GCFT this gives another reconstruction test. If a geometric symmetry or gauge redundancy is claimed to reproduce a symmetry of the effective field theory, then the induced correlation functions and boundary amplitudes must satisfy the corresponding Noether, Ward–Takahashi, or Slavnov–Taylor relations. It is not sufficient for the microscopic geometry merely to possess an analogous symmetry.

An anomaly occurs when a symmetry of the classical description cannot be preserved in the quantum theory with all of the required consistency conditions. Thus the sequence

$$\text{geometric symmetry} \longrightarrow \text{classical Noether identity} \longrightarrow \text{quantum Ward identity}$$

is itself part of the local-to-global reconstruction problem, while anomaly data record an obstruction to completing that sequence.

Summary. Lagrangians arise because they are the natural local, gluing-additive, symmetry-respecting scoring rules on geometric processes, and the variational principle expresses stability of admissible histories under perturbation. In our language, they are the evaluator layer that sits atop a compositional (often topological) core.

5.5 Psi-Geometric

In light of the preceding construction, how might GCMs help inform an interpretation of quantum mechanics?

It is plausible that a quantum state may admit an ontic realization in geometric data carried by a twin helix substrate, while a wavefunction ψ supplies a representation of those data in a suitable chart. Connections, holonomy, admissible gluing, and invariant readouts provide a candidate language for interference and entanglement.

Kinematic ontology. Let M be the relevant carrier region, with a time parameter and spatial configuration domain X in the nonrelativistic setting; a relativistic extension would instead require suitable data on a globally hyperbolic spacetime and its Cauchy surfaces. The proposed beables are:

(O1) A twin helix bundle $\pi : \mathcal{H} \to M$ with oriented-strand and chirality data, together with an associated phase bundle carrying a $U(1)$ connection A and a nonnegative geometric density $\rho_{\mathcal{H}}$

(helix–flux density). The connection specifies phase transport, while its description in a local trivialization is gauge-dependent.

(O2) Global linking, join, and holonomy data, subject to the admissible interface and gluing laws of the substrate. These are candidate geometric carriers of Aharonov–Bohm-type phases and nonfactorizing correlations; their identification with quantum entanglement remains to be established.

Schematically, the space of complete physical configurations is a gauge quotient

$$\Lambda = \big\{(\mathcal{H} \to M,\, A,\, \rho_{\mathcal{H}};\, \text{linking/holonomy and admissible field data})\big\}/\mathcal{G},$$

where $\mathcal{G}$ denotes the relevant gauge redundancies. This quotient should not be confused with the space of positions or other classical readout coordinates.

In a proposed scalar, nonrelativistic chart, write

$$\psi_t(x) = R_t(x)e^{iS_t(x)/\hbar}, \qquad \rho_{\psi,t}(x) := |\psi_t(x)|^2 = R_t(x)^2,$$

with $x \in X$. The density $\rho_{\psi,t}$ is a density on X, whereas $\rho_{\mathcal{H}}$ denotes substrate data; identifying them requires a specified geometric reconstruction map. In the usual minimally coupled scalar model, the associated guidance velocity, away from nodes of ψ, is

$$\mathbf{v}_{\psi,t} = \frac{1}{m}\big(\nabla S_t - e\mathbf{A}_t\big).$$

Here e is the coupling and $\mathbf{A}_t$ is the local vector potential in the scalar quantum model. Treating this potential as a readout of the helix connection is a proposed identification, not a result of the present construction.

Dynamical ontology.

(D1) *Scalar Madelung correspondence.* For a sufficiently regular solution of the minimally coupled Schrödinger equation, writing $\psi = Re^{iS/\hbar}$ gives, where $R > 0$, the standard continuity and Hamilton–Jacobi equations [Mad27]:

$$\partial_t \rho_\psi + \nabla\cdot(\rho_\psi \mathbf{v}_\psi) = 0,$$

$$\partial_t S + e\phi + \frac{|\nabla S - e\mathbf{A}|^2}{2m} + V + Q_\psi = 0, \qquad Q_\psi = -\frac{\hbar^2}{2m}\frac{\nabla^2 R}{R}.$$

The displayed equations give a reformulation of the scalar Schrödinger dynamics; by themselves they do not derive that dynamics from a helix bundle. The scalar potential ϕ and the additional potential V are included here in the usual quantum-mechanical sense.

(D2) *Proposed helix–geometric reconstruction.* A GCT realization would need to define a gauge-invariant scalar $Q_{\mathcal{H}}$ from the relevant amplitude geometry, connection, curvature, torsion, or other admissible data and prove, in an appropriate reduction, that $Q_{\mathcal{H}} = Q_\psi$. In particular, the identification of Q_ψ with a shape-operator or curvature expression is not established by the Madelung decomposition. Likewise, a spinorial or Dirac reconstruction would require additional spin and Clifford data, appropriate field equations, and their compatibility with the proposed geometric flow.

The guidance equation and continuity law have an important antecedent in Bohm's deterministic account of quantum mechanics [Boh52a, Boh52b]. Our proposal is not simply to assign Bohmian particle trajectories to a helical background: its candidate beables are the coupled geometric substrate, connections, and *shared global holonomy* of composite configurations. Bohmian guidance therefore supplies a mathematical point of comparison, not an identification of the two ontologies.

Measurement as bordism surgery. We propose that measurement is a physical surgery on the decorated bordism of the coupled system–apparatus geometry:

$$\mathfrak{S}_A : W_{SA} \longrightarrow W'_{SA}.$$

Here $\mathfrak{S}_A$ modifies the admissible boundary identifications, join structures, and connection-compatible transport histories, without requiring a change in spacetime topology. The resulting dynamics is conjectured to select a stable outcome sector determined by the complete ontic state. Wavefunction collapse is then the effective restriction of the quantum description to that sector, rather than a primitive stochastic intervention.

The precise surgery operation, dynamical stabilization of outcomes, and recovery of Born statistics remain open reconstruction problems.

Probabilities and the Born rule. For the scalar model above, the density $\rho_{\psi,t} = |\psi_t|^2$ obeys a continuity equation under the standard guidance velocity. Consequently, if $\varphi_{t,t_0} : X \to X$ is the corresponding well-defined flow, then, under the usual regularity assumptions,

$$(\varphi_{t,t_0})_*\big(\rho_{\psi,t_0}\, d\mathrm{vol}_X\big) = \rho_{\psi,t}\, d\mathrm{vol}_X.$$

This is equivariance *within the scalar guidance model*. It does not yet establish equivariance for measures on the complete GCT configuration space Λ.

To state the required relation without conflating state spaces, let μ_t be an ensemble probability measure on Λ (assuming a suitable measurable structure), and let

$$q_t : \Lambda \longrightarrow X$$

be a specified, gauge-invariant configuration projection for the preparation under consideration. A Born-compatible ensemble would satisfy the pushforward condition

$$(q_t)_*\mu_t = |\psi_t|^2\, d\mathrm{vol}_X.$$

If the complete dynamics is Φ_{t,t_0}, this relation would be propagated from t_0 provided that

$$\mu_t = (\Phi_{t,t_0})_*\mu_{t_0}, \qquad q_t \circ \Phi_{t,t_0} = \varphi_{t,t_0} \circ q_{t_0},$$

and the initial pushforward equals $|\psi_{t_0}|^2 d\mathrm{vol}_X$. The intertwining relation is a *condition to be demonstrated* for a GCT realization, not a property established here.

Even such equivariance would not explain why physically prepared ensembles satisfy the initial Born condition. Within Bohmian mechanics, Dürr, Goldstein, and Zanghì develop a quantum-equilibrium typicality account [DGZ92], whereas Valentini studies possible nonequilibrium distributions and their coarse-grained relaxation toward equilibrium [Val91, VW05]. The present work adopts neither explanation. The geometric origin or statistical selection of the physically relevant measure, including its relation to observed frequencies, remains open.

PBR and the status of ψ. The ontic–epistemic distinction requires care. In the ontological-models framework, ψ-ontology is a technical condition on the probability measures associated with quantum-state preparations [HS10, PBR12]. For example, distinct pure states ψ_1 and ψ_2 are ψ-ontically distinct in the disjoint-support sense when their induced measures on the ontic state space are mutually singular:

$$\mu_{\psi_1} \perp \mu_{\psi_2}.$$

The PBR result derives restrictions on overlapping ontic distributions under its stated assumptions, including preparation independence [PBR12]. Neither the gauge quotient Λ nor the assignment of a wavefunction chart alone proves the required disjointness, supplies the preparation measures, or establishes the response functions of a completed model.

The position proposed here is therefore *structurally ontic but representationally chart-dependent*. The bundle, its admissible geometric data, and its gauge-invariant relations are proposed as physical; ψ is a local description of an associated quantum state, analogous to a choice of trivialization or gauge. Distinct formulae related by a change of representation need not describe distinct physical quantum states. This does not mean that arbitrary inequivalent quantum states are merely different charts of the same ontic configuration. Whether the completed model is ψ-ontic in the precise support-theoretic sense, and whether it satisfies the assumptions relevant to PBR, must be checked after its state-preparation and measurement maps have been constructed. The possibility of epistemic restrictions in other ontological models remains relevant background [Spe07, KS67].

Bell correlations and nonseparability. The intended GCT position is to retain operational no-signalling and Bell measurement independence while permitting a failure of Bell-local factorization. For a Bell experiment, let a, b denote settings, α, β denote outcomes, and λ_{src} denote the complete source/preparation data relevant to the experiment. We distinguish λ_{src} from a retrospectively specified *entire spacetime history* that already includes the chosen settings. Measurement independence is the condition

$$P(\lambda_{\mathrm{src}} \mid a, b) = P(\lambda_{\mathrm{src}}).$$

For entangled configurations, the proposed completion would instead have to demonstrate a failure of Bell-local factorization, in the sense that the following identity does not hold generally:

$$P(\alpha, \beta \mid a, b, \lambda_{\mathrm{src}}) \not\equiv P(\alpha \mid a, \lambda_{\mathrm{src}}) P(\beta \mid b, \lambda_{\mathrm{src}}).$$

This is a proposed dynamical feature, not a consequence already proved from holonomy [Bel64]. This distinction is independent of the operational no-signalling conditions

$$P(\alpha \mid a, b) = P(\alpha \mid a), \qquad P(\beta \mid a, b) = P(\beta \mid b).$$

For a deterministic completion with free settings and a complete relevant ontic specification, violation of Bell factorization requires the appropriate ontic dependence on a distant setting (or a failure of some other assumption used in the Bell-model formulation); no-signalling must then follow after averaging over inaccessible ontic data. Merely positing shared holonomy or a globally glued configuration does not prove either the observed Bell correlations or this no-signalling property. These are explicit reconstruction tests, not results claimed in the present section.

A Summary of Postulates. The following are proposed interpretive commitments and reconstruction targets rather than established consequences of the preceding GCM constructions.

P1. Ontology. The candidate physical substrate is a twin helix bundle with connection, geometric density, and admissible linking/holonomy data, considered modulo genuine gauge redundancy.

P2. Dynamics. Evolution is proposed to be deterministic and geometric. In a restricted scalar chart it should recover the Schrödinger/Madelung correspondence, while the helix origin of Q_ψ and any Dirac or interacting-field reconstruction remain open.

P3. Equivariance. The usual scalar density $|\psi|^2$ is equivariant under its standard guidance flow. A GCT derivation requires the appropriate configuration projection and measure-intertwining law; selecting Born equilibrium is a further problem.

P4. Measurement. Apparatus coupling induces a proposed bordism surgery on the coupled geometry, yielding a dynamically selected, stable outcome sector without primitive stochastic collapse.

P5. Nonlocality. Entanglement is proposed to arise from shared global holonomy and linking data within a nonfactorizing geometric configuration. The completed theory must reproduce Bell correlations while preserving measurement independence and operational no-signalling.

P6. Relativity. A relativistic completion must admit covariant, compatible evolution across Cauchy surfaces—potentially of Tomonaga–Schwinger type [Tom46, Sch48]—without an empirically distinguished preferred frame.

Future work. The psi-geometric interpretation is a minimal orienting outline, *not* a completed reconstruction of quantum theory. A full account requires, among other things, a well-defined geometric quantum-state map and amplitude prescription; a suitable measure on gauge-reduced configuration spaces and a derivation or independent justification of Born statistics; explicit coupled detector dynamics, decoherence, metastable records, and outcome selection; an account of multiparticle composition, identical particles, and spin–statistics; Bell-violating correlations with no-signalling and measurement independence; a covariant, foliation-independent treatment of interacting quantum fields; recovery of quantum optics, scattering, and perturbative QFT in controlled limits; and agreement with the applicable coupling, renormalization, and anomaly constraints. The present section fixes only the direction of a possible interpretation and separates what follows from established scalar quantum mechanics from what remains to be derived from GCT.

Summary. The proposed ontology is geometric and gauge-invariant; ψ is a representation of an associated physical state rather than a primitive substance or a merely subjective probability assignment. Scalar equivariance is a useful consistency condition, but neither the relevant GCT ensemble measure nor Born equilibrium has been derived. Measurement is proposed to involve bordism surgery on the coupled geometry, while shared global holonomy supplies a candidate mechanism for entanglement and Bell-type correlations. The relevant surgical dynamics, outcome statistics, and Bell correlations remain to be derived. Accordingly, the present interpretation is a research hypothesis, not an alternative completed quantum theory.

Closing Remarks on THM_4 and the role of V_4. We do not identify THM_4 with particular Standard Model particle families, nor do we claim that it directly realizes continuous gauge groups. Its significance is more primitive. At the kinematic level, the twin helix substrate carries two independent involutive operations:

$$\chi : (\text{chirality flip}), \qquad \omega : (\text{orientation flip}),$$

with

$$\chi^2 = \omega^2 = \mathrm{id}, \qquad \chi\omega = \omega\chi.$$

Hence, the substrate supports the minimal nontrivial abelian group generated by two commuting involutions,

$$\langle \chi, \omega \rangle \;\cong\; \mathbb{Z}_2 \times \mathbb{Z}_2 \;\cong\; V_4.$$

Equivalently, if one labels the four helical sectors by

$$\mathcal{H}_4 = \{THM_4^{(\epsilon,\delta)} : \epsilon, \delta \in \{\pm 1\}\},$$

where ϵ records chirality and δ records orientation, then $\mathcal{H}_4$ is naturally a V_4–torsor: the group acts freely and transitively by toggling these two binary invariants. In this sense, V_4 should be understood not as an incidental symmetry, but as the minimal algebraic skeleton of the twin helix substrate.

This point is strengthened by the fact that the same algebra arises in several canonical settings. First, the one-qubit Pauli group modulo its scalar center satisfies

$$\mathcal{P}_1/\{\pm 1, \pm i\} \;\cong\; \{I, X, Y, Z\}/\{\pm 1, \pm i\} \;\cong\; V_4,$$

so that V_4 is precisely the phase-stripped algebra of two independent binary flips. Second, the four Bell states form a natural V_4–torsor under local Pauli operations: starting from any one Bell state, the action of two commuting $\mathbb{Z}_2$ generators traverses the remaining three. Third, on a torus, one has

$$H^1(T^2; \mathbb{Z}_2) \;\cong\; \mathbb{Z}_2 \times \mathbb{Z}_2,$$

corresponding to the four spin structures determined by periodic/antiperiodic boundary conditions along the two independent cycles. In each case, the same abstract pattern appears: two commuting binary distinctions generate a four-sector structure. In our setting, the relevance of V_4 is not that it encodes the exact P or T symmetries of the Standard Model, but that it supplies the smallest nontrivial algebra in which independent binary geometric distinctions can be composed, inverted, and transported [LM89].

This perspective may also help clarify the relation to quantum nonlocality. Historically, Einstein, Podolsky, and Rosen [EPR35] identified a potential incompleteness in any theory satisfying locality and separability; Bell [Bel64] later showed that the corresponding local-causal package is incompatible with the observed quantum correlations. A deterministic but globally constrained theory would preserve no-signalling and measurement independence while abandoning Bell-local factorization: distant outcomes need not be conditionally independent given a putatively complete local state when they arise as boundary readouts of a single nonseparable geometric configuration. Thus the EPR impulse toward a deeper completion may survive, while, in the spirit of Bohm, the specific assumption of local separability would be abandoned.

Our universe may be built from the smallest groups, not just the richest.

A Appendix

A.1 "Hidden" Variables?

It should be noted that two canonical join patterns for twin helices lead to distinct gauge–geometric behaviors.

Definition A.1 (Apex Twin Helix)**.** An *apex–joined* configuration is obtained by collapsing a boundary circle to a point, producing a conical join $C(S^1)$ (a stratified space with a point singularity). Equivalently, remove the apex and view the result as $M \setminus \{p\}$ equipped with a connection whose curvature may carry a localized charge at p (e.g. a Dirac monopole in the abelian case). Such joins model sources/sinks or defect cores, such as optical vortices, but most prominently **Dirac cones**.

By contrast, our THM as in definition 1.7 is the object used for deterministic logic flow, as in the **Schrödinger equation**. The operational distinction is *holonomic*:

Proposition A.1 (Base Transport versus Apex Charge)**.** *Let A be a connection on the relevant gauge bundle, with curvature F.*

(a) ***Base–joined case.*** *Suppose the join lies in a simply connected neighborhood U on which the connection is smooth. If $F|_U = 0$, then parallel transport around every contractible loop $\gamma \subset U$ has trivial holonomy. More generally, when F is smooth but nonzero, sufficiently small contractible loops may acquire nontrivial holonomy determined locally by the enclosed curvature, but this holonomy approaches the identity as the loop is shrunk. Thus no singular topological charge is concentrated at the smooth join.*

(b) ***Apex–joined case.*** *Suppose instead that the join collapses to an isolated point p, and consider a small linking sphere*

$$S_p^2 \subset M \setminus \{p\}.$$

In the $U(1)$ case, the topologically protected datum is the quantized flux

$$c_1 = \frac{1}{2\pi} \int_{S_p^2} F \in \mathbb{Z},$$

with the conventional coupling-dependent normalization understood. This integer is the first Chern number of the restricted line bundle over S_p^2.

Individual loop holonomies may still be computed locally. If a contractible loop $\gamma = \partial\Sigma$ lies in a trivializing patch, then

$$\mathrm{Hol}_\gamma(A) = \exp\left(i \int_\Sigma F \right).$$

However, the monopole charge is carried by the flux through the closed linking sphere rather than by a distinguished Aharonov–Bohm-type loop around the point. In particular,

$$\exp\left(i \int_{S_p^2} F \right) = e^{2\pi i c_1} = 1,$$

even when $c_1 \neq 0$.

For a non-abelian structure group, the corresponding defect data are encoded by the topology of the restricted bundle and its clutching or characteristic data on S_p^2; loop holonomies provide conjugacy-class-valued transport observables but are not, in general, determined by a single scalar flux.

Resolution by blow-up. An isolated apex may be resolved geometrically by the real blow-up of M at p, which replaces the point by its sphere of normal directions S_p^2. The gauge data on the punctured neighborhood may then be represented by bundle data on this new boundary component. In the $U(1)$ case, the stored magnetic charge is measured by

$$c_1 = \frac{1}{2\pi} \int_{S_p^2} F.$$

More generally, the exceptional sphere carries the corresponding clutching or characteristic data appropriate to the structure group. In this sense, an isolated defect may be replaced by a boundary carrying the same topological charge data, while the smooth base-joined case contains no analogous point-supported charge.

Feature	**Twin Helical Manifolds**	**The Apex Twin Helix**
Join point	Smooth base join	Singular apex join
Topology	Globally smooth manifold	Manifold with point singularity
Flow	Bidirectional transport along an annulus	Radial (source/sink) around a defect core
Chirality	Controlled by local geometry	Emerges from defect topology
Singularities	Avoided (non-singular)	Essential (e.g. Dirac monopoles)
Field role	Symbolic/geometric logic (ordered joins)	Physical spinor dynamics
Purpose	Analog computational flow	Topological charge carriers

Summary. The "duality" is a clean dichotomy of join conditions: *smooth* joins emphasize programmable transport (deterministic logic), while *singular* joins emphasize conserved charges (defect logic). Hence, paired helices play two separate roles in physics. Holonomy conjugacy classes and curvature flux rigorously control both.

Emergence of helical normal forms. As illustrated in fig. 4b, a complex plane wave

$$\Psi(x,t) = Ae^{i(kx-\omega t)}, \qquad \Re\Psi = A\cos(kx-\omega t), \quad \Im\Psi = A\sin(kx-\omega t),$$

has two quadrature components which, plotted transversely against a linear propagation coordinate at fixed time, describe a cylindrical phase helix of constant amplitude. The Type 1 normal form represents this abelian phase rotation on the paired conical screw–dilation geometry, with scale and relative chirality/orientation supplied by the geometric substrate. In Maxwell's $U(1)$ sector, it serves as a proposed normal form for abelian phase transport (and, with vector polarization data, polarization transport), not a literal spatial trajectory of a photon.

Question. *But why the difference? Why do photons appear as Type 1 while Yang–Mills instantons (fig. 4a) present as Type 3 dual-cone configurations?*

Helical normal forms for Type 1 and Type 3. We say a localized geometric computational configuration on the twin helix substrate is:

- **Type 1 (Helical Orb Normal Form).** A coaxial pair of counterwinding helices as an abelian wave with a common propagation axis and phase-locked transverse frame; joints are equal-phase loci.
- **Type 3 (Symmetric Flow Normal Form).** A compact, oriented cobordism in spacetime whose incoming/outgoing faces carry oppositely oriented helical frames, visualized as two opposed cones joined along a finite 3-volume.

Proposition A.2 (Gauge-Sector Boundary Normal-Form Correspondence)**.** *Given a gauge sector G and boundary data:*

(a) ***Abelian, propagating waves*** *(e.g. transverse electromagnetic waves in $U(1)$) admit a proposed* Type 1 *helical phase-transport normal form, with a common propagation axis and paired transverse-frame geometry.*

(b) ***Nonabelian, (anti)self-dual finite-action events*** *(e.g. instantons in $SU(2)$ or $SU(3)$) are represented by localized Euclidean gauge configurations carrying nonzero topological charge*

$$k \propto \int_{\mathbb{R}^4} \mathrm{tr}(F \wedge F).$$

For standard finite-action instantons the curvature decays at infinity and the connection approaches a pure-gauge configuration asymptotically. After one-point compactification

$$\mathbb{R}^4 \cup \{\infty\} \simeq S^4,$$

the corresponding bundle data carry the quantized topological class. Within the present geometric semantics, the incoming/outgoing orientation data of such a vacuum-to-vacuum event are represented by the Type 3 dual-cone normal form.

Proof sketch. (1) In the abelian case, holonomy takes values in a commuting phase group. A monochromatic traveling wave has equal-amplitude quadratures that yield a cylindrical phase-helix representation. The Type 1 conical twin supplies an additional screw–dilation representative for the abelian phase channel, including the paired geometric structure; that representative is not fixed by the plane-wave equation alone.
(2) For nonabelian (anti)self-dual solutions, the relevant invariant is the instanton number

$$k = \frac{1}{8\pi^2} \int_{\mathbb{R}^4} \mathrm{tr}(F \wedge F) \in \mathbb{Z},$$

up to the conventional choice of sign and trace normalization. For the BPST family, this integer is represented by a localized curvature profile with algebraically decaying tails and nontrivial bundle data over the compactified space S^4.

Equivalently, when Euclidean time is used to describe the interpolation, an instanton connects asymptotic gauge vacua whose Chern–Simons or winding numbers differ by k. In the GCT normal-form picture, the two faces of the Type 3 dual cone encode these oppositely oriented asymptotic boundary data. □

Summary. Abelian propagating waves admit a proposed Type 1 geometric phase-transport normal form; instantons are nonabelian, topological *events*—represented here by Type 3 dual-cone cobordisms—not particles. The distinct pictures are fixed by (a) symmetry (abelian vs. nonabelian), (b) energetics (wave transport vs. self-dual soliton), and (c) boundary class (open propagation vs. vacuum-to-vacuum interpolation).

Question. *But what about the weak bosons? Why do the $W^{\pm}$ and Z admit Type 1-like propagation while the $SU(2)_L$ gauge sector also supports Type 3 topological configurations?*

The distinction is between the geometric normal form of a propagating excitation and the global field configurations admitted by its gauge theory. The photon and the weak bosons are all spin-1 excitations, and their transverse polarization modes may exhibit similar local helical wave profiles. Thus, Type 1-like geometry is not exclusive to an abelian gauge group: it may also describe the transverse propagation of a nonabelian connection in an appropriate linearized regime.

The physical weak bosons nevertheless differ from the photon. Following electroweak symmetry breaking,

$$SU(2)_L \times U(1)_Y \longrightarrow U(1)_{\mathrm{em}},$$

the photon remains massless with two transverse polarizations, whereas $W^{\pm}$ and Z become massive and possess an additional longitudinal polarization. Their transverse modes may admit Type 1-like representatives, but the complete massive vector field requires further polarization, Higgs, and dynamical data.

The same nonabelian electroweak theory also admits nonperturbative configurations, including instanton-like Euclidean histories and sphaleron-mediated transitions. The former motivate the Type 3 dual-cone normal form through their topological boundary data. A sphaleron is instead an unstable energy-barrier configuration, not itself a self-dual instanton. Its relation to Type 3 is therefore an analogy at the level of nonperturbative transition geometry.

Hence the weak sector does not require a fifth twin helix type. Rather, it illustrates the distinction established in A.1:

$$\text{propagating weak-field excitations} \longrightarrow \text{Type 1-like geometry},$$

$$\text{nonperturbative electroweak histories} \longrightarrow \text{Type 3-like geometry}.$$

These are different configurations of the same underlying gauge sector, not two competing geometric identities assigned to an individual weak boson.

Question. *But what about the Type 2 and Type 4 twin helix configurations? What might they represent, and how do they relate to gluonic interactions and junctions?*

Helical normal forms for Type 2 and Type 4. Unlike Type 1-like propagating waves and Type 3-like topological events, Type 2 and Type 4 are proposed normal forms for paired or extended configurations of gauge-theoretic flow. Their distinction is primarily one of cancellation versus reinforcement of the relevant geometric transport data:

(a) **Type 2 (Twisted Pair Normal Form).** Oppositely organized helical components produce a cancellation-dominated configuration. In QCD, this suggests a possible geometric representative for selected scalar and pseudoscalar gluonic channels, where correlated field components contribute to a gauge-invariant composite observable.

(b) **Type 4 (Co-propagating Twins Normal Form).** Coherently aligned helical components produce a reinforcement-dominated configuration. In QCD, this suggests a possible geometric representative for twisted confining flux tubes and selected tensorial gluonic channels, where coherent winding or aligned transport persists across an extended field configuration.

Heuristic justification. For Type 2, the proposed correspondence is with gauge-invariant scalar and pseudoscalar gluonic operators, schematically

$$\mathcal{O}_{0^{++}} = \operatorname{tr}(F_{\mu\nu}F^{\mu\nu}), \qquad \mathcal{O}_{0^{-+}} = \operatorname{tr}(F_{\mu\nu}\widetilde{F}^{\mu\nu}).$$

These operators distinguish parity sectors and provide natural probes of the corresponding glueball channels. However, cancellation of a designated helicity or twist readout does not alone determine the total J^{PC} quantum numbers. Nor does a two-strand geometric representative imply the existence of exactly two constituent gluons: physical glueball states are determined through gauge-invariant dynamics and correlation functions, with constituent-gluon descriptions furnishing effective models [MBS08].

For Type 4, the proposed correspondence is instead with coherent winding and reinforcement of transport. Helically twisted confining flux tubes provide one possible effective geometric realization, although such geometry is not implied by $SU(3)$ symmetry alone [TN14]. A complementary comparison arises in tensorial gluonic channels, which may be probed by the symmetric traceless gauge-invariant operator

$$\mathcal{O}^{(2)}_{\mu\nu} = \operatorname{tr}(F_{\mu\rho}F_{\nu}{}^{\rho}) - \frac{1}{4}g_{\mu\nu}\operatorname{tr}(F_{\alpha\beta}F^{\alpha\beta}),$$

with the appropriate spin projection. Its spin-2 projection probes tensorial gluonic channels, for which the proposed Type 4 representative emphasizes coherent extended transport.

Relation to gluon junctions. Three- and four-gluon interaction vertices arise from the cubic and quartic terms of the nonabelian gauge-field action, while the baryonic Y-junction organizes three fundamental color lines through an invariant contraction. These are interaction and flux-network structures; Types 2 and 4 instead label proposed extended transport patterns. A composite field configuration may contain several vertices or branching flux segments while retaining the same macroscopic geometric normal form.

Summary. Type 2 and Type 4 are interpreted as distinct composite or extended geometric regimes: Type 2 is cancellation-dominated and admits possible comparisons with scalar and pseudoscalar gluonic channels, whereas Type 4 is reinforcement-dominated and admits possible comparisons with coherent flux tubes and tensorial channels. The selection of either representative depends on the dynamics and boundary data of the gauge sector.

Geometric normal forms, gauge structure, and dynamics. A helical normal form does not, by itself, uniquely determine a particle species, an internal gauge group, or a dynamical field configuration. To distinguish these levels, we may describe an effective geometric-computational field configuration schematically by the structured datum

$$\mathcal{C} = \big(\mathcal{N},\, (E, \nabla^E),\, \mathcal{D}\big),$$

where $\mathcal{N}$ denotes a selected geometric or kinematic normal form, (E, ∇^E) denotes the associated internal representation bundle and gauge connection, and $\mathcal{D}$ denotes the relevant dynamical structure, including field equations, boundary conditions, vacuum data, and excitation spectrum.

This notation is a distinction between descriptive layers, not an assertion of a canonical factorization or three independent microscopic constituents. In particular, $\mathcal{N}$ may depend on a specified framing, projection, or geometric readout and need not uniquely reconstruct the underlying gauge field.

Consequently, different gauge sectors may admit the same local geometric normal form without possessing equivalent internal transport. As previously stated, transverse polarizations of a nonabelian spin-1 connection may exhibit a Type 1-like helical wave profile, even though their connection has

Sector	Object	Dominant functional	Boundary class	Form
$U(1)_{\mathrm{em}}$	Photon	Transverse spin-1 propagation	Massless, asymptotic	Type 1
$SU(2)_L \times U(1)_Y$	$W^{\pm}$, Z bosons	Transverse spin-1 propagation; additional longitudinal mode	Massive, unstable excitations	Type 1-like
$SU(2)_L$, $SU(3)_c$	Instanton	(Anti)self-dual topological event	Vacuum-to-vacuum history ($k \neq 0$)	Type 3
$SU(3)_c$	Scalar/pseudoscalar gluonic channel	Proposed cancellation-dominated paired geometry	Gauge-invariant, confined composite	Type 2-like
$SU(3)_c$	Twisted flux tube / tensor channel	Proposed reinforcement-dominated geometry	Extended, confined or composite	Type 4-like

Table 13: Proposed helical normal-form correspondences classified by gauge sector, dynamical behavior, and boundary data.

noncommuting holonomy and nonlinear self-interactions. This is relevant to the electroweak sector: the photon is a massless excitation of the unbroken $U(1)_{\mathrm{em}}$ connection, whereas the physical $W^{\pm}$ and Z bosons arise from the $SU(2)_L \times U(1)_Y$ gauge theory after Higgs symmetry breaking. Their transverse modes can possess similar local wave geometry, but the massive weak bosons additionally carry longitudinal polarization modes that are not captured by the transverse Type 1 analogy.

Conversely, a single nonabelian gauge sector may support different geometric normal forms according to its dynamical and boundary data. Propagating gauge-field excitations and finite-action instanton histories need not share the same geometric representative, despite belonging to the same underlying gauge theory.

Accordingly, the Type 1–Type 4 classification is understood as a classification of selected geometric normal forms and computational carrier structures, not as a one-to-one classification of elementary particles or gauge groups. Any physical identification requires the accompanying gauge, representation, and dynamical data.

Question. *But why does nature even bother with gluing helices?* A single helix's axial $U(1)$ phase renders a gauge; with a twin, the relative phase $\Delta\theta \in S^1$ is gauge-invariant and robust. This yields an abelian "phase logic" realizing the $C_2 \times C_2$ actions used in the symbolic regime. Likewise, gluing balances torque and stabilizes the framing, thereby making the interfaces implementable. The most commonly cited continuous symmetry of the helix (i.e., rotation about the screw axis) is not amenable to computation.

Question. *Why conical helices?* In contrast to cylindrical helices (orbits of screw isometries), conical helices are orbits of a screw–dilation flow in Sim(3). This additional similarity symmetry makes the radial direction a genuine scale coordinate. Along a conical helix, the Frenet invariants (κ, τ) scale inversely with length, while their ratio remains invariant. The corresponding trajectory in curvature–torsion space therefore follows a ray, interpolating between the straight-rod limit (IR) and a high-curvature apex (UV).

This structure suggests an analogy with the scale modulus of Yang–Mills instantons. As an instanton shrinks toward zero size, its curvature concentrates, and the Uhlenbeck compactification records the degeneration through ideal-instanton boundary strata. At the curve level, the conical helix models the corresponding scale-dependent concentration. For volumetric tubes, the conical profile also accommodates geometric self-contact constraints (see Fig. 3 of [CGM06]), providing an additional physical motivation for the construction.

Question. *Why require smooth end caps rather than allowing singular tips?* Smooth caps enforce regularity at the terminal boundary and prevent concentration of curvature, energy, or gauge flux at a conical or cuspidal endpoint. Charge-like data in the regular model must arise from holonomy, twist, gluing, or explicitly introduced defects. The cap also fixes a terminal closure and framing condition, thereby constraining the admissible global holonomy classes.

Compositional asymmetry of the regimes. The chart of n–logics in table 6 exhibits an asymmetry that is not adequately characterized by the commutativity of its transport operations. Although the regimes admit different algebraic closure structures, they also differ in how a relationship between geometric components becomes part of a computational state. We distinguish two broad mechanisms: *constitutive composition*, in which the operative computational structure is defined through a relation between components, and *ambient composition*, in which independently describable structures are related through shared transport, boundary conditions, or global constraints. This is a distinction between modes of realization, not a claim that the regimes are separated by an absolute requirement of spatial attachment.

The symbolic regime supplies the elementary constitutive example. As established in section 1.3 and theorem 1.5, the canonical THM_4 is constructed by gluing two unit helices into a common framed object. Let their chirality and orientation labels be (χ_A, ω_A) and (χ_B, ω_B), respectively. The relative labels

$$\chi_{\mathrm{rel}} = \chi_A \chi_B, \qquad \omega_{\mathrm{rel}} = \omega_A \omega_B$$

take values in $\{\pm 1\}^2$. The four resulting configurations carry the natural action in V_4 generated by independently changing the relative chirality and orientation labels. In this construction, gluing supplies the common geometric interface and framing required to treat these relations as the state of a single computational cell. It is therefore not merely a convenient arrangement of two otherwise independent symbolic carriers: the relational organization is constitutive of the chosen physical realization of the geobit.

The significance of a shared reference can be expressed independently of the particular embedding. If two component state spaces carry an action of a symmetry group G, their composite state modulo a *common* symmetry action is described by

$$\mathcal{S}_{\mathrm{rel}} = (\mathcal{S}_A \times \mathcal{S}_B)/G_{\mathrm{diag}},$$

where G_{diag} acts simultaneously on both components. In general,

$$(\mathcal{S}_A \times \mathcal{S}_B)/G_{\mathrm{diag}} \ncong (\mathcal{S}_A/G) \times (\mathcal{S}_B/G).$$

Quotienting the components independently can erase relative information that survives under a common reference. A joined, framed THM provides a concrete geometric realization of this distinction. Its relative degrees of freedom are not recoverable merely by treating each constituent as an independently quotiented object.

The quasi–fluidic regime exhibits a different possibility. A single carrier may already possess meaningful phase transport and cyclic holonomy. Two such carriers can be coupled or phase-locked, but a permanent geometric join is not generally required to define their individual transport operations. When a common phase reference is imposed, relative phases can become meaningful composite observables; when the channels decouple, their individual abelian transports remain well-defined. Composition is thus primarily mediated by transport and compatibility rather than by the compulsory formation of a new geometric body.

In the fully fluidic regime, the emphasis returns to constitutive relations, but in a dynamical rather than a discrete form. For interacting multi-carrier configurations, the relevant computational process may be defined by coupled continuous evolution, in which the motion of one component changes the admissible evolution of another. Such coupling can arise through shared fields, interface conditions, or noncommuting transport. We may therefore speak of *dynamical gluing*, provided this means dependence within a common evolution law rather than permanent physical attachment. The constituent histories cease to be independently sufficient descriptions of the interacting process.

Finally, in the gauge regime, composition is governed by the global compatibility of locally represented geometric data. Distinct localized excitations may belong to the same gauge configuration without forming a connected physical body. Connections, transition functions, boundary conditions, and topological sectors constrain their collective description. This does not mean that gauge fixing renders the constituents dynamically independent; gauge transformations identify equivalent descriptions, whereas dynamical independence is a separate property. In this regime, the relevant gluing is most naturally expressed through the descent and compatibility conditions required to reconstruct global geometric data from local representatives.

Regime	Characteristic source of composition	Role of gluing / attachment	Typical closure condition
Symbolic	Shared *relational state* between discrete carriers	*Constitutive geometric gluing* in the canonical THM_4 realization	A common interface/frame supports finite-state operations
Quasi–fluidic	Compatible phases, winding, or cyclic transport	Geometric joining *optional*	Carried by phase relations or abelian holonomy, even when the channels remain spatially distinct
Fluidic	Coupled continuous evolution and ordered transport	*Constitutive dynamical coupling* in interacting realizations	Imposed by the common evolution law: constituent histories no longer suffice independently
Gauge	Global compatibility of local geometric data	Physical attachment *optional*; mathematical gluing remains essential	Expressed by descent/compatibility conditions on connections, transition data, and topological sector

Figure 5: Compositional asymmetry of the four regimes. The distinction is not primarily whether geometric carriers are physically attached, but where the composite computational structure is constituted: at a shared interface, through transported phase relations, through coupled dynamics, or through globally compatible gauge data

The locus of compositional closure. The apparent inner–outer pattern of table 6 can therefore be understood as a change in the *locus at which compositional closure is imposed*. In the canonical symbolic construction, closure is realized through an explicit common interface supporting relative finite-state operations. In the quasi–fluidic regime, closure can be carried by phase transport without requiring such an interface. In interacting fluidic constructions, closure is imposed by the common evolution law and its coupled degrees of freedom. In the gauge regime, closure is expressed through globally compatible connection and equivalence data.

This organization retains the distinction between the symbolic and fluidic regimes, where the relation among components is central to the computational operation, and the quasi–fluidic and gauge regimes, where a global or transported relation may persist without compulsory local attachment. Nevertheless, these are characteristic realizations rather than exclusive possibilities. The same geometric substrate may admit different computational descriptions depending on which interfaces, histories, and invariant observables are retained.

The join commutator of section 4.1 remains relevant, but answers a different question. It detects whether specified transport operations commute; it does not determine whether a geometric join is necessary to constitute a state, whether a dynamical coupling is present, or whether separated constituents satisfy a common global constraint. The regime asymmetry is therefore not a binary division into commuting and noncommuting systems. It reflects different ways in which a composite geometric state acquires its identity and admissible operations.

Question. *Proof of Yang–Mills instantons being composed of holonomic helices has so far not been confirmed. How then can we safely verify their existence?*

The issue is that the helical structure we posit resides in the *connection* A (parallel transport in the internal bundle). In contrast, direct observables are gauge-invariant functionals of the *curvature* $F = dA + A \wedge A$ or of holonomies (Wilson loops). A gauge transformation can erase any purely local feature of A; what survives to observation are scalar densities such as $\operatorname{tr} F_{\mu\nu}F^{\mu\nu}$ and $\operatorname{tr} F \wedge F$, which appear as lumps, rings, or cone-like envelopes in lattice plots and experiments. The micro–handedness of a helical A thus projects to gauge–invariant *envelopes* rather than visible corkscrews.

Helical winding is a property of the *fiber* (the G internal directions) over spacetime. Detectors and standard lattice diagnostics live on the base manifold and access only fiber–invariant combinations. Projecting fiber twist onto base scalars discards orientation data but retains energy and topological charge, yielding the observed dual-cone profiles for instanton-like configurations. Real instruments

and lattice operators average over space, time, and ensembles. Without a phase-locked reference to the internal connection, linear twist contributions cancel, leaving only quadratic or topological signals. Hence, the helical microstructure is washed out, while $\operatorname{tr} F^2$ and $F \wedge F$ remain.

Many diagnostic solutions (instantons, calorons) are Euclidean saddles. The helix lives in the Euclidean/complexified connection; in real time, one measures its *consequences* (selection rules, rates, envelopes), not the helical motion itself. The appropriate observables are *nonlocal* and gauge sensitive:

- **Wilson–loop tomography.** Families of loops $\mathcal{W}(\gamma) = \operatorname{tr} \mathcal{P} \exp \int_\gamma A$ detect non–abelian holonomy; loop–shape/systematic studies can reconstruct local twist consistent with $\operatorname{tr} F^2$ envelopes.
- **Gauge–fixed diagnostics.** In a fixed gauge, one may visualize the Chern–Simons 3–form K_μ to track handedness (useful for diagnosis, though not itself gauge invariant).
- **Analog platforms.** Phase–locked probes in $SU(2)$ optical media, cold atoms with synthetic gauge fields, or superconducting circuits access non–abelian holonomy directly, providing experimental surrogates for helical transport [CZX+19, GJOS14].

Summary. The helical structure is not expected to appear directly as a gauge-invariant observable. Rather, it manifests as the framed geometry of transport encoded by connections, phase accumulation, curvature, and holonomy. Local field plots therefore display gauge-dependent representatives or coarse geometric envelopes. At the same time, physical observables are constructed from gauge-invariant quantities such as curvature densities, characteristic data, and class functions of holonomy. In this sense, the underlying helical organization may be visible only indirectly: either through a chosen gauge or trivialization in which the framed transport admits a helical representative, or through nonlocal observables that retain the corresponding transport data after quotienting by gauge.

Topological boundary readout in classical Maxwell theory. A useful comparison is provided by [BLLN19], who showed that surface Maxwell waves at interfaces between homogeneous isotropic media admit a bulk–boundary description in terms of the complex spectrum of the helicity operator. Their topological invariant may be presented either as

$$w \in \mathbb{Z}_4$$

or as a pair of binary indices

$$\left(w^{\mathrm{TM}}, w^{\mathrm{TE}}\right) \in \mathbb{Z}_2 \times \mathbb{Z}_2,$$

and the change of this invariant across an interface determines the corresponding surface modes.

The relevance to GCT is not an identification of these four Maxwell sectors with the four canonical elements of THM_4. The Maxwell sectors belong to a common abelian wave regime and differ through constitutive and spectral data. They are therefore better interpreted as differently decorated realizations of a common geometric canonical form. The structural parallel lies instead in the sequence

$$\text{continuous bulk dynamics} \longrightarrow \text{finite invariant readout} \longrightarrow \text{interface-localized mode.}$$

The two presentations of the Maxwell invariant are also instructive. The pair-valued form retains two independently readable channels, whereas the $\mathbb{Z}_4$-valued form records their cyclic organization through helicity-spectrum winding. Thus, the same four bulk sectors admit distinct algebraic descriptions depending on which relations the readout preserves. This supplies a physical example of a general principle used throughout GCT: the canonical geometry of a substrate does not by itself determine its observable alphabet; finite information appears only after geometric or spectral data are passed through a specified invariant readout.

From this perspective, a surface Maxwell mode is not a new fundamental geometric atom. It is a robust boundary excitation produced by the mismatch between two decorated bulk sectors. The comparison therefore supports the broader GCT picture in which discrete, topologically stable observables can emerge from continuous deterministic field geometry.

Cross-sectional geometry and matter-like sectors. The physical role of varying cross-sectional geometry on tubular helices is not merely to enlarge the local state space. Upon reaching the fully fluidic regime (4.2), the cross-section determines which internal modes and flow channels exist, which degeneracies can be maintained, and which localized defects can remain coherent under transport.

Gauge transport governs how these modes are carried through the helical frame, while cross-sectional geometry governs what can be carried. Gluing (2.2) then imposes the interaction grammar: boundary data must agree in framing, phase, mode content, and conserved defect structure before two local configurations can compose smoothly. Matter-like excitations may therefore be interpreted, at this level, not as primitive point objects but as persistent soliton, defect, or obstruction sectors of the helical moduli space. Their physical identity is encoded by the deformation-stable data that survive transport, gluing, and coarse-graining.

The analogy with language is useful provided it is read structurally. The cross-section supplies an alphabet of local modes; gluing supplies the syntax of admissible composition; holonomy supplies an invariant semantics; and persistent soliton sectors are the resulting "words" that remain recognizable under deformation. This does not yet identify particular particles with particular cross-sectional contours, nor does it supply a phenomenological mass spectrum. It instead isolates the mathematical problem that must precede such identifications: determining which regions and strata of the helical moduli space support localized composite sectors, how these sectors transform under transport, and which transitions between them are permitted by the gluing laws.

Continuous logic and the proliferation of solitonic composites. A continuous geometric substrate need not produce a continuously observed particle spectrum. Stable, metastable, and resonant sectors may appear as discrete readouts of an underlying continuous moduli problem, much as vortices, solitons, and normal modes form distinguishable objects within continuous media. The continuing proliferation of composite states in collider spectroscopy makes such a picture conceptually natural. By June 2026, CERN referred to eighty-five composite particles discovered at the LHC [Har26], while many additional excited and heavy-flavor states remained to be sought. This empirical abundance does not establish the present model, but it cautions against treating the observed particle catalog as a finite primitive alphabet. A sufficiently expressive continuous geometry should instead be naturally expected to support a large family of effective composites whose discreteness arises from stability, symmetry, and invariant readout rather than from an underlying discrete ontology.

Psi–geometric semantics and "quantum quandaries". Our program does not attempt to explain *why* helices in nature behave as they do or *where* they came from; such work is best left to our colleagues in *adjacent departments*. Rather, it takes seriously what their behavior appears to implement: something simultaneously ordinary and mildly unsettling—they enforce global consistency in a world that, operationally, only permits local access.

A useful way to read this is through the categorical perspective advocated by Baez [Bae06]: many familiar "quantum quandaries" are not additional physical mysteries, but structural consequences of working in a non-Cartesian, process-theoretic setting (closer in spirit to **nCob** than to **Set**). In such a setting, composition is *gluing* rather than pairing; one should not expect a canonical diagonal ("copying") nor a cartesian product that cleanly models independent subsystems. From this viewpoint, interference and AB-type phenomena are the generic signatures of phase transport and holonomy: the relevant compatibility data is global (encoded in connections and their path-dependence), while local descriptions are related by gauge. Entanglement, likewise, is best understood as the failure of factorization of the underlying glued state: two distant "systems" may simply be two boundary ports of a single global geometry prepared in their common past. No superluminal signaling is implied; the observed correlations reflect shared constraints on how boundary data can be capped, compared, and recombined.

A.2 Invariant Content Across Gauge and Duality Frames

A recurring danger in any geometric formulation is to confuse a useful representative with the invariant object it represents. In the present framework, the twin helix is not intended to be a privileged shape in isolation. Its role is to provide a local normal form in which several computationally relevant structures become simultaneously visible: chirality, orientation, phase, winding, framing, transport, and admissible gluing. The invariant content of the theory must therefore be sought in the data that survive the appropriate changes of description.

The phrase "change of description" has several meanings in field theory. A coordinate transformation changes the presentation of the same geometric object. A gauge transformation changes the local representative of the same gauge configuration. A deformation may move within a fixed topological or protected sector. More radically, a duality may relate descriptions whose fields, couplings, operator coordinates, or even gauge groups are different while preserving the same long-distance physics. These

notions should not be conflated, but they suggest a hierarchy of questions:

What survives coordinate/gauge change? $\longrightarrow$ What survives deformation? $\longrightarrow$ What survives duality?

For GCT and GCFT, this hierarchy is important because the microscopic helical presentation is only the beginning of the construction. A candidate physical theory must ultimately be characterized by observable and compositional data that do not depend on accidental choices of coordinates, gauge, embedding, or effective field variables.

From gauge representatives to differential cocycles. The simplest gauge-theoretic lesson is already familiar from holonomy. For a connection A and closed loop γ,

$$U_\gamma = \mathcal{P} \exp\left(\int_\gamma A\right)$$

depends on a choice of local representative, while its conjugacy class and class functions such as

$$\mathrm{tr}_\rho(U_\gamma)$$

are gauge invariant. Curvature and characteristic classes provide further information, but none of these ingredients separately captures the complete global gauge field.

For abelian gauge fields, differential cohomology provides a natural framework in which topology, differential form data, and holonomy are retained simultaneously [Fre02]. A differential cohomology class

$$\widehat{h} \in \widehat{H}^n(M;\mathbb{Z})$$

carries, schematically, three compatible pieces of information:

$$\begin{aligned} I(\widehat{h}) &\in H^n(M;\mathbb{Z}), \\ \mathrm{curv}(\widehat{h}) &\in \Omega^n_{\mathbb{Z}}(M), \\ \mathrm{hol}_{\widehat{h}} &: Z_{n-1}(M) \longrightarrow U(1). \end{aligned}$$

Here $I(\widehat{h})$ is the underlying integral characteristic class, $\mathrm{curv}(\widehat{h})$ is a closed differential form with the required integral periods, and $\mathrm{hol}_{\widehat{h}}$ evaluates the corresponding transport data on cycles. The essential point is that

$$\text{topological class} + \text{curvature} + \text{holonomy}$$

are not three unrelated invariants, but different shadows of one global differential object.

This is close to the invariant package required by geometric computation. A phase ledger without its curvature data is incomplete; a curvature form without its global quantization condition is incomplete; a topological charge without differential transport data is too coarse to describe the process that realizes it. Differential cohomology therefore provides a standard model for the kind of local-to-global organization that GCFT eventually requires.

Ordinary differential cohomology is fundamentally abelian. Genuinely non-abelian gauge fields require corresponding non-abelian or higher-geometric refinements, naturally expressed through bundles, gerbes, higher stacks, and differential non-abelian cocycles. We do not develop that machinery here. The relevant lesson is simply that the invariant gauge object is generally richer than a connection one-form or a characteristic number considered in isolation.

Extended observables and generalized symmetries. The same principle becomes more apparent when the observable algebra is allowed to contain extended operators. Gauge theory is not determined only by local gauge-invariant functions. Wilson lines, 't Hooft lines, surface operators, defects, and boundary conditions may distinguish theories that appear identical at the level of their local Lie algebras.

This viewpoint is organized systematically by generalized global symmetry [GKSW15, SN24]. A p-form global symmetry acts on p-dimensional charged operators, while its topological symmetry operators have codimension $p+1$. Ordinary global symmetry is the case $p=0$; a one-form symmetry acts naturally on line operators. Schematically, if a topological symmetry operator $U_g(\Sigma)$ links a charged extended operator $W(C)$, then

$$U_g(\Sigma)\, W(C) = \chi_g(W)\, W(C)$$

inside correlation functions, with the linking geometry encoding the action.

For pure $SU(N)$ Yang–Mills theory, the center

$$Z(SU(N)) \cong \mathbb{Z}_N$$

provides the canonical electric one-form symmetry, acting on Wilson lines according to their center charge. This immediately shows why the global form of a gauge group is physical information. The groups

$$SU(N) \qquad \text{and} \qquad PSU(N) = SU(N)/\mathbb{Z}_N$$

have the same Lie algebra but different allowed line operators, one-form symmetries, and global sectors. Thus the infinitesimal gauge algebra does not by itself determine the complete theory.

In the present terminology, generalized symmetries identify deformation-stable information stored in extended readouts. They therefore fit naturally with the GCFT emphasis on paths, surfaces, defects, boundaries, and gluing. A local field may fluctuate while a line or defect charge remains protected; conversely, the spectrum of admissible extended operators may distinguish theories whose local equations have the same form.

For continuous abelian higher-form symmetries, their background gauge fields may themselves be organized by differential cohomological data. More generally, generalized symmetries may carry 't Hooft anomalies, which obstruct gauging and impose anomaly-matching conditions across renormalization-group flow. Differential cocycles, extended operators, generalized symmetry, and anomalies are therefore not separate decorations: they are different aspects of the global organization of gauge data.

We restrict attention here to the invertible part of this structure. An invertible generalized symmetry is implemented by a topological defect possessing an inverse under fusion. Modern field theory admits more general non-invertible symmetry defects, but their full categorical structure is not required for the present argument.

The Polyakov loop as a compactified readout. A useful concrete bridge between holonomy and generalized symmetry is provided by the Polyakov loop. On a Euclidean spacetime with a compact thermal direction

$$S^1_\beta,$$

the untraced thermal holonomy at spatial position $\vec{x}$ is

$$U_\beta(\vec{x}) = \mathcal{P} \exp\left(\int_0^\beta A_0(\tau, \vec{x})\, d\tau \right).$$

A gauge-invariant Polyakov-loop observable is obtained by taking a character, for example

$$P_R(\vec{x}) = \operatorname{tr}_R U_\beta(\vec{x})$$

in a representation R [Pol87].

In pure Yang–Mills theory, the Polyakov loop is charged under the center symmetry and provides the familiar probe of confinement and center-symmetry realization. With dynamical matter in representations carrying nontrivial center charge, this symmetry may be explicitly broken, so the Polyakov loop need not remain an exact order parameter.

For geometric computation, the Polyakov loop is useful for a different but compatible reason. It is an invariant readout of transport around a compact direction:

$$\text{local connection data} \longrightarrow \text{compact holonomy} \longrightarrow \text{class-function readout}.$$

It therefore supplies a standard field-theoretic example of the "phase ledger" principle developed earlier, while generalized symmetry explains why such a loop may also carry information about global sectors that cannot be reconstructed from local curvature alone.

Symmetry is not duality. Gauge invariance and generalized symmetry still compare states or operators within a specified theory. Duality is more radical. Two dual descriptions may possess different elementary fields, different couplings, different weakly coupled variables, or even different gauge groups, while describing the same physical system in the regime where the duality applies.

This distinction is central in modern gauge and string theory. The invariant object is not always a particular Lagrangian presentation. One may instead have a web of presentations related by nontrivial maps among observables, defects, charges, moduli, and couplings.

The Seiberg–Witten solution of four-dimensional $\mathcal{N} = 2$ supersymmetric Yang–Mills theory provides a canonical example [Sei95]. The low-energy description is organized over a moduli space on which electric and magnetic variables transform nontrivially under monodromy. No single electric coordinate system provides a globally preferred description of the effective theory. Near appropriate singular loci, magnetic monopoles or dyons become the natural light degrees of freedom. The physical information is therefore encoded not in one fixed choice of electric variables, but in the globally compatible family of duality frames and their monodromy data.

This lesson is especially close to the geometric viewpoint adopted here. A local trivialization of a gauge bundle need not extend globally; analogously, a useful field-theoretic description need not constitute a globally preferred coordinate system on theory space. Duality may therefore be regarded as a higher-level change of presentation: not a gauge transformation of one connection, but a transition between different effective descriptions of the same physics.

Seiberg duality and invariant infrared content. An even sharper example is Seiberg duality in four-dimensional $\mathcal{N} = 1$ supersymmetric gauge theory. In its canonical form, an "electric" $SU(N_c)$ gauge theory with N_f flavors admits a magnetic description with gauge group

$$SU(N_f - N_c),$$

dual quarks $q, \widetilde{q}$, gauge-singlet mesons M, and a superpotential coupling schematically of the form

$$W = Mq\widetilde{q}.$$

The two descriptions have different microscopic gauge fields and different elementary variables, yet in the appropriate regime they flow to the same long-distance physics.

This gives a much stronger meaning to invariant content than ordinary gauge invariance. The gauge group itself is no longer invariant under the change of description. Instead one compares structures such as

global symmetry groups,
't Hooft anomalies,
moduli spaces of vacua,
chiral operator rings,
maps of baryonic and mesonic operators,
protected indices and infrared observables.

Agreement of such quantities provides evidence that two apparently different microscopic theories belong to the same infrared universality class.

This is particularly important for GCFT. If the eventual physical content of a geometric computational field theory depended on the literal appearance of its microscopic helical variables, then it would be too presentation-dependent to behave like an ordinary quantum field theory. Modern duality instead suggests that the physically meaningful object may be an equivalence class of descriptions whose microscopic state spaces look very different.

Duality, line operators, and global structure. The comparison becomes still more restrictive once extended operators and generalized symmetries are included. A proposed duality must map not only local gauge-invariant operators, but the appropriate spectrum of lines, defects, charges, background fields, and anomalies. The global form of the gauge group and the allowed line-operator lattice therefore matter.

In this sense, generalized symmetry provides a refinement of the traditional duality test. Two theories with the same perturbative Lie algebra and similar local correlation functions may nevertheless differ because their extended operator sectors or higher-form symmetries are different. Conversely, a genuine duality may exchange electric and magnetic extended operators while preserving the complete relational structure among them.

For a geometric theory organized by gluing, this observation is especially natural. Extended operators are themselves geometrically supported objects, and duality may be implemented by interfaces

or walls relating two descriptions. Composition of such interfaces then becomes part of the invariant field-theoretic data. This is one reason that bordisms, defect categories, and higher morphisms arise so persistently in modern gauge and string theory: equivalence of physical descriptions is itself a compositional geometric phenomenon.

Implications for GCFT. The hierarchy developed above suggests progressively stronger notions of invariant content:

gauge equivalence	:	same configuration, different local representative,
differential cohomology	:	one global object combining topology, curvature, and holonomy,
generalized symmetry	:	stable extended operators, defects, charges, and anomaly data,
duality	:	same effective physics in different microscopic variables.

These levels should not be collapsed into a single quotient. They identify different kinds of redundancy or equivalence. Nevertheless, they point toward an important requirement for any mature GCFT: physical content cannot be identified solely with a particular embedded helix, a particular connection, or even a particular Lagrangian presentation.

A candidate equivalence between two GCFT presentations should eventually be tested against the data that ordinary field theory treats as robust: holonomy and differential cocycles, extended observable sectors, generalized symmetries, anomalies, boundary data, and infrared observables. At a still stronger level, one would ask whether apparently different geometric computational substrates can flow to the same reconstructed field theory.

The comparison gives a methodological criterion: gauge theory teaches that local representatives are not physical objects; differential cohomology teaches that topology and differential transport must be packaged together; generalized symmetry teaches that extended defects and operator sectors are part of the invariant theory; and duality teaches that even the microscopic fields and gauge group may fail to be fundamental invariants.

Accordingly, the invariant content of geometric computation should be sought not in the visual form of its generators but in the full local-to-global structure they induce:

transport + cocycle data + extended observables
+symmetry/anomaly structure + duality-compatible readout

The twin helix is a proposed geometric generator of this structure. The structure itself is what must survive.

A.3 Higher Dimensional Algebra and Geometric Computational Field Theory

To our knowledge, no single algebraic framework presently captures computation in GCMs across the full symbolic–to–fluidic range. By this we mean a framework that simultaneously (a) composes systems under joins—both commuting and non-commuting, (b) handles local–to–global propagation through interfaces, and (c) couples continuous transport (flows/phases) with discrete readout. Lie groupoids (and stacky variants) currently provide the most serviceable language for local symmetry, defects, and gluing. However, a general categorical semantics that bridges a GCM's geometry with its computability is still lacking.

As one passes from discrete to fluidic regimes, finite combinatorial descriptions cease to capture the full process structure. Continuous phase, path-dependent transport, curvature, and deformation enlarge the space of admissible histories beyond what can be encoded by a finite transition algebra alone. Accordingly, we use "algebra" here in a programmatic sense: the aim is a compositional language in which discrete operations, continuous transport, non-abelian flow, and topological gluing appear as different regimes of the same process structure.

What is needed? A viable semantics for GCMs must be simultaneously symbolic and geometric: it must (a) compose discrete states and interfaces (information–theoretic layer), (b) transport phases and flows continuously (geometric layer), (c) express gluing along boundaries and track joins, and (d) specify how update laws transform the underlying geometry (chirality/orientation/topological data).

The key obstacle is nonlocal constraint propagation across helices: interface compatibility is not decided on a single patch, and path–dependence (holonomy) persists under coarse discretization. Global states are therefore not simple products of local states but solutions of descent/compatibility conditions

along the interface groupoid (as in section 4.1). Consequently, naive local linearization or discretization erases the very invariants that govern computation.

A workable mathematical language for GCMs must support four capabilities and tie each to a concrete compositional device.

(a) **Continuous transformation.** Represent smooth deformations (tube radius, phase, twist) and their flows.

(b) **Local-to-global behavior.** Track how interface–local updates assemble to global states and constraints.

(c) **Structural invariance and laws.** Express conservation and controlled change of chirality, orientation, and topological charges.

(d) **Rich morphism structure.** Compose fragments along boundaries; allow deformations as higher morphisms.

Definition A.2 (Minimal Compositional Spine for GCMs)**.** Let $\mathbb{G}$ be a symmetric monoidal double category of open GCMs, defined as follows:

- **Objects** (0-cells). Interfaces/boundary components equipped with the declared readout structure.
- **Horizontal 1-cells**. Open GCM fragments with specified input/output interfaces, i.e., gluable bordisms equipped with interface rules $\mathcal{I}$.
- **Vertical 1-cells**. Structure-preserving maps of interfaces (refinements, relabelings, or symmetry-compatible identifications).
- **2-cells**. Commuting squares of GCM data, interpreted as compatible deformations/flows/homotopies between fragments.
- **Monoidal product**. Disjoint union $\otimes$ (parallel composition), with horizontal composition given by gluing along matching interfaces.

Decorate $\mathbb{G}$ by a stack (or higher stack) $\mathcal{S}$ of local state objects on the site of open GCMs, valued in the geometric ambient category $\mathcal{E}_{\mathrm{GCM}}$. Thus, each open region U is assigned a local state object $\mathcal{S}(U)$ together with descent data along overlaps and interfaces. Dynamics consists of:

- **Pulses.** Distinguished endo-2-cells representing discrete update steps.
- **Flows.** Connections or transport laws on $\mathcal{S}$ representing continuous evolution.

The point of definition A.2 is to separate the *compositional skeleton* from the choice of local state model. The double-category structure records how GCM fragments glue and deform; the stack $\mathcal{S}$ records what state data live on those fragments. The minimal semantics above should be read as a workable core rather than a final synthesis. A fuller algebraic account of GCM behavior appears to radiate outward in several tightly related directions. We group by function:

Local-to-global semantics. The first extension concerns how local computational states glue into global geometric configurations. Here, the natural language is that of *stacks*, *descent*, and *higher gauge theory* [Lur11, BS06]. One should assign to each open set U a higher groupoid of local states and transports, then recover global configurations as descent data rather than as naive products of local coordinates. In this setting, the quotient or stack language is not merely a formal decoration. Passing to a coarse orbit space may identify gauge-equivalent representatives while forgetting residual automorphisms; these automorphisms can remain physically operative as higher, global, or non-invertible symmetries of gauge data [HK26]. Hence, when local computational states are glued, the relevant global object is not only a set of equivalence classes but a structured descent object retaining the symmetries by which those equivalences are realized. In the abelian/quasi-fluidic band, this collapses to familiar local systems (our $B/T/Z$-type readouts, torus phases, and integer charges), but in the fluidic and gauge regimes, the gluing problem becomes genuinely nonabelian: one must track connections, holonomies, and coherent homotopies of gauge data under refinement and recombination [SW13]. This is exactly the setting in which higher gauge theory becomes the minimal bookkeeping required for nonabelian transport, defect fusion, and feedback under gluing. From this perspective, global GCM states are not tuples of local values but *glued objects in a differential cohesive geometric semantics*.

Differential dynamics and update laws. The second extension concerns the internal mechanics of updates. Here *synthetic differential geometry*, *jet bundles*, and the *Cartan–Spencer formalism* [Koc06, Spe69] provide the natural language for finite-order control, prolongation, and integrability. Working internally to our differential cohesive ∞-topos allows vector fields, flows, infinitesimals, and differential modalities (e.g. $\int$, $\flat$, $\sharp$) to be treated as first-class objects rather than external analytic artifacts. In parallel, a future *bordism type theory* could package the same ideas proof-theoretically: types as stacks of decorated manifolds, terms as global sections or configured geometries, identity types as homotopies/deformations, and Π– and Σ–types as homotopy right/left Kan extensions along fibrations modeling parameterized families and gluing. Followed by a sequent calculus whose cut/elimination rules match horizontal/monoidal composition in the double category of open GCMs. Our aim is not to multiply formalisms for their own sake, but to isolate a setting in which update laws, prolongations, phase slips, and defect motion can be represented as executable geometric rules rather than described informally.

Observables, defects, and stable invariants. The third extension concerns observables in the genuinely higher regimes. Once one allows defects, interfaces, and nontrivial operator insertions, ordinary bundle language quickly becomes too coarse. Here *stratified topological field theory*, *factorization homology*, *K-theory*, and *noncommutative geometry* [Waa25, Con94, AF19] enter naturally. Stratified/extended TFT organizes computations by defect type and gluing pattern; factorization homology provides the corresponding local-to-global integration of observables; (possibly twisted) K-theory classifies stable sectors and conserved charges; and noncommutative geometry becomes relevant when quotienting by holonomy/gauge data destroys any useful ordinary space of states. In the abelian subtheories, these tools reduce to comparatively tame flux and phase bookkeeping, but in the fluidic/gauge band, they are the natural repositories of the data that survive after passing to moduli and quotienting by symmetry. In other words, once the geometry is sufficiently expressive, the correct outputs cease to be "numbers at points" and become stable invariants of operator-valued or defect-decorated structures.

Equivariant and Floer-type refinements. The final extension concerns the onset of genuinely equivariant and cohomological phenomena. Our base symmetry $V_4 \simeq C_2 \times C_2$ embeds in $O(2)$, but in the regimes sensitive to spinorial or orientation-reversing data one should lift along $\mathrm{Pin}(2) \to O(2)$; the corresponding preimage of V_4 is the quaternion group $Q_8 \subset \mathrm{Pin}(2) \subset SU(2)$. Thus, chirality and orientation reversal are not cosmetic labels but genuine equivariant structure, aligning the fluidic/gauge band with the Pin(2)-equivariant viewpoint that has become central in modern Floer theory, particularly in Manolescu's work [Man16]. Practically, the abelian/quasi-fluidic analysis still sees only the V_4 projection, while the higher gauge regime naturally asks for the Pin(2) lift. This is one reason that Floer-type and Donaldson-type refinements appear not as optional embellishments, but as the likely endpoint of any serious attempt to extract stable computational invariants from the highest regime.

Remark A.1. There are, of course, many further directions, but these four themes already indicate the scale of the task. A full algebraic description of GCM behavior likely requires a synthesis beyond the reach of any single mathematician—something closer to a coordinated language than a solitary breakthrough. Grothendieck famously spoke of a rising sea in which difficult problems might eventually be submerged and simplified. Yet when nature insists on phenomena such as quantum mechanics, sometimes no ocean is deep enough. To counter this, we may need to carve a new path, one with a river of flow.

Uses and abuses of GCFT. Geometric Computational Field Theory is intended primarily as a compositional and computational semantics for geometric field processes, rather than a replacement for established dynamical theories. Its natural domain consists of systems in which boundary conditions, defects, holonomy, conserved charges, and admissible gluing determine the information retained under physical evolution. The immediate objective is not to compute the full solution space of a Hamiltonian or field equation, but to organize its admissible histories into composable processes with invariant, physically interpretable readouts.

The most promising initial applications therefore lie in condensed matter, atomic physics, and topological media, where vortices, skyrmions, phase textures, and emergent gauge structures already admit experimentally accessible or mathematically controlled descriptions [BFG+94, NT13, LW05]. In these settings, GCFT could provide a formal language for defect transport, topological charge bookkeeping, interface composition, and the preservation or loss of information under coarse-graining. A subsequent objective is the treatment of nonperturbative gauge theories, where the BF/Yang–

Physical domain	Potential GCFT application	Research status
Superconductivity and superfluidity	Quantized vortices, phase slips, winding ledgers, defect transport, and flux conservation.	First benchmark
Magnetic textures and topological matter	Skyrmion charges, boundary modes, defect histories, and topological information transport.	Early application
Cold atoms and photonics	Controlled phase geometry, synthetic gauge fields, holonomy, and geometric readout.	Early application
Strongly correlated and topologically ordered matter	Emergent gauge sectors, extended excitations, string-net-like structures, and categorical classification of admissible processes.	Intermediate
Lattice gauge theory and constructive QFT	Non-abelian holonomy, Wilson observables, topological-sector tracking, and BF/YM composition.	Long-term target
Quantum gravity	Computational bordisms, geometric histories, emergent metric sectors, and nonperturbative spacetime reconstruction.	Foundational horizon

Table 14: Prospective applications of GCFT, ordered by the accessibility of initial benchmarks rather than their ultimate foundational significance.

Mills separation may provide a useful distinction between topological composition and metric-sensitive dynamics. Quantum gravity remains a longer-term foundational motivation rather than a prerequisite for these applications. Conversely, GCFT should *not* be mistaken for a numerical solver, a substitute for quantum field theory, or established derivations of quantum mechanics, particle spectra, or spacetime dynamics. Its utility will be demonstrated through explicit models, well-defined composition laws, and reproducible physical readouts.

A.4 Topological Kleene Field Theories and Computational Geometric Bordisms

Gonzales, Peralta, and Miranda [GPMPS25] have recently introduced *Topological Kleene Field Theory* (TKFT) as a smooth-topological realization of classical computability. In this field theory, computation is encoded by a *dynamical bordism*: a manifold with boundary equipped with a suitably well-behaved vector field, together with embeddings of discrete input and output data into distinguished boundary components. The associated reaching map recovers a partial recursive function. In this sense, TKFT should be read as a model of computability in the Kleene–Turing sense, not merely as an analogy with it.

What is especially relevant for the present work is that, in TKFT, the topology of the bordism is not ornamental. Branching and iteration are reflected in the topology of the underlying manifold: pair-of-pants type decompositions model conditional branching, while nontrivial handles encode iterative or looping behavior. TKFT, therefore, offers a precise way to view program structure through smooth topology and dynamical flow.

Our use of bordism is related, but conceptually distinct. In TKFT, the bordism is primarily the ambient geometric stage through which a computation is routed between designated boundary components. In GCT, by contrast, the computational content is intended to be carried more intrinsically by the decorated geometry itself: by the manifold, its local interfaces, its admissible deformations, and the algebraic or gauge-theoretic structures placed upon it. This motivates the following definition.

Definition A.3 (Computational Geometric Bordism)**.** Let $\mathcal{S}$ be a class of computational structures on smooth manifolds (for example, principal G-bundles with connection, decoration functors, or other geometric state data). An n-dimensional GCM is a pair (M, σ), where M is an oriented smooth n-manifold, possibly with boundary, and $\sigma \in \mathcal{S}(M)$.

A *computational geometric bordism* from (M_0, σ_0) to (M_1, σ_1) is a compact oriented smooth $(n+1)$-manifold W with boundary, equipped with a collar-preserving identification

$$\partial W \;\cong\; \overline{M_0} \;\sqcup\; M_1,$$

together with a structure $\Sigma \in \mathcal{S}(W)$ whose restrictions along the collars recover the endpoint data:

$$\Sigma|_{M_0} = \sigma_0, \qquad \Sigma|_{M_1} = \sigma_1.$$

Two such bordisms are regarded as equivalent if they are related by a boundary-fixing diffeomorphism together with an isomorphism in $\mathcal{S}$.

Example A.1 (A Helical Cylinder as Bordism). Let

$$C := S^1 \times I, \qquad I = [0,1],$$

so that

$$\partial C = S^1 \times \{0\} \sqcup S^1 \times \{1\}.$$

For any fixed parameter $\lambda \in \mathbb{R}$, the map

$$F_\lambda(\theta, t) = \big(\cos(\theta + \lambda t),\ \sin(\theta + \lambda t),\ t\big), \qquad (\theta, t) \in S^1 \times I,$$

is an embedding into $\mathbb{R}^3$. Its image is a helically twisted cylinder joining two copies of S^1. Thus, the underlying bordism is still the cylinder $S^1 \times I$, but now equipped with an explicitly chiral geometric realization. In the present setting, the point is not that the bordism class changes, but that the geometric structure carried by the bordism can itself become computationally meaningful.

TKFT provides a smooth-topological language in which dynamical bordisms may organize classical computable functions; GCT seeks a more intrinsic implementation in which computational state is carried directly by decorated geometry. The two frameworks should therefore be viewed as complementary rather than competing. Heuristically, one may prototype a computation in the TKFT setting and then seek a geometric implementation of the same computational content within a GCFT, where the relevant data are borne by the manifold itself rather than by an external symbolic encoding alone.

Decategorification and Kleene recursion. The role of classical computability in the present framework is best expressed indirectly. Rather than rebuilding Kleene recursion as an autonomous layer, we place it inside TKFT, and then regard TKFT itself as a decategorified shadow of GCT.

The point is structural. TKFT already shows that smooth dynamical bordisms can realize classical partial recursive computation. What GCT adds is not a different notion of classical computability, but a richer one, geometric semantics in which the computational content is carried intrinsically by decorated geometry: interfaces, local symmetries, holonomy, gauge data, and higher compositional structure.

From computational bordisms to their shadow. Let

$$\mathbf{CGBrd}$$

denote the geometric bordism category whose objects are decorated computational states

$$(M, \sigma),$$

with M a smooth manifold (possibly with boundary) and σ the geometric computational structure carried by M (for example, interface data, bundle data, connection data, chirality/orientation labels, or local state decorations). Morphisms are computational geometric bordisms

$$(W, \Sigma) : (M_0, \sigma_0) \to (M_1, \sigma_1),$$

composed by gluing.

Let

$$\mathbf{TKFT}$$

denote the bordism category underlying topological Kleene field theory, in which one remembers only the smooth bordism together with the dynamical data needed to define the associated reaching map.

We define the *TKFT shadow functor*

$$\mathsf{Sh} : \mathbf{CGBrd} \longrightarrow \mathbf{TKFT}$$

by forgetting all geometric data not visible at the level of the TKFT reaching map. Concretely, Sh retains the underlying manifold with boundary, the input/output boundary components, the ambient dynamical flow needed to define the induced computation and discards, or passes to π_0, local gauge or bundle structure, holonomy and curvature data, defect and higher-form labels, nontrivial interface groupoid structure, distinctions visible only up to higher homotopy or higher representation data.

In this sense, Sh is a *decategorification*: it passes from decorated geometric computation to the smooth-topological computation visible at the TKFT level.

Definition A.4 (TKFT-shadow Equivalence)**.** Two geometric computational bordisms

$$(W, \Sigma),\ (W', \Sigma')$$

are said to have the same TKFT shadow if

$$\mathsf{Sh}(W, \Sigma) \cong \mathsf{Sh}(W', \Sigma')$$

in **TKFT**. Equivalently, they induce the same underlying dynamical bordism computation after all higher geometric decoration invisible to TKFT has been forgotten.

Proposition A.3 (TKFT as Symbolic Boundary of GCT)**.** *Every TKFT computation is realized by a geometric computational bordism whose additional decorations are trivial, abelianized, or otherwise invisible under the shadow functor* Sh*. Hence, TKFT embeds as the decategorified symbolic boundary of GCT.*

Proof sketch. A TKFT computation is given by a smooth bordism equipped with a sufficiently well-behaved vector field and designated input/output embeddings. This data can be regarded as a special case of a geometric computational bordism by equipping the same manifold with only the minimal decoration needed to recover that flow. Applying Sh then returns the original TKFT object. Thus, TKFT appears as the image of the minimally decorated sector of GCT. □

Proposition A.4 (Strict Enrichment Beyond TKFT)**.** *The shadow functor* Sh *is not faithful in general. Distinct GCT computations may determine the same TKFT computation after decategorification.*

Reason. TKFT is insensitive to geometric data that do not alter the reaching map at the level of the underlying dynamical bordism. In particular, nonabelian holonomy, gauge-equivalent but computationally distinct decorations, higher defect data, and order-sensitive interface composition may all survive in GCT while disappearing under Sh. □

What GCT adds. The excess of GCT over TKFT is precisely the part of the computation carried by decorated geometry rather than by the underlying smooth dynamical bordism alone.

Corollary A.5 (Containment of Classical Computability)**.** *Since TKFT recovers partial recursive computation, and since TKFT lies in the image of the shadow functor*

$$\mathsf{Sh} : \mathbf{CGBrd} \to \mathbf{TKFT},$$

classical Kleene computability is contained in GCT as a special case.

In this way, the classical recursion-theoretic layer no longer needs to be treated as a separate foundation for the theory. It appears automatically as the symbolic decategorified boundary of geometric computation. The genuine novelty of GCT begins exactly where the shadow functor ceases to be injective: namely, where geometric decoration, gauge structure, and higher composition contribute computational content that TKFT cannot see.

A.5 Reversible Computing and Gauge Processes

Reversible computation provides a natural point of contact between classical computation and the geometric process semantics developed in this paper. In the discrete setting, a reversible computational step is a bijection of configurations. Bennett showed that irreversible computations may be embedded into reversible ones by retaining sufficient history information [Ben73], while Fredkin–Toffoli gates provide familiar universal reversible primitives [FT82]; see also [Mor17] for a modern treatment.

In continuous physics, the corresponding notion is not a particular gate set but invertibility of evolution. A well-posed Hamiltonian flow on a symplectic phase space consists of symplectomorphisms

$$\phi_t : M \longrightarrow M, \qquad \phi_{t+s} = \phi_t \circ \phi_s, \qquad \phi_{-t} = \phi_t^{-1},$$

while closed quantum evolution is implemented by a unitary family

$$U_t = e^{-itH}, \qquad U_{-t} = U_t^{\dagger}.$$

GCT does not identify these examples with one another. Their common feature is that the fine-grained evolution admits an inverse.

The reversible core of geometric computation. Let

$$\mathcal{C}_{\mathrm{GCT}}$$

denote schematically a category, groupoid, or higher category whose objects are admissible geometric computational states and whose morphisms are admissible processes. Its *core*

$$\mathcal{C}_{\mathrm{GCT}}^{\simeq} \hookrightarrow \mathcal{C}_{\mathrm{GCT}}$$

is the wide subcategory containing all objects and only the invertible morphisms.

This reversible core appears differently in the computational regimes considered above. In the symbolic regime it contains permutations of the microscopic geobit state space. In the quasi-fluidic regime, gauge transformations and parallel transports are invertible even when an effective dynamical realization also contains dissipative relaxation. In the non-abelian regime, ordered transports remain invertible while their composition becomes history-sensitive. Thus reversibility is not identified with commutativity, simplicity, or absence of computational structure.

The distinction is important because the full GCT process category need not be a groupoid. Threshold events, coarse-grainings, dissipative effective dynamics, boundary updates, and later field-theoretic effects may be represented by noninvertible morphisms. The claim is therefore not that every GCM evolution is reversible, but that the theory contains a natural reversible transport sector whose relation to noninvertible readout and effective dynamics can be stated explicitly.

Gauge transport: reversibility without commutativity. Let $P \to M$ be a principal G-bundle equipped with connection A. Parallel transport along a path γ determines

$$U_\gamma = \mathcal{P} \exp\left(\int_\gamma A\right) \in G.$$

For the oppositely oriented path γ^{-1},

$$U_{\gamma^{-1}} = U_\gamma^{-1}.$$

Thus transport itself is invertible.

In an abelian $U(1)$ regime one additionally has

$$U_{\gamma_2} U_{\gamma_1} = U_{\gamma_1} U_{\gamma_2},$$

so reversible transport may be summarized by an additive phase ledger. In a non-abelian regime,

$$U_{\gamma_2} U_{\gamma_1} \neq U_{\gamma_1} U_{\gamma_2}$$

in general, even though each factor possesses an inverse. Reversibility therefore survives the transition into order-sensitive computation. What is gained is not information destruction but an intrinsic memory of composition order.

This gives a useful distinction within the Algebra of Flow:

$$\text{reversible} \quad \not\Longrightarrow \quad \text{commutative.}$$

A process can preserve its complete microscopic information while nevertheless acquiring nontrivial holonomy, path dependence, and history-sensitive computational semantics.

Readout and effective irreversibility. The more characteristic GCT issue arises when an invertible microscopic process is viewed through a non-injective readout. Let

$$U : X \longrightarrow X$$

be a bijective microscopic update and let

$$\rho : X \longrightarrow B$$

be a chosen observable map. Define the observational equivalence relation

$$x \sim_\rho y \qquad \Longleftrightarrow \qquad \rho(x) = \rho(y).$$

The microscopic dynamics need not induce a closed dynamics on the observable alphabet B. For such an induced update

$$\overline{U} : B \longrightarrow B$$

to exist, observationally indistinguishable states must remain observationally indistinguishable after applying U.

Proposition A.6 (Reversible Descent Criterion)**.** *Let $U : X \to X$ be a bijection and $\rho : X \to B$ a surjective readout map.*

The microscopic update U descends to a well-defined map

$$\overline{U} : B \longrightarrow B$$

satisfying

$$\rho \circ U = \overline{U} \circ \rho$$

if and only if

$$x \sim_\rho y \quad \Longrightarrow \quad U(x) \sim_\rho U(y).$$

The induced map $\overline{U}$ is itself reversible if and only if the observational equivalence relation is preserved in both directions:

$$x \sim_\rho y \quad \Longleftrightarrow \quad U(x) \sim_\rho U(y).$$

Proof. If $\overline{U}$ exists and $x \sim_\rho y$, then

$$\rho(Ux) = \overline{U}(\rho(x)) = \overline{U}(\rho(y)) = \rho(Uy),$$

so $Ux \sim_\rho Uy$.

Conversely, suppose U preserves the equivalence relation. Define

$$\overline{U}(\rho(x)) := \rho(Ux).$$

The assumed implication makes this independent of the representative x, so $\overline{U}$ is well defined.

Finally, $\overline{U}$ is invertible precisely when the same construction applies to U^{-1}, which is equivalent to preservation of $\sim_\rho$ in both directions. □

This proposition separates microscopic reversibility from observable reversibility. Even when U is perfectly invertible, three cases are possible:

(a) U preserves the readout fibers in both directions, so the observable dynamics is itself reversible;

(b) U preserves the fibers only in the forward direction, so an observable dynamics exists but need not retain the full reversible structure;

(c) U fails to preserve the fibers, so no autonomous update on the chosen observable alphabet exists at all.

For a *finite* observable alphabet B, the second case cannot occur when U is a bijection of the entire microscopic state space and ρ is surjective: any descended $\overline{U}$ is surjective, hence bijective. The forward-only possibility is relevant for infinite readout spaces or for a proper forward-admissible sampled domain on which the restricted dynamics need not be surjective, as in definition 3.4.

The third case is particularly important for geometric computation. Two microscopic configurations may initially produce the same geobit readout while carrying hidden geometric information that later affects their evolution. The coarse state then fails to be dynamically closed: predicting its future requires restoring information discarded by the readout.

For example, the relational twin helix readout

$$\rho_{\mathrm{rel}} : C_2^4 \longrightarrow C_2^2$$

forgets the absolute chirality and orientation labels of the two unit helices while retaining only their relative values. A microscopic update on C_2^4 induces a genuine four-state dynamics on the THM_4 readout only when it respects the fibers of ρ_{rel}. Otherwise, two configurations represented by the same

visible THM_4 state may evolve to different visible outputs. The information was not destroyed by the microscopic update; it had already been omitted by the chosen description.

Thus,

$$\text{microscopic reversibility} \not\Longrightarrow \text{reversible readout dynamics.}$$

This is the reversible-computation counterpart of the distinction made throughout the paper between microscopic state, gauge redundancy, and observable quotient.

Reversibility and computational bordisms. A second distinction becomes necessary in GCFT. Let

$$W : Y_0 \longrightarrow Y_1$$

be a decorated computational bordism. Reversing its orientation gives an opposite bordism

$$\overline{W} : Y_1 \longrightarrow Y_0.$$

This operation should not be confused with taking a categorical inverse. In general,

$$\overline{W} \circ W \not\simeq \mathrm{id}_{Y_0}, \qquad W \circ \overline{W} \not\simeq \mathrm{id}_{Y_1}.$$

The composite may contain nontrivial topology, defects, gauge data, or other internal structure and need not reduce to a cylinder.

Accordingly, the existence of duals in a bordism category is weaker than invertibility of its morphisms. The Cobordism Hypothesis is organized around *dualizability*, not around the assertion that every bordism is reversible. This distinction is essential for GCFT, whose general process semantics must accommodate topology change, defect creation, gluing, and other processes lying outside the reversible core.

One should therefore distinguish path reversal from process duality or categorical inversion. For gauge transport along a fixed path, reversal supplies an inverse. For a general geometric history, reversing its orientation supplies a dual history but not necessarily an inverse computation.

Effective irreversibility in GCFT. The resulting architecture separates several levels that are often collapsed into the single word "irreversibility." At the fine-grained level, geometric transport may lie inside $\mathcal{C}^{\simeq}_{\mathrm{GCT}}$. At the effective level, one may introduce dissipative relaxation, thresholding, or coarse-grained evolution. At the observational level, a many-to-one readout

$$\rho : X \longrightarrow B$$

forgets distinctions present in the microscopic state. At the field-theoretic level, measurement, renormalization, boundary restriction, and other effects may likewise be represented by maps that are not invertible on the chosen semantic target.

This viewpoint is compatible with the quasi-fluidic normal forms used earlier. Their gradient-flow dynamics are intentionally dissipative and are not claimed to belong to the reversible core. They provide stable effective realizations of the abelian computational corridor. The underlying gauge transport, by contrast, remains invertible. GCT therefore does not require every level of description to possess the same reversibility structure.

The principal lesson is that reversibility is a property of a *specified process at a specified level of description*. A microscopic geometric computation may be reversible while its observable quotient is irreversible; an order-sensitive non-abelian transport may be reversible without being commutative; and a GCFT bordism may possess a natural opposite without being an invertible morphism.

Reversible computation in GCT is therefore not merely the importation of classical reversible gate theory into geometry. It is the study of how invertible geometric transport sits inside a larger process category, and of how coarse-graining, readout, gluing, and field-theoretic effects modify or destroy that invertibility.

A.6 Parallel Composition and Geometric E_∞-Structure

A particular issue concerns the composition of several GCM components. The paper repeatedly uses two different forms of composition that should be distinguished.

Processes compose *serially* through matched interfaces or boundary data. Such composition may be order-sensitive and, in the non-abelian regime, may carry noncommuting holonomy. Independent

subsystems, however, may also be assembled *in parallel*. In that case there is no preferred ordering of the components themselves. Swapping or regrouping two independent components should not alter the resulting composite system except through the appropriate coherent equivalence.

This parallel structure admits a natural E_∞-description.

Definition A.5 (Geometric E_∞-Algebra of Parallel GCM States)**.** Let $\mathcal{H}$ be an ∞-topos of smooth spaces or stacks, equipped with its Cartesian symmetric monoidal structure, and let

$$X \in \mathcal{H}$$

denote the moduli object of admissible states of a single GCM component.

Define its finite symmetric configuration object by

$$\mathrm{Sym}(X) := \coprod_{n \geq 0} \left(X^{\times n}\right)_{h\Sigma_n},$$

where $(-)_{h\Sigma_n}$ denotes the homotopy quotient by permutation of the n independent components.

For $m, n \geq 0$, juxtaposition of finite configurations induces maps

$$\mu_{m,n} : \left(X^{\times m}\right)_{h\Sigma_m} \times \left(X^{\times n}\right)_{h\Sigma_n} \longrightarrow \left(X^{\times (m+n)}\right)_{h\Sigma_{m+n}}.$$

Together with the empty configuration

$$\mu_0 : * \longrightarrow \mathrm{Sym}(X),$$

these operations define a coherently associative and commutative multiplication. Hence

$$\mathrm{Sym}(X)$$

is a commutative monoid object, equivalently an E_∞-algebra object, in the chosen smooth ∞-categorical setting [Lur17]. We call $\mathrm{Sym}(X)$ the *geometric E_∞-algebra of parallel GCM states*.

The definition concerns *independent parallel composition*. It does not assert that the full process algebra of a GCM is commutative. Indeed, the same geometric theory may simultaneously possess

$$\text{coherently commutative parallel composition}$$

and

$$\text{noncommutative ordered transport.}$$

The distinction is analogous to the familiar separation between a symmetric monoidal product of independent systems and the generally noncommuting operators acting within each system.

Thus, if

$$x_1, x_2 \in X$$

represent independent GCM components, their unordered parallel configuration determines a point of

$$(X \times X)_{h\Sigma_2} \subset \mathrm{Sym}(X).$$

By contrast, if

$$U_{\gamma_1}, \qquad U_{\gamma_2}$$

are non-abelian transports internal to a component, one may have

$$U_{\gamma_2} U_{\gamma_1} \neq U_{\gamma_1} U_{\gamma_2}.$$

The E_∞-structure organizes the former operation and places no commutativity requirement on the latter.

Independent geometric computational systems admit symmetric monoidal composition, while boundary-to-boundary histories compose through gluing and gauge transport records ordered internal evolution. The E_∞-algebra therefore captures one layer of the higher compositional structure of the theory rather than the whole of its dynamics.

A.7 Comparison with Real and Quantum Computation

The Blum–Shub–Smale (BSS) model [BSS89] provides a natural comparison point for continuous computation. A BSS machine replaces the discrete registers of an ordinary register machine by elements of a field such as $\mathbb{R}$, and permits exact field operations together with algebraic branching tests. In this way, the model develops a theory of computability and complexity directly over continuous numerical domains rather than first encoding them into strings or natural numbers.

GCT shares with BSS the refusal to identify computation exclusively with a discrete alphabet, but the two frameworks enlarge classical computation in different directions. BSS retains an essentially algebraic machine semantics while changing the domain on which that machine operates. GCT instead changes the operational substrate itself: states are geometric configurations, processes are admissible deformations or transports, composition is implemented through interfaces and gluing, and outputs are specified by geometric or gauge-invariant readouts.

Schematically,

$$\begin{aligned} \text{BSS}: &\quad \text{continuous numerical registers} + \text{exact algebraic operations}, \\ \text{GCT}: &\quad \text{geometric state space} + \text{admissible processes} + \text{structured readout}. \end{aligned}$$

The comparison is therefore contextual rather than reductive: GCT is not obtained by replacing the BSS registers with manifolds, and the BSS model is not asserted to be a special case of GCFT.

Continuous state does not imply an exact-real oracle. This distinction is especially important in the continuous regimes. The appearance of smooth configuration spaces, compact phases, connections, or moduli does not imply that a physical GCM is granted unit-cost access to an arbitrary exact real number. Continuous state belongs to the geometry of the substrate; computational access is determined separately by the allowed preparations, controls, transformations, and readouts.

For example, the quasi-fluidic regime may contain a phase

$$\theta \in S^1$$

whose evolution is continuous, while the operational information retained from that phase may consist only of a finite partition, a winding number, a phase difference, or another invariant readout. Likewise, a smooth differential evolution may explore an infinite-dimensional solution or configuration space even though only a small family of boundary and observable data participates in the computation.

This is the same separation used in the "computation by structure" viewpoint developed in section 3.1. The cardinality of the underlying state space therefore does not by itself determine the computational power of the physical device. What matters is which portions of that space are reachable, how they may be composed, and which distinctions can be operationally extracted.

In this respect, BSS and GCT ask complementary questions. BSS studies what changes when exact continuous quantities are admitted as primitive computational values. GCT asks how a continuous physical substrate can acquire computational semantics without identifying its complete geometric state with an exact numerical register. The BSS model shows that continuous domains can support a rigorous theory of computation without reducing every value to a discrete symbol. GCT accepts this lesson but relocates the primitive computational structure from exact field arithmetic to geometric reachability, composition, and readout.

Quantum computation and geometric transport. Quantum computation provides a second, distinct comparison. Deutsch's universal quantum computer [Deu85] and the standard circuit model [NC10] formulate computation through states in complex Hilbert spaces, unitary transformations, tensor-product composition, and probabilistic measurement. Unlike BSS computation, the continuous quantities appearing in quantum amplitudes are not arbitrary exact-real registers equipped with unit-cost arithmetic. Their computational role is constrained by coherent evolution, interference, entanglement, and physically admissible preparation and measurement.

The relationship to geometry becomes more explicit in holonomic quantum computation (HQC). Zanardi and Rasetti [ZR99] showed that adiabatic loops in a manifold of classical control parameters can induce non-Abelian geometric holonomies on degenerate quantum eigenspaces, thereby implementing computational gates. With a suitable connection A, the resulting transport takes the form

$$U_\gamma = \mathcal{P} \exp\left(- \oint_\gamma A \right).$$

Separately, Nielsen and collaborators [NDGD06] related quantum circuit synthesis to shortest paths in a penalty-weighted Riemannian geometry on the unitary group, connecting computational gate complexity to geometric distance.

These approaches establish that geometric paths, connections, and transport can play operational roles in quantum computation. Their explanatory direction nevertheless differs from that of GCT: conventional quantum computation assumes the quantum state space and its unitary semantics, while HQC and geometric circuit synthesis exploit additional structures within that framework. GCT instead investigates whether suitable state spaces, transport laws, and computational readouts can arise from the geometry of a more primitive substrate. The present construction does not claim to derive quantum Hilbert-space composition, universal quantum gates, Born probabilities, or the complexity class BQP. Its relationship to quantum computation is therefore a structural comparison and a prospective reconstruction problem, not an established equivalence.

A.8 Fourier Mode Calculations

We examine how rotational symmetry constrains the angular degrees of freedom available to a helical cross-section and to the continuous fields carried by it. These are kinematic selection rules: they determine which geometric modes and couplings are admissible under a prescribed symmetry, without by themselves establishing a corresponding increase in computational expressive power.

Cross-sectional shape modes. Consider a smooth, star-shaped cross-section represented in polar coordinates by

$$\Gamma_r(\theta) = r(\theta) \begin{pmatrix} \cos\theta \\ \sin\theta \end{pmatrix}, \qquad r(\theta) > 0.$$

Its radial profile admits the Fourier expansion

$$r(\theta) = a_0 + \sum_{k=1}^{\infty} \left(a_k \cos(k\theta) + b_k \sin(k\theta) \right).$$

Suppose the cross-section is invariant under a rotation of order n, so that

$$r\left(\theta + \frac{2\pi}{n}\right) = r(\theta).$$

Fourier orthogonality then requires

$$a_k = b_k = 0 \qquad \text{whenever } n \nmid k.$$

Consequently, the admissible profile has the form

$$r(\theta) = a_0 + \sum_{m=1}^{\infty} \left(a_{nm} \cos(nm\theta) + b_{nm} \sin(nm\theta) \right).$$

For a fixed angular cutoff K, let

$$\mathcal{F}_K = \operatorname{span}_{\mathbb{R}} \{1, \cos(k\theta), \sin(k\theta) \mid 1 \le k \le K\}.$$

Then

$$\dim \mathcal{F}_K = 2K + 1.$$

Its C_n-invariant subspace has dimension

$$\dim \mathcal{F}_{n,K} = 2 \left\lfloor \frac{K}{n} \right\rfloor + 1.$$

We therefore define the relative angular-mode fraction

$$E_K(n) := \frac{\dim \mathcal{F}_{n,K}}{\dim \mathcal{F}_K} = \frac{2\lfloor K/n \rfloor + 1}{2K + 1}.$$

For example, when $K = 8$ and $n = 4$, the permitted angular frequencies are

$$k = 0, \pm 4, \pm 8,$$

so

$$E_8(4) = \frac{5}{17}.$$

For fixed K, the mode fraction is nonincreasing with n, and

$$E_K(n) = \frac{1}{2K+1} \qquad \text{whenever } n > K.$$

Thus,

$$\lim_{n\to\infty} E_K(n) = \frac{1}{2K+1},$$

rather than zero: the angular zero mode survives.

For fixed finite n, however,

$$\lim_{K\to\infty} E_K(n) = \frac{1}{n}.$$

Accordingly, a finite rotational symmetry restricts the permitted harmonics without making the unrestricted smooth shape space finite-dimensional.

Full continuous rotational symmetry imposes the stronger condition

$$r(\theta+\varphi) = r(\theta) \qquad \text{for every } \varphi \in S^1.$$

It follows that

$$r(\theta) = a_0,$$

so the cross-sectional contour is circular.

Hence the transition from a fully rotationally symmetric cross-section to a general smooth cross-section releases infinitely many independent angular shape parameters. The finite-cutoff formula $E_K(n)$ quantifies this restriction at a chosen resolution.

Angular modes of continuous flow. A related calculation applies to continuous fields defined on a circular reference cross-section.

Let

$$\mathbf{v}(r,\theta) = v_r(r,\theta)\,\mathbf{e}_r + v_\theta(r,\theta)\,\mathbf{e}_\theta$$

be a smooth planar vector field, expressed in the rotating polar basis.

Its scalar components admit expansions

$$v_r(r,\theta) = \sum_{k\in\mathbb{Z}} a_k(r) e^{ik\theta},$$

and

$$v_\theta(r,\theta) = \sum_{k\in\mathbb{Z}} b_k(r) e^{ik\theta},$$

with the usual conjugate-symmetry conditions ensuring that the velocity field is real.

Rotational equivariance of order n requires

$$\mathbf{v}(R_{2\pi/n}x) = R_{2\pi/n}\mathbf{v}(x).$$

Because the polar basis itself rotates covariantly, this is equivalent to

$$v_r\left(r,\theta+\frac{2\pi}{n}\right) = v_r(r,\theta),$$

and

$$v_\theta\left(r,\theta+\frac{2\pi}{n}\right) = v_\theta(r,\theta).$$

It follows that

$$a_k(r) = b_k(r) = 0 \qquad \text{for } k \notin n\mathbb{Z}.$$

Thus the flow components admit only the angular harmonics

$$k = 0, \pm n, \pm 2n, \ldots.$$

If the flow is additionally incompressible, then

$$\nabla \cdot \mathbf{v} = \frac{1}{r}\frac{\partial (r v_r)}{\partial r} + \frac{1}{r}\frac{\partial v_\theta}{\partial \theta} = 0.$$

Substitution of the Fourier expansions gives, for each angular frequency k,

$$\frac{d}{dr}\big(r a_k(r)\big) + ik\, b_k(r) = 0.$$

Hence incompressibility imposes a differential relation between the radial coefficient functions within each permitted angular sector. The number of angular sectors therefore must not be confused with the number of independent degrees of freedom of an incompressible velocity field.

Under full rotational equivariance, only $k = 0$ survives:

$$v_r = v_r(r), \qquad v_\theta = v_\theta(r).$$

Incompressibility then gives

$$\frac{d}{dr}\big(r v_r(r)\big) = 0,$$

and therefore

$$v_r(r) = \frac{C}{r}.$$

On a disk containing the origin, smoothness requires $C = 0$. Nevertheless, nontrivial azimuthal flow $v_\theta(r)$ may remain. For instance,

$$\mathbf{v}(r, \theta) = \Omega r\, \mathbf{e}_\theta$$

is a smooth, incompressible, rotationally equivariant solid-body rotation.

Thus full rotational symmetry eliminates nonzero angular harmonics, but does not force a continuous flow to be uniform or dynamically trivial.

Mode coupling and symmetry breaking. The preceding calculations can be extended from permitted modes to permitted interactions between modes.

Let L be a linearized transport or coupling operator acting on angular fields. Suppose L commutes with the action of C_n. Then the angular function space decomposes into invariant sectors classified by angular momentum modulo n.

A simple example is an angular coupling profile $w(\theta)$ acting by multiplication:

$$(M_w f)(\theta) = w(\theta) f(\theta).$$

Write

$$w(\theta) = \sum_{q \in \mathbb{Z}} w_q e^{iq\theta}.$$

In the Fourier basis, its matrix elements satisfy

$$\left\langle e^{im\theta}, M_w e^{im'\theta} \right\rangle = w_{m-m'},$$

where the inner product is normalized over S^1.

If w is C_n-invariant, then

$$w_q = 0 \qquad \text{unless } q \in n\mathbb{Z}.$$

Consequently,

$$\left\langle e^{im\theta}, M_w e^{im'\theta} \right\rangle = 0 \qquad \text{unless } m \equiv m' \pmod{n}.$$

The coupling operator therefore preserves the angular-momentum classes modulo n. Breaking the C_n symmetry permits additional Fourier coefficients w_q, and consequently additional off-diagonal couplings between angular sectors. This is the precise sense in which cross-sectional anisotropy can enlarge the family of admissible transport channels.

The selection rule does not imply that transport operators within an invariant sector commute. If a sector contains multiple internal states, the corresponding operator blocks may be matrix-valued and noncommuting. Whether these blocks generate non-abelian holonomy depends on the realized connection and admissible control operations, not on the Fourier decomposition alone.

Interpretation for geometric computation. These calculations establish a distinction between the symmetry of the geometric carrier and the algebra of its transport. Continuous rotational symmetry strongly restricts the angular shape of a helical cross-section. Finite residual symmetry permits additional modes subject to harmonic selection rules, while removal of rotational constraints admits the full infinite-dimensional family of smooth angular profiles. The resulting geometric freedom supplies potential degrees of control: anisotropies, deformations, coupled angular channels, and changes in the internal geometry of the helical cell. It does not follow that every newly admitted shape implements a distinct computational operation, or that symmetry breaking automatically produces non-abelian gauge dynamics. The latter requires an internal representation and connection whose realized holonomies fail to commute, as examined in section 4.2.

A.9 Disclaimers

Regarding Scope and Fundamental Assumptions

This paper does not challenge the empirical validity of quantum field theory, Quantum Chromodynamics, Yang-Mills theory, or the Standard Model. Its purpose is instead to investigate whether some of the geometric and computational structures underlying gauge theory can be reformulated in terms of prequantum geometry. Our work here is best viewed as a candidate semantics for organizing known physical structures, rather than as a competing phenomenological theory.

Glossary and Scope of Terminology

To avoid ambiguity, we distinguish two related but non-identical layers of the present program.

(a) **Geometric Computability Theory (GCT).** The broad research program concerns computation realized through geometric, topological, and gauge-theoretic structures, as well as the logical, complexity-theoretic, and physical consequences of such realizations. In this sense, GCT is the umbrella field of study more concerned with pure mathematics. It includes, for example, the classification of computational regimes, the role of helicoidal substrates, the EVT hypothesis, and *possible* future connections to number theory/arithmetic geometry (e.g., Berry-Keating).

(b) **Geometric Computational Field Theory (GCFT).** The constructive (total) formalism (4.5) developed within GCT, in which geometric histories are interpreted as composable computational processes. In a GCFT, boundaries carry typed state data, gluing corresponds to evaluation or composition, gauge equivalence is handled at the level of observable output, and physical observables arise as gauge-invariant, coarse-grained results of computation. GCFT is thus the most structured and formal layer of the program: it is to GCT what a functorial field theory is to the broader study of field-theoretic phenomena.

Author's Note on Naming Conventions

If the twin helix manifold (THM) described here ultimately proves to be of lasting foundational significance, the author would prefer that it not be given an eponymous name. This preference is not intended as a rejection of historical naming conventions. Still, it reflects the view that *geometric* objects of genuinely fundamental scope are often better served by descriptive terminology that emphasizes mathematical content rather than personal attribution. This is in contrast to *theorems*, *conjectures/hypotheses*, and *lemmas*, which would be more appropriate.

Still, the emphasis of this paper is therefore not on personal legacy, but on the development of Geometric Computability Theory and its possible mathematical, physical, and pedagogical consequences. The work is written from the perspective of the computational sciences, and readers are encouraged to interpret its terminology in that spirit. Likewise, the author must disclose that he is not a classically trained physicist, and as such, it would be inappropriate to identify him in this manner. The best term of description for the author would be "physical mathematician and/or computer scientist" [Moo14].

Funding Sources

None.

Conflicts of Interest

None.

Data Availability

There is no associated data with this manuscript.

AI Contributions and Acknowledgments

Google Gemini and OpenAI ChatGPT were used as research and writing assistants during the development of this work. Their use included assistance with literature navigation, mathematical and conceptual discussion, checking and refining formulations, editorial revision, LaTeX typesetting, exploratory experimental design, and the generation of GAP and Sage code for THM models and geobit state spaces.

The author directed the research program, determined which suggestions and formulations were incorporated, and assumes full responsibility for the mathematical claims, interpretations, errors, and conclusions presented in this manuscript.

References

[AB59] Yakir Aharonov and David Bohm. Significance of electromagnetic potentials in the quantum theory. *Physical Review*, 115(3):485–491, 1959.

[AB24] Mohammed Abouzaid and Andrew J. Blumberg. Foundation of floer homotopy theory i: Flow categories. *arXiv preprint arXiv:2404.03193*, 2024.

[ABV$^+$05] Juan A. Acebrón, Luis L. Bonilla, Conrad J. Pérez Vicente, Félix Ritort, and Renato Spigler. The kuramoto model: A simple paradigm for synchronization phenomena. *Reviews of Modern Physics*, 77(1):137–185, 2005.

[Ada09] Toshiaki Adachi. Foliation on the moduli space of helices on a real space form. *International Mathematical Forum*, 4(35):1699–1707, 2009.

[ADHM78] Michael F. Atiyah, Vladimir G. Drinfeld, Nigel J. Hitchin, and Yuri I. Manin. Construction of instantons. *Physics Letters A*, 65(3):185–187, 1978.

[AF19] David Ayala and John Francis. A factorization homology primer. *arXiv preprint*, 2019. arXiv:1903.10961.

[AGM93] Paul S. Aspinwall, Brian R. Greene, and David R. Morrison. Multiple mirror manifolds and topology change in string theory. *Physics Letters B*, 303:249–259, 1993.

[AGM94] Paul S. Aspinwall, Brian R. Greene, and David R. Morrison. Calabi–yau moduli space, mirror manifolds and spacetime topology change in string theory. *Nuclear Physics B*, 416:414–480, 1994.

[AHT14] Nima Arkani-Hamed and Jaroslav Trnka. The amplituhedron. *Journal of High Energy Physics*, 2014(10):30, 2014.

[AJ90] M.F. Atiyah and L. Jeffrey. Topological lagrangians and cohomology. *Journal of Geometry and Physics*, 7(1):119–136, 1990.

[Arn89] V. I. Arnold. *Mathematical Methods of Classical Mechanics*. Springer, 2 edition, 1989.

[AS53] Warren Ambrose and Isadore M. Singer. A theorem on holonomy. *Transactions of the American Mathematical Society*, 75(3):428–443, 1953.

[AS63] Michael F. Atiyah and Isadore M. Singer. The index of elliptic operators on compact manifolds. *Bulletin of the American Mathematical Society*, 69(3):422–433, 1963.

[Ati57] M. F. Atiyah. Complex analytic connections in fibre bundles. *Transactions of the American Mathematical Society*, 85(1):181–207, 1957.

[Ati88] Michael F. Atiyah. Topological quantum field theories. *Publications Mathématiques de l'Institut des Hautes Études Scientifiques*, 68:175–186, 1988.

[Ati02] M. Atiyah. Mathematics in the 20th century. *Bulletin of the London Mathematical Society*, 34:1–15, 2002.

[AW84] Luis Alvarez-Gaum'e and Edward Witten. Gravitational anomalies. *Nuclear Physics B*, 234(2):269–330, 1984.

[Bae98] John C. Baez. Spin foam models. *Classical and Quantum Gravity*, 15(7):1827–1858, 1998.

[Bae06] John C. Baez. Quantum quandaries: A category-theoretic perspective. In Steven French, Dean Rickles, and Juha Saatsi, editors, *The Structural Foundations of Quantum Gravity*, pages 240–265. Oxford University Press, 2006.

[Bae22] John C. Baez. Getting to the bottom of noether's theorem. In James Read and Nicholas J. Teh, editors, *The Philosophy and Physics of Noether's Theorems*, pages 66–99. Cambridge University Press, 2022.

[Bar91] John W. Barrett. Holonomy and path structures in general relativity and yang–mills theory. *International Journal of Theoretical Physics*, 30(9):1171–1215, 1991.

[Bar97] Manuel Barros. General helices and a theorem of lancret. *Proceedings of the American Mathematical Society*, 125(5):1503–1509, 1997.

[Bar25] Jacob A. Barandes. The stochastic-quantum correspondence. *Philosophy of Physics*, 3(1):8, 2025.

[BD95] John C. Baez and James Dolan. Higher-dimensional algebra and topological quantum field theory. *Journal of Mathematical Physics*, 36(11):6073–6105, nov 1995.

[Bel64] John S. Bell. On the Einstein Podolsky Rosen paradox. *Physics Physique Fizika*, 1(3):195–200, 1964.

[Ben73] Charles H. Bennett. Logical reversibility of computation. *IBM Journal of Research and Development*, 17(6):525–532, 1973.

[Ber84] Michael V. Berry. Quantal phase factors accompanying adiabatic changes. *Proceedings of the Royal Society of London. Series A, Mathematical and Physical Sciences*, 392(1802):45–57, 1984.

[BFG+94] G. Blatter, M. V. Feigel'man, V. B. Geshkenbein, A. I. Larkin, and V. M. Vinokur. Vortices in high-temperature superconductors. *Reviews of Modern Physics*, 66:1125–1388, 1994.

[Bis75] Richard L. Bishop. There is more than one way to frame a curve. *The American Mathematical Monthly*, 82(3):246–251, 1975.

[BLLN19] Konstantin Y. Bliokh, Daniel Leykam, Max Lein, and Franco Nori. Topological non-Hermitian origin of surface Maxwell waves. *Nature Communications*, 10, 2019.

[Boh52a] David Bohm. A suggested interpretation of the quantum theory in terms of "hidden" variables. i. *Physical Review*, 85(2):166–179, 1952.

[Boh52b] David Bohm. A suggested interpretation of the quantum theory in terms of "hidden" variables. ii. *Physical Review*, 85(2):180–193, 1952.

[Bou02] Raphael Bousso. The holographic principle. *Rev. Mod. Phys.*, 74(3):825–874, Aug 2002.

[BPST75] A. A. Belavin, A. M. Polyakov, A. S. Schwartz, and Yu. S. Tyupkin. Pseudoparticle solutions of the yang-mills equations. *Physics Letters B*, 59(1):85–87, 1975.

[BRS76] Carlo Becchi, Alain Rouet, and Raymond Stora. Renormalization of gauge theories. *Annals of Physics*, 98(2):287–321, 1976.

[bru13] brusspup. Amazing water and sound experiment #2. YouTube, 2013. Accessed: 2025-07-01.

[BS06] John C. Baez and Urs Schreiber. Higher gauge theory, 2006.

[BS10] J. Baez and M. Stay. *Physics, Topology, Logic and Computation: A Rosetta Stone*, pages 95–172. Springer Berlin Heidelberg, 2010.

[BSS89] Lenore Blum, Mike Shub, and Steve Smale. On a theory of computation and complexity over the real numbers: NP-COMPLETENESS, recursive functions and universal machines. *Bulletin (New Series) of the American Mathematical Society*, 21(1), jul 1989.

[BSZ92] John C. Baez, Irving E. Segal, and Zhengfang Zhou. *Introduction to Algebraic and Constructive Quantum Field Theory*. Princeton University Press, Princeton, NJ, 1992.

[BT82] Raoul Bott and Loring W. Tu. *Differential Forms in Algebraic Topology*, volume 82 of *Graduate Texts in Mathematics*. Springer, 1982.

[BT91] Matthias Blau and George Thompson. Topological gauge theories of antisymmetric tensor fields. *Annals of Physics*, 205(1):130–172, 1991.

[BV81] Igor A. Batalin and Grigori A. Vilkovisky. Gauge algebra and quantization. *Physics Letters B*, 102(1):27–31, 1981.

[CCRF+98] Alberto S. Cattaneo, Paolo Cotta-Ramusino, Francesco Fucito, Maurizio Martellini, Maurizio Rinaldi, Alessandro Tanzini, and Mauro Zeni. Four-dimensional yang–mills theory as a deformation of topological bf theory. *Communications in Mathematical Physics*, 197:571–621, 1998.

[CF03] Marius Crainic and Rui Loja Fernandes. Integrability of lie brackets. *Annals of Mathematics*, 157(2):575–620, 2003.

[CFL28] Richard Courant, Kurt Friedrichs, and Hans Lewy. Über die partiellen differenzengleichungen der mathematischen physik. *Mathematische Annalen*, 100:32–74, 1928.

[CFP18] Bruno T. Costa, Michael Forger, and Luiz Henrique P. Pêgas. Lie groupoids in classical field theory i: Noether's theorem, 2018.

[CG17] Kevin Costello and Owen Gwilliam. *Factorization Algebras in Quantum Field Theory*, volume 31 of *New Mathematical Monographs*. Cambridge University Press, 2017.

[CGM06] Nadia Chouaieb, Alain Goriely, and John H. Maddocks. Helices. *Proceedings of the National Academy of Sciences*, 103(25):9398–9403, 2006.

[CH88] Thierry Coquand and Gérard Huet. The calculus of constructions. *Journal of Symbolic Computation*, 6(2):113–129, 1988.

[CJS95] Ralph L. Cohen, John D. S. Jones, and Graeme B. Segal. Floer's infinite-dimensional morse theory and homotopy theory. In *The Floer Memorial Volume*, volume 133 of *Progress in Mathematics*, pages 297–325. Birkhäuser, 1995.

[CMPSP21] Robert Cardona, Eva Miranda, Daniel Peralta-Salas, and Francisco Presas. Constructing turing complete euler flows in dimension 3. *Proceedings of the National Academy of Sciences*, 118(19):e2026818118, may 2021.

[CMR14] Alberto S. Cattaneo, Pavel Mnev, and Nicolai Reshetikhin. Classical bv theories on manifolds with boundary. *Communications in Mathematical Physics*, 332:535–603, 2014.

[Coh19] Ralph L. Cohen. Floer homotopy theory, revisited. *arXiv preprint arXiv:1901.08694*, 2019.

[Col77] S. Coleman. Nonabelian plane waves. *Physics Letters B*, 70(1):59–60, 1977.

[Con94] Alain Connes. *Noncommutative Geometry*. Academic Press, 1994.

[Coo04] Matthew Cook. Universality in elementary cellular automata. *Complex Systems*, 15(1):1–40, 2004.

[CPGW15] Toby S. Cubitt, David Perez-Garcia, and Michael M. Wolf. Undecidability of the spectral gap. *Nature*, 528(7581):207–211, 2015.

[CS74] Shiing-Shen Chern and James Simons. Characteristic forms and geometric invariants. *Annals of Mathematics*, 99(1):48–69, 1974.

[CSCS23] F. M. Castela Simão, Alberto S. Cattaneo, and Michele Schiavina. Bv equivalence with boundary. *Letters in Mathematical Physics*, 113(25), 2023.

[CZX+19] Yuntian Chen, Ruo-Yang Zhang, Zhongfei Xiong, Zhi Hong Hang, Jensen Li, Jian Qi Shen, and C. T. Chan. Non-abelian gauge field optics. *Nature Communications*, 10(1), jul 2019.

[dB78] Carl de Boor. *A Practical Guide to Splines*, volume 27 of *Applied Mathematical Sciences*. Springer-Verlag, New York, NY, 1 edition, 1978.

[Deu85] David Deutsch. Quantum theory, the Church–Turing principle and the universal quantum computer. *Proceedings of the Royal Society of London. Series A*, 400(1818):97–117, 1985.

[DGZ92] Detlef Dürr, Sheldon Goldstein, and Nino Zanghì. Quantum equilibrium and the origin of absolute uncertainty. *Journal of Statistical Physics*, 67(5–6):843–907, 1992.

[Don83] S. K. Donaldson. An application of gauge theory to the topology of 4-manifolds. *Journal of Differential Geometry*, 18:279–315, 1983.

[DW90] Robbert Dijkgraaf and Edward Witten. Topological gauge theories and group cohomology. *Communications in Mathematical Physics*, 129(2):393–429, 1990.

[EGH00] Yakov Eliashberg, Alexander Givental, and Helmut Hofer. Introduction to symplectic field theory. In Noga Alon, Jean Bourgain, Alain Connes, Mikhael Gromov, and Vitali Milman, editors, *Visions in Mathematics*, pages 560–673. Birkhäuser / Springer, 2000.

[Ehr59] Charles Ehresmann. Catégories topologiques et catégories différentiables. In *Colloque de Géométrie Différentielle Globale*, page 137, Bruxelles, 1959. Centre Belge de Recherches Mathématiques.

[EM70] David G. Ebin and Jerrold Marsden. Groups of diffeomorphisms and the motion of an incompressible fluid. *Annals of Mathematics*, 92(1):102–163, 1970.

[EPR35] A. Einstein, B. Podolsky, and N. Rosen. Can quantum-mechanical description of physical reality be considered complete? *Physical Review*, 47(10):777–780, 1935.

[Fel91] Matthias Felleisen. On the expressive power of programming languages. *Science of Computer Programming*, 17(1-3):35–75, 1991.

[FI25] Angel Ferrández Izquierdo. *Helices*. RSME Springer Series. Springer Cham, 2025. Edition 1.

[FK99] Laurent Freidel and Kirill Krasnov. Spin foam models and the classical action principle. *Advances in Theoretical and Mathematical Physics*, 2:1183–1247, 1999.

[Flo88] Andreas Floer. Morse theory for lagrangian intersections. *Journal of Differential Geometry*, 28(3):513–547, 1988.

[Fon15] Brendan Fong. Decorated cospans, 2015.

[Fre02] Daniel S. Freed. Dirac charge quantization and generalized differential cohomology. In *Surveys in Differential Geometry*, volume 7, pages 129–194. 2002.

[Fre12] Daniel S. Freed. The cobordism hypothesis. *arXiv preprint*, 2012. Expository; arXiv:1210.5100.

[Fre14] Daniel S. Freed. Anomalies and invertible field theories. In *String-Math 2013*, volume 88 of *Proceedings of Symposia in Pure Mathematics*, pages 25–45. American Mathematical Society, 2014.

[FRS16] Domenico Fiorenza, Christopher L. Rogers, and Urs Schreiber. Higher $U(1)$-gerbe connections in geometric prequantization. *Reviews in Mathematical Physics*, 28(06):1650012, 2016.

[FS12] Laurent Freidel and Simone Speziale. On the relations between gravity and bf theories. *SIGMA*, 8:032, 2012.

[FT82] Edward Fredkin and Tommaso Toffoli. Conservative logic. *International Journal of Theoretical Physics*, 21(3–4):219–253, 1982.

[GAP] The GAP Group. *GAP – Groups, Algorithms, and Programming*. Version 4.

[Gei08] Hansjörg Geiges. *An Introduction to Contact Topology*, volume 109 of *Cambridge Studies in Advanced Mathematics*. Cambridge University Press, 2008.

[Gir87] Jean-Yves Girard. Linear logic. *Theoretical Computer Science*, 50(1):1–101, 1987.

[Gis19] Nicolas Gisin. Real numbers are the hidden variables of classical mechanics. *Quantum Studies: Mathematics and Foundations*, 7(2):197–201, oct 2019.

[GJ87] James Glimm and Arthur Jaffe. *Quantum Physics: A Functional Integral Point of View*. Springer, 2 edition, 1987.

[GJOS14] N Goldman, G Juzeliunas, P Ohberg, and I B Spielman. Light-induced gauge fields for ultracold atoms. *Reports on Progress in Physics*, 77(12):126401, nov 2014.

[GKSW15] Davide Gaiotto, Anton Kapustin, Nathan Seiberg, and Brian Willett. Generalized global symmetries. *Journal of High Energy Physics*, 2015(2):172, 2015.

[GMN10] Davide Gaiotto, Gregory W. Moore, and Andrew Neitzke. Four-dimensional wall-crossing via three-dimensional field theory. *Communications in Mathematical Physics*, 299(1):163–224, 2010.

[GMN13] Davide Gaiotto, Gregory W. Moore, and Andrew Neitzke. Wall-crossing, hitchin systems, and the WKB approximation. *Advances in Mathematics*, 234:239–403, 2013.

[Gol67] Hubert Goldschmidt. Integrability criteria for systems of nonlinear partial differential equations. *Journal of Differential Geometry*, 1(3–4):269–307, 1967.

[Gor17] Alain Goriely. *The Mathematics and Mechanics of Biological Growth*, volume 45 of *Interdisciplinary Applied Mathematics*. Springer, New York, 2017.

[GP21] Daniel Grady and Dmitri Pavlov. The geometric cobordism hypothesis. *arXiv preprint*, 2021. arXiv:2111.01095.

[GPMPS25] Angel Gonzalez-Prieto, Eva Miranda, and Daniel Peralta-Salas. Topological kleene field theories as a model of computation, 2025.

[Gra04] Alfred Gray. *Tubes*, volume 221 of *Progress in Mathematics*. Birkh"auser, Basel, 2 edition, 2004.

[Gro21] Alexander Grothendieck. Pursuing stacks, 2021.

[GW73] David J. Gross and Frank Wilczek. Ultraviolet behavior of non-abelian gauge theories. *Physical Review Letters*, 30(26):1343–1346, 1973.

[Har26] Rory Harris. LHCb discovers the final missing member of a doubly charmed particle family. CERN News, 2026.

[Hit87a] Nigel J. Hitchin. The self-duality equations on a riemann surface. *Proceedings of the London Mathematical Society*, 55(1):59–126, 1987.

[Hit87b] Nigel J. Hitchin. Stable bundles and integrable systems. *Duke Mathematical Journal*, 54(1):91–114, 1987.

[HK64] Rudolf Haag and Daniel Kastler. An algebraic approach to quantum field theory. *Journal of Mathematical Physics*, 5(7):848–861, 1964.

[HK26] Po-Shen Hsin and Ryohei Kobayashi. Automorphism in gauge theories: Higher symmetries and transversal non-clifford logical gates. *SciPost Physics*, 20(6):159, 2026.

[HKLR87] Nigel J. Hitchin, Anders Karlhede, Ulf Lindström, and Martin Roček. Hyper-kähler metrics and supersymmetry. *Communications in Mathematical Physics*, 108(4):535–589, 1987.

[Hol06] Barry R. Holstein. Graviton physics. *American Journal of Physics*, 74(11):1002–1011, nov 2006.

[HS10] Nicholas Harrigan and Robert W. Spekkens. Einstein, incompleteness, and the epistemic view of quantum states. *Foundations of Physics*, 40(2):125–157, 2010.

[Int14] Int'l Centre for Theoretical Physics. Conversation: Salam, sciama, witten and budinich, Oct 2014. Accessed: 2025-06-18.

[Ish92] Chris J. Isham. Canonical quantum gravity and the problem of time, 1992.

[Jac95] Ted Jacobson. Thermodynamics of spacetime: The einstein equation of state. *Physical Review Letters*, 75(7):1260–1263, aug 1995.

[JW06] Arthur Jaffe and Edward Witten. Quantum yang–mills theory. In James Carlson, Arthur Jaffe, and Andrew Wiles, editors, *The Millennium Prize Problems*, pages 129–152. American Mathematical Society, 2006.

[Kam26] Benjamin Kaminsky. Expressiveness, verifiability, tractability: Toward a computational thermodynamics. Hexagon preprint hexagon:2611.00323v1, 2026.

[Kas83] H. A. Kastrup. Canonical theories of lagrangian dynamical systems in physics. *Physics Reports*, 101(1-2):151, 1983.

[Kle52] Stephen Cole Kleene. *Introduction to Metamathematics*. North-Holland, Amsterdam, 1952.

[KM84] F. R. Klinkhamer and N. S. Manton. A saddle-point solution in the Weinberg-Salam theory. *Physical Review D*, 30(10):2212–2220, 1984.

[Koc06] Anders Kock. *Synthetic Differential Geometry*. Cambridge University Press, 2 edition, 2006.

[Kog79] John B. Kogut. An introduction to lattice gauge theory and spin systems. *Reviews of Modern Physics*, 51(4):659–713, 1979.

[Kos70] Bertram Kostant. Quantization and unitary representations. In C. T. Taam, editor, *Lectures in Modern Analysis and Applications III*, volume 170 of *Lecture Notes in Mathematics*, pages 87–208. Springer, Berlin, Heidelberg, 1970.

[KS67] Simon Kochen and Ernst P. Specker. The problem of hidden variables in quantum mechanics. *Journal of Mathematics and Mechanics*, 17(1):59–87, 1967.

[KS17] Igor Khavkine and Urs Schreiber. Synthetic geometry of differential equations: I. jets and comonad structure. arXiv preprint arXiv:1701.06238, 2017.

[KT25] Subhash Kantamneni and Max Tegmark. Language models use trigonometry to do addition, 2025.

[Kur84] Yoshiki Kuramoto. *Chemical Oscillations, Waves, and Turbulence*, volume 19 of *Springer Series in Synergetics*. Springer, Berlin, Heidelberg, 1984.

[Kv98] T. C. Kraan and P. van Baal. Periodic instantons with non-trivial Holonomy. *Nuclear Physics B*, 533(1-3):627–659, 1998.

[KW07] Anton Kapustin and Edward Witten. Electric-magnetic duality and the geometric langlands program, 2007.

[LM89] H. Blaine Lawson and Marie-Louise Michelsohn. *Spin Geometry*, volume 38 of *Princeton Mathematical Series*. Princeton University Press, 1989.

[Lor02] Gino Loria. *Spezielle algebraische und transscendente ebene Kurven. Theorie und Geschichte.* B. G. Teubner, Leipzig, 1902.

[LS21] Matthias Ludewig and Augusto Stoffel. A framework for geometric field theories and their classification in dimension one. *SIGMA*, 17:072, 2021.

[Lur09] Jacob Lurie. On the classification of topological field theories. *Current Developments in Mathematics*, 2008:129–280, 2009.

[Lur11] Jacob Lurie. Derived algebraic geometry xi: Descent theorems, sep 2011. Preprint, September 28, 2011.

[Lur17] Jacob Lurie. Higher algebra, 2017. Available at https://www.math.ias.edu/~lurie/papers/HA.pdf.

[LW90] Joohan Lee and Robert M. Wald. Local symmetries and constraints. *Journal of Mathematical Physics*, 31(3):725–743, 1990.

[LW05] Michael A. Levin and Xiao-Gang Wen. String-net condensation: A physical mechanism for topological phases. *Physical Review B*, 71:045110, 2005.

[Mac05] Kirill C. H. Mackenzie. *General Theory of Lie Groupoids and Lie Algebroids*, volume 213 of *London Mathematical Society Lecture Note Series*. Cambridge University Press, 2005.

[Mad27] Erwin Madelung. Quantentheorie in hydrodynamischer form. *Zeitschrift für Physik*, 40(3–4):322–326, 1927.

[Man03] Ciprian Manolescu. Seiberg–witten–floer stable homotopy type of three-manifolds with $b_1 = 0$. *Geometry & Topology*, 7:889–932, 2003.

[Man16] Ciprian Manolescu. Pin(2)-equivariant seiberg–witten floer homology and the triangulation conjecture. *Journal of the American Mathematical Society*, 29(1):147–176, 2016.

[Man19] N. S. Manton. The inevitability of sphalerons in field theory. *Philosophical Transactions of the Royal Society A: Mathematical, Physical and Engineering Sciences*, 377(2161):20180327, nov 2019.

[MBS08] Vincent Mathieu, Fabien Buisseret, and Claude Semay. Gluons in glueballs: Spin or helicity? *Physical Review D*, 77(11), jun 2008.

[Met03] David Metzler. Topological and smooth stacks, 2003.

[ML84] Per Martin-Löf. *Intuitionistic Type Theory*. Bibliopolis, 1984.

[MLM92] Saunders Mac Lane and Ieke Moerdijk. *Sheaves in Geometry and Logic: A First Introduction to Topos Theory*. Universitext. Springer, New York, 1992.

[Mog91] Eugenio Moggi. Notions of computation and monads. *Information and Computation*, 93(1):55–92, 1991.

[Moo14] Gregory Moore. Physical mathematics and the future. Written version of a talk given at Strings 2014, Princeton University. Available at https://www.physics.rutgers.edu/~gmoore/PhysicalMathematicsAndFuture.pdf, 2014.

[Mor17] Kenichi Morita. *Theory of reversible computing*. Springer, 2017.

[MS17] Dusa McDuff and Dietmar Salamon. *Introduction to Symplectic Topology*. Oxford University Press, 3 edition, 2017.

[MZ96] Maurizio Martellini and Mauro Zeni. The bf formalism for yang-mills theory and the ‘t hooft algebra, 1996.

[NC10] Michael A. Nielsen and Isaac L. Chuang. *Quantum Computation and Quantum Information*. Cambridge University Press, 10th anniversary edition, 2010.

[NDGD06] Michael A. Nielsen, Mark R. Dowling, Mile Gu, and Andrew C. Doherty. Quantum computation as geometry. *Science*, 311(5764):1133–1135, 2006.

[Noe18] Emmy Noether. Invariante variationsprobleme. *Nachrichten von der Gesellschaft der Wissenschaften zu Göttingen, Mathematisch-Physikalische Klasse*, pages 235–257, 1918.

[NT13] Naoto Nagaosa and Yoshinori Tokura. Topological properties and dynamics of magnetic skyrmions. *Nature Nanotechnology*, 8:899–911, 2013.

[Oec05] Robert Oeckl. *Discrete Gauge Theory: From Lattices to TQFT*. Imperial College Press, London, 2005.

[OS73] Konrad Osterwalder and Robert Schrader. Axioms for euclidean green's functions. *Communications in Mathematical Physics*, 31(2):83–112, 1973.

[PAD10] T. PADMANABHAN. Equipartition of energy in the horizon degrees of freedom and the emergence of gravity. *Modern Physics Letters A*, 25(14):1129–1136, May 2010.

[Pau40] Wolfgang Pauli. The connection between spin and statistics. *Physical Review*, 58:716–722, 1940.

[PBR12] Matthew F. Pusey, Jonathan Barrett, and Terry Rudolph. On the reality of the quantum state. *Nature Physics*, 8(6):475–478, 2012.

[Pen71] Roger Penrose. Angular momentum: An approach to combinatorial space-time. In Ted Bastin, editor, *Quantum Theory and Beyond*, pages 151–180. Cambridge University Press, Cambridge, 1971.

[Pen87] R. C. Penner. The decorated Teichmüller space of punctured surfaces. *Communications in Mathematical Physics*, 113:299–339, June 1987.

[Pen89] Roger Penrose. *The Emperor's New Mind: Concerning Computers, Minds, and the Laws of Physics*. Oxford University Press, Oxford, UK, 1989. Foreword by Martin Gardner.

[Pic19] Sébastien Picard. Calabi–yau manifolds with torsion and geometric flows. In Daniele Angella, Leandro Arosio, and Eleonora Di Nezza, editors, *Complex Non-Kähler Geometry: Cetraro, Italy 2018*, volume 2246 of *Lecture Notes in Mathematics*, pages 57–120. Springer International Publishing, 2019.

[Ple77] Jerzy F. Plebański. On the separation of einsteinian substructures. *Journal of Mathematical Physics*, 18(12):2511–2520, 1977.

[PM73] R. Penrose and M. A. H. MacCallum. Twistor theory: An approach to the quantisation of fields and space-time. *Physics Reports*, 6(4):241–315, 1973.

[Pol87] A. M. Polyakov. *Gauge Fields and Strings*, volume 3 of *Contemporary Concepts in Physics*. Harwood Academic Publishers, 1987.

[Pos21] Emil L. Post. Introduction to a general theory of elementary propositions. *American Journal of Mathematics*, 43(3):163–185, 1921.

[PP09] Gordon Plotkin and Matija Pretnar. Handlers of algebraic effects. In *Programming Languages and Systems*, volume 5502 of *Lecture Notes in Computer Science*, pages 80–94. Springer, 2009.

[Pra66] Jean Pradines. Théorie de lie pour les groupoïdes différentiables: relations entre propriétés locales et globales. *C. R. Acad. Sci. Paris Sér. A-B*, 263:A907–A910, 1966.

[Ric53] H. G. Rice. Classes of recursively enumerable sets and their decision problems. *Transactions of the American Mathematical Society*, 74(2):358–366, Mar 1953.

[RS95] Carlo Rovelli and Lee Smolin. Spin networks and quantum gravity. *Physical Review D*, 52(10):5743–5759, 1995.

[Sau89] David J. Saunders. *The Geometry of Jet Bundles*, volume 142 of *London Mathematical Society Lecture Note Series*. Cambridge University Press, 1989.

[Sch48] Julian Schwinger. Quantum electrodynamics. i. a covariant formulation. *Physical Review*, 74(10):1439–1461, 1948.

[Sch13] Urs Schreiber. Differential cohomology in a cohesive infinity-topos, 2013.

[Sch14] Urs Schreiber. Quantization via linear homotopy types. arXiv preprint arXiv:1402.7041, 2014.

[Sch16] Urs Schreiber. Higher prequantum geometry, 2016.

[Sch20] Frederic P. Schuller. Constructive gravity: Foundations and applications, 2020.

[Sed82] Steven Sedlacek. A direct method for minimizing the yang–mills functional over 4-manifolds. *Communications in Mathematical Physics*, 86:515–527, 1982.

[Sei95] Nathan Seiberg. Electric–magnetic duality in supersymmetric non-abelian gauge theories. *Nuclear Physics B*, 435(1–2):129–146, 1995.

[SMO04] LEE SMOLIN. An invitation to loop quantum gravity. In *Quantum Theory and Symmetries*, pages 655–682. WORLD SCIENTIFIC, Oct 2004.

[SN24] Sakura Schäfer-Nameki. ICTP Lectures on (Non-)Invertible Generalized Symmetries. *Physics Reports*, 1063:1–55, 2024.

[Sou70] Jean-Marie Souriau. *Structure des systèmes dynamiques*. Maîtrises de mathématiques. Dunod, Paris, 1970.

[Spe69] Donald C. Spencer. Overdetermined systems of linear partial differential equations. *Bulletin of the American Mathematical Society*, 75(2):179–239, 1969.

[Spe07] Robert W. Spekkens. Evidence for the epistemic view of quantum states: A toy theory. *Physical Review A*, 75:032110, 2007.

[ST06] Jeremy G. Siek and Walid Taha. Gradual typing for functional languages. In *Scheme and Functional Programming Workshop*, pages 81–92, 2006.

[SvdH07] E. L. Starostin and G. H. M. van der Heijden. The shape of a Möbius strip. *Nature Materials*, 6(8):563–567, Aug 2007.

[SW94] Nathan Seiberg and Edward Witten. Monopoles, duality and chiral symmetry breaking in N=2 supersymmetric Yang–Mills theory. *Nuclear Physics B*, 431(3):484–550, 1994.

[SW13] Urs Schreiber and Konrad Waldorf. Connections on non-abelian gerbes and their holonomy. *Theory and Applications of Categories*, 28:476–540, 2013.

[Szu12] Matthew P. Szudzik. *The Computable Universe Hypothesis*, pages 479–523. WORLD SCIENTIFIC, oct 2012.

[Tao18] Terence Tao. On the universality of the incompressible Euler equation on compact manifolds. *Discrete and Continuous Dynamical Systems*, 38(3):1553–1565, 2018.

[Tay71] J. C. Taylor. Ward identities and charge renormalization of the yang–mills field. *Nuclear Physics B*, 33(2):436–444, 1971.

[TCK+20] TB Thompson, P Chaggar, E Kuhl, A Goriely, and Alzheimer's Disease Neuroimaging Initiative. Protein-protein interactions in neurodegenerative diseases: A conspiracy theory. *PLoS Computational Biology*, 16(10):e1008267, Oct 2020.

[tH79] G. 't Hooft. A property of electric and magnetic flux in nonabelian gauge theories. *Nuclear Physics B*, 153:141–160, 1979.

[THF06] Sam Tobin-Hochstadt and Matthias Felleisen. Interlanguage migration: From scripts to programs. In *Companion to the 21st ACM SIGPLAN Symposium on Object-Oriented Programming Systems, Languages, and Applications*, OOPSLA '06, pages 964–974, New York, NY, 2006. Association for Computing Machinery.

[TN14] Šárka Todorova-Nová. Quantization of the qcd string with a helical structure. *Physical Review D*, 89(1), jan 2014.

[Tom46] Sin-itiro Tomonaga. On a relativistically invariant formulation of the quantum theory of wave fields. *Progress of Theoretical Physics*, 1(2):27–42, 1946.

[TS97] Walid Taha and Tim Sheard. Multi-stage programming with explicit annotations. In *Proceedings of the 1997 ACM SIGPLAN Symposium on Partial Evaluation and Semantics-Based Program Manipulation*, PEPM '97, pages 203–217, New York, NY, 1997. Association for Computing Machinery.

[Uhl82] Karen K. Uhlenbeck. Connections with L^p bounds on curvature. *Communications in Mathematical Physics*, 83(1):31–42, 1982.

[Val91] Antony Valentini. Signal-locality, uncertainty, and the subquantum h-theorem. i. *Physics Letters A*, 156(1–2):5–11, 1991.

[vB96] Pierre van Baal. Instanton moduli for t3 × r. *Nuclear Physics B - Proceedings Supplements*, 49(1–3):238–249, jun 1996.

[VW05] Antony Valentini and Hans Westman. Dynamical origin of quantum probabilities. *Proceedings of the Royal Society A: Mathematical, Physical and Engineering Sciences*, 461(2053):253–272, 2005.

[Waa25] Lukas Waas. Presenting the topological stratified homotopy hypothesis, 2025.

[Wad90] Philip Wadler. Linear types can change the world! In Manfred Broy and Cliff B. Jones, editors, *Programming Concepts and Methods*. North-Holland, 1990.

[Wal95] Robert M. Wald. Quantum field theory in curved spacetime. *arXiv preprint*, 1995. arXiv:gr-qc/9509057.

[War50] J. C. Ward. An identity in quantum electrodynamics. *Physical Review*, 78:182, 1950.

[Wei96] Alan Weinstein. Groupoids: Unifying internal and external symmetry. *Notices of the American Mathematical Society*, 43:744–752, 1996. Also available as arXiv:math/9602220.

[Wei00] Klaus Weihrauch. *Computable Analysis: An Introduction*. Texts in Theoretical Computer Science. Springer, Berlin, 2000.

[Wil74] Kenneth G. Wilson. Confinement of quarks. *Phys. Rev. D*, 10(8):2445–2459, Oct 1974.

[Wit88] E. Witten. Topological Quantum Field Theory. *Communications in Mathematical Physics*, 117(3):353–386, 1988.

[Woi22] Peter Woit. Notes on the twistor $\mathbf{p}^1$, 2022.

[WW20] Juven Wang and Xiao-Gang Wen. A non-perturbative definition of the standard models. *Physical Review Research*, 2:023356, 2020.

[WY75] Tai Tsun Wu and Chen Ning Yang. Concept of nonintegrable phase factors and global formulation of gauge fields. *Physical Review D*, 12(12):3845–3857, 1975.

[WZ84] Frank Wilczek and A. Zee. Appearance of gauge structure in simple dynamical systems. *Physical Review Letters*, 52(24):2111–2114, 1984.

[Yau78] Shing-Tung Yau. On the Ricci curvature of a compact Kähler manifold and the complex Monge-Ampère equation, I. *Communications on Pure and Applied Mathematics*, 31(3):339–411, 1978.

[Yet92] David N. Yetter. Topological quantum field theories associated to finite groups and crossed g-sets. *Journal of Knot Theory and Its Ramifications*, 1(1):1–20, 1992.

[YM54] C. N. Yang and R. L. Mills. Conservation of isotopic spin and isotopic gauge invariance. *Physical Review*, 96(1):191–195, 1954.

[Zad65] Lotfi A. Zadeh. Fuzzy sets. *Information and Control*, 8(3):338–353, 1965.

[ZR99] Paolo Zanardi and Mario Rasetti. Holonomic quantum computation. *Physics Letters A*, 264(2–3):94–99, 1999.